The Pathogenesis and Regulation of Cell Death in Glioblastoma: Experimental Studies using Glioma Spheroid Cultures

Helen Susan Bell BSc
Department of Clinical Neurosciences
Western General Hospital
Edinburgh
EH4 2XU

Thesis submitted for the Degree of Doctor of Philosophy
Edinburgh 2002

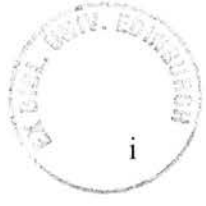

ABSTRACT OF THESIS

Understanding the pathways by which endogenous cell death occurs in tumours may be of considerable value when identifying potential therapies. In glioblastoma, two main types of cell death are observed, apoptosis and necrosis. Although the regulatory mechanisms leading to necrotic and apoptotic morphologies are thought to vary widely, their close association in glioblastoma suggests they may share some regulatory function. High levels of Fas (APO-1), HIF-1α and PARP found within perinecrotic tissue *in vivo* suggests regulatory factors do exist. The presence of these regulatory factors, sub-lethal stress and a high apoptotic index suggests the p53 pathway may be involved in the cell death response around these areas. In order to investigate cell death regulatory factors *in vitro*, particularly those relating to the p53 pathway, the glioma spheroid system was utilised. Glioma spheroids are known reproduce some of the regional heterogeneity found *in vivo* and they form areas of necrosis as the spheroids become larger and the central core of cells becomes metabolically compromised.

Using spheroids derived from four glioma cell lines, the aims of this project were (i) to fully characterise the glioma spheroid system for the four glioma cell lines, U87, U373, MOG-G-CCM and A172 and to establish that the system adequately reflects many of the features found in glioblastoma cell populations *in vivo*; (ii) to define the exact time point in spheroid growth when central cell death occurs and to identify the modes of cell death present (iii) to establish which p53-related proteins are associated with areas of cell death within stressed glioblastoma cell populations and to determine any correlations between this distribution and the genetic status of the cell lines; and finally, (iv) to ascertain whether modulation of the *P53* status of the cells has an effect on the development of cell death and the expression of p53-related proteins within glioma spheroid cultures.

Regions of proliferation, death and differentiation were first assessed using a variety of immunohistochemical and microscopical techniques. Spheroid growth and apoptotic index were also quantitatively recorded. Onset of central cell death was seen to occur over week 3 and these spheroids were examined using electron microscopy to establish the primary mode of cell death (apoptosis or necrosis). HIF-1α expression was used as a marker to determine

the metabolic status of spheroid central regions at this time point. The *P53* genotype of the cell lines was then determined and the reactivity of p53, Bax, p21 and MDM2 in monolayer cultures of the 4 lines was assessed following exposure to hypoxia and free radical stress. Perinecrotic expression of p53, Bax, p21 and MDM2 was recorded in both week 3 spheroid cultures and in glioblastoma biopsy material. The cell lines were transfected with wild-type and dominant negative *P53* transcripts to investigate the effect of increasing and decreasing levels of endogenous p53 on cell death susceptibility within 3-dimensional spheroid cultures.

Cross-sections of large glioma spheroids appeared highly representative of GBM tissue, modeling the span from blood vessels to nutritionally compromised, necrotic tissue distinct from the vasculature. The primary cell death morphology observed was necrosis, followed by increases in perinecrotic apoptotic index. Increases in HIF-1α expression coincided with the onset of necrosis. HIF-1α, p53 and p21 accumulation were associated with U87 and A172 monolayer cultures (p53 wild-type), but not U373 and MOG-G-CCM monolayer cultures (*P53* mutant), following exposure to oxidative stress. No increases in p53, Bax and p21 expression were found within perinecrotic tissue in spheroid cultures derived from any of the cell lines. A 60kDa MDM2 isoform was found to be upregulated within perinecrotic tissue in both spheroids and in 80% of biopsy cases irrespective of *P53* status. The addition of a wild-type *P53* transcript to U87 cells did not effect cell death susceptibility within U87 spheroids. U373 cells transfected with wild-type *P53* died 3 days post transfection. Cell death susceptibility was not altered in either U87 and U373 spheroids following transfection with dominant negative *P53*.

In conclusion, in large 3-dimensional glioma spheroid cultures, necrosis is the primary cell death event, followed by increases in perinecrotic apoptotic index. Although increases in p53-related expression are observed in *P53* wild-type lines in response to oxidative stresses, p53, Bax and p21 accumulation do not appear to be important for the regulation of cell death in spheroid cultures, irrespective of the *P53* status of the cell lines. Although the *P53*gene appears to be essentially redundant within perinecrotic tissue, high levels of 60kDa MDM2 may associate with other cell death regulatory factors thus significantly influencing cell death susceptibility in both *P53* wild-type and mutant cell populations.

To my parents,
Graham and Sheila

ACKNOWLEDGMENTS

Firstly, I would like to thank Dr Stephen Wharton and Professor Ian Whittle for their friendship, patience and overall excellent supervision. Equal thanks also goes to Dr Scott Bader at the Sir Alastair Currie Laboratories for his invaluable input. The help of Dr Mark Walker and Frank Donnelly at the University of Edinburgh and Kevin Corke at the University of Sheffield was also very much appreciated. Also, I would like to thank my colleagues both in the Department of Clinical Neurosciences and Prostate Research Group; YH Yau, Ioannis Fouyas, Gail Valler, Shom Goel, Douglas Thomson, Ewan Grant, Colin Bayne, Vanessa Cobb, Rosalind Launchbury and Margaret Ross for their friendship, good humour and support over the past 4 years.

Finally, I would like to extent my gratitude to the Samantha Dickson Research Fund for supporting the studies contained within this thesis.

DECLARATION

I, Helen Susan Bell, hereby declare, that unless otherwise stated, the work embodied in this thesis is the result of my own independent investigation. This is in accordance with the rule 3.4.7. of the University of Edinburgh Postgraduate Study Programme.

PUBLICATIONS AND PRESENTATIONS ARISING FROM THIS THESIS

Full Papers

Bell HS, Whittle IR, Walker M, Leaver HA, Wharton SB. The development of necrosis and apoptosis in glioma: experimental findings using spheroid culture systems. ***Neuropathol Appl Neurobiol***. 2001 Aug;27(4):291-304.

Bell HS, Whittle IR, Bader SA and Wharton SB. Discovery of a Perinecrotic 60kDa MDM2 Isoform within Glioma Spheroids and Glioblastoma Biopsy Material. ***Carcinogenesis.*** Submitted.

Abstracts

Bell HS, Bader SA, Whittle IR and Wharton SB. A study of the relationship of p53 status to the susceptibility to apoptosis, necrosis and to the expression of p53-related proteins in glioma spheroid models. ***Neuropathol Appl Neurobiol*** 2001; 27:410-418.

Bell HS, Whittle IR, Bader S, Wharton SB. The spheroid system as a model to investigate cell death in glioma. ***Brain Path*** 2000 ; 10(4): 731-732.

Bell HS, Whittle IR, Wharton SB. The spheroid system as model to investigate cell death in glioma. ***Brit J Neurosurg*** 2000; 15: 125.

Bell HS, Whittle IR, Wharton SB. A multicellular glioma spheroid model: phenotypic characteristics and development of necrosis. ***Brit Neuroscience Ass*** Abst 1999; 15:116.

TABLE OF CONTENTS

LIST OF FIGURES AND TABLES

ABBREVIATIONS

ABC:	Avidin-Biotin complex
Adp53:	Adenoviral p53
AGT:	O^6 alkylguanine-DNA alkyltranferase
AhR:	Aryl hydrocarbon receptor
ALS:	Amyotrophic lateral schlerosis
ARF:	Alternative reading frame
ARNT:	AhR-nuclear translocator
ATM:	ataxia telangiectasia mutated
ATP:	adenosine 5' triphosphate
ATR:	Ataxia telangiectasia mutated and Rad-3 related
BCNU:	Bis(chloroethyl)nitrosourea
Bp:	Base pair
BPDE:	r-7,t-8-dihydroxy-t-9,10-epoxy-7,8,9,10-tetrahydrobenzo[a]pyrene
BrDU:	5-Bromo-2-deoxyuridine
BSA:	Bovine serum albumin
CAMS:	cell adhesion molecules
CAT:	Chloramphenicol acetyl transferase
CCNU:	N-(2-chloroethyl)-N'-cyclohexyl-N-nitrosourea
CDK:	Cyclin dependent kinase
CDKN2A:	Cyclin dependent kinase inhibitor 2A
CMV:	Cytomegolovirus
CoA:	Co-enzyme A
DAB:	Diaminobenzidine tetrachloride
DCC:	Deleted in Colon cancer
DIABLO:	Direct IAP binding protein
DISC:	death inducing signalling complex
DMEM:	Dulbecco's modified eagles medium
DMSO:	Dimethyl sulphoxide
DNA-PK:	DNA protein kinase
dNTP:	deoxyribonucleoside triphosphate

E1a:	Early region 1a
ECM:	Extracellular matrix
EGFP:	Enhanced green fluorescent protein
EGFR:	Epidermal growth factor receptor
ER:	Endoplasmic reticulum
ERCC:	Excision repair cross complementation group
FACS:	Flourescence activated cell sorter
FADD:	Fas-associated death domain protein
FCS:	Foetal calf serum
g:	Gram
GBM:	Glioblastoma multiforme
GF:	Growth factor
GFAP:	Glial fibrillary acid protein
GY:	Gray
H&E:	Haematoxylin and eosin
HIF-1α:	Hypoxia inducible factor- 1α
HRP:	Horseradish peroxidase
IAP:	Inhibitor of apoptosis protein
IFN-γ:	Interferon gamma
IL2:	Interleukin 2
INK4:	Inhibitors of cdk4
kDa:	Kilodalton
L:	Litre
μ:	Micro
m:	Milli
M:	Mole
MAPK:	Mitogen activated protein kinase
MDM2:	3-mouse double minute 2, human homolog of; p53-binding protein
MEK:	Mitogen activated protein/ERK kinase
MEKK:	MEK kinase
MMPs:	Matrix metalloproteases
MTT:	3-[4,5-Dimethylthiazol-2-yl]-2,5-diphenyltetrazolium bromide

MyD:	Myeloid differentiation
n:	Nano
NO:	Nitric oxide
PARP:	Poly(ADP-ribose) polymerase
PBS:	Phosphate buffered saline
PCNA:	Proliferating cell nuclear antigen
PCR:	Polymerase chain reaction
PDGFR:	Platelet derived growth factor receptor
PERP:	P53 apoptosis Effector Related to PMP-22
PI(3)K:	phosphatidylinositol 3-kinase
PI:	Propidium iodide
PIGS:	p53 induced genes
PMP-22/Gas:	Peripheral Myelin Protein 22/growth arrest specific 3
PMSF:	Phenylmethylsulphonyl fluoride
PS:	Phosphotidylserine
PTEN:	Phosphatase and tensin homologue deleted on chromosome 10
RB:	Retinoblastoma
ROS:	Reactive oxygen species
RVV:	Recombinant vaccinia virus
SAP:	Shrimp alkaline phosphatase
SBA:	Sodium 5,6-benzylidene-L-ascorbate
SCID:	Severe combined immunpodeficiency disease
SDS-PAGE:	SDS POLYACRYLAMIDE GEL ELECTROPHORESIS
SEM:	Standard error of the mean
SPANOVA:	Split plot analysis of variance
SV40:	Simian virus 40
TBS:	Tris buffered saline
TBST:	TBS tween
TNF-α:	Tumour necrosis factor alpha
TRAIL:	TNF-related apoptosis inducing ligand
TUNEL:	TdT-mediated dUTP-X nick end labelling
UV:	Ultraviolet

VEGF:	Vascular endothelial growth factor
WHO:	World Health Organisation
WT:	Wild-type
XPB/XPD:	Xeroderma pigmentosum helicases B and D

CHAPTER 1

INTRODUCTION

1.1. General Introduction

The prognosis for patients suffering from highly malignant brain tumours such as glioblastoma multiforme (termed GBM, WHO grade IV) is uniformly fatal with a mean survival time for patients with GBM of 8 months (Whittle, 1996). Because the search for an effective therapy remains elusive, understanding the molecular basis of gliomas, to identify novel therapeutic strategies has become of utmost importance. Because large increases in tumour volume and subsequent death of eloquent brain tissue occur in such a short period of time, many novel strategies are being designed around increasing levels of cell loss within tumour cell populations.

Cell loss in tumours may occur due to apoptosis or necrosis (Steel, 1977). Apoptosis is a process that often requires new gene transcription and the triggering of complex regulatory pathways (Wyllie, 1995). As a result, these pathways have begun to be thoroughly researched in recent years as potential therapeutic targets. In contrast, necrosis is sudden and accidental cell death brought on by a large stimulus sufficient to kill the cell and generate an inflammatory response (Trump et al., 1997). Necrosis is generally regarded as an unregulated process, which, in contrast to apoptosis, is not under genetic control. However, necrosis is a poorly understood process and it is possible that there are regulatory mechanisms involved, perhaps separate from those involved in apoptosis (Clarke, 1998).

In the diffuse astrocytoma group of tumours, apoptotic index increases with tumour grade, thus glioblastomas have the highest apoptotic index. Necrosis is only associated with high grade tumours and is a diagnostic feature to allow the categorisation of an astrocytoma as glioblastoma multiforme (Alvord, 1992; Kleihues et al., 1993). It has been suggested that there are two types of necrosis, ischaemic necrosis with an infarct-like pattern and smaller areas of necrosis surrounded by pseudopallisading layers of tumour cells (Kleihues et al., 2000). It is unclear whether these two types of necrosis are linked or whether they arise independently as a result of different pro-death signals. Understanding endogenous cell death in glioblastoma is important as it could elucidate specific pathways and target molecules that are switched on when a tumour cell is stressed.

Susceptibility to cell death within normal and tumour cell populations is often decided by a complex series of pathways central to which lies the p53 protein (Vogelstein et al.,

2000). p53 up-regulates the expression of proteins such as p21, which induces cell cycle arrest, and pro-apoptotic members of the Bcl family such as Bax (Wylie, 1995). *P53* mutations are prevalent in secondary glioblastomas i.e. those arising from a lower grade glioma (Nagane et al., 1997). Another protein called MDM2 binds to and inactivates the p53 protein. Upregulation of this protein can result in abrogation of p53-mediated cell death. Abnormal MDM2 over-expression is common in primary tumours (Yu et al., 2000; He et al., 1994). The constant acquisition of mutations picked up throughout the life span of each individual tumour (Rasheed et al., 1999; Collins et al., 1999), suggests that cell death associated with areas of necrosis in GBM most likely occurs via assorted pathways that have retained some residual function. In many cell types, p53 has been implicated in stress-induced cell death involving various mediators such as the activation of intracellular reactive oxygen species, Fas (CD95) and HIF-1α (Chandel et al., 2000; Edwards et al., 2000; Vogt et al., 1998; An et al., 1998). Fas and HIF-1α have been found to be increased within perinecrotic tissue in GBM (Tachibana et al., 1996; Zagzag et al., 2000). Although this is the case, it remains unclear as to whether areas of cell death, which are pathologically similar in most glioblastomas regardless of progression, occur as a result of a p53 related mechanism or whether other pathways are involved.

A number of *in vitro* and *in vivo* models have been developed to study the characteristics of glial tumour cell growth (Bernstein et al., 1987; Geise et al., 1995; Schor et al., 1982; Bjerkvig et al., 1986). Monolayer and cell suspension systems are of great value when assessing detailed cell function and to study the regulation of apoptosis, but they do not reconstruct the cellular microenvironments present within a tumour cell mass and there are no simulated nutrient gradients. In addition, many *in vitro* models are limited in the study of cell death in that they do not model necrosis. The spheroid system for cell culture is a three-dimensional model which creates areas of proliferation, differentiation and cell death within a tumour cell mass (Kunz-Schughart et al., 1998; Tamaki et al., 1997; Sutherland et al., 1988). These areas can be studied individually when the spheroid becomes larger and a nutrient gradient forms across the radius of the spheroid. It is the intention to utilise this system to investigate the pathogenesis and regulation of cell death within hypoxic and nutritionally-deprived tumour cell populations.

Four factors have to be taken into consideration when identifying potential candidates in the search for target genes and pathways activated around areas of endogenous cell death

in glioblastoma. Firstly, the typical characteristics of the diffuse astrocytoma group of tumours should be fully understood. These include general patterns of growth, death, differentiation, invasion and progression. Secondly, the morphology of the cells associated with regions of cell death need to be taken into consideration. The existence of apoptotic morphologies suggests that regulatory molecules are involved. In contrast, the presence of necrosis implies that fewer regulatory mechanisms are involved. Thirdly, the type and intensity of insult applied to the tissue can result in different cell death pathways being activated. A broad knowledge of the molecules and pathways associated with necrotic and apoptotic cell death, in response to a wide variety of cell stresses, such as hypoxia and nutrient deprivation, is therefore vital. And lastly, the genetic background of the tumour has to be established. Mutations occurring in specific cell death pathways may alter the expression of certain proteins around and within areas of cell stress. The following four sections of this project are therefore dedicated to these issues (1.2-1.5), followed by a review of the literature on 3-dimentional culture systems (1.6), by which the evolution of areas of cell death in glioblastoma will be studied.

1.2. The diffuse astrocytomas

1.2.1. Introduction to the diffuse astrocytoma group

This study focuses mainly on the most malignant of the diffuse astrocytoma group, glioblastoma multiforme. However, it is important to fully understand the diffuse astrocytoma group as a whole because these tumours are related not only in terms of their glial status, but also by their genetic progression and overall biological behaviour. Diffuse astrocytic tumours share the following characteristics: (i) they may arise at any site in the central nervous sytem (CNS), preferentially in the cerebral hemispheres; (ii) they usually manifest clinically in adults; (iii) they possess a wide range of histopathological features; (iv) they show diffuse infiltration of adjacent and distant brain structures; (v) they have a tendency to progress to a more malignant phenotype.

1.2.2. Incidence

Diffusely infiltrating astrocytomas are the most frequent intracranial neoplasms and account for more than 60% of all primary brain tumours. Approximately 6 new cases per 100,000 are diagnosed each year. Glioblastoma multiforme is the most common tumour type within the diffuse astrocytoma group and accounts for approximately 12-15% of all intracranial neoplasms and 50-60% of all astrocytic tumours. In most developed countries 2-3 new cases per 100,000 population are diagnosed each year (Kleihues, 2000).

1.2.3. Localization of diffuse astrocytomas

Diffuse astrocytomas most commonly occur in the cerebral hemispheres, in particular in the fronto temporal and parietal regions. Infiltrative spread is a common feature of all diffuse astrocytic tumours (Burger et al., 1988). However, it is glioblastomas, the most malignant of the diffuse astrocytoma group, that are renown for their rapid invasion into neighbouring brain structures. Tumour infiltration occurs most often in the cerebral hemispheres and tumour infiltration often extends into the contralateral hemisphere creating the image of a bilateral symmetrical lesion ('butterfly glioma'). Similarly, rapid spread is observed in the internal capsule, fornix, anterior commisure and optic radiation. Increased intracranial pressure resulting from the fast growth of these tumours is the greatest threat to survival resulting in the sudden onset of symptoms such as headache and personality changes. Although diffuse astrocytomas are highly invasive they tend not to metastasise and do not invade the subarachnoid space, cerebrospinal fluid or vessel lumen

(Giordana et al., 1995). In addition, haematogenous spread to extraneural tissue is very rare in patients that have not received neurosurgical intervention (Hoffman et al., 1985).

1.2.4. Histological grading of diffuse astrocytomas

The length of the patients history and chance of a long, recurrence-free survival are closely associated with the intrinsic biology of the neoplasm. Significant indicators of anaplasia in gliomas include nuclear atypia (coarse nuclear chromatin, nuclear pleomorphism, multinucleation and pseudoinclusions), mitotic activity, cellularity, vascular proliferation and necrosis. These histological characteristics have been used by the World Health Organisation (WHO) to produce a grading scheme for the diffuse astrocytoma group. As a general rule, grading is based on areas showing the highest degree of anaplasia, on the assumption that this tumour cell population eventually determines the course of the disease. WHO grade I astrocytomas (eg pilocytic astrocytomas) are the least malignant of the astrocytoma group. These tumours rarely possess any of the above described histological criteria and are biologically distinct clinicopathological entities. WHO grade II astrocytomas consist of astrocytomas which have no histological criteria, and low-grade diffuse astrocytomas which exhibit nuclear atypia. WHO grade III astrocytomas are designated anaplastic astrocytomas and these tumours possess 2 histological criteria, nuclear atypia and mitotic activity. WHO grade VI astrocytic tumours are designated glioblastoma multiforme and are identified by the presence of three out of four histological criteria. These include the presence of; (I) nuclear atypia (II) microvascular proliferation, (III) high mitotic activity and/or (IV) the presence of necrosis (Daumas-Duport et al., 1988).

1.2.5. Histological evaluation of glioblastoma multiforme

The level of intra- and inter-tumoural heterogeneity is almost endless in glioblastoma. However, some tissue patterns are more commonly observed than others. Poorly differentiated, round, fusiform and pleomorphic cells are very common in GBM, although more differentiated neoplastic cells, such as gemistocytes and fibrillary astrocytes, are also often observed (Burger, 1989). Areas containing recognisable astrocyte differentiation and highly anaplastic cells are often observed side by side within the same tumour. Although fibrillary and poorly differentiated morphologies are most prevalent, other tissue patterns such as the presence of giant, sarcoma-like and epithelial-like cancer cells are also common.

Although glioblastomas are derived from glial tissue, GFAP (glial fibrillary acid protein) expression is very variable between tumours. Well differentiated, astrocyte-like cells are generally positive for GFAP and small undifferentiated cells tend to be negative or stain weakly. Although large portions of a GBM may lack GFAP expression, usually occasional cells are found to be positive after extensive examination.

In addition to the presence of highly anaplastic cells, the presence of microvascular proliferations are typical of GBMs. These are mitotically active endothelial cells recruited by the glioma cells to encourage vascularization of poorly oxygenated areas of the tumour (Nagashima et al., 1987). VEGF (vascular endothelial growth factor) is the most important regulator of vascular functions in glioma-induced angiogenesis and acts specifically on endothelial cells and vascular permeability *in vivo* (Cheng et al., 1996). VEGF is hypoxia-inducible and is often found within areas of perinecrotic tumour cells (Plate et al., 1992).

A high proliferative index is also a feature of GBM. The Ki67 index (labels cells in G1, S, G2 and M phase) shows great regional variation and average values are around the 15-20% mark (Gerdes et al., 1983; Deckert et al., 1989). Small undifferentiated cells generally show high higher proliferative indices than better differentiated neoplastic astrocytes and gemistocytes (Watanabe K., 1997).

It has been suggested that two major types of necrosis can be distinguished in GBM. The first type consists of huge areas of destroyed tumour tissue, which may comprise more than 80% of the total tumour mass. These appear as yellowy -white coaggulated masses that often contain some remnants of the vasculature (Burger et al., 1983). The second type of necrosis observed is that of small necrotic foci surrounded by layers of pseudopallisading small, fusiform glioma cells (Lantos et al., 1996). Necrosis in GBM will be discussed at length in section 1.4.2.

1.2.6. Primary and secondary glioblastoma

Glioblastomas can be split into two categories by their clinical duration (Scherer, 1940). Secondary glioblastomas can arise from a low grade diffuse or anaplastic astrocytoma and can develop over months or years. Low-grade diffuse astrocytomas frequently develop recurrent lesions with the second biopsy often showing histopathological evidence of

increased nuclear atypia, hyperchromasia, mitotic activity and in some cases vascular proliferation and /or necrosis, i.e. features of the glioblastoma. The acquisition of these anaplastic features, though an inherent property of diffuse astrocytomas, is largely unpredictable in terms of both clinical and histological outcomes. While some astrocytomas show no change in histological grade over more than 10 years following the first resection, others show a rapid transition to malignancy within 1-2 years. This type of tumour usually effects younger adults (aged 30-45 years). Primary GBMs have a short clinical history (usually of less than six months) and do not have any clinical or histopathological evidence of a precursor lesion. They normally occur in older adults (around 55 years).

Histologically the two tumour types are very similar with respect to the highly heterogeneous nature of the tissue. However, secondary GBMs are generally found to have a greater number of the better differentiated fibrillary morphologies and primary GBMs show a prevalence of the more monotonous, small, largely GFAP negative cells that congregate at high density.

1.2.7. Genetic progression of the diffuse astrocytomas

Extensive studies examining the molecular genetics of the diffuse astrocytoma group have revealed the presence of huge numbers of genetic abnormalities. Loss or mutation of the *P53* gene has been detected in many types of glioma and represents an early genetic event in a subset of astrocytomas. *P53* is a tumour suppressor gene which, in normal cells, activates either cell cycle arrest or apoptosis (programmed cell death) in response to stress (Watanabe et al., 1996) (see section 1.4 for review). Allelic loss of chromosome 17p and *P53* mutations are observed in approximately one-third of all three grades of adult astrocytomas, suggesting that inactivation of *P53* is important in the formation of grade II tumours. In addition, high-grade astrocytomas with homogenous *P53* mutations can evolve clonally from subpopulations of similarly mutated cells present in tumours that are initially low grade. An important consequence of the loss of wild-type *P53* activity is increased genomic instability, which appears to accelerate neoplastic progression. Thus, *P53* appears to play a role in both the formation of low grade disease and in the progression towards secondary glioblastoma. *P53* mutations occur in approximately 60-70% of secondary tumours. In contrast, *P53* mutations are rare (approximately 10%) in primary glioblastomas. This theory is supported by the observation that younger

astrocytoma patients not only had higher incidences of *P53* mutations but also survived longer than those without mutations. Therefore, glioblastomas evolve by one of at least two distinct pathways: one that requires *P53* inactivation and one that does not. The *P53* pathway and glioblastoma will be discussed in detail later in the project (1.5.). Other combinations of mutagenic events commonly occur during astrocytoma progression such as *RB* (retinoblastoma protein) alterations (~25%), *PDGFR* (platlet derived growth factor) amplification (~10%) and the loss of expression of *DCC* (deleted in colorectal cancer gene, ~50%) (Kleihues et al., 2000; Collins, 1999).

Primary GBMs most commonly fall into the group of glioblastomas that do not require *P53* mutations to evolve. One of the most common genetic abnormalities is the overexpression and/or mutation of the epidermal growth factor receptor gene (*EGFR*). EGFR is a transmembrane receptor responsible for sensing extrecellular ligands, EGFR and transforming growth factor beta (TGF-β). EGFR mitogenisis appears to encompass many pro-proliferative systems including ligand-driven dimerization of receptor monomers and tyrosine kinase activation. Overexpression of the *EGFR* gene in cancerous cells results in abnormally high numbers of the EGFR receptors being expressed on the cell surface. This can often occur in conjuction with the generation of an abnormal receptor resulting in a mutant transcript that is constitutively activated (Nishikawa et al., 1994). *EGFR* amplification and/or overexpression occurs in approximately 60% of primary GBM s and only 5% of secondary tumours (Lang et al., 1994). Another common finding in primary tumours is the loss of specific alleles known to encode for the tumour suppressor PTEN (~30%) (Bostrom et al., 1998). PTEN expression inhibits the proliferation of glioma cells by inducing G1 arrest and elicits astrocytic differentiation. Inactivation of *PTEN* therefore plays an important role in the enhancement of unregulated growth of undifferentiated glioma cells (Adachi et al., 1999). *CDKN2A* mutations are also common in primary tumours (Ueki et al., 1996). This locus encodes for p16 and $p14^{ARF}$ proteins which are important for regulating both cell cycle control and apoptosis respectively (Stewart et al., 2001). $P14^{ARF}$ helps govern levels of intracellular p53 by regulating the movement of the MDM2 protein. The implications of the latter will also be discussed at length later in the project (1.4.7. and 1.5.3.)

It is therefore clear that in glioblastoma, in terms of primary and secondary tumours, different sets of mutations can result in phenotypically similar endpoints. These

progressive events can lead to disruption of both proliferative and cell death regulatory pathways.

1.2.8. Current therapeutic strategies for glioblastoma

Glioblastomas are essentially incurable and current treatments are limited to marginally increasing quantity and quality of life. The management of glioblastoma is based on a combination of surgery, radiation therapy and chemotherapy (Prados & Levin, 2000). Surgery is usually initially performed to debulk the tumour, followed by involved-field radiation (cumulative dose of up to 60Gy). Unfortunately, due to the diffusely infiltrative nature of glioblastomas and the intrinsic resistance of many gliomas to irradiation induced cytotoxicity, the combination of these two treatments usually only adds 2-3 months onto the overall prognosis. Chemotherapy is generally used selectively on recurrent tumours. The most commonly used chemotherapy drugs are alkylating agents, particularly nitrosoureas (Jeremic B et al., 1992; Levin V et al., 1990). These have been commonly used as single agents or in combination with other drugs such as procarbazine or etoposide. At present, response rates to chemotherapy are rather limited, with only 20-30% of tumours responding at all to chemotherapy and even then the prognosis is only lengthened by 2-3months (Stewart, 1989).

1.2.9. Recent advances in glioblastoma therapy

At a clinical level, improvements in the delivery of the above mentioned chemotherapeutic drugs combined with different therapeutic schedules (eg chemotherapy before surgery) are currently being tested and have been shown to improve prognosis in some patients (Prados & Levin, 2000). In addition, new chemotherapeutic drugs, such as temozolomide have been shown to be more effective in infiltrating the blood brain barrier and have shown progression free survival after 6 months (Yung et al., 1998). The effectiveness of alkylating agents can been further enhanced by the use of O^6-benzylguanine, which inactivates O^6 alkylguanine-DNA alkyltranferase (AGT) reducing tumour cell survival after DNA damage (Wedge et al., 1996). AGT is involved in the repair of alkylator based DNA crosslinks.

Much recent research has focused on immunotherapeutic strategies for glioma. Antibody-targeted immunotherapy involves the targeting of tumour cells with antibodies conjugated to radioisotopes or toxins. However, this relies heavily on the tumours cells expressing the

same specific markers. Transferin and EGFR receptors are preferentially expressed on tumour cells and immunotherapies targeting these have been tested on gliomas in nude mice with very mixed results (Laske D et al., 1994; Wikstrand et al., 1998). Cytokine-based immunotherapy (eg IL2) and the use of interferons (eg IFN-γ) have also showed promise as prospective therapeutic agents. Although when used on their own there is little tumour regression, it is thought they may enhance the activity of some other anti-tumourgenic drugs by stimulating direct immune responses against cancerous cells (Gansbacher et al., 1990). TNF-α is another prospective therapeutic agent and has been shown to induce death in some tumour types. It has a range of functions in the immune system including stimulating T cell growth and enhancing the cytotoxicity of monocytes . Unfortunately, cultured glioma cells are usually resistant to TNF-α, and clinical trials studying the therapeutic efficacy of TNF-α have been disappointing (Weller et al., 1994).

As a consequence of the limited success of the above strategies, a considerable amount of research has focused on combating the resistance of glioma cells to various cytotoxic agents and to the actions of immune cells. The phenotype of resistance is thought to depend on the pattern of genes expressed, and most importantly, those responsible for cell cycle arrest and apoptosis. For this reason, considerable time and effort has been put into investigating systems regulating cell death that could potentially be employed to overcome these problems. Currently, great hope is placed on the ability of death ligands (namely TRAIL and CD95) to induce cell death in tumour cells without damaging healthy tissue. The mechanisms behind this approach and other experimental treatments aimed at targeting apoptotic pathways will be discussed later in the project (1.5.5.). However, it is also possible that by investigating the pathogenesis and regulation of endogenous tumour cell death, which is particularly abundant in glioblastoma, specific molecules/pathways may come to light that may provide a 'gateway' to altering tumour cell death susceptibility.

1.3. The pathology of cell death in glioblastoma

1.3.1. General introduction to cell death

In the last 30 years, the two fundamentally different forms of cell death, apoptosis and necrosis, have been defined in terms of their morphology, biochemistry and incidence. The realisation that one of the two processes, apoptosis, has the theoretical potential to be influenced to produce a desired outcome in clinical problems such as cancer and neurodegenerative disease, is of particular interest to scientists and clinicians alike. Most tumour types exhibit some level of endogenous cell death, whether it be low levels of apoptosis as observed in astrocytomas or high levels of apoptosis and necrosis seen in the more malignant glioblastoma group. It is possible that this intrinsic cell death may help find the key to identifying key regulatory pathways involved in these systems, which could potentially be targeted therapeutically. Because different modalities of cell death, such as apoptosis and necrosis, can be activated as a result of different regulatory mechanisms, understanding the morphology and incidence of specific cell death types is vital. The following is a summary of the key morphological changes associated with apoptosis and necrosis and their distribution within glioblastoma tissue.

1.3.2. Pathology of apoptosis and necrosis

Apoptosis was first seen to be discrete from necrotic cell death by an individual series of morphological changes (Kerr, 1971; Wylie,1981). The living cell begins with segregating chromatin into condensed masses that cling to the inside of the nuclear envelope. The nucleus then fragments into several discrete fragments usually bound by a double membrane. Cytoplasmic changes also occur at this time and cytoskeletal elements, such as smooth ER, aggregate parallel to the cell surface. Eventually, in cells with abundant cytoplasm, extensive surface blebs form and these separate out into membrane bound apoptotic bodies of varying size which are engulfed or phagocytosed by adjacent cells or macrophages.

Apoptosis occurs in many circumstances, both in normal tissue and in cancer. Because it does not stimulate an inflammatory response, in normal tissue it is used by organisms to break down unwanted cells in a slow and controlled manner without causing undue harm to surrounding tissue (Cummings et al., 1997). In cancer it is thought to be stimulated by low level stress caused by oxidative stress, nutrient deprivation and growth factor withdrawal (Bellamy., 1995; Graeber et al., 1996; Shiffer et al., 1995). Because a complex

series of pathways are involved in regulating apoptosis. If abnormal alterations or mutations occur in these pathways, the malignant potential of a cell is enhanced because the ability of the cell to apoptose is reduced (Wyllie, 1997).

Necrosis, in contrast to apoptosis, is thought of as an accidental passive process. This results in the progressive breakdown of ordered cell structure and function after irreversible damage caused by a major environmental change such as severe ischemia, chemical trauma or extremes of temperature. Necrosis has no role in normal tissue physiology or development but is a common phenomenon when tissue is severely mechanically damaged, diseased or highly malignant (Trump et al., 1997).

Unlike apoptosis, the necrotic cell is already dead when morphological changes are seen to occur. These changes begin with the breakdown of cytoplasmic components. Initially, irregularities form in the cytoskeleton, intramatrical granules are lost from mitochondria, the plasma membrane begins to bleb and the ER and golgi elements become dilated. Following this, the cell membrane begins to lose its integrity, the mitochondria become swollen and the cytoskeleton and ER fragment. The cell membrane then completely breaks apart, spilling the contents of the cell into the extracellular space. The cell contents, particularly mitochondrial proteins, can induce an inflammatory reaction. Following this, the nucleus, which by this stage contains condensed chromatin, breaks down (Trump & Berezesky, 1998; Phelps et al., 1989). The mechanisms thought to be responsible for this series of events are not thought to be controlled by a complex series of pathways as with the apoptotic response. Because the stress is usually so great, membranous/cytoplasmic changes occur first, preceeding nuclear damage. In apoptosis, changes to the nuclear morphology are one of the first to occur because the cell has made a 'decision' to apoptose as a result of a series of extra- or intranuclear molecular signals.

1.3.3. Methods of detecting apoptotic and necrotic cells

Because of the recent interest in apoptosis as a target for anticancer therapies, scientists have spent considerable time designing ways to detect apoptotic cells. The four most popular ways of detection are currently electron microscopy, high resolution light microscopy, the TUNEL assay and Annexin V labelling. High resolution light microscopy using slides stained with haematoxylin and eosin (H&E) is the simplest way of identifying and counting apoptotic figures. However, because considerable cell shrinkage occurs in

the apoptotic process, apoptotic cells are sometimes difficult to detect compared to other methods. Electron microscopy (EM) is easily the best way for morphologically identifying apoptotic figures. However, EM is time consuming, expensive and only relatively small areas of tissue can be examined. To make the detection process easier, more complex assays have been designed to label apoptotic cells. One such assay is the TUNEL (TdT-mediated dUTP-X nick end labelling) labelling system. One of the hallmarks of apoptosis is DNA degradation. As a result, many nicks (both single and double standed) appear in the DNA exposing free 3'-OH termini. The TUNEL assay involves using the enzyme terminal deoynucleotidyl transferase (TdT) to label free 3'-OH termini with modified nucleotides. These nucleotides are conjugated to biotin or fluorescein as a secondary detection system. The cells can then be examined using either light/fluorescence microscopy or flow cytometry. Unfortunately, the TUNEL method has previously been shown to lack specificity, in that it may label necrotic as well as apoptotic cells (Grasl-Kraupp et al., 1995). In addition, other studies have shown that it may also label actively transcribing nuclei (Kockx et al., 2000).

Another trademark of apoptosis, preceding that of DNA degradation, is the translocation of phosphotidylserine (PS) from the interior side of the plasma membrane to the outer leaflet. It was discovered that a Ca2+ dependent phospholipid-binding protein, named Annexin-V, had a high affinity for PS. The Annexin-V protein, which is normally conjugated to a fluorescent marker, was therefore developed as a marker for apoptotic cells. Because necrotic cells also expose PS with a loss of membrane integrity, apoptotic cells are differentiated by the addition of propidium iodide (PI) which is incorporated into the nucleus of necrotic cells thus distinguishing them from the PI negative, apoptotic cells. The cells can then be examined using fluorescence microscopy or flow cytometry. There are two main problems surrounding this method. Firstly, fresh tissue has to be used for the labelling process. Fixed cells have permeabilized cell membranes and thus allow the entrance of both Annexin-V and PI into healthy cells. Secondly, a single cell suspension has to be used. This is particularly awkward when using tissue biopsies or three-dimentional cell culture systems. Aggressive disaggregation protocols could unwittingly permeabilize the cell membranes of healthy cell populations. It is therefore clear that a combination of detection systems has to be used when analysing cells/tissue for apoptotic indices. In monolayer cultures, a combination of H&E counts and Annexin V flow cytometry is possibly the best way to measure apoptotic indices, whereas when using

fixed, paraffin embedded material, a combination of TUNEL labelling and H&E apoptotic counts may be more appropriate.

The only guaranteed way of identifying individual necrotic cells is by using electron microscopy. This is because the necrotic process usually encompasses more than one cell making it difficult to distinguish individual cells from a necrosing cell population. In addition, necrotic cells often become swollen and burst thus rendering the outline of such cells difficult to see using conventional light microscopy. The resolution of the electron microscope is high enough to identify the outlines of such cells. Theoretically Annexin V labelling is also a possibility for the measurement of necrotic cells. However, necrotic cells rarely retain an intact morphology for long enough for proper flow cytometric analysis. Because of these difficulties, necrosis tends to be measured by the area of tissue lost in tissue biopsies and three-dimentional cultures systems, and by cell viability assays (such as the MTT assay) in monolayer culture systems.

1.3.4. Distribution of apoptosis and necrosis in the diffuse astrocytoma group

Although high grade diffuse astrocytomas, such as GBMs, are highly heterogeneous tumours, specific patterns of apoptosis and necrosis, can be distinguished both between different tumours and within individual tumour cell populations.

Apoptotic indices in astrocytic tumours have been found to increase with increased anaplasia and is therefore indicative of a poor prognostic outcome. This general pattern of apoptotic indices in a broad spectrum of different brain tumour types of various grades has been observed in many previous studies (Tew, 1999; Kordek et al., 1996; Migheli et al., 1994; Patsouris et al., 1996; Wharton et al., 1998). To quote one example, in a series of astrocytomas, Ellison et al found that apoptotic indices increased across a spectrum of astrocytic tumours from grade II to grade IV. In addition, there was a strong correlation between growth fraction (cells labelled with Ki67 antibody) and apoptotic index (Ellison et al., 1995). In normal tissues, cell proliferation, which may be sustained by growth factors, is usually inversely correlated with apoptosis which is the natural response of some tissues to withdrawal of these factors (Kerr et al., 1994).

The presence of necrosis is a defining feature of a glioblastoma multiforme (Kleihues et al., 2000). Generally, two distinct types of necrosis are observed in GBM; large ischaemic

areas of necrosis and smaller foci of necrosis surrounded by pseudopallisading tumour cells. The large areas of geographic necrosis in GBM are thought to arise due to insufficient blood supply and as a result have been termed ischemic in type. These are most common in primary (de novo) tumours (Kleihues et al., 2000). Poorly differentiated, highly anaplastic cells generally have a high proliferative index resulting in areas of hypercellularity with high energy requirements. As a consequence, cells distant from the tumour vasculature are more susceptible to necrosis due to acute hypoxia and nutrient deprivation. The perinecrotic cells situated at the periphery of this type of necrotic tissue often exhibit Fas expression (Tachibana et al., 1994). Fas is a member of the cell death receptor family and is associated with an apoptotic response (Waring & Müllbacher, 1999).

Smaller, irregularly shaped, band like, necrotic foci are common in both primary and secondary tumours. These are generally surrounded by radially orientated, densely packed, fusiform tumour cells in a 'pseudopallisading' pattern which often exhibit a high apoptotic index (Lantos et al., 1996). These regions also often contain regions of high VEGF expression which is thought to be induced in response to hypoxia (Plate et al., 1992). Also thought to be induced in response to hypoxia within pseudopallisading cell populations is the HIF-1α protein. In a study by Zagzag et al.(2000), 100% of all GBMs (n=12) tested exhibited high levels of HIF-1α around such areas. The combination of VEGF expression, HIF-1α expression and the appearance of apoptotic figures suggests a less acute stress than with the ischemic necrosis resulting in the activation of specific pathways to activate both apoptosis and neovascularisation.

It is unknown whether these two types of necrosis are related. The fact that patterns of VEGF and Fas expression are usually specific to each of the above types of necrosis, suggests that this is unlikely. However, the general consensus in the literature is that the small foci of necrosis eventually become enlarged, forming the huge ischaemic type areas of necrosis (Lantos et al., 1996; Kleihues et al., 2000). Regardless of the type of necrosis that eventually evolves, the mode of cell death that occurs first, necrosis or apoptosis, remains an unanswered question that could have implications in our knowledge of brain tumour biology. There are two possible theories that can describe the events that occur preceding the appearance of necrotic tissue. Firstly, small clusters of apoptotic cells may form first within areas of cell stress. As this stress becomes greater, necrotic cells become

interspersed within these foci. As these areas expand, pseudopallisading morphologies arise containing scattered apoptotic figures containing a central core of necrosis. Large areas of ischaemic necrosis eventually arise when the central necrotic core becomes extremely large. A second theory is that necrosis is the first event to occur due to the high energy requirements of the surrounding tissue and the fast growth of the invasive tumour cell mass into normal brain. Vascular thrombosis may also contribute to a sudden onset of necrosis without an initial onset of apoptosis. The existence of these small foci of necrosis may encourage the onset of apoptosis as a secondary response due to sub-lethal levels of hypoxia or pro-apoptotic signals from the central core of necrotic cells. Again, this may lead to the eventual creation of large areas of ischaemic tissue. Elucidation of the primary morphological changes occurring within these areas of cell death is important as it may implicate specific target molecules activated when glioblastoma tumour cells are under stress.

1.4. Regulation of cell death

1.4.1.General introduction to cell death regulation

To identify likely pro-death candidates/pathways that are associated within and around regions of necrosis in glioblastoma, the complexity of the pathways involved in a normal cell death response must first be understood. It has generally been assumed that stresses such as hypoxia and nutrient deprivation activate an unregulated necrotic mode of death when the stress is too great and too acute to activate the more regulated series of events that is associated with apoptosis. However, recent evidence suggests that there may be some overlap between the two processes. This may be of particular relevance to glioblastoma where necrosis and apoptosis are seen within close proximity to each other. The following is a review of the key regulatory changes that are associated with both apoptosis and necrosis in response to cell stress in normal tissue. Also discussed is a summary of key pathological and regulatory events that indicate these processes may not be entirely separate cell death entities.

1.4.2. The regulation of apoptosis

From a developmental perspective, apoptosis is a common occurrence programmed into the genetic make-up of an organism to remove excess cells from in organs, vessels and epithelia as they grow and differentiate (Meier et al., 2000). In certain pathological states, apoptosis can also remove damaged tissue in order to reduce inflammation, infection and abnormal cellular proliferation (Wyllie, 1997a). Although there are differences in the regulatory pathways responsible for activating apoptotic cell death under these circumstances, there are also many universal regulatory molecules that are involved in both. It is likely that although aberrations in apoptotic pathways are present in many glioma cells, some similar molecular strategies may be employed with glioblastoma cell populations in response to endogenous stress.

Injury to DNA, injury to cell membranes, mitochondrial damage and cytotoxic T lymphocyte killing can all stimulate an apoptotic response in human cells (Wyllie, 1997A). Direct damage to DNA can initiate apoptosis by a powerful, early activated mechanism dependent on the nuclear protein p53 via the checkpoint sensors ATM (ataxia telengiectasia mutated), ATR (ataxia telengiectasia Rad-3 related) and DNA-PKs (the catalytic subunit of DNA-dependent kinase). The main role of p53 is in the decision making process in which the cell is directed towards the completion of repair or apoptosis.

This mechanism is critical in the cellular response to double stranded DNA breaks (eg. damage inflicted by ionizing radiation), the generation of nucleotide dimers (eg. damage inflicted by UV light) and other DNA damaging agents (such as drugs that cause DNA alkylation) (Smith et al., 1999; Smith & Jackson, 1999; Hoekstra, 1997).

Injury to the cell membrane can result in the activation of acid sphingomylinase which generates the second messenger ceramide from membrane lipids (Figure 1). Ceramide can alter cellular susceptibility to apoptosis via MAP/JUN kinase signalling pathways (Sawada et al., 2001; Basu & Kolesnick, 1998). Active p53 protein has also been shown to regulate ceramide formation by neutral sphingomyelinase during periods of oxidative stress. Both the production of reactive oxygen species (ROS) from the mitochondria and upregulation of hypoxia-inducible factor 1α (HIF-1α) are capable of stabilising the p53 protein under these circumstances (An et al., 1998; Carmeliet et al., 1998; Chandel et al., 2000; Graeber et al., 1996). Similar pathways are thought to be activated when cells are exposed to glucose deprivation (Moley & Mueckler, 2000) and growth factor withdrawal (Asschert et al., 1998). Direct damage to the mitochondria can lead to the depolarisation of the mitochondrial membrane and the release of certain pro-apoptotic factors such as cytochrome C (Kroemer, 1997). Finally, T cell killing (by cytotoxic T lymphocytes, T helper cells, natural killer cells) works by releasing factors such as TNFs (tumour necrosis factor) and Fas/CD95 ligand which activate cell surface receptors resulting in the activation of pro-apoptotic pathways inside the target cell (Waring and Müllbacher, 1999; Krammer, 2000). Cytotoxic T cells also release granules, such as perforin which increase the permeability of the target cell membrane, and various proteases including Granzyme B (Greenberg, 1996).

The above insults culminate in the activation of a family of proteases called caspases (Figure 1). All known caspases possess an active cysteine which can cleave substrates after aspartic acid residues. Caspases are responsible for cleaving specific target proteins (eg. nuclear lamins and cytoskeletal proteins such as fodrin and gelsolin) resulting in the characteristic morphology of nuclear fragmentation and cell membrane blebbing (Wyllie, 1997). Approximately 14 caspases have been identified thus far, some of which are involved in the inflammatory response, and others that act as initiator and effector caspases as part of the apoptotic response (Yuan, 2000). Caspases are synthesized as enzymatically inert zymogens. They are composed of 3 domains, the N-terminal domain

(pro-domain), and the p20 and p10 domains, which are found in the mature enzyme. The mature enzyme forms a tetramer containing two p20/p10 heterodimers and two active sites. Most caspases are activated by proteolytic cleavage of the zymogen between the p20 and p10 domains at Asp-X sites. Thus, the easiest way of activating a caspase is by exposing it to another activated caspase resulting in a 'caspase cascade'. This strategy is employed by the 3 effector caspases, caspases 3, 6 and 7. These effector caspases are activated by initiator caspases and usually possess short pro-domains. Once activated, effector caspases are responsible for cleaving the specific cellular target proteins mentioned above. Initiator caspases have long pro-domains as they are not activated by other caspases but by complex combinations of other pro-apoptotic proteins (Earnshaw et al., 1999).

Two important initiator caspases involved in the apoptotic response are caspases 8 and 9. Caspase 8 is the key initiator caspase in the death-receptor superfamily. Upon ligand binding, caspase 8 is recruited by receptors such as Fas (Apo-1/CD95) to form membrane bound signalling complexes with other caspase 8 molecules and various adapter proteins. The caspase 8 molecules can then mutually cleave and activate each other. Caspase 9 has an even more complex mode of activation. The key requirement for caspase 9 activation is its association with a protein cofactor, Apaf-1. Apaf-1 becomes associated with caspase 9 when it is activated by cytochrome c. Cytochrome c is released into the cytosol from the mitochondria through pore-forming, Bcl-2 family homodimers such as Bax. The entire complex containing cytochrome c, Apaf-1 and the activated caspase 9 molecule is known as the apoptosome (Hengartner, 2000).

Caspases are regulated by a family of proteins called inhibitors-of-apoptosis (IAP) proteins (Miller, 1999). These are thought to provide a dampner on the very final step of caspase induction should an apoptotic fate not be required. Recent evidence has been shown that IAPs can be inhibited by signals from the mitochondria to allow full activation of the apoptotic machinery. Two of these inhibitors of IAPs have been named Smac (for second mitochondria-derived activator of Caspases) and DIABLO (for direct IAP-binding protein with low pI) (Du et al., 2000; Verhagen et al., 2000).

1.4.3. The p53 protein

Mediation of the apoptotic response from the initial insult to caspase activation occurs through a complex series of molecular events (Figure 1). A protein often central to this sequence of events is the p53 protein. p53 is partly responsible for mediating the apoptotic signal, in all of the described modes of injury described above.

The *P53* gene is situated on chromosome 17p. When transactivated, the resulting protein is modular, containing several regions with distinct functions that interact to integrate various stimuli from a range of cellular stresses to protect against adverse cellular activity. The p53 protein is essentially a transcription factor, capable of regulating a range of downstream genes including those directly responsible for cell cycle arrest, DNA repair and apoptosis (Prives & Hall, 1999). Because many types of tissue are ultimately reliant on this proteins ability to perform these functions, a lack of p53 function is thought to be directly responsible for the malignant progression of many tumours.

The core of the p53 protein is a region which folds in such a way as to form a domain which can interact with DNA in a sequence specific manner (el-Deiry et al., 1992). The binding of DNA in normal cells is optimal when the p53 protein is in a tetrameric state, that is when 4 separate p53 molecules interact via the tetramerization domain (Jeffrey et al., 1995). The C terminal domain of the protein forms a region thought to contain key regulatory properties associated with post-translational modification of the p53 protein. Acetylation, phophorylation and O-glycosylation and RNA binding have all been reported to occur in this region although the significance of all of these occurrences remains unclear. One theory is that this region regulates the conversion of a 'latent' p53 molecule to one that is active for DNA binding (Hupp & Lane., 1994). Another theory suggests that the C terminus somehow regulates the DNA binding capabilties of the p53 protein on longer DNA molecules (Bayle et al., 1995). Between the DNA binding domain and the N-terminus lies the SH^3 domain. This region can interact with with signal transduction molecules that contain a SH^3 domain including the c-abl oncogene (Yuan et al., 1996). The N-terminus allows the p53 protein to recruit the transcriptional machinery required for transcribing the new mRNA of specific target genes and is also involved in the self-regulation of the p53 molecule (Kubbutat et al., 1997).

1.4.4. p53 and apoptosis

Probably the best documented cases of p53 mediated activation of apoptosis are those involving the Bcl-2 family of proteins. Although these proteins share a combination of similar domains, Bcl-2 family members can be either pro-survival (eg Bcl-2, Bcl-X) or pro-apoptotic (eg Bax, Bad, Bid, Bak). It is thought the Bax protein, a pro-apoptotic member of the Bcl-2 family, can homodimerize on the outer membrane of the mitochondria to form pores allowing the release of cytochrome c from the intermembrane space. Cytochrome c then appears to mediate the activation of initiator caspase 9, which triggers a caspase release resulting in apoptosis. The proteins smac and DIABLO are also released at this time, which inactivate inhibitors-of-apoptosis proteins (Du et al., 2000; Verhagen et al., 2000). The Bcl-2 protein, a pro-survival member of the Bcl-2 family can heterodimerize with Bax preventing cytochrome c release. Wild-type p53 protein can transactivate the Bax promoter, boosting levels of mitochondrial Bax to increase the likelehood of Bax homodimer formation (Reviewed in Kroemer, 1997; Adams & Cory., 1998). The relative contribution of Bax to p53-mediated apoptosis appears to be cell-type dependent. For example, Bax is not required for radiation induced, p53-dependent apoptosis in thymocytes (Knudson et al., 1995) but Bax-deficient fibroblasts appear to be compromised in DNA-damage induced apoptosis (Schmitt et al., 1999). It is also thought that p53 is responsible for regulating levels of the pro-apoptotic Bcl-2 family member Bad. Bad heterodimerizes with the Bcl-2 protein, thus allowing more free Bax molecules to homodimerize resulting in subsequent caspase activation (Chao & Korsmeyer., 1998). Other Bcl-2 family members have more ambiguous functions such as Bag-1. Bag-1 is a heat shock (Hsp70)-binding protein that can collaborate with Bcl-2 in suppressing apoptosis after growth factor withdrawal, but can slow proliferation when over-expressed (Roth et al., 2000).

Although ligand binding stimulates an apoptotic response via members of the death-receptor family, transcription of the death receptor Fas is induced by p53 through a p53 responsive element (Figure 1). Fas ligand/Fas receptor binding serves many crucial physiological functions including tumour cell killing, lymphocyte culling and establishing zones of immune privilege (Waring and Müllbacher., 1999; Krammer, 2000). Fas has also been implicated in the cellular response to hypoxia (Kwon et al., 2001). The increased production of the Fas receptor increases susceptibility of the target cell to apoptosis via the Fas (CD95) ligand. Binding of the Fas ligand to the Fas receptor leads to the formation

of a submembrane death inducing signalling complex (DISC). FADD (Fas-associated death domain protein, also known as Mort1) instantly binds to the Fas receptor after ligand engagement and then recruits DED- containing procaspase 8 (also known as FLICE). Caspase 8 is then activated into the cytoplasm to initiate the caspase cascade (Kischkel et al., 1995). p53 can also stimulate the expression of another death receptor, KILLER/DR5. Like the Fas receptor, when KILLER/DR5 binds to the extracellular signaling molecule TRAIL, a signaling cascade is activated that results in caspase activation (Wu et al, 1997). Elaborate molecular control mechanisms have been found to exist to prevent either inappropriate or inadequate cell killing within the TNF-receptor super family. Decoy receptors exist that lack the 'death domain'and can prevent engagment of the apoptotic pathway (Rasper et al., 1998). Also, recruitment of caspase 8 into the successfully ligated death receptor complex can be prevented by c-flip, a catalytically incompetent pseudocaspase (Thome et al., 1997).

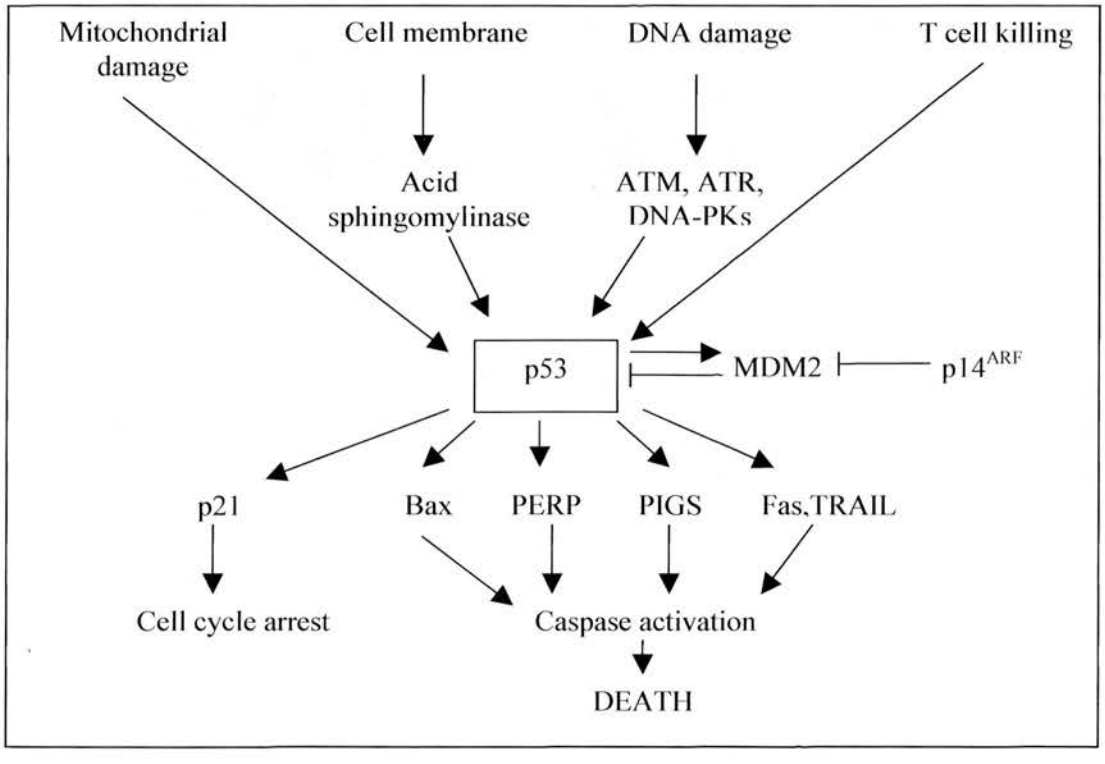

Figure 1. p53 mediated apoptotic pathways

Other p53 mediated pro-apoptotic target molecules are currently being researched and recently a group of PIGS (p53-induced genes) were identified that appear to increase cellular oxidation. When oxidation was blocked, p53-mediated apoptosis was inhibited, suggesting that p53 may activate apoptosis via cellular oxidation (Polyak et al., 1997).

The advent of microarray technology has also allowed the identification of another p53 dependent newcomer called PERP. PERP is a four span plasma membrane protein with similarity to the PMP-22/Gas3 family and is associated exclusively with the apoptotic machinery (Attardi et al., 2000). p53 has also been shown to associate with the c-abl protein tyrosine kinase that is distributed in the nucleus and the cytoplasm of proliferating cells (Shaul, 2000). Although c-abl is thought to cause the dissociation of DNA repair machinery during DNA repair, its other roles include the prevention of nuclear export and subsequent degradation of p53 by MDM2 (Sionov et al., 1999).

1.4.5. p53 and cell cycle arrest

A critical mediator of the p53 response to cell damage is the CDK inhibitor p21. p21 is transcriptionally regulated by p53 and can function as a dual specific inhibitor of cell proliferation by two independent and functionally distinct mechanisms. Firstly, p21 is a member of the Cip/Kip family of CDK (cyclin dependent kinase) inhibitors, a family that includes p27 and p57 (Mainprize et al., 2001). Cip/Kip proteins bind to and inhibit cyclin/cyclin dependent kinase complexes that are required for cell cycle progression. Each Cip/Kip protein has distinct functional properties, attributable to structural differences at their C-termini. This results in differing binding affinities of these proteins to CyclinD/ cdk4&6 and CyclinE/cdk2 (Russo et al., 1996).

p21 also associates with the DNA replication factor PCNA (Waga et al., 1994). PCNA is an auxiliary protein to certain DNA polymerases required for DNA synthesis. These p21/PCNA complexes can block DNA replication but not PCNA-mediated DNA repair. These p21/PCNA complexes also associate with the cyclin/cdk complexes suggesting that p21 may help to coordinate CDK-dependent cell cycle progression together with processes regulating DNA replication and /or repair (Li et al., 1994). Since the majority of p21 is found in activated cyclin/cdk complexes in proliferating cells and is required for proper assembly of cyclinD/cdk2 complexes, low levels of p21 may aid progression of the cell cycle (Zhang et al., 1994)

GADD45 is another target for p53 function involved in growth arrest. It is one of a family of genes called MyD that have been shown to interact with the stress responsive MTK1/MEKK complex and the p21/PCNA/CDK complex, both of which actively inhibit

cell cycle progression (Azam et al., 2001). p53 can also activate the 14-3-3 protein, 14-3-3σ, which has been shown to block the cell cycle at the S/G2 transition (Fu et al., 2000).

Not only does p53 have an active role in arresting the cells to allow repair to take place, the p53 protein itself is thought to be directly involved in maintaining DNA integrity. While cells are arrested for DNA repair, p53 can bind to and inactivate Rad51, a protein involved in homologous recombination (Buchhop et al., 1997). p53 also interacts through its C-terminal domain with the transcription repair TFIIH-associated factors ERCC2 and ERCC3 (XPB and XPD), that are involved in strand-specific DNA repair (Wang et al., 1996). A ribonucleotide reductase gene is also thought to be involved as a p53 dependent cell cycle checkpoint for DNA damage. P53R2 is activated in response to DNA damage and supplies urgent precursors (dNTPs) for DNA synthesis at the actual site of repair in the nucleus (Tanaka et al., 2000).

1.4.6. p53 regulation

In normal mammalian cells, p53 is expressed at extremely low levels because the protein is rapidly degraded following synthesis. The MDM2 (murine double minute-2) protein is known as the key protein involved in the regulation and stability of the p53 protein (Kubbutat et al., 1997). MDM2 interacts with p53 in undamaged cells and targets it for ubiquitin-mediated degredation. MDM2 also binds to the p53 protein and inhibits the ability of p53 to act as a transcription factor. The promoter of the *MDM2* gene contains a p53 binding site and is transcribed in a p53 dependent manner. This has led to a model in which p53 up-regulates the MDM2 protein, therefore providing a negative feedback loop for p53 activity (Wu et al., 1993). The control that MDM2 exerts over p53 is essential for normal cell growth and the death of MDM2 deficient mice can only be rescued by the simultaneous deletion the p53 gene (Montes de Oca Luna et al., 1995).

The $p14^{ARF}$ protein indirectly influences levels of intracellular p53. This protein was initially identified when researchers were examining the role of the *CDKN2A* locus. The *CDKN2A* locus has been shown to encode a family of proteins called INK4. These proteins (p15, P16, p18 and p19) have been shown to inhibit various cyclin dependent kinases that are important for cell cycle progression (Roussel, 1999). Alternative splicing of the *CDKN2A* locus produces the $p14^{ARF}$ protein. The $p14^{ARF}$ protein is a nuclear protein, which is localized specifically to the nucleolus. Here, it binds and sequesters

MDM2, preventing MDM2-mediated export of p53 to the cytoplasm for degradation (Kamijo et al., 1998). It has also been found that wild-type p53 can down-regulate transcription from the *p14^{ARF}* promoter despite that fact that this promoter does not appear to have p53 binding sites. Therefore, like the relationship between p53 and MDM2, the relationship between p53 and p14^{ARF} produces an autoregulatory negative feedback loop (Stott et al., 1998). The participation of p14^{ARF} in specific signalling pathways upstream of p53 still however requires some elucidation.

Another factor that is thought to be involved in the regulation of p53 is a member of the E2F family of transcription factors, E2F-1. The E2F-1 transcription factor is a regulator of both cell cycle progression and apoptosis (Strachan et al., 2001). E2F-1 controls cell cycle transit in part by regulating transcription of genes whose products are involved in DNA synthesis. E2F-1 accomplishes this by binding DNA as a heterodimer with a Dp family member (La Thangue, 1994; Lam et al., 1994). The ability of E2F-1 to regulate transcription is in turn controlled by the retinoblastoma protein (Rb), which inhibits E2F-1 activity by binding to the C-terminal transactivation domain of E2F-1 (Dyson, 1998). Phosphorylation of Rb by cyclin D-dependent kinase is a defining event of G1/S checkpoint progression because it results in the dissociation of Rb from the E2F-1/Dp1 complex thus allowing E2F-1 to activate transcription of target genes. The activation of apoptosis is thought to be unique to E2F-1 among E2F family members and can occur via multiple mechanisms including both p53 dependent and independent pathways. In terms of its association with the p53 pathway, E2F-1 is able to transcriptionaly activate p14^{ARF}, which, as described above, stabilizes p53 (Pierce et al., 1999) by increasing the degradation of MDM2. Interestingly, MDM2 can bind to the C-terminal domain of the E2F-1 protein and modulate E2F-1 transcriptional activity. Another way by which E2F-1 increases the pro-apoptotic function of p53 is by binding to the p53 protein directly resulting in an increase in the half-life of the protein (Kowalik et al., 1998). E2F-1 can also transcriptionally activate the p73 gene, the action of which is discussed below.

Finally, because of its association with perinecrotic tissue in glioblastoma, it is important to mention the hypoxia inducible factor-1 (HIF-1) group of proteins. Following mild hypoxic insult, HIF-1α binds to HIF-1β (to form the complex HIF-1) and genes are activated that are important for cell survival. These include factors such as VEGF, nitric oxide synthase, transferrin, endothelin-1, IGF-2 and many glucose transporters (Zhong et

al., 1999). However, if very high levels of HIF-1α are induced as a result of a large hypoxic insult or in the presence of low level HIF-1β, HIF-1α can bind to p53, increase the half-life of the p53 molecule and promote p53 dependent apoptosis. Phosphorylated HIF-1α is thought to bind to HIF-1β and unphosphorylated HIF-1α is thought to bind to p53. HIF-1α can also prevent MDM2 mediated degradation of p53 (Suzuki et al., 2001). When HIF-1α binds to p53 it can stimulate transcription of Bax and p21 genes and suppresses Bcl-2 transcription (Carmeliet et al., 1998). These findings suggest that HIF-1α plays a vital role in hypoxia induced apoptosis in many systems. HIF-1α dependent induction of p53 has also been implicated in regions of glucose deprivation (Moley & Mueckler., 2000). HIF-1α was initially thought to be stimulated via PI(3)K (phosphatidylinositol 3-kinase) and Akt kinase signalling pathways following hypoxic insult (Zundel et al., 2000). However, recent evidence suggests that activation of the PI(3)K/Akt pathway may be be activated concurrently with HIF-1α and may not be necessary for HIF induction (Arsham et al., 2002; Alvarez-Tejado et al., 2002).

1.4.7. p63 and p73

Most genes occur in families, and until recently p53 was thought to be an exception to this rule. However, two new members of the p53 family have now been identified. Although neither of these genes is examined in this study, it is important that their existence is briefly mentioned. p73 is a putative tumour suppressor with considerable structural homology to p53 and has a 63% similarity in the DNA binding region (Kaghad et al., 1997). Like p53, p73 is able to induce cell cycle arrest by activating p21 and recently it has been shown that p73 is a target of c-abl in response to DNA damaging agents (Davis & Dowdy, 2001). However, p73 does not degrade after MDM2 binding and other p53-like functions have not yet been identified. It was thought that p73 could play a role in the pathogenesis of malignancies in a similar way to p53. However, although p73 is mapped to 1p36, a region frequently deleted in a variety of human cancers, several studies have documented only rare mutations (Tsujimoto et al., 2000; Yokomizo et al., 1999). p63 (also known as p51) more closley resembles p73 than p53 and is also able to induce growth arrest in a similar manner to p53. Although it is also maps to a chromosome frequently deleted in some cancers (3q27-28), like p73, mutations in p63 appear to be rare (Shimada et al., 1999). Findings by Celli et al found that knock out mice for p63 do not develop cancers but have developmental problems, suggesting this p53 analogue may be more important for development than the cellular response to stress (Celli et al., 1999).

1.4.8. Molecular events leading to the onset of necrosis

Unlike apoptosis, cell death has already occurred when the characteristic necrotic morphology is seen to occur. As a result, the short period of time preceding these changes, when molecular changes arise, has been termed 'oncosis' by some researchers (Trump, 1997). However for consistency in this summary, the entire process from onset of the insult until the cells exhibit a necrotic morphology, will be referred to as necrosis. Necrosis has attracted less interest than apoptosis due its status as an uncontrolled and accidental process.

Necrosis often follows a variety of injuries, such as toxins (eg. metabolic inhibitors such as antimycin and ATPases) and ischemia. Because many of these interfere with ATP synthesis, they destroy control of the interior environment of the cells by destroying control at the plasma membrane (Bonventre, 1993). This loss of control usually occurs because the balance between Na+ entry and Na+extrusion is lost.

Alternatively, direct damage to the cell membrane can also result in a necrotic outcome and ATP loss. Cell membrane damage may occur as a result of mechanical damage, modification of membrane lipids (eg. detergents), variations in pore/channel formation (eg complement C5-9) and the influence of ionophores (such as sodium and calcium). Lack of ATP and/or loss of cell membrane integrity means that control of cellular ion content, again resulting from a balance between Na^+ entry and active Na^+ removal is lost. This in turn results in a massive influx of water causing cell swelling and eventual rupture of the cell membrane (Trump et al., 1998). The initiation of a necrotic response can also result in a reduction of the mitochondrial membrane potential. It is thought that the change in mitochondrial membrane transition (MPT) is a result of a combination of Ca^{2+} influx (Bernardi & Petronelli, 1996), cytoskeletal alterations (Evtodienko et al., 1996) and increasing levels of intracellular phospholipases (particularly phospholipase A2) (Lemasters et al., 1999).

1.4.9. Similarities in the regulation of apoptosis and necrosis

Recently, much evidence has come to light suggesting that the definition of apoptosis versus necrosis may not be so clearcut. Many researchers have found overlapping molecules involved in both modalities of cell death. Others have found dead or dying cells in situ exhibiting morphologies common to both processes.

As previously discussed, during necrogenesis a sudden decrease in ATP occurs very rapidly. This is not the case during apoptosis where ATP levels are maintained longer during a 'reversible phase', that is, when the cell is able to revert back to a path of survival (Trump et al., 1997). Indeed, some researchers have suggested that ATP levels can act as a type of switch, determining either an apoptotic or necrotic fate (Eguchi et al., 1997). During the 'reversible phase' the apoptotic cell shrinks implying the loss of ions such as K^+ and Cl^- . Because the necrotic process is ultimately more acute, no such shrinkage occurs. However, the loss of K^+ and Cl^- ions in the apoptotic process is thought to be due to a massive increase in Ca^{2+} and stimulation of Ca^{2+} activated K^+ channels. Interestingly, huge increases in the level of intracellular calcium also plays a role in 'oncosis' the process preceeding death of the cell by necrosis (Trump et al., 1997; Trump & Berezesky., 1998; Clarke, 1998). Movement of intercellular calcium has increasingly been implicated in various aspects of gene transcription and cytoskeletal function (Bootman et al., 2001). These factors suggest that there may be a regulative aspect to necrotic cell death.

This idea has been supported by the identification of a regulatory enzyme upstream of ATP depletion called Poly(ADP-ribose) polymerase (PARP). It is thought PARP can alter the cells fate according to the intensity of an insult such a hypoxia or irradiation. During low level stress, PARP acts as a DNA repair enzyme which is activated by single stranded DNA damage. If the damage is too severe for proper repair of DNA, the enzyme can catalyse the poly(ADP-ribosyl)ation of proteins, including histones. Because NAD is a precurser in this reaction, NAD levels within the cell drop resulting in reduced ATP production (D'Amours et al., 1999). This in turn results in cell death via the oncotic/necrotic process. Because the apoptosis effector Caspase 3 has PARP as its major substrate and cleaves the enzyme as soon as breaks becomes present on the DNA backbone, PARP is thought to be involved in the regulation of both apoptosis and necrosis. Recently, the presence of poly(ADP-ribose)groups within perinecrotic cells in glioblastoma was discovered (Wharton et al., 2000). The involvement of the PARP enzyme in necrogenesis again supports the idea that regulative elements are present.

Further evidence for an element of regulation in necrotic cell death was established in 1995 when Fukunaga-Johnson et al and Kane et al found that the anti-apoptotic protein, Bcl-2 (mechanism of Bcl-2 action described fully in 3.1.5), could inhibit necrosis in erythroleukemia cells and in neurons. It was later shown that Bcl-2 hyperexpression on

the mitochondrial membrane impeded the mitochondrial permeability transition and blocked the release of various proteases released during a necrotic response (Susin et al., 1996). These findings suggest that cellular susceptibility to necrosis in these cells may alter following increases in p53 related proteins such as Bax. In addition, various inhibitors of protein synthesis (which is normally associated with apoptosis) have been shown to be very effective at inhibiting necrosis. This has been shown in both hepatic lesions in rat and in both immature and mature neurons deprived of retrograde support (Torvik & Heding, 1967; Catsicas & Clarke, 1990; Popp et al., 1978).

Intermediate phenotypes possessing both necrotic and apoptotic features have been identified in some systems which also suggests the morphological definitions of the two processes may not be so clear cut. Clarke et al have described 3 types of cell death that occur in neuronal development (Clarke, 1998). The first of these was termed necrosis, another type was termed autophagic cell death which contained large abundant autophagic vacuoles and some membrane blebbing. The third type was named nonlysosomal disintegration and possessed dilation of organelles and a cytoplasmic type of death more characteristic of classic necrosis. Although only one or two apoptotic features are present, the variation between these types of morphology at least suggests variations in the regulatory mechanisms that governs these cells. Sperandio et al have also identified a non-apoptotic, non-necrotic type of cell death characterised by cytoplasmic vacuolation (Sperandio et al., 2000). This death was termed 'parapoptosis' as it utilised some regulatory functions of apoptosis but was functionally and morphologically disimilar.

The implications of a regulative element to necrosis are of particular interest to neurooncologists because of the large amounts of intratumoural necrosis. Cell death within glioblastoma cell populations is thought to occur as a result of a combination of a decrease in metabolites and appropriate GFs, together with a build up of waste products and changes in pH. These factors form gradients which vary in intensity from the centre of the ischaemia to the periphery. Regions containing moderate levels of stress may be prime locations for the appearance of a combination of pro-apoptotic and pro-necrotic cell death signals. It is possible that factors normally associated with an apoptotic response, such as p53, may have the ability alter glioma cell susceptibility to both apoptosis and necrosis.

1.5. The p53 pathway and carcinogenesis

1.5.1. General introduction to cancer and the p53 pathway

When cells acquire mutations that either abolish the function of pro-apoptotic genes (e.g. *P53*) or up-regulate anti-apoptotic genes (eg. *MDM2*), normal cell death responses are not activated and cells can remain alive under conditions that normal cells would find impossible. This in turn can lead to tumour formation depending on the series of mutations that occur in a particular cell type. Theoretically, by identifying specific abnormalities in cancerous cells, therapeutic strategies can be adjusted accordingly. Therefore, intact cell death pathways can be targeted depending on the molecular background of the tumour, rather than using therapies that are unlikely to be effective and may cause unnecessary damage to normal tissue.

Because *P53* has been implicated in the cellular response to stresses such as hypoxia (An et al., 1998; Carmeliet et al., 1998; Chandel et al., 2000; Graeber et al., 1996), nutrient depletion (Moley & Mueckler, 2000) and growth factor withdrawal (Asschert et al., 1998), it may be important for the onset of cell death within glioma cell populations. However, to assess the likelehood of the *P53* gene playing a role in the onset cell death in glioblastoma it is first important to understand the implications of *P53* and *P53* related aberrations in human cancers and also the frequency by which they occur.

1.5.2. Mutations in the *P53* gene

The large number of pathways in which p53 is involved constitutes an explanation for the high frequency of mutations found at the *P53* locus in human tumours. Cells harbouring such mutations are at a selective advantage compared to normal tissue due the impairment of mechanisms activating both cell cycle arrest and apoptosis. As a result, the commonest *P53* mutations are those that add significant malignant potential to the cell (Sigal and Rotter, 2000).

When examining human tumours as a whole, all classes of mutation (deletions, insertions, transitions and transversions) have been found to occur in the *P53* gene. Point mutations, which alter p53 function, cluster in the hydrophobic central region (the DNA binding domain- Figure 1) of the protein (87% in exons 5-8), where base substitutions alter the proteins conformation and/or its function. Although more than 250 codons in the *P53*

gene are potential mutation sites, 25% of all mutations found in human tumours comprise only 5 of these codons (175, 245, 248, 249 and 273) (Greenblatt et al., 1994).

Approximately 30% of glioblastomas contain *P53* mutations. Primary glioblastomas show mutations in approximately 11% of tumours, whereas in secondary tumours this figure is much higher (~67%). Because *P53* mutations occur in glial tumours from grades II- IV it is suggested that the acquisition of *P53* mutations is one of the earliest events in tumours of this type. However, in a study examining the clonal expansion of astrocytic brain tumours, the original tumour biopsies were found to contain variable percentages of *P53* mutant cells compared to wild-type cells (20-75%) (Tada et al., 1996). Therefore, as only a fraction of cells in the low grade tumours harbour *P53* mutations it is unlikely to be 'the' initiation event. However, it is difficult to differentiate tumour and non-tumour cells in some low grade tumours. In addition, in patients with germ-line *P53* mutations, 73% acquire astrocytomas, suggesting a *P53* mutation could be a primary occurrence in the malignant progression of some malignancies. The most frequent alterations found in glioblastomas are GC-AT transversions that occur at CpG sites by deamination of 5' methylcytosine and are considered spontaneous (reviewed in Fulci, Ishii and Van Meir, 1998). There are no brain tumour specific mutations and the three most commonly mutated codons in order of frequency are 273, 248 and 175. In other human tumours codon 248 is most commonly mutated followed by 249 and 175 (Bögler et al., 1995). Whether these data are of any value is uncertain, as no work has been completed indicating a defined role for specific mutants in brain tumourgenesis.

Two classes of *P53* mutant are generally found: mutations within codons directly involved in DNA binding (eg 248W and 273H) and mutations within residues important for the stable folding of the p53 protein (eg 175H). Although these mutations generally result in abnormal proteins that seriously impair downstream function (eg the activation of *P21, MDM2* and *Bax* promoters) of the p53 molecule, they can result in p53 proteins with varying transactivation abilities (Sigal & Rotter, 2000; Saintigny et al., 1999). Many mutant proteins (such as the full length murine *P53* (A to V)) are able to form tetrameric complexes with wild-type p53 proteins which result in complete cessation of downstream transciption in a dominant negative manner. However, although the two DNA binding mutants 273(R toH) and 248(R to W), have completely lost p53 biological activity, they do retain 98% and 86% wild-type p53 conformation respectively and heterooligomers

between these mutants and wild-type p53 are often able to bind DNA. Another common p53 conformational mutant,175(R to H), is not always fully dominant over endogenous wild-type p53. This was shown by the maintenance of wild-type p53 activity when colorectal cancer cells were transfected with a vector containing 175H-p53 DNA (Williams et al., 1994). Some mutants are actually capable of conferring increased tumourigenic potential to the cell, ie. separate than those simply causing attenuation of cell death/growth arrest responses. These type of mutants (such as the murine *P53* mutant 132F) are referred to as gain of function mutants. This gain of function can be achieved through a variety of mechanisms including the blocking of differentiation (Shaulsky et al., 1991), the increasing of metastatic potential (Crook et al., 1992) and the induction of vascularisation (Kieser et al., 1994).

Because p53 plays a role in cell cycle arrest and in DNA repair, p53 mutant isoforms are thought to lead to an increase in the mutation frequency of tumour cells. As is mentioned earlier, wild-type p53 is actively involved in the repair of damaged DNA by inhibiting homologous recombination via the RAD protein family (Buchhop et al., 1997). Mutant p53 proteins allow spontaneous recombination events to occur which can lead to the acquisistion of additional mutations (which may or may not be tumourigenic). Like transactivation ability, different p53 mutants show varying abilties to stimulate spontaneous recombination. 175H and 273P show the highest levels of recombination events, 273H has a moderate effect on recombination and 175G has no effect on spontaneous recombination (Marmorstein et al., 1998). Theoretically, the effects of spontaneous recombination are further exacerbated by the inability of mutant protein to activate p53R2 (a ribonucleoside reductase gene). This would result in a lack of additional dNTPs required to rectify any mistakes made during recombination or DNA damaging events (Tanaka et al., 2000).

1.5.3. Mutations in the CDKN2A locus

Mutations found in other p53 related genes in glioblastoma are relatively rare. In a study looking at the *P21* gene in 81 gliomas including 48 GBMs, no mutations were noted after screening the entire coding region (Jung et al., 1995). In addition, another report found no alterations in P21 in 10 different cell lines (Zhang et al., 1996). Similarly, no alterations in the *Bax* gene have been demonstrated in glioma (Chou et al., 1996).

One well-described exception to this are mutations in the *INK4* locus (*CDKN2A* locus). Because the *INK4* locus is responsible for encoding p16 which inhibits cyclin dependent kinases (CDK4 and CDK6), mutations can lead to dysregulated cell proliferation at the G1 checkpoint due to the hyperphosphorylation of Rb (Hara et al., 1996). *INK4* also encodes the $p14^{ARF}$ protein which regulates levels of nuclear p53. When high levels of p53 are required, $p14^{ARF}$ shifts MDM2 from the nucleus to the nucleolus leading to the stabilization and accumulation the p53 protein (Pomerantz et al., 1998). If the $p14^{ARF}$ protein is not capable of undertaking this function, increasing levels of nuclear MDM2 cause p53 protein levels to drop. This supports the observation that $p14^{ARF}$ is able to induce G1 arrest only in the presence of wild-type P53 (Kamijo et al., 1997). Thus deletion of the *CDKN2A/INK4* locus leads to the alteration of both the p53 and pRB-dependent tumour suppressor pathways (Ivanchuck et al., 2001).

Mutations in the *INK4* locus occur second only to *P53* mutations in human cancers (Ruas & Peters, 1998). Point mutations and small deletions (usually found on exon 2) in the *INK4* locus are relatively common in some cancers, and depending on the position of the mutation, generally result in either conformational changes in the p16 protein or affect p16s ability to bind CDK4. No nonsense mutations have been found in $p14^{ARF}$ mRNA (Koh et al., 1995; Byeon et al., 1998). However, most mutations in the *INK4* locus eliminate the entire coding region for both p16 and $p14^{ARF}$ (reviewed in Ruas & Peters, 1998). Over half of high grade gliomas lack a functional *INK4* locus and most of these are in tumours that do not contain *P53* mutations ie. in primary (de novo) cancers (Jen et al., 1994; Schmidt et al., 1994). Therefore, MDM2 upregulation due to endogenous overexpression /loss of the *INK4* locus in some tumours and the presence of *P53* mutations in other tumours without large homozygous deletions in the INK4 locus, results in p53 pathway disruption in a large percentage of all glioblastomas (Ichimura et al., 2000; Fulci et al., 2000). This implies that the p53 pathway is absolutely critical in cell growth and control in glial cell populations.

Although the p53 system may be be compromised in most glioblastomas, other genes besides $p14^{ARF}$/MDM2 are capable of influencing levels of the p53 protein in wild-type p53 tumours. For example, the proto-oncogene *c-abl* can prevent p53 export to the cytoplasm by MDM2 (Shaul, 2000). In addition, the transcription factor E2F-1 possesses two p53 binding domains and has been shown to be responsible for the accumulation of

the p53 protein (Nip et al., 2000). The relationship between various $p14^{ARF}$ mutants and MDM2 can also vary (see 1.6.4). This means that the *P53* gene may yet play an active role in tumours with a wild-type *P53* gene but with $P14^{ARF}$ abberations. In *P53* mutant tumours, p53-independent regulation of p21 has been demonstrated via an E2F-1/Ras pathway and TNF-α (Gartel et al., 2000). In addition, overexpression of E2F-1 can lead to p53-independent apoptosis (Shu et al., 2000). Increases in intracellular levels of Bax have been associated with p53-independent induction of apoptosis in ovarian cancer cell lines (Strobel et al., 1996). This shows that downstream targets of p53 may still function at some level without wild-type *P53*. In addition, some so-called 'p53 mutants' can actually activate most of their downstream targets, particularly those where the mutation resides outside the DNA binding domain. The p53 system may therefore function at some level in both *P53* mutant and non-mutant tumours. As a result, the p53 system may also be functional to some extent within and around areas of cell death in a large percentage of both primary and secondary glioblastomas. It is possible that tumours harbouring *P53* mutations and those with wild-type *P53* may activate endogenous cell death via separate mechanisms.

1.5.4. p53 related protein expression in glioblastoma

The extensive knowledge of the genetic aberrations found in glioblastoma cell populations suggests that levels of p53 related protein expression (such as Bax, p21 and MDM2) can be accurately predicted, if, for example, the *P53* genotype is known. However, the complexity of p53 related signalling pathways, the influence of some non-p53 related genes and the varying half-lives of molecules in abrogated systems means that this is rarely the case.

Only minute quantities of the p53 protein are found in normal cells, but accumulation of the p53 protein is a feature of the 20-40% of GBMs containing *P53* mutations. This phenomenon is well described in many different types of cancer. This is because the MDM2 protein cannot recognise and bind to mutant forms of the p53 protein and thus fails to label it for degradation by the proteosome (Haupt et al., 1997 ; Anker et al., 1993). However, the correlation between *P53* mutation and positive immunohistochemistry is incomplete, since *P53* gene deletions may not give rise to translatable mRNA and since wild-type p53 may also accumulate (Weller et al., 1998). Therefore, upregulation of the p53 protein in brain tumour biopsy material may indicate the presence of *P53* mutations

but 100% accuracy cannot be obtained. Thus far, no correlation has been found between *P53* status and the levels of apoptosis found in glioblastoma tissue (Ellison et al., 1995; Kalid et al., 1998).

In a study by Krajewski et al, the Bax protein was found to be overexpressed in nearly 100% of the 49 diffuse astrocytoma biopsies examined. In addition, Bax expression increased with tumour grade. This coincided with a drop in the anti-apoptotic proteins Bcl-2, Bcl-X and Mcl-2 (Krajewski et al., 1997). This suggests that the Bcl-2 family may be differentially regulated in association with tumour progression and differentiation. However, study by Strik et al (1999) examined levels of Bcl-2, Bcl-X, Bax and Mcl-1 proteins from first glioblastoma resections and their recurrences and found that levels of anti-apoptotic Bcl-2 increase with tumour grade whereas levels of the pro-apoptotic Bax protein decrease with tumour grade. These contradictory findings therefore suggest that patterns of Bax expression in glioblastoma still require some elucidation. From a therapeutic perspective, Bax has been shown to be an important determinant of chemosensitivity in pediatric glioma cell lines (McPake et al., 1998) and in some glioblastoma cell lines (Weller et al., 1998). In these sudies, wild-type *P53* status was not found to be associated with chemosensitivity (Weller et al., 1998). This suggests that *Bax* may be activated by molecules other than p53 in response to chemotherapeutic agents. This is supported by the above described findings using the chemotherapeutic drug Paclitaxel (1.5.3.) (Strobel et al., 1996). No similar correlation has been found between Bcl-2 family expression and sensitivity to chemoradiotherapy (Strik et al., 1999). Another study examining Bcl-2 family members found that the heat shock binding protein Bag-1 (see 1.4.5.) was expressed in 15 out of 19 glioblastoma biopsies (Roth et al., 2000). *In vitro* work in the same study suggested that interaction of Bag-1 with Bcl-2 may provide a survival advantage to cancer cells in ischaemic/hypoxic tumour cell populations, such as those found in glioblastoma.

Like Bax, p21 expression as assessed immunohistochemically does not reflect the functional status of p53. Khalid et al found that 2 out of 20 p21 positive GBMs whereas 15 out of 26 mutant p53 GBMS were positive for p21 (Khalid et al., 1998). This suggests that the p21 observed in this study is not regulated by p53. However, in addition to the cell cycle arrest function, p21 also has an anti-apoptotic effect susceptible to modulate the p53 apoptotic signal in gliomas. Thus the expression of p21 and absence of p53 could

confer a selective advantage to healthy tumour cells (Gomez-Manzano et al., 1997; Li et al., 1998). How p21 is activated under these circumstances however remains unclear. Whether p21 is activated when cells are subjected to oxidative stress and whether this is governed by a p53 related mechanism also remains unknown.

MDM2 gene amplification occurs in approximately 10% of GBMs as assessed by southern blot analysis (Reifenberger et al., 1993). However, MDM2 immunohisto-chemistry has revealed that more than 50% of primary GBMs contain cells that over express MDM2, although the fraction of immunoreactive cells varies considerably between cases (Biernat et al., 1997). Work using cell lines has shown that MDM2 amplification and over expression occurs only in cells containing wild-type p53 (He et al., 1994). However, Biernat et al found that although MDM2 over expression was most common in primary GBMs (>50%), 10% of secondary GBMs (which most often contain p53 mutations) also showed MDM2 positivity thus suggesting that there may be some overlap between the 2 tumour types. This supports the conclusion by Biernat that the relationship between MDM2 amplification and overexpression is complex, as tumours may show simultanous amplification and overexpression, amplification without over expression, or overexpression without amplification. Therefore, although intrinsic amplification of the MDM2 gene may be solely responsible for MDM2 overexpression in some tumour cells, variations in the *P53* status and $P14^{ARF}$ status also may play a part, resulting in the varied expression patterns seen in both primary and secondary GBMs.

Immunodetection of MDM2 protein expression in tumour biopsies and cell lines often results in the identification of more than one MDM2 isoform. In addition to full length MDM2 (90kDa in mouse and 97kDa in humans), three lower bands (85kDa, 75kDa, 55kDa) are often observed (Olson et al., 1993; Bartel et al., 2001). These three proteins are missing the N-terminus region including the p53 binding domain, and are thought to have arisen due to alternative spicing or leaky scanning ribosomes (Olsen et al., 1993; Bartel et al., 2001). Two other MDM2 isoforms have been detected by Rallapalli and colleagues (1999) and were termed MDMX (80kDa) and MDMX-S (27kDa). The former is thought not be transcriptionally activated by p53 and is thought to have a much weaker affinity for p53 than full length MDM2. The MDMX-S isoform is thought to be transcriptionally activated by p53 and is found in low levels in a variety of mouse and human transformed cell lines.

Another MDM2 isoform that is often observed in cell lines is a 57-60kDa sized protein (Olsen et al., 1993; Zauberman et al., 1995; Blaydes et al., 1997). This 60kDa isoform is able to bind to p53 but is lacking the C-terminus ring-finger domain after residue 361. The C-terminus ring finger domain contains the cysteine residue that is vital for ubiquitin-mediated p53 degradation in the cytosol. It is thought therefore that the 60kDa isoform can bind p53 and prevent p53 transcriptional activity but is unable to mark it for degradation (Honda et al., 1997). This 60kDa MDM2 isoform is thought to arise via two different pathways, where both are truncated at the same residue, 361. The first of these is produced during the apoptotic response by Caspase 3 cleavage of the full length MDM2 97kDa protein (Chen et al., 1997). The Caspase 3 substrate poly(ADP-ribose) polymerase (PARP) is also cleaved in cells producing this 60kDa MDM2 isoform (Rosen & Casciola-Rosen, 1997). During the apoptotic response, cleavage of the entire cellular population of MDM2 occurs, completely inhibiting MDM2-mediated p53 turnover, thus promoting cell killing by p53 (Pochampally et al., 1998). Because this 60kDa MDM2 isoform is rapidly degraded in cells undergoing apoptosis, it is thought there is insufficient to prevent p53-mediated transactivation of pro-apoptotic downstream target molecules (Pochampally et al., 1998). The second 60kDa isoform is also thought to arise by protease cleavage of full length MDM2. However, Caspase 3 is not thought to be responsible since caspase 3 substrate PARP is not cleaved (Pochampally et al., 1999). This 60kDa MDM2 isoform is thought to be produced in non-apoptotic tumour cells and is prevalent in a subset of breast and lung tumours where it is found in higher levels than the full length MDM2 molecule (Bueso-Ramos et al., 1996; Gorgoulis et al., 1996). It has been suggested that this 60kDa isoform may function as dominant negative regulator by competing with full-length MDM2 for p53 binding (Pochampally et al., 1998).

1.5.5. Novel therapeutic strategies designed to target apoptotic pathways

Because of the wealth of current research in this area it is impossible to mention every therapy or prospective therapy currently being researched/ developed in this vast field. Switching on the production of, and/or introducing pro-apoptotic proteins to glioblastoma cells has shown mixed results. This is mainly because of the difficulties of tumour cell selectivity and methods of delivery *in vivo*.

The most obvious choice for a novel therapeutic agent was initially p53 itself, as it provided a mode of activation of so many pro-cell cycle arrest and apoptotic pathways.

Many *in vitro* studies have shown the benefits of using the p53 pathway as a target for apoptosis inducing therapies. The introduction of wild-type *P53* expessing plasmids into tumour cells can induce over-expression of recombinant wild-type p53 protein and drive cells into either growth arrest or apoptosis. This has been shown in many cancer types with widely diverse genetic backgrounds including glioma (Yonish-Rouach et al., 1991; Mercer et al., 1990; Merzak et al., 1994; Van Meir et al., 1995; Gomez-Manzano et al., 1996). In addition, further experiments have demonstrated that the transfer of exogenous *P53* alone or in combination with radio or chemotherapy improves the survival of animals bearing brain tumours (Badie et al., 1995; Kock et al., 1996; Lang et al., 1998). However, in addition to the difficulties involved in successfully targeting and tranducing *in vivo* tumour cells, a combination of other factors suggests that random introduction of *P53* gene sequence into patients suffering from GBMs may be problematic. Firstly, as most *in vitro* and *in vivo* experiments have shown, p53 most often activates *P21* and cell cycle arrest in brain tumour cell lines (Van Meir et al., 1995; Gomez-Manzano et al., 1997). This may actually result in an increase in relative resistance to therapy in some tumours (Gomez-Manzano et al., 1997; Li et al., 1998). Secondly, some human brain tumours possess mutant *P53* isoforms which possess 'gain-of-function mutations' which would nullify any exogenous wild-type p53 activity (Trepel et al., 1998; Sigal et al., 2000). And thirdly, some wild-type *P53* cell lines are resistant to the introduction of additional wild-type p53 and/or other combined therapies (Komata et al., 2000; Badie et al., 1999).

Gene transfer of *Bax* also induces apoptosis and can enhance the effectiveness of radiotherapy and some chemotherapeutic drugs *in vitro* (Craperi et al., 1999; Strobel et al., 1996; Arafat et al., 2000). Although it has not been tested in glioma, tumours with high levels of endogenous Bax are generally more responsive to various chemotherapeutic reagents (McPake et al., 1998). Antisense Bcl-2 therapy has also shown promise *in vitro*. It is thought that the Bcl-2/Bax balance can be tipped in favour of Bax (the pro-apoptotic family member) when the Bcl-2 antisense oligonuceotide G-3139 (Genta pharmaceuticals) is introduced to tumour cells. The G-3139 oligonucleotide prevents Bcl-2 mRNA being translated into protein. Clinical trial data using this technique on patients with malignant melanomas and in non-hodgkins lymphoma (with the chemotherapeutic agent dacarbazine) has shown some positive results (Nicholson, 2000; Waters et al., 2000). However, other Bcl-2 family members will be the dominant anti-apoptotic effector in some types of cancer and only a 14-45% patient impovement (little to total regression)

has been noted. At this stage, probably the most promising pro-apoptotic therapies involve the cell death receptor super family. CD95 (Fas) ligand and the TRAIL (Apo2 ligand) can trigger apoptosis in cells that possess the CD95 receptor and the KILLER/DR5 receptor respectively (Waring and Müllbacher, 1999; Wu et al., 1997). Some studies have shown that, like Bax, the role of the TNF super family in p53 mediated apoptosis appears to be cell type and signal specific (Malkin, 2001; Takimoto & El Deiry, 2000). However, recent evidence has shown that approximately 80% of human cancer cell lines inluding glioma cell lines are sensitive to TRAIL, whereas most normal tissue is relatively resistant (Zhang et al., 1999; Van Valen et al., 2000; Hao et al., 2001). No testing has yet has been done on humans although experiments using recombinant TRAIL on human xenografts (including glioma tissue) in SCID mice have shown very promising results (Ashkenazi et al., 1999; Walczak et al., 1999; Ashkenazi et al., 2000).

1.5.6. Summary of the p53 pathway and glioblastoma

It is therefore clear that knowledge of the molecular aberrations present in tumour cells is vital when trying to identify genes/proteins that may responsible for areas of cell death/necrosis in GBM. It is possible that tumours harbouring *P53* mutations may activate cell death pathways different to those activated in wild-type *P53* tumours. In contrast, it is also possible that due to the presence of p53 pathway abnormalities in a large percentage of GBMs, a universal mechanism may be employed to activate cell death. Knowledge of the pathways that activate endogenous cell death within these tumours would therefore be of considerable importance when devising treatment strategies for individual patients with glioblastoma. Further ellucidation of the role of p53 and p53 related proteins around such areas, is therefore required. Unfortunately, it is difficult to use human glioblastoma biopsy material for such studies. Genetic analysis, such as those described above, using biopsy tissue, can provide some answers as to likely intact pathways in glioblastoma. In addition, studies examining regions of cell death in biopsy tissue for changes protein/mRNA expression and cellular morphology may also answer some questions as to likely candidates for cell death activation. However, tumour biopsy material does not allow the evolution of such areas to be assessed. This material provides a 'snap-shot' of a particular cell population at a specific point in time. Glioblastoma cell populations need to be modelled over time to examine gene and protein expression as areas of cell death develop.

1.6. The brain tumour spheroid system

1.6.1. Introduction to *in vitro* cell culture systems

Since the introduction of cell culture techniques in 1907 using nerve fibre outgrowths, *in vitro* experimentation using both primary cultures and cell lines is now common place in many biological laboratories. Using these techniques, the effects of drugs, growth factors and hormones can be studied in relation to the physiology, morphology and pathology of individual cell populations. These experiments can be performed without the confounding influences of the immune system and the complexity of the *in vivo* scenario. Two main types of cell culture exist, primary culture using ex vivo tissue and cell lines.

1.6.2. Primary culture techniques

Cells prepared directly from the tissues of an organism are called primary cultures. In most cases, cells primary cultures can be removed from the culture dish and used to form a large number of secondary cultures; they may be repeatedly subcultured in this way for weeks or even months in some cases. Glioblastoma cultures of this nature have been thought to be useful as they retain the heterogeneity present *in vivo* and are useful for examining growth factors/growth factor receptors, invasion and susceptibility to the toxicity of prospective anti-cancer agents (Bouterfa et al., 2000; Engebraaten et al., 1993; Narla et al., 1998). They are also useful for establishing and preserving xenograft tissue before insertion into immunosuppressed mice (Sasaki et al., 2001).

Although cultures of non-cancerous cells are generally difficult to preserve, as their life span is often limited to a certain number of generations, highly malignant glioblastoma cells can survive much longer. However, monolayer cultures derived from brain tumour biopsies generally lose their heterogeneity/*in vivo* qualities quickly due to the selective pressure of the medium. Experiments performed while primary tumour cell populations are at their most viable may be misleading as the tissues are going through a transition period involving changes in growth patterns and the death of some tumour cell populations less suited to the *in vitro* scenario. The best example of this is the presence of normal tissue being admixed with the malignant tissue. This can lead to very confusing results, for example, if the specimens are being used for drug efficacy assays measuring cell death/ cell cycle control. Normal tissue does not survive as long as cancerous tissue *in vitro* thus cell death assays may pick up dying normal cells rather than tumour cells. If glioma cell populations explanted from patients are left to grow for up to 40-50 passages,

they can develop (in approximately 10% of cases) into more homogenous cell populations which are more resilient and thus are often more malignant. These cells are termed glioma cell lines (Ishii et al., 1999; Matsumura et al., 1994).

Attempts to encourage 3-dimentional growth of primary glioblastoma tissues have had mixed results. One advantage of explanting solid tumour tissue in fragments is that cell and tissue components, which run the risk of disappearing in monolayer, have a chance to survive for prolonged periods in organotypic cultures. Many studies have shown that capillaries, macrophages and areas of connective tissue can survive throughout a culture period of up to 70days (Bjerkvig et al., 1990). Monolayer cultures derived from both primary cultures and cell lines have a tendency to change their chromosome number and DNA content over time. In contrast, studies examining 3-dimentional spheroid explants do not allow for the selection of specific cellular subpopulations and show the same DNA profiles as obtained from the original biopsy (Shapiro & Shapiro, 1985). This is most likely due to the retention of original cell-cell contacts present *in vivo* thus preventing the cells from exposure to alien environmental situations. Studies by Janka et al also found that DNA amplifications found in the original glioblastoma tissue by reverse chromosome imprinting (RCI) retained the same amplification domains using tumour fragment spheroids (Janka et al., 1996). All amplifications which were detected in the biopsy material were lost by passage 5 using monolayer cultures.

Spheroid fragments derived from biopsy material have been useful for various modes of research. These revolve centrally around assessing cell proliferative, migratory and invasive capacities of human primary brain tumour spheroids when exposed to various drug therapies and growth factors. For example, Engebraaten et al found that the addition of EGF could increase tumour volume and invasive capacity in primary spheroids derived from 10 out of 13 GBMs examined (Engebraaten et al., 1993). In addition, Bouterfa et al found that retinoids could inhibit glioma cell proliferation and migration in primary spheroid cultures and also that migration was inhibited in the presense of high concentrations of a drug (Lovastatin) that inhibits beta-hydroxy-beta-methylglutary CoA reductase (Bouterfa et al., 2000a; Bouterfa et al., 2000b). Therefore, although primary monolayer cultures are useful when testing various substances on cells, using this ex-vivo material, cell-cell interactions and protein expression (particularly extracellular matrix proteins) can be examined in a model that more acurately reflects the *in vivo* situation.

Disadvantages of using tumour fragment explants revolve mainly around the growth kinetics of the tumour cell populations within the fragments. Unlike the *in vivo* scenario where the tumour cell mass has layers of rapidly dividing cells increasing the size and volume of the tumour, glioblastoma fragments do not generally increase or decrease in size under normal culture conditions. Flow cytometric analyses of BrdU labelled cells revealed that approximately 10% of the cells in spheroids derived from 8 tumour biopsies were positive (Bjerkvig et al., 1990). This suggests that a significant level of cell loss accompanies this proliferation. Therefore, although the heterogeniety of these tumours is somewhat more preserved than in monolayer culture, the lack of expansive growth means that the onset of necrotic cell death, as seen *in vivo* cannot be studied in normal culture conditions ie. without adding various growth factors and artificial growth enhancers.

1.6.3. Glioma cell lines

By far the most popular way of examining the behaviour of tumour cells *in vitro* is by using established cell lines. Glioblastoma cell lines have been used by many researchers in various fields thus providing a useful database on information such as genetic background and growth kinetics of cell lines. Most of the commonly used cell lines have retained their genetic stability over many generations, in terms of known oncogenes and antioncogenes. Unfortunately, established glioma cell lines often lose many of their *in vivo* characteristics. For example, a reduction in EGFR expression, which is abnormally upregulated in de novo tumours (see 1.2.5.), and ATM (ataxia telangiectasia mutated) expression (see 1.3.4.), which is involved in the cellular response to DNA damage (Bilzer et al., 1991; Tribius et al., 2001). Dedifferentiation also often occurs, where all of the cells take on a bipolar fusiform appearance with little or no expression of GFAP (Franks & Burrow, 1986; Bilzer et al., 1991b). Although many cells do adopt these characteristics *in vivo*, thus providing some validity to this technique, highly heterogeneous tumours (such as GBMs) *in vivo* also contain tumour cell populations with more differentiated morphologies and high levels of GFAP expression

1.6.4. Genetics of glial tumour cell lines

Many studies have examined glioblastoma cell lines in order to categorise their genetic defects to compare with similar abnormalities found *in vivo* (see1.2.6). In terms of cell death regulatory mechanisms, the most informative of these was performed by Ishii et al in 1999 examining the frequent co-alterations of *p53*, *p16*, *p14*^{ARF} and *PTEN* tumour

suppressor genes in 34 glioblastoma cell lines. Of these 34 four cell lines, over 75% (26) contained *P53* mutations. This figure is much higher than found *in vivo* where the figure is around 25% (Ohgaki et al., 1995). What is suprising is that the cell lines examined in this study were all thought to be derived from de novo tumours where *P53* mutations are rare. However, this can partly be explained by the suggestion that some low grade precursor lesions may have escaped detection in some secondary tumours. In addition, cells with mutated *P53* have a survival advantage *in vitro*. Thus if a small number of cells within a highly heterogeneous cell population contain *P53* mutations, these will survive the lengthy selection process many generations after the initial plating of the biopsy material. Only about 10% of GBMs will generate permanent cell lines when put in culture in standard medium (Ishii et al., 1999). Alternatively, *P53* mutations could arise in culture, but this has been shown to be an uncommon event (Anker et al., 1995; Tada et al., 1996).

$P14^{ARF}$ function was lost in 21 out of the 34 glioma cell lines examined in the above study due to homologous deletions in the gene. This loss of $p14^{ARF}$ expression is expected to lead to increased cellular MDM2 levels and augmented p53 degradation (see 1.5.3). Because 26 of the 35 cell lines had *P53* mutations and 6 cell lines that had wild-type *P53* but had $p14^{ARF}$ loss, nearly 95% of the cell lines examined had an altered p53 pathway. However, there are 3 main reasons why mutations in these 2 genes are unlikely to result in complete cessation of the p53 pathway response in these cell lines. Firstly, as was mentioned earlier (1.5.2), different *P53* mutants result in different proteins with varying transactivation abilities. Secondly, different $p14^{ARF}$ mutants vary in their ability to inhibit intracellular MDM2 levels. For example, changes in exon 2 of the *INK4* locus do not affect the ability of $p14^{ARF}$ to induce cell cycle arrest (Ruas & Peters., 1998). Thirdly, recent research examining E2F-1 mediated apoptotic pathways in human lung carcinogenesis has brought to light evidence suggesting that the model of p14ARF/p53 interaction is a complex network rather than a simple linear pathway (Nicholson et al., 2001).

The finding that 15 (44%) of the 34 cell lines with $p14^{ARF}$ mutations also contained p53 mutations further supports this theory. Although this phenomena has only been observed in cell lines, if $p14^{ARF}$ loss occurs first (which is most likely as all the cell lines were thought to be derived from de novo tumours), the resulting reduction in wild-type p53 levels were unlikely to be sufficient to alleviate selection for a *P53* mutation during the

initial plating phase (Ishii et al., 1999). Therefore, in GBMs and cell lines containing wild-type *P53* but null $p14^{ARF}$, wild-type *P53* may still play an important role in mediating the cell death and cell cycle arrest responses in these cells.

Three of the most commonly used cell lines in experimental glioma biology are the cell lines U87, U373 and A172. These 3 cell lines are all derived from malignant gliomas and exhibit features similar to glioblastoma when implanted into SCID mice. They possess different *P53* genotypes and have often been used separately or together to investigate the effects of various anticancer therapies and other stimuli on cell death (Hirose et al., 2001; Yee et al., 2001; Komata et al., 2000; Badie et al., 1999). U87 and A172 cell lines possess a wild-type *P53* genotype and U373 cell line possesses a mutant *P53* genotype (Ishii et al., 1999). U87 and A172 both possess mutations in the *CDKN2A* locus resulting in deletions in both *p16* and $p14^{ARF}$ genes (Ishii et al., 1999). U373 is wild-type for these genes according to most studies. Confusingly, identical names of cell lines used in different laboratories (particularly when using U87 and U373 cell lines) have displayed different genetic alterations. This means that when using these cell lines, further genetic characterisation is required. Another less well-known astrocytic tumour cell line is MOG-G-CCM. MOG-G-CCM is derived from an anaplastic astrocytoma and nothing is currently known about the status of any apoptosis- or cell cycle-related genes.

1.6.5. Monolayer and suspension culture using cell lines

Monolayer and suspension culture is by far the most popular way of growing and experimenting with cell lines including those mentioned above. These cultures are of great value when assessing detailed cell function and to study regulation of apoptosis. An example of the latter is the use of *P53* gene transfer to examine the effect of excess levels of wild-type p53 protein on the life span of glioma cells possessing different *P53* backgrounds (Komata et al., 2000; Kock., 1996). Other researchers have used cell lines transfected with recombinant adenovirus *P53* to assess the effects of combined radiation therapy and various chemotherapeutic drugs on levels of downstream target proteins such as Bax and p21 (Badie et al., 1995; Kock et al., 1996; Lang et al., 1998). Artificial induction of sense and nonsense RNA encoding for many other proteins associated with apoptosis have also been investigated in this way (Naumann & Weller, 1998; Gomez-Manzano et al., 1999). Monolayer cultures are suitable for these experiments because of their homogeneity and ease of use.

The main problem when using monolayer systems is that they do not reconstruct the cellular microenvironments present within a tumour cell mass and there are no simulated nutrient gradients. In addition, monolayer cultures derived from cell lines represent only one type of cell in a specific level of differentiation, which is very different than the vivo situation and most primary cultures. Most importantly for this research, they do not model necrosis.

1.6.6. Spheroid culture derived from cell lines

By changing the culture conditions, many permanent cell lines can be grown as three-dimensional spheroid cultures as well as monolayer cultures. The major advantage of spherical cultures derived from cell lines is their well-defined geometry with a reproducible concentric arrangement of different cell populations (Sutherland et al. 1981). This means that multicellular spheroid cultures are characterised by the emergence of cellular heterogeneity which is an inherent property of most solid tumours. In tumours *in vivo*, such heterogeneous cell populations often show a chaotic and unpredictable distribution pattern, whereas the diverse properties of cells in spheroids are clearly related to their radial position (Mueller-Klieser, 2000). In addition, unlike spheroids derived from primary cultures, spheroids derived from cell lines grow larger and from areas of central cell death that are phenotypically similar to those seen in glioblastoma *in vivo* (Figure 2). To investigate the pathogenesis of endogenous cell death in glioma, a model capable of forming geographically distinct areas of necrosis, similar to those found *in vivo* was vital.

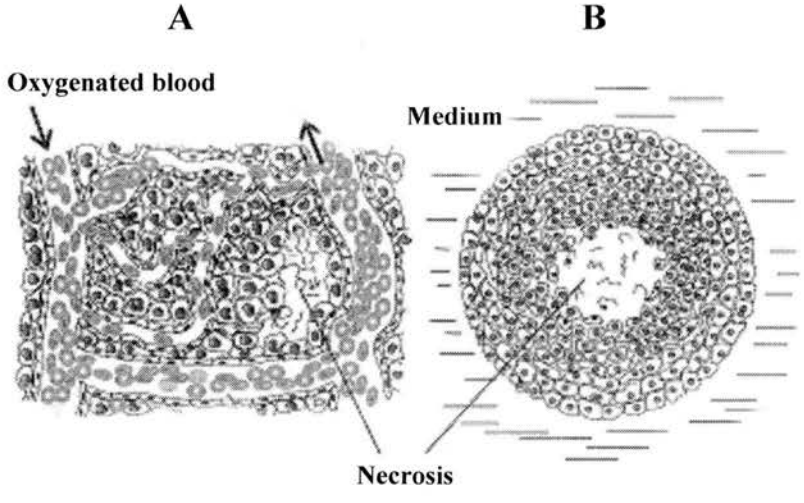

Figure 2. Diagram of intratumoural necrosis versus intraspheroidal necrosis. A, *in vivo* tumour tissue containing necrosis and B, *in vitro* 3-dimentional spheroid containing

necrosis. The medium in B acts as the 'blood-supply' where tissue distinct from this supply necroses at a particular spheroid size. Diagram from Mueller-Klieser, 2000.

Multicellular spheroids derived from cell lines are made by agitating a tumour cell suspension to prevent the cells adhering to a surface, such as in monolayer culture. This is usually done using the spinner flask technique although roller bottles and tubes can be used. Spherical aggregates of tumour cells form spontaneously and reach diameters of approximately 100-200μm at the end of the first week in normal growth medium (Mueller-Klieser, 1987; Lund-Johansen et al., 1992). There are variations in spheroid formation abilities between cell lines. In some cases, such as the U87 glioblastoma cell line, spheroids form spontaneously in monolayer culture and detach at a certain size (Deisboeck et al., 2001). Other cell lines, such as the ovarian carcinoma cell line A2780, will not form spheroid aggregates in either monolayer or using the spinner flask technique (Rainaldi et al., 1999). When spheroids do form in culture, they can be removed from the spinner flask environment and examined immunohistchemically (after being fixed and embedded in paraffin or frozen) or can be placed in another medium for further analysis e.g. to examine invasive/migratory activity. Collagen matrices are commonly used for the latter (Tamaki et al., 1997; Bell et al., 1999).

Although there is considerable variation between tumour types, multicellular spheroids derived from established cell lines exhibit many features similar to tumours *in vivo*. Five of the most well described features include spatially distinct areas of differentiation, proliferation and invasion, the deposition of extracellular matrix molecules and differences in the patterns of growth factor expression.

In terms of differentiation, tumour specific patterns are often observed within the tumour cell mass such as neural rosette formation in teratocarcinoma spheroids (derived from the cell line PA-1/NR) and the generation of myotube-like, multinucleated giant cells in the central regions of large, non-necrotic spheroids made from human rhabdomyosarcoma cells (A673 cell line) (Kawata et al., 1991; Karbach et al., 1992). Cells within tumour spheroids that exhibit increased differentiation are generally found within a quiescent cell population situated in a concentric arrangement around the spheroid centre (Mueller-Klieser, 2000). These observations are important as they suggest that spheroids derived

from cloned cell populations are capable of re-differentiating into cells more closely resembling the tumours from which they originated.

Growth factor expression in spheroid cultures can also mimic the *in vivo* situtation. A series of experiments performed by Sutherland et al (1988), showed that using a squamous cell carcinoma cell line A431, highly differentiated cells found in spheroids were characterised by a three fold increase in the transcription of TGF-α as well as increased heme-oxygenase expression compared to monolayer cultures (Knuechel et al., 1990; Laderoute et al., 1992; Murphy et al., 1993). In addition, wild-type EGFR expression was reduced in these cells in spheroid culture compared to monolayer and addition of EGF stimulated growth in spheroid cultures but not in monolayer (Mansbridge et al., 1992; Laderoute et al., 1992b). All of these results are thought to mirror findings within squamous cell carcinomas *in vivo*. These findings are likely to be tumour type specific, as studies by Ness et al (1994), using 5 glioma cell lines (D-37MG, D-54MG, D-263MG, GaMG and U-251-MG) found increases in EGFR and TGF-α expression by northern blot analysis in spheroids as compared to monolayer cultures. These again refect the expression patterns of these growth factors/growth factor receptors in gliomas *in vivo*. In addition, other studies using glioma cell lines (rat C6 glioma cells) and a colon carcinoma cell line (HT29) have shown that angiogenic factors such as VEGF are induced by 3-dimentional growth (Acker et al., 1990; Schweiki et al., 1995; Waleh et al., 1995). These are normally exclusively associated with areas of cell death *in vivo* and are not found in monolayer cultures under normal culture conditions.

In vivo, it is vital that normal cells form adhesions to the substratum in order to exit from G_0 and proliferate (Donaldson et al., 2000; Fuchs et al., 1997). Many cancer cells do not require such adhesion and grow well attached to plastic or in suspension, which are artificial states for the growth and proliferation of tumour cells. The development of a 3-dimensional culture model allows tumour cells to form aggregates and secrete similar levels of extracellular matrix molecules as those found *in vivo*. Varying levels of ECM molecules may alter the tumour cells susceptibility to divide, invade and metastasise. The deposition of extracellular matrix molecules such as fibronectin, collagens I, II and III have been observed within spheroids derived from squamous cell carcinoma (Knuechel et al., 1990). Waleh et al (1994) found that integrin subunits α6, β1 and β4 were significantly reduced in spheroids derived from the A431 cell line as opposed to

monolayer cultures. This was proven at both the protein and mRNA level. These results together with data using glioblastoma cell lines and the colorectal cancer cell lines HRT-18 and CX-2, found that spheroids mimic the pattern of integrin expression found *in vivo* (Paulus et al., 1994; Hauptmann et al., 1995). These findings indicate that cell-cell contact and microenvironment regulate expression and distribution of a subset of integrin molecules. This was found not to occur in monolayer culture using the same cell lines. More recently, the cell adhesion molecules (CAMs) CD44, ICAM-1 and LFA-3 have been found to be implicated in the very early stages of tumour formation using 6 day old spheroid cultures derived from a colon cancer cell line (HT29) and a squamous epidermal cancer cell line (A431) (Rainaldi et al., 1999). In addition, Byers et al (1995) have shown that intact E-Cahedrin (another cell adhesion molecule) expression and proper linkage of this molecule to the cytoskeleton is an essential factor for strong cell adhesion in a 3-dimentional model of breast and colon carcinoma.

1.6.7. Invasion and migration studies using multicellular spheroids

Migratory and invasive characteristics of tumour cells have been examined at length using the multicellular spheroid model. When spheroids (of any size) are embedded in a collagen matrix, cells on the spheroid periphery invade the surrounding matrix (Tamaki et al., 1997). The separation of the invading cells from the tumour cell mass allows them to be assessed as an independent cell population. These cells can be examined in terms of their protein expression in order to identify potential targets to inhibit metastatic growth. For example, EGFR amplification *in vivo* has been shown to promote glioblastoma cell infiltration *in vitro* (Humphrey et al., 1991). Recent evidence has shown that tryphostin A25 (a specific EGFR-TK inhibitor) can inhibit EGFR activity significantly thus reducing the invasive capacity of the invading cell population stemming from implanted glioma spheroids (Penar et al., 1997). A COX-2 inhibitor (NS-398) has also been tested on glioma spheroid cultures (using U87 and U251 cell lines) and a significant reduction in tumour cell migration was observed (Joki et al., 2000). Various current therapeutic strategies have also been tested on the invading cell population using the spheroid system. The anticancer drug Paclitaxel (Taxol) was recently tested on glioma spheroids (derived from cell lines GaMG and D-54MG) and showed a dose dependent decrease in the invasive capacity of the migrating cell population (Terzis et al., 1997). The dose responses of irradiation, BCNU and dexamethasone have also been tested on invading cell

populations derived from glioblastoma spheroids (derived from cell lines C6, U251, U373 and A172) with differing outcomes (Bauman et al., 1999).

The use of glioblastoma derived spheroids in collagen matrices has also provided insight into the importance of extracellular matrix proteins in tumour cell invasion. Using the human glioblastoma cell lines SNB19, U251, UWR1 and UWR2, the invasive capacity of the cells was increased by adding laminin, collagens type I and IV, fibronectin and hylauric acid to the embedding matrices (Chintala et al., 1996). To the contrary, rat C6 astrocytoma invasion was not effected by adding these proteins to the matrix (Tamaki et al.,1997).

Another method of testing both invasion and extracellular matrix molecules is using the tumour confrontation model. Confrontation models involve taking two separate types of tissue and setting them apart in a chamber within a matrix containing a basement membrane component (collagens, laminins and proteoglycans) and matrix degdrading enzyme/their inhibitors and growth factors. A tumour cell aggregate is usually placed in the gel together with a type of tissue attractant that actively encourages tumour cell migration in that direction. Specific molecules can then be isolated for their pro-/anti-invasive properties and various inhibitors and agonists can be tested to reduce that invasion. Neuro-oncological experimentation using this technique started in 1986 when Bjerkvig et al set a up simple system analysing the mechanism of invasion and subsequent death of normal brain using normal fetal rat brain aggregates and tumour cells derived from fetal BD IX rats. More complex experiments have since been set up examining the properties of anti-invasive drugs. Tonn et al in 1999 found that matrix-metalloproteinase inhibitors (MMPI) could inhibit tumour cell migration towards Fetal rat brain aggregates. Fetal rat brain aggregates produce specific growth factors such as EGF that encourage monodirectional growth. The reduction in invasion can be then be quantitatively assessed in response to varying MMPI concentrations.

1.6.8. The spheroid model and proliferation

Beyond a certain size (usually between 100-300μm), a viable rim of cells form consisting of proliferating cells on the spheroid periphery and quiescent, yet intact and viable cells nearer the centre. The thickness of the proliferative layer can vary between cell lines and can be measured after labelling with BrDU (encorporated into cells during S-phase) or the

Ki67 antibody (labels all cycling cells). The concentric arrangement of the proliferating cell populations within spheroids clearly mimics the initial avascular stages of solid tumours *in vivo* and/or intercapillary tumour microregions with high proliferative activity close to the capillaries. The medium surrounding the spheroid cultures acts as the 'blood supply' (Mueller-Klieser, 2000). The behaviour/size of the proliferating cell population can therefore be studied in relation to the genetics of the cell line used (Kunz-Schughart et al, 1996) or with the addition of various additives to the medium. The latter has been achieved using commonly used chemotherapeutic drugs such as paclitaxel and novel therapeutic drugs such a essential fatty acids, folate antagonists and Protein kinase C inhibitors (Bell et al., 1999; Terzis et al., 1997; Sommers & Alfieri, 1998).

1.6.9. Spheroid culture and cell death

Probably the least studied aspect of tumour spheroid biology are the regions of central cell death. It has generally been accepted that the central regions of most large tumour spheroids derived from cell lines consist of necrotic tissue. However, considering that metabolic gradients form across the spheroid radius, and that apoptosis has been associated with sub-lethal stress, it is suprising that little has been mentioned of apoptosis and the pathways that activate apoptosis in these systems. Because of the apparent similarity of tumour spheroid growth and tumour growth *in vivo*, the spheroid model could potentially be very useful in the identification of the control mechanisms that initiate these cell death events.

The precise cause of the central regions of cell death in spheroids remains undefined. Several investigators have tried to link development of central cell death and the adjacent region of cell senesence in the spheroid system to deficiencies in energy-related metabolites. For some spheroid types such as WiDr human colon adenocarcinoma and tumourigenic Rat-T1 embryo fibroblasts, a coincidence of emergence of cell death and hypoxia during growth has been documented with the thickness of the viable rim reflecting oxygen availability (Kunz-Schughart et al, 1996). Interestingly, in the same study, 'pseudo-normal' immortalised Rat 1 fibroblasts aggregates in the same study showed no decrease in pO_2 levels toward the centre of the spheroids at the same size although areas of cell death were present. This suggests that not only do different cell types possess different metabolic requirements, but spheroids may become centrally depleted via different insults. These findings support the theoretical considerations by

Groebe and Mueller-Kleiser (1996) suggesting that a single limiting factor such as oxygen depletion or lack of growth factors might explain the development of necrosis. The single limiting factor may be different in spheroids derived from different cell lines in various types of medium. However, other research in this field has shown that cell death in multicellular spheroids could be a multifactoral event affected by lack of oxygen/nutrients/GFs, accumulation of waste products and low pH as discussed by Acker and colleagues (Acker et al., 1987).

The modality by which the cells die within central regions in tumour spheroids also remains undefined. Most studies report that inner spheroid regions may adapt their metabolism to environmental stress thus maintaining intracellular homeostasis until shortly before the onset of a wave of necrotic cell death. This is reflected in the steady state levels of glucose, lactate and energy rich phosphates (including ATP) across the radius of EMT-6 mouse spheroids (Bredel-Geissler et al., 1992; Teutsch et al., 1995; Walenta et al., 1990). Reduced numbers of mitochondria towards the spheroid centre support this theory. To the contrary, several reports suggest that in some spheroid types apoptotic cell death preceeds the onset of necrosis. In V79 (hamster lung) spheroids, apoptotic cells are dispersed singular events in small spheroids. These accumulate with increasing frequency in the spheroid centre as spheroid growth progresses and eventually merge together to form a central area of cell destruction which morphologically resembles necrosis (Mueller-Kliesser, 1997). In addition, rat rhabdomyosarcoma spheroids also exhibit an accumuation of apoptosis in the spheroid centre which subsequently changes into necrotic morphology possessing an element of structural disintegration (Mueller-Kliesser, 1997). Interestingly, the latter study also demonstrated a suppression of cell death by spheroid-mediated differentiation. Thus far, no studies have examined the means by which cells die within central regions of glioblastoma spheroids.

From a mechanistic stand point, very little research has been completed into the specific death pathways employed by tumour cells subjected to increasing levels of stress around and within spheroid central regions. This has been mostly due to the assumption that these cells die by necrosis and thus do not activate regulative pathways. This theory has previously been applied to glioblastoma tumour cell populations because areas of necrosis are observed *in vivo* and in the centre of glioblastoma spheroid cultures at a particular time point once the threshold for the onset of cell death has passed. However, the above

research using various cell lines suggests that apoptosis may preceed the onset of necrosis and thus regulatory pathways may exist. The few studies examining the expression patterns of cell death/cell cycle arrest related genes in tumour spheroid cultures are included below.

The p53 dependent-CDK inhibitor p21 has been implicated in the regulation of G1-phase arrest in inner-spheroid zones using MR1 (ras/myc transfected rat embryo fibroblasts)and MLEC10 (immortalised normal mouse liver) cells (LaRue et al., 1998; Lee et al., 1999). In the latter study using the MLEC10 cell line, the cells grown as spheroids exhibited a 75% decrease in viable cell number without any association between p53 and apoptosis. A study using V79 immortalised hamster lung cells has shown that there are significant increases in the potent antioxidant glutathione associated with the accumulation of centrally located increases in apoptotic index (Romero et al., 1997). Glutathione has previously been shown to inhibit p53 mediated apoptosis in various human cell lines (Lee et al., 2001). Although these findings imply that p53 may not be involved in intraspheroidal cell death in these cell lines, there are considerable variations in the response of different cell types to different types of cell stress. It is possible that using glioblastoma cells, which possess very different genotypic alterations compared to the above mentioned immortalised normal cell lines, p53 or p53 related genes may play a role in the onset of central cell death in multicellular spheroids.

In summary, glioblastoma biopsy material does not allow the pathogenesis of endogenous cell death to be studied. Large areas of pseudopallisading cells and ischaemic tissue can easily be identified but the events leading to their formation cannot be solely explained by immunohistochemicial and genetic analysis. The glioblastoma spheroid system allows preliminary and progressive cell death-associated events to be monitored spatio-temporally, in terms of both morphology and patterns of protein expression. In addition, unlike primary cultured biopsy tissue, cell lines can be stably transfected to produce proteins that can be studied in relation to the cell death response within growing tumour cell populations.

1.7. Aims

The aims of this project were:

(i) to fully characterise the glioma spheroid system for the four glioma cell lines, U87, U373, MOG-G-CCM and A172 and to establish that the system adequately reflects many of the features found within glioblastoma cell populations *in vivo*.
(ii) to define the exact time point in spheroid growth when central cell death occurs and to record the different modes of cell death present both qualitatively and quantitatively.
(iii) to establish which p53-related proteins are associated with areas of cell death within glioma spheroids and to determine whether any correlation exists between this distribution and the genetic status of the cell lines.
(iv) to determine whether the distribution of p53 related proteins in spheroid culture is comparible with that seen *in vivo*
(iv) to ascertain whether modulating levels of endogenous intracellular p53 will have an effect on the development of cell death and the expression of p53-related proteins within glioma spheroid cultures.

These findings should hopefully give us greater insight into the modes and mechanisms of cell death employed within glioblastoma cell populations when they are exposed to cellular stresses similar to those found around areas of necrosis *in vivo*.

CHAPTER 2

MATERIALS AND METHODS

2.1. Preparation of tissue

2.1.1. Cell lines

Four human glioma cell lines derived from anaplastic astrocytoma or GBM were used in this study. All cell lines were supplied by the European Collection of Cell Cultures, Centre for Applied Microbiology & Research, Salisbury, Wiltshire, UK. A172 was derived from a glioblastoma removed from a 53 year old male. This cell line is non-tumourigenic in anti-thymocyte serum treated NIH Swiss mice. The culture was at passage 314 on arrival. MOG-G-CCM was established from an anaplastic astrocytoma of normal adult brain. This culture was at passage number 54 on arrival. U373 cell line was derived from a malignant glioma by explant technique. This culture was at passage number 177 on arrival. The U87 cell line was derived from a malignant glioma from a patient by explant technique also. It is reported to produce a malignant tumour consistant with glioblastoma in nude mice. The passage number on arrival of U87 cell line was 4. Cell lines were grown to confluency at passage 1 from purchase and frozen into aliquots to preserve maximum heterogeneity throughout this series of experiments.

2.1.2. Culture of cell lines

The cell lines were grown in monolayer in Corning 75cm^2 culture flasks (Merck) in Dulbecco's Modified Eagles Medium (DMEM) supplemented with 10%v/v foetal calf serum (FCS), penicillin (100units/ml), streptomycin (100μg/ml) and L-glutamine (2mM). These were all purchased from from GibcoBRL, Life Technologies, Paisley, Scotland. The flasks were placed inside a humidified incubator (Heareaus 'function line' incubator, Heraeus Instruments Ltd, 9 Wates Way, Brentwood, Essex, UK) supplied with an atmosphere of 95% air and 5% CO_2 at 37°C. All tissue culture procedures were carried out aseptically in a laminar flow cabinet (Microbiological Class II (Envair 2+); Envair Ltd, York Avenue, Haslingden, Rossendale, UK) using sterile disposable plastic pipettes and pipette tips. To ensure that a sterile environment was preserved, the laminar flow cabinet was thoroughly cleaned before, during and after all operations with a solution of 70% ethanol. In addition, all handling of cell lines was performed using disposable latex gloves.

Continuous cell growth was sustained through regular subculture and examination of the cultures was performed using a Leica MDIL inverted microscope (Leica Microsystems (UK) Ltd, Davy Avenue, Knowhill, Milton Keynes, UK). When 100% confluency was

reached, the cells were harvested through trypsinisation, diluted 1:10 in medium and delivered into fresh flasks. Excess cells were either thrown away or centrifuged (at 2000rpm in a Hereaus function line centrifuge) and frozen at –70°C in the above medium containing 1 part dimethyl sulphoxide (DMSO) (Sigma-Aldrich Company Ltd, Fancy Road, Poole, Dorset, UK) to 15 parts medium for future use. The process of subculture involved the aspiration of spent medium from the cells, followed by 2 washes with Dulbecco 'A' phosphate buffered saline (PBS tablets from Oxoid Ltd, Basingstoke, Hampshire, UK) and a 5 minute incubation at 37°C in 5mls 1xTrypsin-EDTA (O.5ml of 10xtrypsin (Gibco-BRL) in 4.5ml PBS). The cells were detached through gentle/heavy agitation and 15mls of the appropriate medium added to the subsequent cell suspension. 1.5ml of this cell suspension was then seeded into each new flask and was supplemented with 13.5mls of fresh medium. The flasks were then incubated for 2-3 days until the cells became confluent.

2.1.3. Monolayer culture experiments

In order to perform immunohistochemistry efficiently on monolayer cultured cells, Lab-Tek chamber slides were used (Nalge Nunc International, 2000 Aurora Road, Naperville, IL60563, USA). These slides allow the culture of tissue directly onto glass slides which can be used in standard immunohistochemical procedures. The day preceeding immunohistochemical labelling, one flask of cells corresponding to each cell line to be analysed was trypsinised and 3000 cells (counted using a haemocytometer) were plated into each well (8 wells per slide). The following day, all of the cells used in this study were 70-100% confluent. To fix the cells, 500µl of 4% buffered paraformaldehyde (Merck Ltd, Hunter Boulevard, Magna Park, Lutterworth, Leicstershire, UK) was added to each well for 15 minutes. Following 2 washes in PBS, the plastic cover providing the 'wells' was removed and the resulting slides with adherant cells were placed in Tris Buffered Saline (TBS- 6.05g trizma base (Merck), 8.2g NaCl, 1L ddH2O, Ph7.6).

2.1.4. Monolayer cultures treated with oxidative and free radical stress

To examine the effects of oxidative and free radical stress on the expression of p53 related protein expression, the four cell lines were exposed to hypoxia in one experiment and H_2O_2 in another. For the H_2O_2 experiment monolayer layer cultures derived from each of the four cell lines were grown in $25cm^2$ flasks (Corning) until 70% confluent. They were then exposed to a 1mM concentration (in the above medium) of H_2O_2 (30%v/v solution

from Sigma) for 6 hours. This concentration and time point have been shown to be optimal when examining p53 reactivity under these circumstances (Kitamure et al., 1999). which The cells were then trypsinised, pelleted at 2000rpm (as in 2.1.2)and lysed for western blot analysis (see 2.3). A $25cm^2$ flask set up with the same number of cells for each cell line was also set up to act as a 0mM H_2O_2 control for this experiment.

For the hypoxia experiment, the two cell lines U87 and U373 were grown in $25cm^2$ flasks (Corning) until 70% confluent. They were then exposed to hypoxia (5% CO_2 and 0.5% oxygen) for 0,1,2,6,12 and 24 hours in a hypoxia chamber (Heto Holten Cell House 170 multigas incubator). The cells were then trypsinised, pelleted at 2000rpm (as in 2.1.2) and lysed for western blot analysis (see2.3). This procedure was performed by Kevin Corke at the Academic Unit of Pathology, University of Sheffield Medical School, Beech Hill Road, Sheffield.

2.1.5. Spheroid formation

Confluent cultures derived from each cell line were trypsinized and seeded into spinner culture flasks (Pyrex/Shott flasks from Merck) at a density $3x10^6$ cells/100ml of medium (DMEM medium as described in 2.1.2). These were spun at 180 rpm for 5 weeks (previously described in Bell et al, 1999) on a 4 position magnetic stirrer (Estem corporation stirrer from Merck) (Figure 3). The medium was replaced when the phenol red indicator in the medium turned orange. This occurred more frequently as the spheroids became larger (approximately every 3 days). Around 200 spheroids from each cell line were harvested from culture at weekly intervals, 25% for paraffin embedding, 25% for flow cytometric analysis, 25% for EM processing and 25% for western blot analysis.

2.1.6. Biopsy material

Twenty-five archival cases of glioblastoma multiforme were selected at random from the Neuropathology files of the Western General Hospital. Following a review of all available haematoxylin and eosin stained sections by a neuropathologist (Dr S. Wharton), a representative paraffin block (tissue processed in an identical manner as in 2.1.7) which contained viable tumour, necrosis and regions of tumour/necrosis interface was selected for each case.

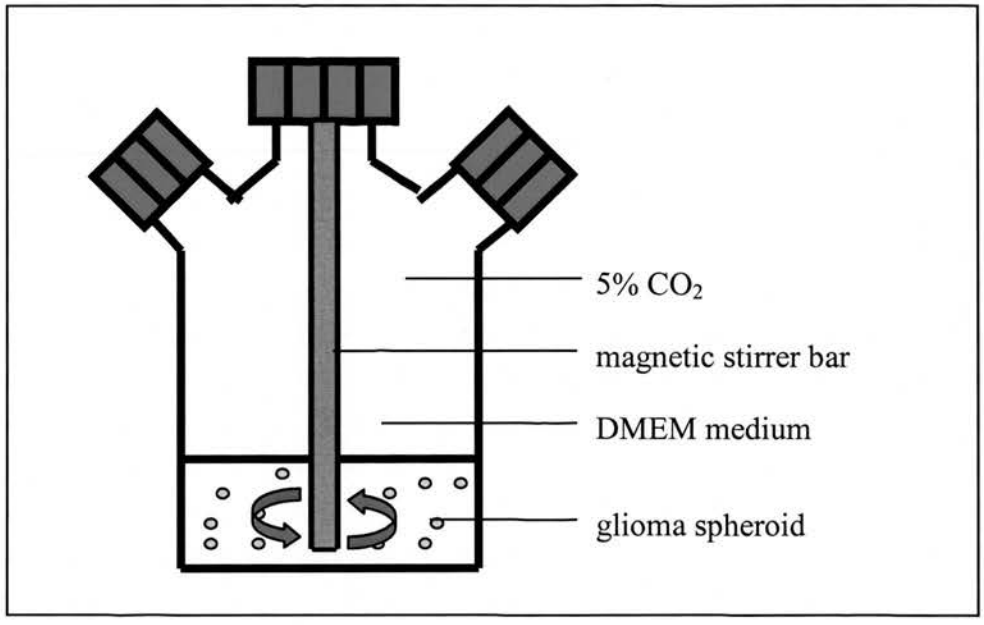

Figure 3. Diagram of glioma spheroid culture

2.1.7. Tissue processing for paraffin sections

The brain tumour spheroids derived from each cell line and time point were fixed in 10% paraformaldehyde (Merck)for 15minutes. Following this, approximately 50 spheroids were placed in each well of a 24 well plate and a 4% hot agarose (Sigma) solution was added to a depth of 75mm. Once the 24 well plate had been refrigerated for 30minutes, the plate was removed and the wells emptied of their contents. The contents of each well consisted of an agarose disk containing approximately 50 spheroids aligned along the base of the disk. The disks were then deposited into plastic holding cassettes and placed in a Tissue-Tek 100 Processor (Bayer Plc, Diagnostics Division, Bayer House, Strawberry Hill, Newbury Berkshire, UK). The tissue processor saturates the tissue with paraffin for sectioning. The tissue passes through a series of alcohols (2x70% for 1hour each, 1x80% for 1hour, 1x90% for one hour and 3x100% for 1 hour each) then a series of xylenes (4x100% xylene for 1 hour each) and then into paraffin (4 x100% for 1 hour each). Once paraffinised, the tissue was embedded in a Tissue-Tek III Embedding System (Bayer) into metal holders with the spheroids facing on the outward edge of the block.

The blocks containing the brain tumour spheroids and biopsy tissue (which was already embedded) were then cut into 5μm sections using a Leica G283 microtome and the sections placed onto Superfrost electrostatically coated slides (Merck). Paraffin sections of the brain tumour spheroids were used for haematoxylin and eosin (H&E) staining,

imunohistochemical analysis and TUNEL labelling. Biopsy sections were used for immunohistochemistry only. To prepare the tissues for staining the slides were placed in xylene for 5 minutes to remove the paraffin. This was followed by 2 minutes in 100%, 80% and 70% alcohol (Merck) respectively. The sections were then placed in water to allow full rehydration.

2.2. Staining & Labelling protocols

2.2.1. Haematoxylin and eosin

The spheroid sections were removed from water and stained in a 10% haematoxylin solution (Merck) for 2 minutes. They were then washed in tap water and placed in saturated Lithium Carbonate (Merck) in ddH_2O (double distilled water) for 10 seconds for the haematoxylin to oxidise to a blue colour. They were then washed in water and stained in eosin solution (Merck) for 2 minutes. Following another wash in tap water, the slides were then placed in a saturated solution of potassium aluminium phosphate for 10 seconds. Finally the sections were washed (in tap water), dehydrated (in 70, 80, 100% alcohols), cleaned and mounted using DEPEX (Merck) mounted and coverslips (Chance Propper coverslips from Merck). With this method nuclei appear blue and cytoplasm, connective tissue, red blood cells and muscle appear pink.

2.2.2. TUNEL labelling

Spheroid sections were dewaxed and rehydrated as in 2.1.7 and incubated with proteinase K (Roche Diagnostics Ltd, Bell Lane, Lewes, East Sussex, UK) for 20 minutes at a concentration of 20μg/ml in 10mM/HCl (Sigma), pH7.6 at room temperature. After washing in PBS, the sections were incubated in TUNEL reaction mixture (TdT-mediated dUTP-X nick end labeling). This involves the labeling of free 3'-OH termini with modified nucleotides in an enzymatic reaction. In this kit terminal deoxynucleotidyl transferase (TdT) catalyzes polymerization of nucleotides to free3'-OH DNA ends in a template-independent manner to label DNA strand breaks. Fluorescein is conjugated to these nucleotides which can be detected using either fluorescent microscopy or by using a secondary detection system. The secondary detection system in this kit contains an anti-fluorescein antibody to visualise the fluorescent markers for light microscopy (instructions as described for In Situ Cell detection kit, AP/POD from Roche).

Two different kits were used in this study. One contained a secondary antibody conjugated to horseradish peroxidase thus requiring a DAB substrate. The other kit

contained a secondary antibody conjugated with alkaline phosphatase. The substrate in this case was 5-Bromo-4-Chloro-3-Indolyl Phosphate/Nitro Blue Tetrazolium Tablets (BCIP/NBT-from Sigma). This meant that positively labelled cells were blue as opposed to brown as with the peroxidase secondary system. Following the visualization procedure the sections were washed, dehydrated, counterstained and mounted as above.

2.2.3. Immunohistochemistry

The immunohistochemistry performed in this study was divided into two groups. The characterisation phase included GFAP, vimentin and Ki67 antibodies. The cell death phase included antibodies to p53, Bax, p21, MDM2 and $p14^{ARF}$. An antibody against HIF-1α was also tested.

GFAP, vimentin and Ki67 immunohistochemistry was performed on wild-type monolayer cultures and spheroid cultures to fully characterise the cell lines and spheroid model. These antibodies were not used on biopsy tissue as their expression in glioblastoma is well documented (Kleihues et al., 2000; Hirato et al., 1994; Bouvier-Labit et al., 1998; Watanabe K., 1997). P53, Bax, p21, MDM2 and $p14^{ARF}$ immunohistochemstry was performed on monolayer culture, spheroid culture (both wild-type and transfected cell lines) and on biopsy tissue. HIF-1α immunohistochemistry was performed on monolayer and spheroid cultures.

The monolayer cultures, spheroid cultures and biopsies were treated as in 2.1.6/2.1.7 and removed from tap water/buffer. The slides that required citrate pretreament were submersed in citrate buffer (x10 stock buffer- 6g citric acid, 48.24g of sodium citrate (anhydrous), 2Litres of ddH_2O, pH6) and microwaved on full power for 15minutes (see Table 1 for details of pretreaments, types of animal sera used etc). This was also performed on the monolayer cultures where virtually no cell loss was observed.The slides were then placed in a 3%solution of H_2O_2 for 20minutes to block any endogenous peroxidase.

After washing in TBS, the sections were placed in a sequenza (Shandon Life Sciences International, Astmoor, Runcorn, Cheshire, UK) for the application of blocking agents and antibodies. The sequenza allows rapid application of liquids evenly across the surface of the slide. After 2 washes in TBS, a 20% solution of animal sera in TBS was added to

the slides as a blocking agent. Following this, the primary antibodies diluted in 20% serum were added to the slides at the appropriate concentration for 1hour at room temperature. Following a further 2 washes in TBS, the appropriate biotinylated secondary antibody was added to the slides for 30minutes at room temperature at a concentration of 1:200 in animal serum. The avidin-biotinylated enzyme complex (ABC kit)used was a vector elite kit (Vector Laboratories, 3 Accent Park, Bakewell Road, Peterbourgh, UK). This binds to the biotin that is conjugated to the secondary antibody and provides a target (horseradish peroxidase) for the subtrate chromagen. The solutions were made up as per instructions in the kit and added to the slides after a further 2 washes in TBS. The sections were incubated in the ABC reagent for 30minutes at room temperature. Following a further two washes in TBS the slides were removed from the sequenza and incubated in a 3,3'-Diaminobenzidine Tetrahydrochloride (DAB) solution (kit from Vector Ltd.) for approximately 5minutes. Consequently, positively labelled tissue appeared brown in colour. All sections were then lightly counterstained with haematoxylin, washed, dehydrated, cleared and mounted in DEPEX as in 2.2.1.

Antibody	Mono/poly clonal	Raised in	PrimaryAb concentrat -ion	Pre-treatments	Serum blocker	Secondary antibody	Western concentrat -ion
GFAP[1] (αCOW)	poly	rabbit	1:1000	non	swine[5]	swine anti-rabbit[1]	N/A
Vimentin[1] (Vim3B4)	mono	mouse	1:500	non	rabbit[5]	rabbit anti-mouse[1]	N/A
Ki67[2] (MM1)	mono	mouse	1:400	microwave in citrate	rabbit[5]	rabbit anti-mouse[1]	N/A
P53[3] (Pab1801)	mono	mouse	1:200	microwave in citrate	goat[5]	goat anti-mouse[4]	1:500
P53[3] (Bp53-12)	mono	mouse	1:200	microwave in citrate	goat[5]	goat anti-mouse[4]	1:500
Bax[3] (B-9)	mono	mouse	1:200	microwave in citrate	goat[5]	goat anti-mouse[4]	1:200
P21[3] (F-5)	mono	mouse	1:100	microwave in citrate	goat[5]	goat anti-mouse[4]	1:100
MDM2[3] (SMP-14)	mono	mouse	1:200	microwave in citrate	goat[5]	goat anti-mouse[4]	1:400
MDM2[3] (C-18)	poly	rabbit	1:200	microwave in citrate	swine[5]	swine anti-rabbit	1:100
$P14^{ARF-3}$ (C-18)	mono	mouse	1:200	microwave in citrate	goat[5]	goat anti-mouse[4]	1:500
HIF-1α[3] (28b)	mono	mouse	1:200	microwave in citrate	goat[5]	goat anti-mouse[4]	1:500
HIF-1α[6] (HIF1α67)	mono	mouse	1:1000	microwave in citrate	Goat[5]	goat anti-mouse[4]	1:1000

[1]Dako Ltd, Angel Drive, Ely, Cambridgeshire, UK.

[2]Novocastra, Ballilol Business Park West, Benton Lane, Newcastle-Upon Tyne, UK.

[3]Santa Cruz, Autogen Bioclear Ltd, Holly Ditch Farm, Mile Elm, Wiltshire, UK.

[4]Vector Laboratories, 3 Accent Park, Bakewell Road, Peterbourgh, UK.

[5]Scottish Antibody Production Unit, Law Hospital, Carluke, Lanarkshire, UK.

[6]Abcam Ltd, 31 Cambridge Science Park, Milton Road, Cambridge, UK.

Table 1. Antibodies used for immunohistochemistry and western blotting experiments

2.2.4. Flow cytometry (FACS analysis)

Wild-type brain tumour spheroids were disaggregated following centrifugation (2000rpm for 5 minutes) in universal tubes using trypsin (0.5g trypsin and 0.2g EDTA in 250ml PBS) in a water bath at 37°C for 5 minutes. To avoid membrane damage, cycles of resuspension were used to break down spheroids from weeks 3-5. Disaggregated cells were removed after each cycle and added to 10mls of DMEM (containing 10% FCS, as above) to inhibit the action of the trypsin. The cells were then centrifuged again , the supernatent removed and the cells suspended in 100µl of Annexin V/propidium iodide solution (Roche Diagnostics Ltd) for 15minutes at room temperature. 400µl of PBS was then added and the resulting cell suspensions were analysed using a Coulter EPICS XL flow cytometer with EPICS XL-MCL System II software. This identified apoptotic and necrotic cells on the basis of side scatter and fluorescence associated with Fluorescein labelled Annexin V and propidium iodide (Creutz, 1992). In the early stages of apoptosis, phosphatidyl serine residues flip to the external side of the cell membrane. These can be labeled with the Annexin V probe. The cell membranes of necrotic cells become permeabilized early on, allowing the entry of both the Annexin V probe and Propidium Iodide. Therefore, the combination of high Annexin V labeling with low propidium iodide labeling indicates an apoptotic cell whilst high labeling for both Annexin and Propidium iodide indicates a necrotic cell.

2.3. Western blotting protocol

2.3.1. Isolation of protein from cultured cells

Cells were grown in monolayer culture to 80-100% confluency in 75cm^2 culture flasks. The cells were washed twice in 10mls of PBS, drained completely and trypsinised using the above described technique (2.1.2). The cells were then centrifuged at 2000rpm in PBS in universal tubes (Sterilin tubes from Merck) and the supernatent removed. For the spheroid cultures, approximately 50 spheroids were removed from culture and washed in 10mls of PBS (x2). Centrifugation was not required as the spheroids could easily be separated from the medium by leaving them to settle at the bottom of the universal tubes. 1ml of RIPA buffer was then added to the monolayer pellet/spheroids (RIPA buffer-

1xPBS, 1% Igepal CA-630 (Sigma), 0.5% sodium deoxycholate, 0.1% SDS) and the samples vortexed for 20seconds. The samples were then incubated on ice for 30minutes (1hour for spheroid cultures) and then sonicated for one 5second pulse using a Sanyo Soniprep 150 sonicator. The samples when then centrifuged in a microcentrifuge for 15minutes at 4°C and the supernatant removed. 1mM of PMSF (phenyl-methyl-sulphonyl fluoride) was then added to each sample (as a proteinase inhibitor) and the samples were stored at -70°C.

2.3.2. Quantification of total protein concentration

In order to standardise the quantity of protein in each well for each sample the Coomassie Plus-200 Protein Assay Reagent (Pierce, 3747 N. Meridian Road, P.O. Box 117, Rockford, IL61105, USA.) was used.

A fresh set of protein standards were first set up. This involved diluting a 2.0mg/ml BSA (bovine serum albumin) stock sample into standards of 25μg/ml, 125μg/ml, 250μg/ml, 500μg/ml, 750μg/ml, 1000μg/ml, 1500μg/ml in ddH_2O. 10μl of each sample (plus a 0μg/ml control) was pipetted into 8wells (x2 for an average reading)of a 96 well plate. 300μl of the Coomassie Plus reagent was added to each of the 8standard wells and placed on a bench top shaker for 30seconds. For each unknown sample, 10μl of sample was added to 300μl of Coomassie Plus reagent and added to other wells on the standard plate. The plate was read on a Bio-Rad540 plate reader at a 580nm absorbance reading. A standard curve was then prepared by plotting the average blank corrected 580nm reading for each BSA standard versus its concentration in ug/ml. Using the standard curve, the protein concentration for each unknown sample could be determined.

2.3.3. SDS-Polyacrylamide Gel electrophoresis of proteins (PAGE)

This procedure is based on the discontinuous buffer system described by Laemmli (1970). Electrophoresis was performed using the Mini-Protean II vertical electrophoresis system (Biorad laboratories Ltd).

The electrophoresis glass plates were washed in a weak detergent solution, rinsed thoroughly and the side to be in contact with gel washed in 100% ethanol. The plates were then assembled according to Bio-rad instructions. The resolving gel was prepared (protocol in Table 2) and then poured (~4mls) into the gap between the plates up to about

3cm from the top of the plates. This was over laid with 0.5ml ddH_2O to flatten the surface of the gel. This was removed using blotting paper once the gel had set. Once the resolving gel had set (after ~15minutes), the stacking gel was prepared (Table 2) and poured into the remaining space at the top of gel. A ten-well Teflon comb (6mmx10mm for each well) was then inserted, ensuring no airbubbles were trapped. The gel set up was then left to polymerise for 30 minutes at room temperature.

After completion of polymerisation the comb was removed and the wells washed with de-ionised water to remove unpolymerised acrylamide. The gel could then be mounted into the gel mounting apparatus and reservoir buffer (Table 2) placed in the top and bottom reservoirs. 50μg protein samples (volume determined by the Coomassie Blue Assay)were then set up containing a 1 in 4 dilution of 4x PAGE loading buffer (Table 2). The samples were then boiled in a water bath for 10minutes and incubated on ice prior to loading into the bottom of the wells using Prot/Elec tips (Bio-Rad Laboratories Ltd). The samples were loaded alongside 10μl of prestained SDS-Page standards (Low range- 24,000-102,000Daltons). The gel was run at 200mVolts (60Amps) until the bromophenol blue was seen to run off the bottom of the gel (approximately 45minutes). The Ampage at this point drops to approximately 20mA. Bromophenol blue run alongside 15kDa proteins.

2.3.4. Transfer of Proteins from SDS-Polyacrylamide Gels to Nitrocellulose.

The gel was removed from the glass plates and the stacking gel part of the gel removed using a gel cutting device. The remaining resolving gel was then measured and the dimensions taken used to cut 2 pieces of blotting paper (Whatmann 3Mmpaper) and a piece of nitrocellulose the same size. The blotting paper and nitocellulose were then immersed in transfer buffer (Table 2) for a few seconds. Blotting paper, nitrocellose, gel, and blotting paper were then positioned on top of a transfer cassette in that order. The cassette was then placed inside the transfer apparatus (TE 22 Mighty Small Transfer Tank, from Amersham Pharmacia Biotech) with the nitrocellulose on the side of the anode. This means the current passes from the cathode to the anode displacing the proteins from the gel onto the nitrocellulose. The remaining transfer buffer was then poured intothe transfer apparatus and the voltage set at 220Volts (400mA). The transfer took place in approximately 30minutes after which the nitrocellulose was removed from the cassette and emmersed in TBS (Table 2).

2.3.5. Immuno-detection of p53 related proteins immobilised on nitrocellulose

Protein detection was carried out using the luminol western detection system (Santa cruz). The nitrocellulose membrane was removed from the TBS and incubated in blocking serum (5%milk solution in TBST) for 1 hour at room temperature in a shallow container on an orbital shaker. This solution was then removed and the primary antibody solution (antibodies all diluted in blocking solution at varying dilutions-see Table 1) added for 1hour. The actual total volume added depended on the size of container. The membrane was subsequently drained and washed for 5minutes (x3) in TBST. Once the wash buffer had been removed, the secondary antibody was then added to the membrane (mouse IgG horseradish peroxidase-linked whole antibody) diluted 1:1000 in TBST for 45minutes. The membrane was then drained completely and washed 3 times in TBST for 5 minutes and once in TBS for 5 minutes to irradicate the high levels of detergent. The nitrocellulose was then incubated for 1minute with the two luminol detection detection reagents (0.125mls per cm^2) previously mixed in equal quantities. HyperfilmTM-ECL was exposed to the membrane for 30seconds, 1 minute, 2minutes and 4 minutes to ensure optimum exposure. The film was then passed through a photographic hyperprocessor to develop the film.

Resolving gel buffer (x4)	Stacking gel buffer (x4)
15.25g Tris base	45.5g Tris base
250ml ddH_20	250ml ddH_20
pH6.8	pH8.8
Resolving gel	Stacking gel
2.5ml 4x resolving gel buffer	1.25ml 4x stacking gel
3.4ml ddH_20	3.0ml ddH_20
4.0ml 30% acrylamide	0.67ml 30% acrylamide
50µl 10% SDS	25µl 10% SDS
100µl APS (Ammonium persulphate)	50µl APS
10µl TEMED	5µl TEMED
Reservior buffer (x10)	PAGE-loading buffer (x4)
30.2g Tris base	0.125ml stacking gel buffer
144g glycine	0.300ml 10% SDS
1LddH_2O	0.100ml Glycerol
0.1% SDS in final 1x buffer (5mls 10%	0.050ml 2-mercaptoethanol

SDS in 500mls)	0.200ml 0.1% bromophenol blue 0.225ml ddH_2O
Transfer buffer 4.5g Tris base 21.6g Glycine 15ml 10%SDS 1200ml ddH_2O 300ml methanol	Blot washing buffer (TBST) 5ml 1M Tris 15mls 5M NaCl 500ml ddH_2O 0.250ml Tween-20

Table 2. List of reagents used in western blotting experiments

2.4. Electron microscopy

Tissue processing for electron microscopy was performed by Mr Frank Donnelly, Department of Neuropathology, Western General Hospital, Edinburgh.

Wild-type brain tumour spheroids derived from the cell lines U87, U373, MOG-G-CCM and A172 were fixed for 2 hours at 4°C in 3% gluteraldehyde in 0.1M Sodium Cacodylate/HCl buffer pH 7.2-7.4. They were then washed 3 times in double distilled water for 20 minutes and fixed for 45minutes in 1% osmium tetroxide. Following dehydration to 100% ethanol, the spheroids were submerged in propylene oxide for 30 minutes then left overnight in Emix resin (Taab Laboratories, Aldermaston, Berks, UK) at room temperature. Once the spheroids had polymerised (20 hours at 70°C), 90nm sections were cut with a glass knife on a Reichert OMU2 microtome and mounted on 300 mesh copper grids. The sections were then stained by the Uranyl Acetate/Lead Citrate method and examined using a Jeol 100CXII transmission electron microscope with an operating voltage of 60KV. Photographs were taken using Kodak 4489 film and developed using Ilford P&Q Universal developer on Ilford Multigrade glossy photographic paper.

The spheroids were examined to identify any ultrastructural differences between the modes of central cell death employed by the different cell lines. This was done over the 5 week spheroid growth period. Any interesting phenotypic observations were also recorded.

2.5. *P53* sequencing

2.5.1. Isolation of genomic DNA from cultured cells

The four wild-type cell lines U87, U373, A172 and MOG-G-CCM were washed and pelleted using a Haereaus function line centrifuge at 2000rpm. The cells were then transferred to a 1.5ml eppendorf tube and 500µl of lysis buffer (0.32M sucrose, 10mM tris-HCl, pH7.5, 5mM $MgCl^2$, 1% Triton X-100). These were inverted 5-6 times and centrifuged at 10,000rpm for 5 minutes. Following this, 500µl of phenol and 250µl chloroform: isoamyl alcohol were added to the samples. These were mixed then centrifuged for 3minutes at 10,000rpm. The supernatent was then transferred to a fresh tube and 250µl of phenol and 500µl chloroform:isoamyl alcohol were added. These were again centrifuged at 10,000 rpm and the supernatent removed. This last step was repeated until the supernatent became clear. Subsequently, 50µl NaOac (Sodium Acetate) and 1ml EtOH were added to the supernatent and the mix lightly tilted until a precipitation was seen. The sample was then spun at 10,000 rpm and the supernatant discarded. The pellet was resuspended in 50-100µl ddH_2O and stored at 4°C for 24hours to allow the DNA to dissolve.

2.5.2. Amplification of genomic *P53* sequences

The entire coding region of the *P53* gene (exons 2-11) was polymerase chain reaction amplified (PCR). A series of primers were used that spanned across all 11exons (Figure 4). The coding sequences were divided into 3 segments of 500-1000 base pair fragments. The primer sequences were all situated on exons and were between 15 and 25 base pairs longs (Table 3).

Genomic DNA isolated from the cell lines was diluted to approximately 100ng/µl. All PCR reactions were carried out in 500µl microtest tubes on a Hybaid Omni-Gene PCR machine. Because multiple samples were to be analysed, bulk solutions containing Taq polymerase, reaction buffer, dNTPs, primers and water were prepared. The total volume of solutions was 300µl and was made up of 193µl ddH_2O, 30µl reaction buffer(x10), 48µl dNTPs (1.25mM of each dNTP), 15µl of sense primer (50µg/ml), 15µl of antisense primer (50µg/ml) and 1µl Taq DNA polymerase (5units/µl). The reaction buffer, dNTPs and Taq polymerase were purchased from Life Technologies Ltd, 3 Fountain Drive, Inchinnan Business Park, Paisley, UK. The primer combinations were made by Genosys (a Sigma subsidiary). This 300µl stock mix was divided into 50µl aliqouts and 1µl of

DNA (100ng/μl) of DNA to be tested from each cell line was added to each tube. The contents of the tubes were thoroughly mixed and 50μl of mineral oil (Sigma) added to prevent evaporation. In all PCRs 30 amplification cycles were employed. Each cycle consisted of 1minute at 95°C for the denaturation phase, 30seconds at 58°C for the annealing phase and 1 minute at 72°C for the extention time.

Region 1 (Product size 694bp)		
P53ex.2.1	$^{5'}$G GAG CGT GCT TTC CAC GA$^{3'}$	(143-204)
P53ex.6.1	$^{5'}$CAG TAG GTT TAT GAG GTG TGC G$^{3'}$	(837-815)
Region 2 (Product size 814bp)		
P53ex4.1	$^{5'}$TCC CAA GCA ATG GAT GAT TTG$^{3'}$	(322-342)
P53ex8/9.2	$^{5'}$C ACG AGC GAA TCA CGA GGG A$^{3'}$	(1136-1117)
Region 3 (Product size 675bp)		
P53ex5.1	$^{5'}$AC CAT GAG CGC TGC TCA GAT A$^{3'}$	(745-767)
P53ex11.1	$^{5'}$CAC CCC TTG TTC TTC ACC$^{3'}$	(1420-1402)

Table 3. Primer sequences for regional amplification of the *P53* gene

2.5.3. Gel electrophoresis of PCR products

The PCR products (see Figure 4 for regions) were analysed by electrophoresis in 2% agarose gels. 100mls of 2% gel was prepared using 1xTAE buffer (made from a 50x stock of 242g Tris base, 57.1g glacial acetic acid, 100ml 0.5M EDTA pH 8.0, made up to 1L) and 2g of PCR grade agarose (Sigma). 1μl of 10mg/ml ethidium bromide was added prior to pouring the agarose into a sealed, level mini-gel tray carrying a 12 well comb. The gel was run in a mini-gel apparatus (Bio-Rad) containing enough buffer to cover the gel. 8μl of each PCR reaction together with 2μl of DNA loading buffer (0.25% Bromophenol blue, 0.25%xylene cyanol FF, 15% Ficoll Type 4000, 120mM EDTA) was added to each well alongside 10μl of 100bp ladder. Electrophoresis was performed for 30-45 miuntes at 100mV, after which the gel was examined and photographed under UV transillumination.

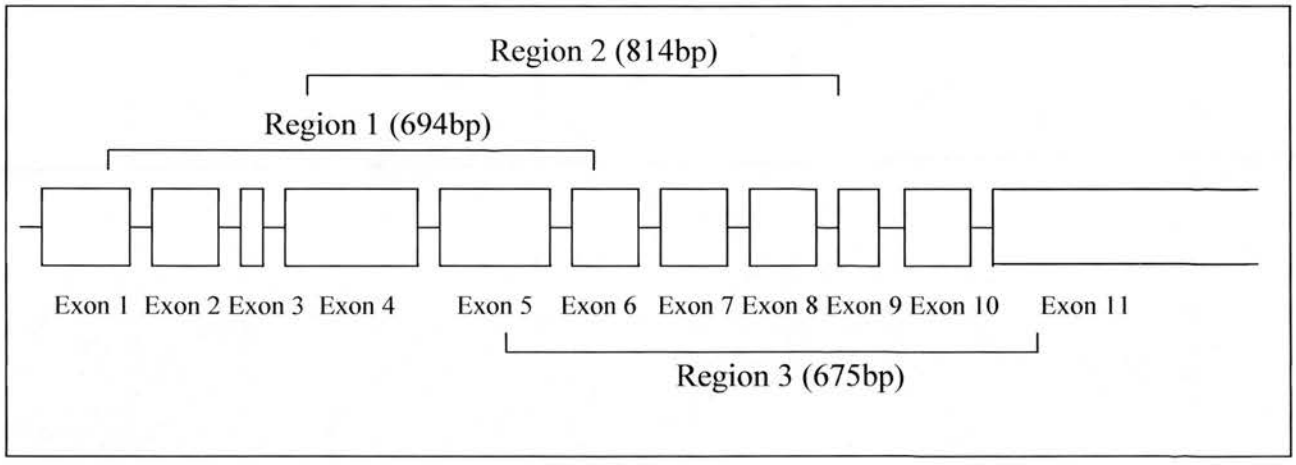

Figure 4. Map of the *P53* gene with region locations

2.5.4. Preparation of samples for chain termination sequencing

The 3 regions of DNA for each sample were directly sequenced using Thermosequenase radio-labelled terminator cycle sequence kits (Amersham-USB Life Sciences, 26111 Miles Road, Cleveland, Ohio 44128, USA). All of the following reagents, excluding the termination [α-^{33}P]ddNTPs, were used from this kit.

Following identification of the correct sized bands (Region 1, 694bp; Region 2, 814bp; Region 3, 675bp) for each region to be sequenced, 5µl of each PCR product was mixed with 1µl of Exonuclease 1 (10units/µl) and 1µl of Shrimp alkaline phosphatase (2.0units/µl) and incubated at 37°C for 15minutes. The samples were then incubated at 80°C for 15minutes to denature the enzymes. Exonuclease I removes residual single stranded primers and any extraneous single stranded DNA produced by the PCR. The shrimp alkaline phosphatase (SAP) removes the remaining dNTPs from the PCR mixture which would interfere with the labelling procedure in the sequencing process.

To set up the sequencing reaction, the termination mixes were prepared using 2µl of dNTPs and 0.5µl of each[α-^{33}P]ddNTP (G, A, T, or C-one of each per sequence) to produce a termination mix for each ddNTP. Therefore 4 tubes were set up for each sample to be sequenced.

To set up the reaction mixture, a stock solution of ddH_2O, reaction buffer, primer, polymerase and sample DNA was made up to be divided between the four above tubes. The quantities used in the reaction mixture were: 2µl reaction buffer (x10), 7µl

DNA(from the exonuclease/SAP stage), 1μl Primer (only 1μl of one primer is required as the mix only contains DNA ending or beginning with this oligonucleotide sequence), 8μl ddH_2O, 2μl Thermo Sequenase Polymerase- added last (4U/μl). 4.5μl of the reaction mixture was then added to each of the four permination tubes ie. 4.5μl to the 'G' tube , 4.5 μl to the 'A' tube etc. Each termination mix was then mixed and overlaid with 25μl mineral oil (Sigma). The cycling programme was then started, again using a Hybaid Omni-Gene PCR machine, using the same programme as described above (at 94°30", 58°30", 72°1'). Once the programme had finished, 4μl of stop solution was added to each of the termination mixes and the samples were briefly mixed and centrifuged to separate the oil from the aqueous phase. The samples were then stored at 4°C overnight before loading the sequencing gel the following day.

2.5.5. Separation of termination sequences using 6% polyacrylamide gels

Before pouring the sequencing the gel, the plates were thoroughly washed and the sides facing the gel were wiped down with 100%ethanol to remove any excess water. Spacers were then placed between the two plates with the shorter plate on top. Crocodile clips were used to hold the plates together in position. The gel mixture was then prepared (see Table 4 below). A 50ml syringe without needle was used to fill the gap between the plates with the gel solution. This was done with relative haste to prevent polymerisation of gel before the gel was fully poured. The gel was tilted to encourage the flow of the solution and to prevent air bubble formation. Once the plates were full, two sequencing combs were inverted and the flat side pushed into the top end of the gel by around 2cm. This provides a flat surface for the samples when the combs are orientated to provide wells. The gel was then left to polymerise for 30minutes. The total size of the gel was 30x40x0.4cm.

Once polymerisation had occurred the gel was moved into an upright position and clamped into the gel running apparatus (Life Technologies Sequencer II). 1xTBE was then poured into the top and bottom chambers of the apparatus. The combs were removed from the inverted position and were placed with the serrated edge down into the well, with the teeth slightly penetrating the gel. The gel was then set up for a pre-run to warm up the plates for 30minutes at 100W.

TBE (x10) buffer (1L)	6% stock sequencing sol.	6% sequencing gel
108 g Tris base	190ml ddH2O	65ml 6% stock sequencing solution
55 g boric acid	50ml TBE(x10)	400µl APS
40ml 0.5M EDTA	75ml 30% Acrylamide Solution (19:1-Acrylamide/Bis-acrylamide mix)	30µl TEMED
pH8.0	240g urea	

Table 4. List of reagents for sequencing gel

The termination reactions were then removed from the fridge and heated to 90°C on a hot plate for 3 minutes. The wells in the gel were then washed using 1xTBE with a fine gauge needle. 4µl of each termination mix (which were kept on ice) was then loaded into each well in the order of G, A, T and C for each set of samples. These were left to run for 2 hours at 80W. A second batch of the same samples were then introduced to the spare wells on the gel to provide a short run and a long run thus allowing more of the gel to be read when sequencing was complete. After another 2 hours the buffers were drained from the gel running apparatus and the gel separated from two plates using a sequencing gel separator. The whole gel was then spread onto Whatmann T4 blotting paper, covered in clingfilm and dried using a large Bio-Rad 650 gel dryer for a further 2 hours. Subsequently, the clingfilm was removed and the blotting paper was exposed to autoradiographic film over night. The film was then developed in a photographic hyperprocessor. The films were then screened p53 mutations by comparison with the wild type sequence using the website; www.perso.curie.fr/ p53/Thierry.Soussi/ index).

2.6. Production of mutant and wild-type *P53* transfectants

2.6.1. Construction of P53WTEGFP vector

The wild-type p53 vector (Figure 5) was purchased from Clontech Laboratories Inc, 1020 East Meadow Circle, Palo Alto, California, USA. This plasmid encodes a p53-EGFP signalling probe, which is a fusion of enhanced greeen fluorescent protein (EGFP) and p53. The expression of the p53-EGFP is driven by the human CMV immediate-early

promoter. The SV40-poly A sequence directs proper processing of the 3' end of the fusion construct. The vector backbone also contains an SV40 origin for replication in mammalian cells expressing the SV40 T- antigen. A pUC origin of replication for propagation in E. Coli is also included. A neomycin resistance cassette (neo^r) allows kanamycin resistance in E.Coli and geneticin (G418) resistance in eukaryotic cells. The p53-EGFP signalling probe can be used to monitor the presence of transfected p53 in target cells by observing changes in EGFP flourescence. The EGFP signalling probe was used in all the of the expression vectors in this study as a means of standardizing protein expression and detection.

After the transformation and cloning procedures were performed using two selected colonies (2.7.1), a PCR for a section of the *P53* gene was set up to confirm the cloning procedure had amplified the *P53* wild-type vector correctly. The reactions were set up as in 2.5.2 using the primers ex2.1 and ex6.1 (Table 3).

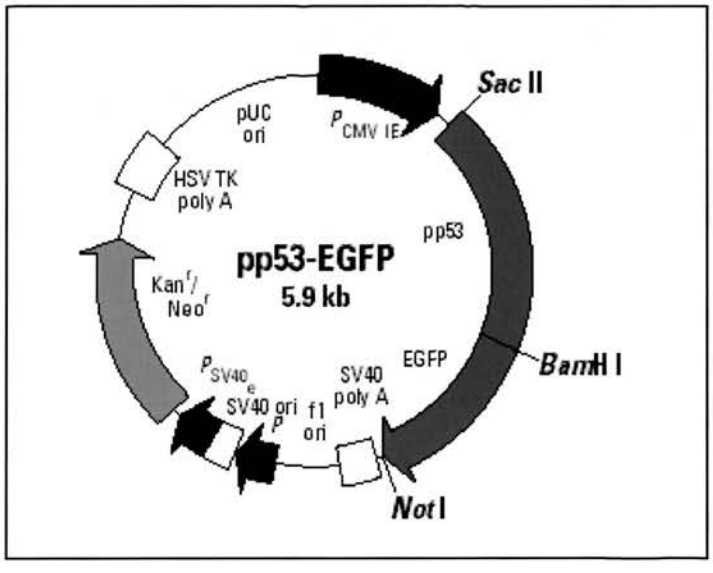

Figure 5. The pp53-EGFPvector construct

2.6.2. Construction of the Plasmid Only vector

In order to perform a controlled experiment for the presence of the *P53* vector in transfected cell lines, a plasmid-only control vector was created. This was done by digesting the above plasmid to remove the 1.2kilobase *P53* encoding region and re-ligating the free ends. This was done between the CMV promoter sequence and the *P53* sequence and also between the *P53* sequence and EGFP sequence. The resulting vector is shown in Figure 6 (also without pCMV promoter region at the start of the p53 sequence).

The digestion to remove the *P53* insert was performed using the restriction enzymes HindIII (restriction site-A/AGCTT) and BglII (restriction site-A/GATCT). This resulted in free complcmcntary base pairs (GATC/CTAG) that could be ligated together to create a circular vector for cloning and transfection procedures. The digestion mix (Table 5) was incubated at 37°C in either a water bath or the Hybaid Omni-Gene PCR machine.

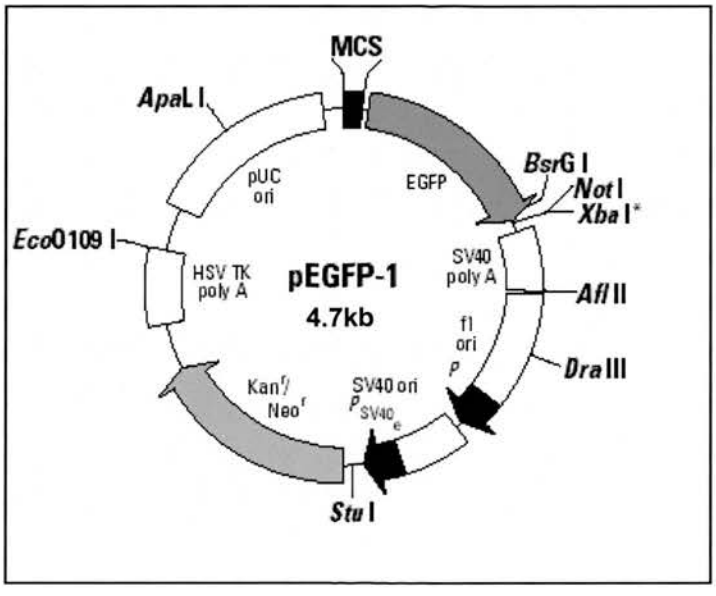

Figure 6. The plasmid-only vector construct

Digestion of pp53-EGFP	Ligation of free ends of empty vector
83μl ddH_2O	7.5μl cut vector
10μl buffer (x10) –React 2 (Life Tech)	0.5μl ligase
1μl Hind III/ Bgl II (Life Tech)	2μl buffer (x5)
5μl pp53-EGFP vector (Clontech)	

Table 5. List of reagents for the creation of PO-EGFP

The digestion products (all 100μl of the digestion mix) were then run on a 0.7% agarose gel (2.5.3) for 45 minutes. This allowed the two vector fragments (1.2Kb and 4.7kb) to be fully separated. Using a UV light box, the 4.7kB fragment (the empty EGFP vector) was cut from the gel with a scalpel. To purify the 4.7kB fragment from the 0.7% agarose gel, 0.5 mls of paper water (ddH_2O containing shredded Whatmann paper) was added to a 1.0ml eppendorf tube with a small hole in the bottom. This was then placed inside a 2.0ml

eppendorf tube and briefly centrifuged on a desk top centrifuge for 10 seconds. This created a small paper filter in the base of the smaller tube. The larger tube was then emptied and the 4.7kB agarose fragment was inserted into the tube containing the filter and spun at 10,000rpm for 15 minutes. The liquid collected at the bottom of the larger tube contained the purified plasmid. 8µl of this product was then run a 1% agarose gel to confirm that the purification procedure was successful. 7.5µl of the plasmid was then used for the ligation reaction (Table 5), which was performed overnight at 16°C. The plasmid was then removed from the waterbath and stored at -20°C.

AvaI		NcoI	
With *P53* insert	Without *P53* insert	With *P53* insert	Without *P53* insert
1938bp	2290bp	1904bp	1904bp
1844bp	1938bp	1809bp	1809bp
1676bp	445bp	770bp	703bp
448bp		717bp	257bp
		70 bp	

Table 6. Restriction fragment sizes with the presence or absence of the *P53* insert

Once the vector copy number was increased using the transformation and cloning procedures (2.7), various checks were performed on the plasmid in order to confirm the absence of the *P53* insert. This was done using a variety of restriction enzymes followed by sequencing. The restriction enzymes used were AvaII (restriction site - G/GWCC) and NcoI (restriction site – C/CATGG). These were set up in 20µl reactions (1µl vector, 1µl enzyme, 2µl buffer (x10) and 16µl water) and run on 1% agarose gels (2.5.3). Table 6 shows the fragment sizes that reflected the presence or absence of the *P53* insert. To confirm absolutely the absence of the *P53* insert, the vectors were then sequenced back from exon 6 (using primer 6.1 – Table 3) over the ligation point. This technique followed the same protocol as in 2.5.4/2.5.5, excluding the shrimp alkaline phophatase/exonuclease I stage (there were no free ddNTPs in the vector solution). In addition, because the plasmid DNA from each vector was extremely concentrated, only 0.5µl of dissolved vector was required for the sequencing procedure (as opposed to 5µl of genomic DNA from the cell lines). The sequencing protocol was otherwise unchanged.

2.6.3. Construction of P53Mt135EGFP vector

The p53Mt135EGFP (5.9kbp) vector was constructed by removing the p53mt135 sequence from a pCMV vector (also by Clontech) called pCMV-p53mt135 (4.7kbp) and ligating it into an empty EGFP vector. The *P53* mutant contains a G∏A mutation at codon 135 (TGC∏TAC: Cys∏Val), resulting in a protein that can interact with wild-type *P53* and inhibit DNA binding. Two enzymes were used for this assay, HindIII (restriction site-A/AGCTT) and BamHI (restriction site-G/GATCC). These were used to cut both pCMV-p53mt135 and pp53-EGFP. Both these vectors contained a HindIII and a BamHI site at either end of the *P53* insert. Thus this restriction digest provided the corresponding ligation points necessary for joining the p53mt135 sequence to the empty EGFP vector.

5µl of each vector was used in the two restriction digests (Table 7). 0.7% agarose gels were then run of the cut sequences to separate the inserts from the vectors (2.5.3). The pp53-EGFP vector resulted in a 4.7Kb EGFP -containing fragment (similar to that in 2.6.2 with a different tail end sequence) and a 1.2 Kb fragment containing the wild-type *P53* insert. The pCMVp53mt135 vector resulted in a 3.5kBp fragment and a 1.2kb fragment containing the mutant p53 insert. The EGFP 4.7kb fragment was then cut from the gel, together with the 1.2kb mutant135 p53fragment. These were then purified from the 0.7% agarose as in 2.6.2 and ligated at 16°C overnight (Table 7). A greater amount of the 1.2kb insert was introduced to the mixture to ensure no ligation of mis-matching base pairs at the free ends of the 4.7kb EGFP vector. This would theoretically result in empty 4.7kb EGFP vectors that would multiply during the cloning procedure. Following the ligation procedure the samples were stored at -20°C.

After the transformation procedure (2.7.1), PCR reactions were set up using 10 random colony lysates (a cocktail stick was inserted into the middle of each colony, mixed into 10µl of ddH_2O and heated to 90°C) to amplify and detect the p53mt135insert within the EGFPvector. This was done using 2 primers, one of which recognised a sense sequence on the CMV promotor region (CMV1) and antisense primer ex4.3 (on exon 4) which was postioned well into the p53gene (630bp). The PCR reaction was set up as in 2.5.2. Once the samples had been run on a 1% agarose gel (2.5.3), 2 positive colonies were chosen at random, cloned, purified then sequenced from the anisense primer 6.1 (on exon 6) over nucleotide 1017 to confirm the presence of the point mutation. Because the purified vector

was sequenced directly, the protocol was followed exactly as that in 2.5.4./2.5.5. excluding the shrimp alkaline phosphatase/exonuclease I stage.

Digestion of pCMVp53mt135	Digestion of pp53-EGFP	Ligation of mt135 insert with EGFP vector
81μl ddH_2O	81μl ddH_2O	14.5μl 1.2kb mt135insert
10μl buffer (x10) –React 1	10μl buffer (x10) –React 1	1μl 4.7kb empty EGFP vector
3μl Hind III	3μl Hind III	0.5μl T4 ligase
1μl BamHI	1μl BamHI	4μl buffer (x5)
5μl pCMVp53mt135 vector (Clontech)	5μl pp53-EGFP vector (Clontech)	

Table 7. List of reagents for the creation of p53mt135EGFP. All reagents are from Life technologies unless otherwise stated.

2.6.4. Construction of P53Mt144EGFP vector

The p53mutant144 insert (mutation at codon 144: CAG[]TAG) encodes a mutant p53 protein that is incapable of activating the down stream effector molecules of p53. It does not have a dominant negative effect similar to the mt135 protein. The mutant144 sequence was PCR amplified from the pC53-SCX3 vector, originally designed by Vogelstein et al in 1990, and ligated into an empty EGFP vector. The pC53-SCX3 vector does not have compatible HindIII/BamHI restriction sites either end of the *P53* insert that correspond with sites on the empty EGFP vector. As a result, of the two primers used to amplify the mutant 144 *P53* insert, one contained a 'free' HINDIII site attached to the sense primer sequence on exon 2 (2.1HIND)and the other contained a BamHI site attached to the antisense primer sequence on exon 11(11.1BAM). The primer sequences are shown in Table 8. An ACGT sequence was added to the restriction sites on each primer to aid restriction enzyme recognition. A large volume PCR reaction was set up (100μl) in order to amplify enough mt144 insert for the ligation phase (Table 9). The PCR reaction was set up for 30 cycles at 94°C for 30 seconds, 58°C for 30 seconds and 72°C for 1 minute for each cycle. Once the PCR reaction was complete, 8μl of the product was run on a 1% agarose gel (2.5.3) to confirm the size of the insert was correct (1.2Kb). The remaining PCR product was digested using HindII and BamHI restriction enzymes (Table 9) at 37°C for 1 hour to clear the ligation ends of ddNTPs. Following this, a ligation reaction was

performed using the digested 1.2Kb fragment and the empty 4.7Kb EGFP vector from 2.6.3 that contained the appropriate compatible ligation points (Table 9). This reaction was performed at 16°C overnight and then stored at –20°C preceeding the transformation of chemically competent cells.

Ex2.1BAM 5' ACGT**G^GATCC**GTGGGGAACAAGAAGTGG
Ex11.1HIND 5' ACGT**A^AGCTT**CAGCCAGACTGCCTTCCG

Table 8. Primer sequences for the amplification of the mutant 144 vector. Restriction sites are marked in ^bold.

PCR of mutant144 insert	Digestion of mutant 144 insert	Ligation of mt144 insert with EGFP vector
95µl ddH2O	84µl mt144insert PCR product	14.5µl 1.2kb mt144insert
15µl reaction buffer	10µl buffer (10x, react 1)	1µl 4.7kb empty EGFP vector
24µl ddNTPs	1µl BamHI	0.5µl T4 ligase
7.5µl Ex2.1HIND primer	3µl HindIII	4µl T4 buffer (x5)
7.5µl Ex11.1BAM primer		
1µl Taq polymerase		
1µl pC53-SCX3 vector		

Table 9. Reagent list for the development of p53mt144EGFP. All reagents are from Life technologies unless otherwise stated

To confirm the presence of the mt144 form of *P53*, PCR reactions were set up, using 3 colony lysates (only 3 colonies grew on the plate), to amplify the fragment between sense primer ex4.1 and antisense primer ex6.1 (Table 3). After the gel was run the samples which contained a band at 518bp were digested with the enzyme HhaI. HhaI recognises and cuts DNA at G/CGC. Because a vector containing the mutant 144 insert contains one more GCGC site than the WT insert, this restriction digest could distinguish between the two inserts should the WT insert have remained attached to the EGFP vector. The mt144PCR product cuts into a 320bp fragment plus 4smaller fragments, whereas the WT fragments cuts into a 370bp fragment plus 3 smaller fragments. Once a sample was found

to contain the 320bp fragment, ie. a mt144 vector identified, the PCR product was sequenced as in 2.5.

2.7. Cloning procedure

2.7.1. Transformation of chemically competent E.Coli

Invitrogen One Shot TOP10 chemically competent cells (Invitrogen BV, PO Box 2312, 9704 CG Groningen, The Netherlands) were transformed with the above plasmids (pp53-EGFP, PO-EGFP, pp53mt135-EGFP and pp53mt144-EGFP). The ligation reactions were thawed, centrifuged and placed on ice. For each transformation, one 50μl vial of One Shot cells was also thawed on ice. 1 to 5μl of each ligation reaction was pipetted directly onto the competant cells and mixed by gentle tapping. The remaining ligation mixture was stored at –20°C. The vials were then incubated on ice for 30 minutes. Following this, the vials were incubated for exactly 30seconds at 42°C in a waterbath then promptly removed and placed on ice. 250μl of pre-warmed SOC medium was then added to each vial under sterile conditions. The vials were then placed in a microcentrifuge rack on it side and shaken at 37°C for 1hour at 225rpm in a shaking incubator. Approximately 100μl of each transformation mixture was then spread onto LB agar plates (12g bactoagarose in 1L ddH2O, autoclaved and poured into petri dishes)containing a 200μM concentration of kanamycin. The plates were then inverted and incubated overnight at 37°C.

The following day colonies were picked and in some cases tested for the possession of the appropriate insert (for the mutant vectors, see 2.6.3 and 2.6.4) using boiled cell lysates. Single colonies derived from bacteria containing each of the 4 vectors were then picked using cocktail sticks and placed in 500ml of nutrient broth (5g yeast extract, 10g bactoagarose, 10g NaCl, 1L ddH_2O) containing 300μl (50mg/ml) kanamycin in 1.5L conical flasks. These were then grown at 37°C for 12-16hours with vigorous shaking (~300rpm) until a cell density was reached of approximately 2-4x10^9 cells per ml.

2.7.2. Plasmid purification protocol

Plasmid purification was performed using a Qiagen Plasmid Maxi-prep kit (Qiagen, Boundary Court, Gatwick Road, Crawley, West Sussex, UK). Each 500ml bacterial suspension was divided between two 250ml sorvall containers and centrifuged at 6000g for 15 minutes at 4°C using a Sorvall SS15 rotor. 5mls of resuspension buffer was then added to each container and mixed to resuspend the pellet. The resulting 10mls of

resuspended bacteria was then transferred to a 30ml centrifuge tube and 10mls of lysis buffer added. The lysate was then mixed gently by inverting 4-6 times and incubated at room temperature for 5 minutes. 4mls of precipitation buffer was then added and the mixture was inverted 4-6 times and incubated on ice for 20minutes. A white fluffy material then formed and the lysates became less viscous. This precipitated material contained genomic DNA, proteins, cell debris and SDS. The mixture was then centrifuged at 20,000g for 30minutes using a sorvall SS-34 rotor. While the lysate was being centrifuged, 10mls of equilibrium solution was added to equilibrate the Qiagen-tip before adding the dissolved plasmid DNA. The Qiagen-tip column contains a filter which traps plasmid DNA. It flows automatically by a reduction in surface tension due the presence of detergent in the equilibium buffer.

Immediately after the centrifugation process was finished, the supernatent (which should be clear) was removed from the tube and pipetted into an equilibriated Qiagen-tip column. Often a second centrifugation step was required to maximise transfer of plasmid DNA and to remove as much protein as possible. Once the supernatent had passed completely through the column, 20ml of wash buffer was added to remove any contaminants from the plasmid DNA and to ensure all of the DNA had passed into the filter. The DNA was then eluted by adding 15mls of elution solution to the column and collecting the eluate in another 30ml tube. The DNA was then precipitated by adding 0.7 volumes (10.5mls) of room-temperature isopropanol. The resultant solution was then mixed and centrifuged at 15000g for 1hour at 4°C. A small white pellet should be apparent at the base of the tube. The supernatant was then removed and 1ml of 70% ethanol was added in order to wash the pellet. The pellet was then dislodged from the 30ml tube and transfered it to a 1.5ml eppendorf tube. The tube was then centrifuged at 15000g for 10minutes using a benchtop centrifuge. Once the supernatent was removed the pellet was airdried for 5-10 minutes and 0.5ml of ddH_2O added. The plasmid could then be stored at 4°C until required.

2.8. Linearisation of EGFP vectors

2.8.1. ApaLI restriction digest

To increase the likelyhood of stable transfectants forming during the transfection procedure (2.9.1 and 2.9.2), the plasmid only/ *P53* signalling vectors were linearised. This was done using a restriction digest using the restriction enzyme ApaLI (Table 10). One suitable restriction site existed on all 4 vectors created. This site was situated on the pUC

origin of replication for the propagation of E. Coli. This region was no longer required as the cloning procedure had been completed. Once the restriction digest was complete (after 1hr at 37°C), a 1μl sample was run on a 0.7% gel (for 1hour). This was run to check that the product was the correct size, 4.7kb in the case of the plasmid only vector and 5.9kb in the case of the vectors containing the various *P53* sequences. Non-linearised vectors are usually supercoiled and do not run on agarose gels at the correct size.

Linearisation restriction digest
300μl plasmid
150μl buffer (x10) (NEB)
15μl BSA (x100) (NEB)
5μl ApaLI (NEB)
1030μl H_2O

Table 10. ApaLI restriction digest

2.8.2. Precipitation of linearized vectors

The DNA was then precipitated and reconstituted to reduce the volume of the linearised vector back to the original 300μl. This technique also removed any residual protein present from the cloning procedure and also the restriction enzyme from the linearisation digest. The 1500μl samples were split into 1.5 eppendorf tubes in 300μl aliquots and 300μl of Phenol and 300μl chloroform added to each. They were then spun at 10,000rpm for 2 minutes and the top layer of transparent liquid transferred into separate tubes. Care was taken not to disturb the intermediate layer containing any impurities such as protein. 60μl of Sodium Acetate (NaOAc) was then added to each sample together with 500μl of 100% ethanol. The samples were then mixed and spun at 10000rpm for 10minutes to precipitate and pellet the plasmid. The supernatent was then poured off and 70% ethanol added to wash the sample. The plasmid samples were then spun again for 10minutes and the supernatent removed. Following airdrying for 5 minutes, 60μl of ddH2O was added to each of 5 tubes containing the same plasmid. These were then mixed together to produce 300μl of linearised plasmid. To determine the concentration of each of the four plasmids a spectrophotometer was used.

2.9. Liposomal Transfection of U87 and U373 cell lines

2.9.1. 24-Well Optimization Protocol using Lipofectin™ reagent

In order to optimise the quantity Liposome and plasmid DNA for maximum transfection efficiency, a 24-Well Optimization Protocol was used. For each cell line to be tested a 24 well tissue culture plate was seeded with 2000 cells per well (DMEM with 10%FCS) and incubated overnight at 37°C. The following day the cells were approximately 80% confluent at the time of transfection.

To a 96 well plate, 20μl of serum free Opti-MEM medium was then added in a 6x4 format to 24 wells (similar to that of a 24well plate). For each of the two 24 well plates 60μl of Lipofectin™ reagent (LifeTechnologies Ltd) was diluted 1:5 with Opt-MEM medium (LifeTechnologies Ltd) to a final volume of 350μl. From this solution, 5, 7.5, 10, 12, 5, 15, 17.5μl were then added to the appropriate wells of the 96well plate: one lipid volume per column (Figure 7). The lipofectin mixes were then left to incubate for 30minutes at room temperature. These dilutions give a final range of 1 to 3.5μl of stock lipid.

The DNA solutions were then prepared. The plasmid only vector was used to optimize DNA concentration. For each 24 well plate to be tested, 1.4,2.8, 5.6, 8.4μg plasmid DNA (calculated from a 1.22mg/ml plasmid-only stock solution) was pipetted into 140μl volumes of Opti-MEM (giving a range of 0.2-1.2μg per 20μl well) (Figure 7). 20μl of DNA solution was then added to the appropriate wells in the 96-well plate (one DNA concentration per row) and incubated at room temperature for 45 minutes to allow DNA-lipid complexes to form..

The cells in the 24well plates were then washed in PBS and incubated at 37°C in 5%CO_2 for 30minutes in Opti-MEM to remove traces of serum. 160μl of Opti-MEM was then added to each lipid/DNA solution. The medium was then removed from the cells and the lipid-DNA complexes added. The cells were then incubated for 4 hours in an a 37°C incubator with 5%CO_2. Following this, the DNA/lipid solutions were removed from the wells and replaced by normal growth medium containing serum and antibiotics. The cells were examined after 24 and 48hours using fluorescent microsopy to assess transfection efficiency. The greatest number of viable green fluorescent cells indicated the highest transfection efficiency.

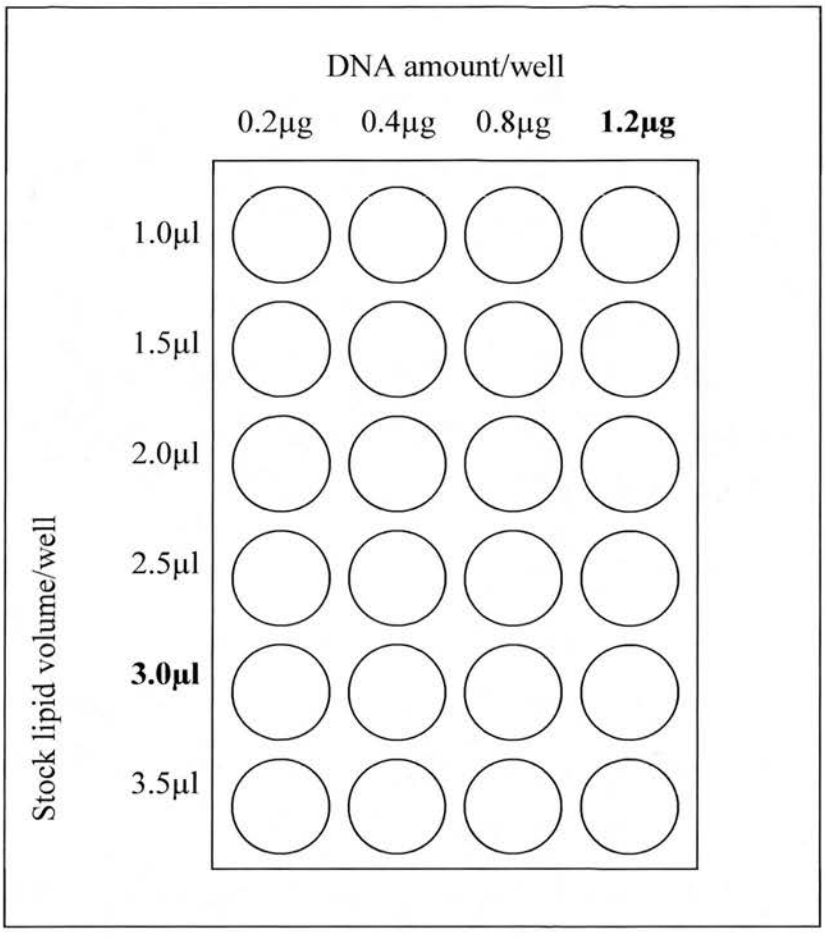

Figure 7. Liposome/DNA concentrations in 24well optimization protocol

2.9.2. Transfecting cell lines using $8cm^2$ petri dishes

Once the optimum transfection concentrations of lipid and DNA were established, the U87 and U373 cell lines were grown to 60% confluency in $8cm^2$ petri dishes in order that a large number of cells could be transfected for experimental procedures. 3mls of opti-MEM serum free medium was added to the cells 30minutes preceeding exposure to the DNA/liposome complexes.

To set up the DNA/lipid complexes, 160µl of Opti-MEM was first added to small universal containers for each dish to be transfected. The liposomal mix was then made using Lipofectin™ reagent diluted 1:5 with Opt-MEM medium. 120µl of this was then added to each universal container and incubated for 30minutes at room temperature. This quantity corresponds with the 3µl dilution as optimized from above (in bold). The stock DNA solutions were then made up using the 4 linearized vectors at 9.6µg/160µl (corresponds to the highest DNA dose from the optimization study). The plasmid stock

solutions, as read on the spectrophotometer, were: plasmid-onlyEGFP, 1.22mg/ml; p53WTEGFP, 1.28mg/ml; p53mt135EGFP, 0.98mg/ml; p53mt142EGFP, 1.15mg/ml. Each 160μl dilution was then added to the universals and incubated for 45minutes at room temperature. 1280μl of opti-MEM was then added to the DNA/lipid complexes. The medium was then removed from the cells and the total volume of each universal added to the cells for 4hours in a 37°C/CO_2 incubator. Following this, normal growth medium medium was added to the cultures for 2 days.

2.9.3. Geneticin (G418) selective antibiotic response curve

Because spheroid cultures are grown for 6 weeks, it was important that stable transfectants were developed. Transient transfections can lose their EGFP signalling probes thus reverting them back to their WT genotype.

The neomycin resistance cassette (neo^r) within the EGFP signalling probe allows geneticin (G418) resistance in eukaryotic cells. To establish the optimal concentration of G418 required to maintain and select cells containing the neo^r cassette, a G418 selective antibiotic response curve was created using the Wild-Type cell lines.

G418 antibiotic (Sigma) was diluted to a concentration of 50mg/ml in tissue culture grade ddH_2O. A 24 well plate was then set up containing 200 cells per well in normal growth medium and left to grow overnight in a 37°C/5% CO_2 incubator. The following day the medium was removed and 1ml of medium containing G418 was added to the wells. A range from 100-1200μg/ml in 100μg increments was used. 2 wells were used for each concentration. The medium was changed every 3 days and the appropriate dilution of antibiotic added. After 10days the medium was removed and the cells were washed in PBS and stained with 0.5%methylene blue and 50% methanol for 20minutes. The plates were then scored by calculating the percentage of survival by the number of individual colonies for percent confluence. A dose response curve was then generated by plotting the percentage of survival on the Y axis versus the concentration of G418 selective antibiotic in μg/ml on the X axis. The minimum concentration at which 100% of wild-type cells were non-viable was the concentration used to select for resistant neo^r containing cells.

2.9.4. Selection procedure for transfected cells containing the neo^r cassette

48hours after the transfection procedure the G418 antibiotic was added to the 8cm culture dishes. A concentration of 400μg/ml (600μM) G418 was chosen from the antibiotic selection curve for both U87 and U373 cell lines. Following 4 days at this concentration the cells in the petri dishes were washed with PBS and examined under the fluoresencent microscope. As a result of the selection process, most of the cells that remained fluoresced green. A cell scraper was used to disadhere each viable green colony from the bottom of the dish and the cells were washed into separate petridishes. These were grown for 1 month in selective medium to ensure stable transfectant had been selected. Fortunately, due to the high cell turnover, large numbers of stably transfected cells (derived from each of the 4 vectors) were produced and could be used for experiments 1.5 months after the initial transfection procedure.

The U87 and U373 transfected cell lines were grown as both monolayer and spheroid cultures (2.1.2, 2.1.3 & 2.1.5). Spheroid cultures were grown for 3 weeks where they reached a pre-necrotic state. They were then assessed immunhistochemically and by immunoblot analysis for p53, Bax, p21, MDM2 and p14 expression using the methods described (2.2 & 2.3).

2.10. MTT assay

The proliferative rates of cultured cell lines (including transfected cell lines) were determined using the MTT (3-[4,5-Dimethylthiazol-2-yl]-2,5-diphenyltetrazolium bromide) assay.

Cells were grown in 96well plates and supplemented with 100μl of growth medium per well. 50μl of MTT solution at a concentation of 1.5mg/ml of culture medium was aliquoted into each test well using a multi-channel pipette (Titertek plus; ICN biochemicals Ltd.) and the cells incubated at 37°C for 2 hours. Subsequently, 130μl of the assay mixture was carefully aspirated from each well. The formazan crystals, produced as a result of the activity of intracellular dehydrogenases, were solubilised by suspension in 150μl of dimethylsulphoxide contaiing 0.5%v/v FCS. The plates were then shaken at room temperature on an orbital shaker for 15minutes to ensure complete dissolution of the crystals and the absorbance of the resulting solution measured at 540nm on a

microplate reader (model 450; Bio-Rad Laboratories, Hemel Hempstead, Hertfordshire, UK).

5 plates corresponding to days 0-4 were used for both the MTT assay and cell counts, with 8 wells employed for each sample cell line. Each well was plated at a density of 500 hundred cells per well. Every 48 hours the medium was removed and replaced by 100μl of fresh medium. At every 24hour interval 1 plate was removed from the incubator and the cell number assessed using the MTT assay (4 wells) or by counting using a haemocytometer (4 wells).

Cells to be counted were washed twice with PBS and incubated with 20μl of 1xtrypsin – EDTA for 2 minutes at 37°C. 80μl of growth medium was then added and the 100μl of mix was pipetted into the growth chamber of the haemocytometer. The cell counts were used to validate the findings of the MTT assay for the assessment of cell proliferation and were not used for every MTT assay performed in this study.

2.11. Light microscopy

2.11.1. Phenotypic characterisation of wild-type monolayer and spheroid cultures

All light microscopy and photomicroscopy was done using an Olympus BX40 microscope with camera attachment.

Monolayer and spheroid wild-type cultures were initially examined and photographed for GFAP, vimentin and Ki67 labelling in terms of the number of positive cells and intensity of staining. The spheroid sections were also examined to establish the regional staining patterns of TUNEL, Ki67, GFAP and vimentin staining. These were all recorded photographically. This allowed comparisons to be made in terms of the qualitative distribution of these markers between monolayer and spheroid cultures. Phenotypic differences between the cell lines were also recorded.

Ki67 and apoptotic indices were quantitatively analysed for the monolayer cell lines. For consistency with spheroid cultures, H&E morphological counts were used to assess apoptotic index. A basic 'square grid' optical graticule was used to count ten 100μm random quadrants. The indices were calculated as a percentage of total cell number in each quadrant.

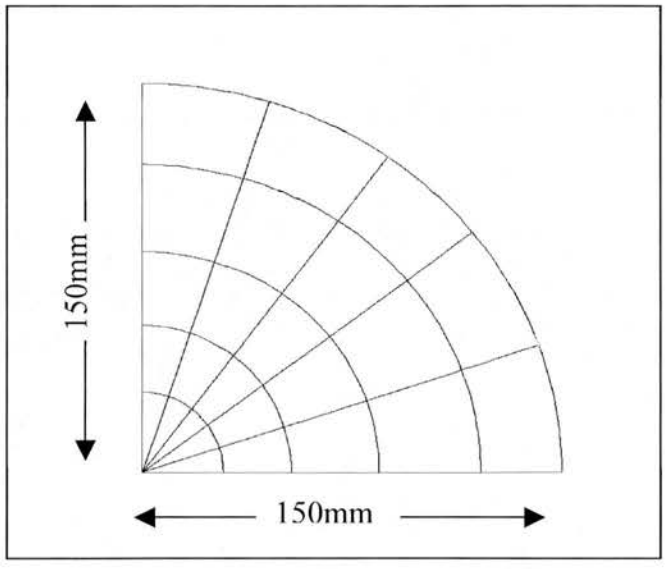

Figure 8. Diagram of the spherical graticule used for spheroid counts

H&E stained preparations were used for measurement of the radius of the spheroids for each cell line at each given time point (over the 5 week period) using a graticule. The 10 largest spheroids were measured on each slide and the average taken. These sections were also used to establish the time point for each cell line when a central area of cell death first appears. The number of cells per spheroid were also counted to determine spheroid packing density. This was done using a specially designed graticule (Graticules Division Pyser-SGI Ltd, Edenbridge, UK), to count individual segments of each spheroid examined (Figure 8). A segment representing 10% of the area of each spheroid was counted and the 10 largest spheroids (as above) from each slide were chosen. Morphological apoptotic counts were also recorded using H&E stained sections using the above technique. An apoptotic index was determined for each cell line as a percentage of total cell counts per spheroid (AI).

2.11.2. Assessment of HIF-1α expression in monolayer and spheroid cultures

A qualitative assessment of HIF-1α distribution was recorded for the monolayer cultures and wild-type spheroid cultures. Examination was particularly focused on spheroid central regions and areas of necrosis *in vivo*. Wild-type monolayer cells were assessed to establish basal levels of HIF-1α expression.

2.11.3. Qualitative assessment of p53 and p53 related antigens in monolayer cultures, spheroid cultures and human glioblastoma biopsies

The immunohistochemical staining of biopsy sections, monolayer culture sections and spheroid culture sections were assessed semi-quantatively according to staining intensity (0 absent, 1 weak, 2 moderate, 3 strong) and by an estimate of the proportion of cells staining (+ <25%, ++ 25-50%, +++ 50-75%, ++++ 75-100%). The presence of only isolated positive cells was considered negative.

The expression of Bax, p21, MDM2 and $p14^{ARF}$ was compared to the p53 status of the cell lines used in the spheroid experiments and the extent of p53 protein expression in the biopsy cases. Over expression of the p53 protein in morphologically healthy tumours cells suggests the presence of *P53* mutations (both the antibodies used in this study labelled both mutant and wild-type p53 protein). For the purposes of statistical analysis the biopsy cases were divided into two groups for each antibody, those with no, or focal expression and those with higher expression. In the case of p53, where staining ranged from none to very strong and diffuse, the low expression group was defined as those with scores of 0, 1+ or 2+ and the high expressor group as >2+. For p21, Bax and MDM2, expression was generally weaker and more focal.

In addition to recording the staining intensity and number of stained cells, the distribution of staining within the study material was also examined. Any enhancement of protein expression was recorded within central regions of pre-necrotic spheroids and around the perinecrotic zone in larger spheroid cultures (weeks 3-5) and biopsy material. Enhancement of staining around the periphery of the spheroid cultures and any variation in the cellular localization of the proteins was also recorded (eg.a nuclear to cytoplasmic shift).

2.11.4. Analysis of cell death in spheroids transfected with wild-type and mutant *P53* vectors

The U87 and U373 cell lines transfected with wild-type *P53* vectors and mutant *P53* vectors were labelled with H&E as in 2.2.1 and the size and apoptotic index recorded as in 2.11.1. The different clones could then be compared in terms of overall growth patterns and type and extent of central cell death.

2.11.5. Analysis of p53 and p53 related antigens within transfected week 3 spheroids

Week 3 spheroids derived from the U87 and U373 transfected cells lines were labelled with p53 and p53 related antibodies. These could be compared in terms of level, intensity and distribution using the same criteria as in 2.11.2. Particular care was taken to observe any changes in protein distribution around central areas of necrosis.

2.12. Statistics

A split plot analysis of variance (SPANOVA) was used to assess the MTT data for the four cell lines examined (MOG-G-CCM, U87, U373 and A172). The null hypothesis was set up where 'total cell number remains the same between monolayer cell lines over the 5 day period'. After finding that Mauchly's test of sphericity was significant (establishes that the values are spread within a normal curve), the F-ratio was obtained using the new degrees of freedom calculated using the Huynh-Fel Epsilon value.

A split plot analysis of variance (SPANOVA) was used to assess the in situ cell counts, apoptotic index results and growth data over the 5 week period of spheroid growth. To analyse the in situ cell counts, the null hypothesis was set up where 'the total number of cells per spheroid remains the same between cell lines and transfected cell lines over time'. After finding that Mauchly's test of sphericity was significant (establishes that the values are spread within a normal curve), the F-ratio was obtained using the new degrees of freedom calculated using the Huynh-Fel Epsilon value. To analyse the distribution of apoptotic index over time, the null hypothesis was set up where 'The apoptotic index of each spheroid remains the same between cell lines over time'. After finding that Mauchly's test of sphericity was significant, again the F-ratio was obtained using the new degrees of freedom calculated using the Huynh-Fel Epsilon value. To analyse spheroid size between cell lines over time, the null hypothesis was set up where 'The radius of each spheroid remains the same between cell lines over time'. Again, after finding that Mauchly's test of sphericity was significant, again the F-ratio was obtained using the new degrees of freedom calculated using the Huynh-Fel Epsilon value.

A split plot analysis of variance was also used to assess the in situ cell counts, apoptotic index results and growth data over the 5 week period of growth for U373 and U87 spheroids transfected with *P53* wild-type and mutant vectors. The null hypotheses were set up where 'The number of cells within spheroids derived from U87 cells transfected with *P53* wild-type and mutant vectors spheroids remain the same over time' and 'the

number of cells within spheroids derived from U373 cells transfected with *P53* wild-type and mutant vectors remain the same over time'. Also the null hypotheses were set up where 'The radius of spheroids derived from U87 cells transfected with *P53* wild-type and mutant vectors spheroid remain the same over time' and 'The radius of spheroids derived from U373 cells transfected with *P53* wild-type and mutant vectors spheroid remain the same over time'. In addition, the null hypotheses were set up where 'The apoptotic index of spheroids derived from U87 cells transfected with *P53* wild-type and mutant vectors spheroid remain the same over time' and 'The apoptotic index of spheroids derived from U373 cells transfected with *P53* wild-type and mutant vectors spheroid remain the same over time'. After testing these hypotheses using the SPANOVA test, Mauchly's test of sphericity was applied. After being found to be significant, the F-ratio was obtained using the new degrees of freedom calculated using the Huynh-Fel Epsilon value.

To analyse the ultrastructural data (the electron microscopy), a Chi^2 analysis was completed to determine whether the observed apoptotic and necrotic indices where significantly different between cell lines at week 3.

For the biopsy cases, distributions of high and low expression for different p53 related antibodies (Bax, p21, MDM2) were compared with extent of p53 expression using the Chi-squared test with continuity correction for small numbers. Multiple pairwise comparisons were made and the Bonferroni correction procedure was used. Five comparisons were made with each antibody, so that a threshold for significance of $P = 0.01$ was used.

All statistical analyses were performed with help from Dr Mark Walker at the Department of Clinical Neurosciences, Western General Hospital, Edinburgh.

CHAPTER 3

GLIOMA SPHEROID CHARACTERISATION

3.1. Introduction

Most studies utilising the glioma spheroid system have focused on invasion and the importance of certain extracellular matrix molecules (Bell et al., 1999; Terzis et al., 1997; Paulus et al., 1994; Tamaki et al., 1997). This is not surprising, due to the highly invasive nature of the diffuse astrocytoma group of tumours. However, no studies, as yet, have purely concentrated on the regulation of central cell death within glioma spheroids. Studies using spheroids derived from other tumour types have previously examined metabolite levels within populations of cycling, non-cycling and dying cell populations (Durand et al., 1998; Walenta et al., 2000; Mueller-Kleiser et al., 1986). These studies have come to very interesting conclusions about the way in which tumour cell populations respond to stress. A summary of these findings published in 2000, suggests that different cell types possess different cell death responses to metabolic stress (Mueller-Klieser, 2000). For example, V79 hamster lung cancer spheroids form areas of central apoptosis preceding changes which morphologically resemble necrosis. In contrast, other spheroid types such as EMT6 sarcoma spheroids, exhibit massive necrosis as the preliminary cell death event. The variation in the cell death responses of these two cell types suggests that the pathways involved in activating cell death in these systems are different. To investigate the development and control of cell death in glioblastoma spheroids it is therefore vital to elucidate the primary cell death events. Because spheroid studies examining endogenous patterns of glioma cell growth and death are rather limited, it was first important to fully characterize the glioma spheroid system using a variety of cell lines.

In the first part of this study, glioma spheroids derived from the cell lines U87, U373, MOG-G-CCM and A172 were assessed over a 5 week growth period. The aims of these experiments were (i) to determine the phenotypic similarity of glioma spheroids to glioblastoma tissue *in vivo* (ii) to identify overall growth patterns and specific zones of proliferation, differentiation and death (iii) to define the time course of the onset of central cell death (iv) to establish the initial and subsequent modes of cell death employed by cells in the centre of the glioma spheroids (v) to determine whether proteins that are normally upregulated in response to metabolic stress in glioblastoma are associated with these areas of cell death.

3.2. Results

3.2.1. Phenotypic characterisation of monolayer and spheroid cultures

In monolayer culture, the 4 cell lines U87, U373, MOG-G-CCM and A172 exhibited a mainly epithelial-like morphology. U373 and A172 cultures rarely contained cells dissimilar to this, although a few cells exhibiting fibroblast-type (spindle shaped with process formation) morphologies were seen. U87 cell line formed 3-dimensional aggregates in monolayer culture, which would often dissociate from the culture flask (Figure 9A). In between this 3-dimentional network, a fine mesh of fibroblast-like cells grew across areas of the flask not inhabited by the epithelial-like cultures (Figure 9A). MOG-G-CCM cells were the most phenotypically diverse in culture (Figure 9C), with approximately 30% of cells exhibiting a fibroblast-like morphology and others with large cell bodies, centrally located nuclei and up to 5-10 processes, imparting a morphology similar to that of neurons.

Examination of spheroids derived from the 4 cell lines revealed that U87, MOG-G-CCM and A172 shared almost identical phenotypic traits (Figure 10). Two days after seeding the cells formed aggregates in culture, which after 7 days formed uniform spheres of a similar size. These spheres continued to grow over the 5 week period in the same uniform shape. In contrast, U373 formed spheroids after 7 days that were often irregularly shaped. Examination under the inverted microscope revealed that this was due to small spheroids (from days 1-3) sticking together to form irregularly shaped aggregates (Figure 14C). As the U373 spheroids grew over the 5 week period, the shape of the aggregates did not appear to become more complex. Therefore the initial 2-3 days of U373 culture seemed to be the single time point when the small spheroids fused together. Because the U373 spheroids continued to grow in consistent shapes from this time point onwards, measurements could be taken in cross-section at the narrowest point from the spheroid periphery to the spheroid centre in an identical manner to the more spherical U87, MOG-G-CCM and A172 spheroids.

In cross section, large spheroids (weeks 3-5) derived from all 4 cell lines appeared to consist of 3 concentric zones. At the periphery, small, rounded cells were present. Inside this layer of cells, a tightly packed layer of concentrically orientated, bipolar cells were present, circling the spheroid centre (Figure 10C). These two zones were collectively

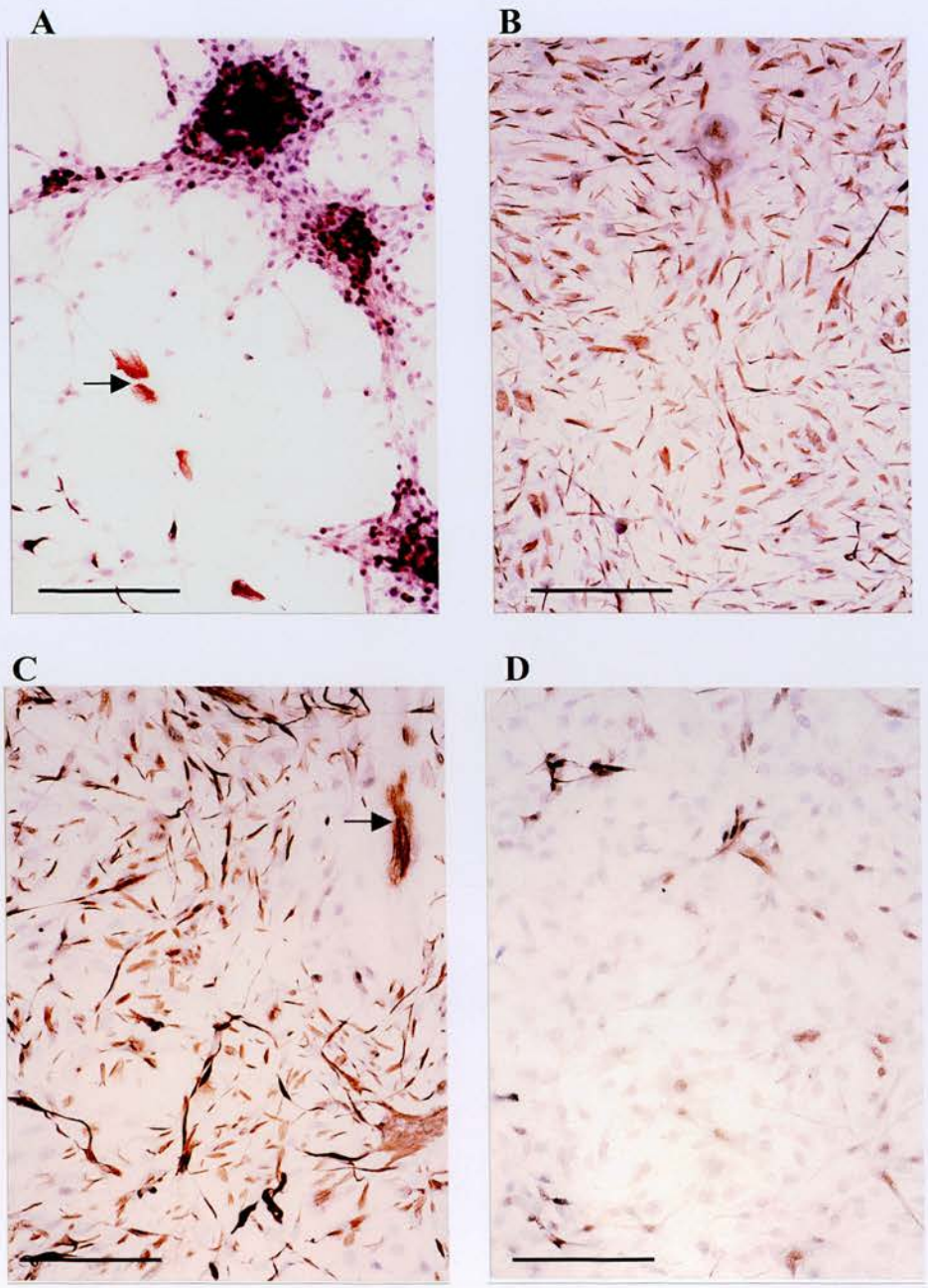

Figure 9. Photomicrograph of U87 (A), U373 (B), MOG-G-CCM (C), A172 (D) monolayer cultures exhibiting GFAP labelling. Arrows point to strongly labelled fibroblast-like cells. All bars=100μm

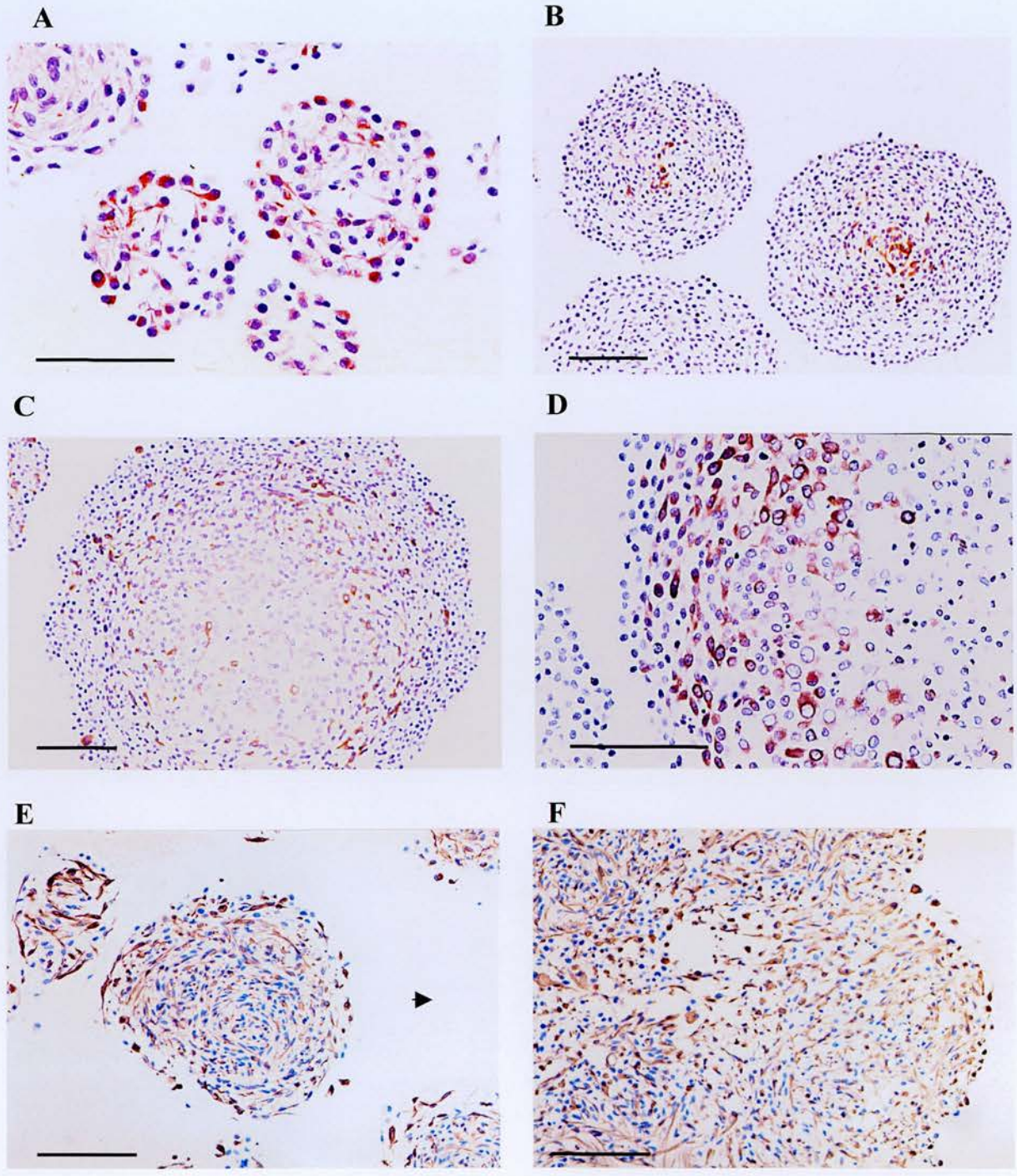

Figure 10. GFAP labelling in spheroid cultures. A, week 1 U87 spheroids showing random GFAP labelling across the radius B, central labelling pattern observed at week 2 in U87 spheroids. C&D, concentric arrangement of GFAP labelling around the spheroid centre from weeks 3-5 in U87 spheroids. E&F, U373 spheroid exhibiting uniform GFAP labeling pattern at weeks 1 and 4 respectively. All bars=100μm.

termed the 'viable rim'. In the spheroid centre, areas of necrosis formed containing numerous pyknotic and karyorrhactic cells (Figure 10D).

Ultrastructural examination of individual spheroids derived from the 4 cell lines revealed that the cells formed intermediate junctions and became closely packed together as the spheroids became larger (Figure 15A). This was particularly apparent within the viable rim at weeks 3-4. The cells around the periphery of the spheroid became polarised with the nucleus basally located towards the spheroid centre (Figure 15B). The cells situated within the region of differentiation (GFAP positive cells) formed a concentric arrangement around the spheroid centre (data not shown).

3.2.2. GFAP and Vimentin labelling

Expression of glial fibrillary acidic protein (GFAP) in the 4 cell lines, MOG-G-CCM, U87, U373 and A172 confirmed their glial status in monolayer culture (Figure 9). Staining was strongest in U373 and MOG-G-CCM (Figures 9B and C) cell line followed by U87 cell line and A172 cell line (Figures 9A and D). A172 possessed isolated, strongly labelled GFAP positive cells. Strong GFAP labelling was seen within the centre of the 3-dimentional aggregates in U87 monolayer culture. In addition, flat, fibroblast-like cells were observed in U87 and MOG-G-CCM cells and these labelled very strongly with the GFAP antibody (Figure 9A). Approximately 60-90% of cells were weakly/strongly GFAP positive in the four cell lines examined.

In spheroid cultures the distribution of GFAP labelling varied over the 5 week period. In spheroids derived from the cell lines U87, MOG-G-CCM and A172, GFAP positive cells were diffusely scattered across the radius of the spheroid at week 1(Figure 10A). As the spheroids became larger at week 2, GFAP labelling was observed in the centre of the spheroids (Figure 10B). By week 4 GFAP positive cells were found in a ring around the centre of the spheroid (Figure 10C and D), with loss of staining in the spheroid centre and no labelling of the outer proliferating cells. In U373 cell line, strong GFAP labelling was distributed across the entire spheroid mass from weeks 1 to 5 (Figure 10E and F). The antibody against human vimentin demonstrated a similar pattern to GFAP although the staining was fainter (data not shown).

3.2.3. Monolayer and spheroid growth kinetics

To assess cell proliferation in monolayer culture, accurate comparisons could not be made between different cell lines using the MTT assay alone. This is because the activity of intracellular dehydrogenases in different cell lines may vary. However, initial experiments using cell counts in parallel with the MTT assay showed that in the case of the four cell lines used in this study, the MTT assay was an accurate way of measuring the viable cell population over a 5 day period (Figure 11A). The A172 cell line was found to have a significantly faster growth rate than the other cell lines studied ($p<0.01$). This was followed by U87 and U373 cell lines which had very similar growth rates. MOG-G-CCM cell line possessed the slowest growth rate compared to the other 3 cell lines ($p<0.01$) (Figure 11B).

The 4 cell lines showed similar shaped growth curves when grown as spheroids (Figure 12A). At the end of the first week the spheroids were approximately 100μm in diameter. This increased over 4 weeks until the spheroids reached an average diameter of approximately 1.2mm. There was a significant difference in the radius measurements taken between A172 and MOG-G-CCM cell lines over time ($p<0.01$). A172 spheroids grew to nearly 1.4mm in diameter compared to approximately 1mm by week 5 in the MOG-G-CCM cell lines. There was no significant difference between U87 and U373 and any of the other cell lines. Between weeks 1-3 the cell counts remained low (below or around 2000 cells/spheroid). This was followed by a large increase in cell number from weeks 3-4 (Figure 12B). By week 5 the cell numbers had plateaued out at approximately 10,000 cells per spheroid. The differences in cell number over time were statistically significant over time between cell lines. A172 spheroids contained the largest number of cells over the 5 week period compared to the other 3 cell lines ($p<0.001$) with a maximum cell number of 14,000 cells at week 5. There was no significant difference in cell number between U87, MOG-G-CCM and U373 cell lines. The low number of cells present between weeks 1 and 3 was reflected in the packing density (number of cells per mm^2), which dropped considerably over this time frame (Figure 12C).

3.2.4. Ki67 labelling in monolayer and spheroid culture

Ki67 labelling was observed in the four cell lines as a granular nuclear stain (Figure 13). MOG-G-CCM had less Ki67 positive cells than the other 3 cell lines (Figure 13C). U87,

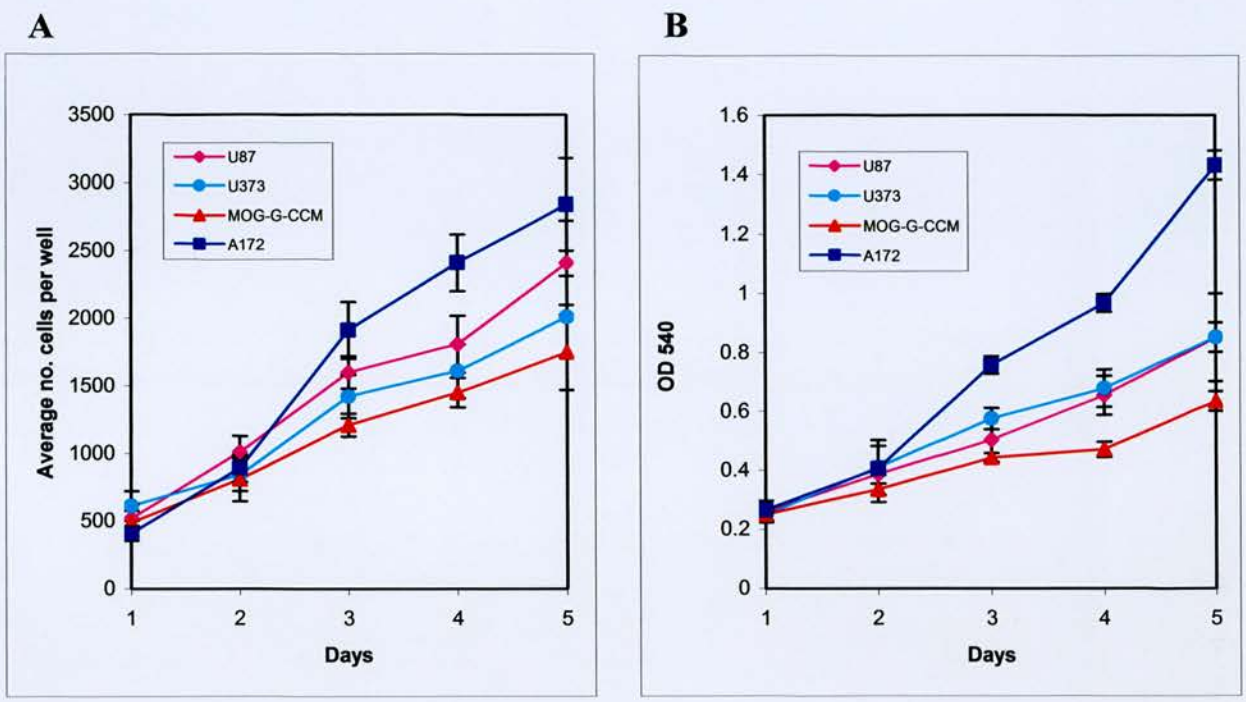

Figure 11. Graph showing the growth of U87, U373, MOG-G-CCM and A172 cells when grown in monolayer culture. A, number of cells per well (n=10) over 5 days. B, optical density MTS reading (n=10) over 5 days. Error bars illustrate the standard deviation from the mean.

Figure 12. Graphs showing the growth characteristics of U373, U87, MOG-G-CCM and A172 cell lines when grown as spheroids. A, length of spheroid radius over time for each cell line. B, number of cells per spheroid for each cell line over time. C, packing density for each spheroid derived from each cell line over time (number of cells per mm^2). D, extent of necrosis in each cell line over time, ie. the percentage of the radius consisting of necrotic cells. E, graph showing the percentage of spheroids (derived from all four cell lines) containing areas of necrosis over weeks 1-5. F, apoptotic index (AI) for each spheroid derived from each cell line over time. N=10 for each point on the above graphs. Standard error bars are shown.

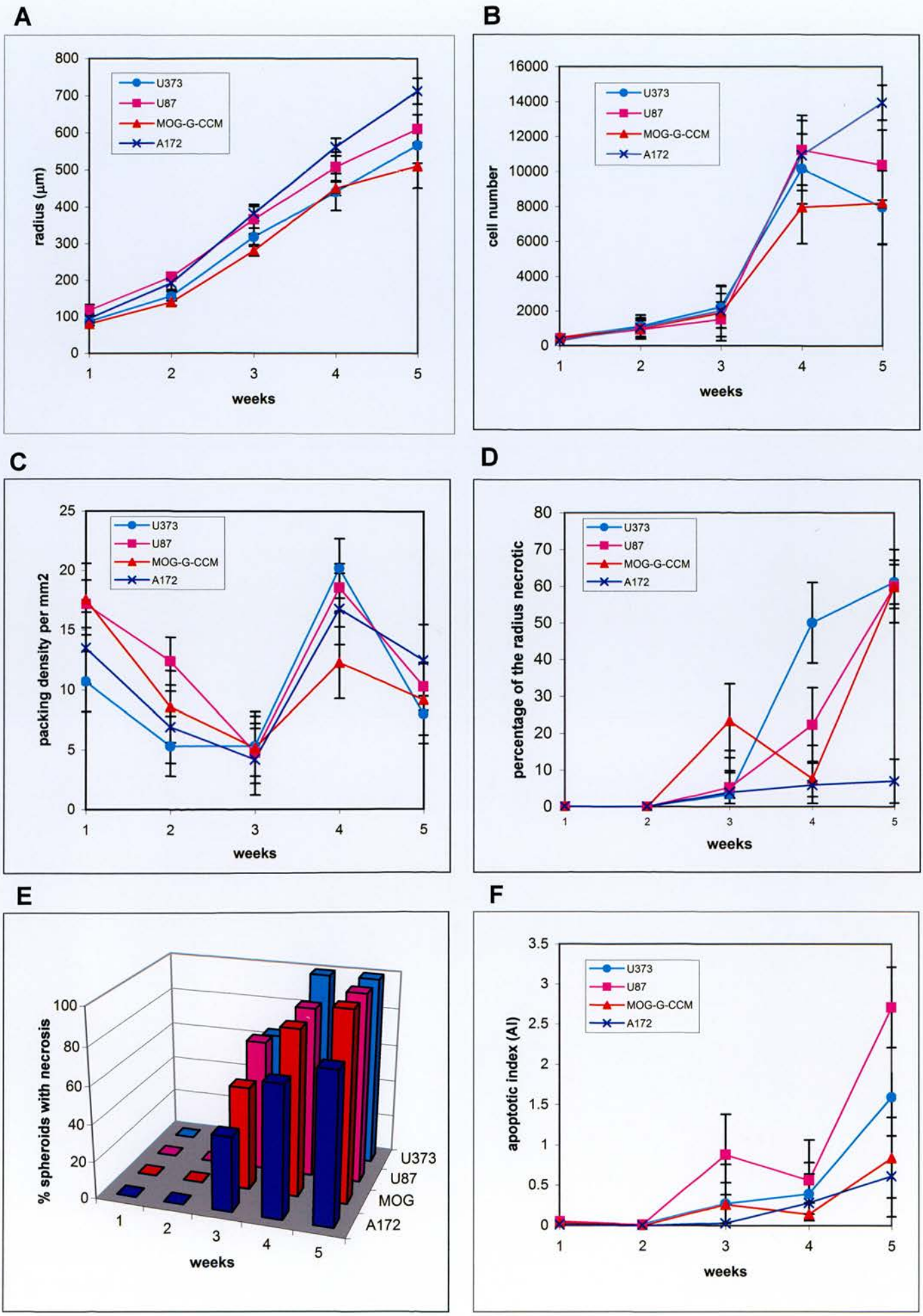
A
radius (µm)
weeks
U373
U87
MOG-G-CCM
A172
B
cell number
weeks
C
packing density per mm2
weeks
D
percentage of the radius necrotic
weeks
E
% spheroids with necrosis
weeks
U373
U87
MOG
A172
F
apoptotic index (AI)
weeks

U373 and A172 all had Ki67 labelling indices of around 65-70%, whereas MOG-G-CCM cell line had a Ki67 labelling index of approximately 30%.

In spheroids derived from the above cell lines, the Ki67 antibody labelled cells randomly across the radius of the spheroids with a similar distribution to GFAP but with a nuclear pattern of staining at week 1 (Figures 14A and C). However, by week 2 Ki67 was confined to the perimeter of the spheroids and no positive cells were observed in the centre (Figures 14B and D). This proliferative rim was approximately 100μm in diameter and was consistent in all of the cells lines examined. Because of the irregular shape of U373 spheroids, the Ki67 peripheral labelling was often not as evenly distributed as with the other cell lines (Figures 14C and D).

3.2.5. Qualitative analysis of cell death in monolayer and spheroid cultures

In monolayer culture, random apoptotic cells were observed in each of the cell lines at 80% confluence. These were identified by the appearance of pyknotic nuclei, nuclear fragmentation and/or membrane blebbing (Figures 16A and B).

In spheroid culture, central cell death developed over week 3 in all four cell lines examined although the spheroids varied in size at this time point (approx.600μm-800μm). The extent of necrosis varied considerably between lines (Fig 12D). At week 3 nearly all the spheroids derived from each cell line contained areas of necrosis (Figure 12E). Thus necrosis could be accurately predicted at a certain time point and size for each cell line. By week 5 the areas of necrosis were very large in 3 of the 4 cell lines, U87, MOG-G-CCM and U373 (Figure 12D). Although unlike U87 and U373 spheroids, some cellular regrowth appeared in MOG-G-CCM line over week 4. The remaining cells became closely packed together around the periphery thus no significant changes were observed in overall packing density (Figure 12C). A172 exhibited a different pattern of necrosis where the percentage of the radius that was necrotic over weeks 3-4 did not increase above 10% (Figure 12D).

Using week 3 spheroids it was possible to identify three morphological types of cell death using electron microscopy. The first type was characteristic by large swollen cells, dilation of organelles and break up of the cell membrane, features typical of necrosis (Figure 15C). The second type was characteristic of apoptosis: electron dense cells

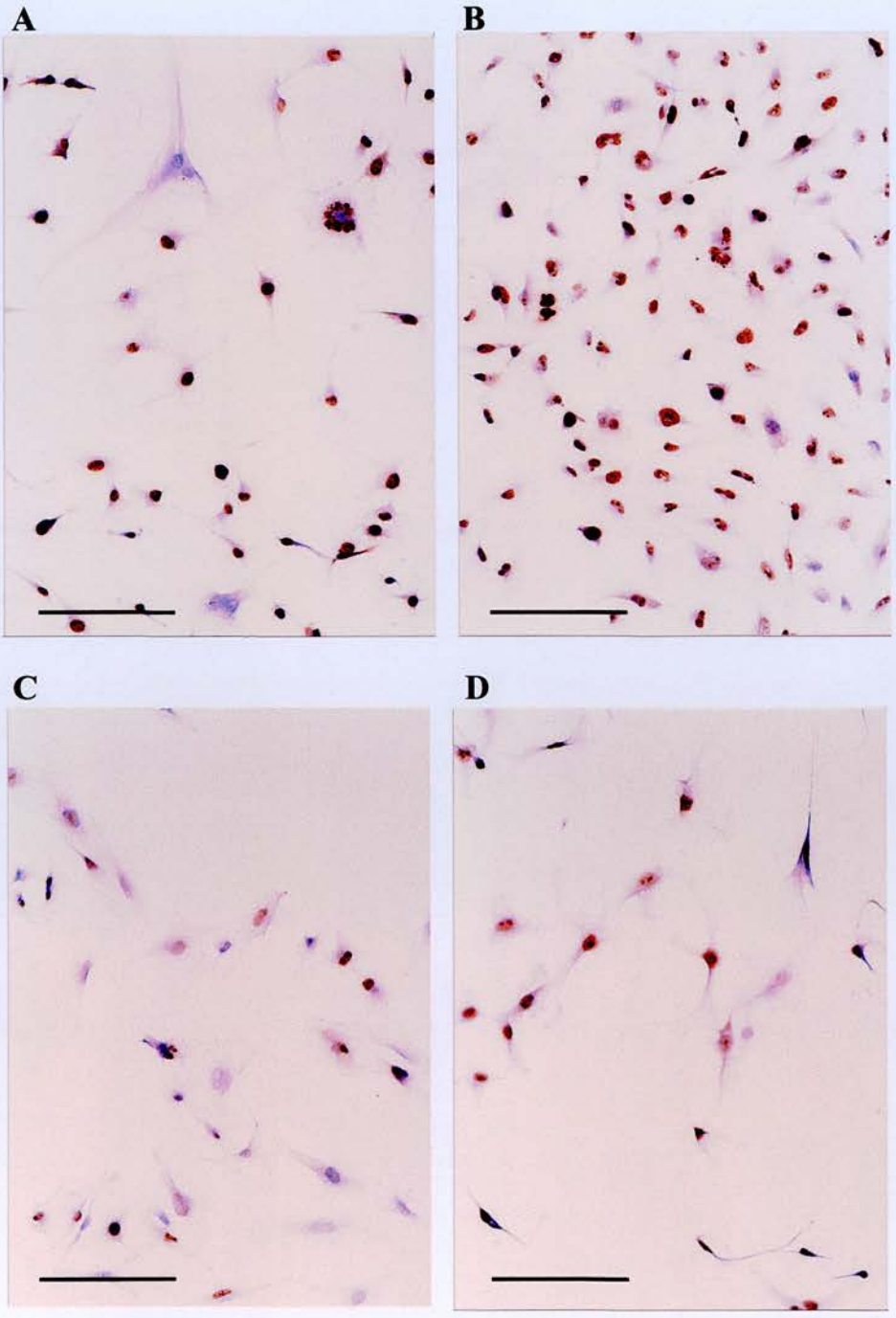

Figure 13. Ki67 labelling in monolayer culture. A, U87 cell line (65% labelling index). B, U373 cell line (70% labelling index). C, MOG-G-CCM cell line (30% labelling index). D, A172 cell line (70% labelling index). All bars=100μm.

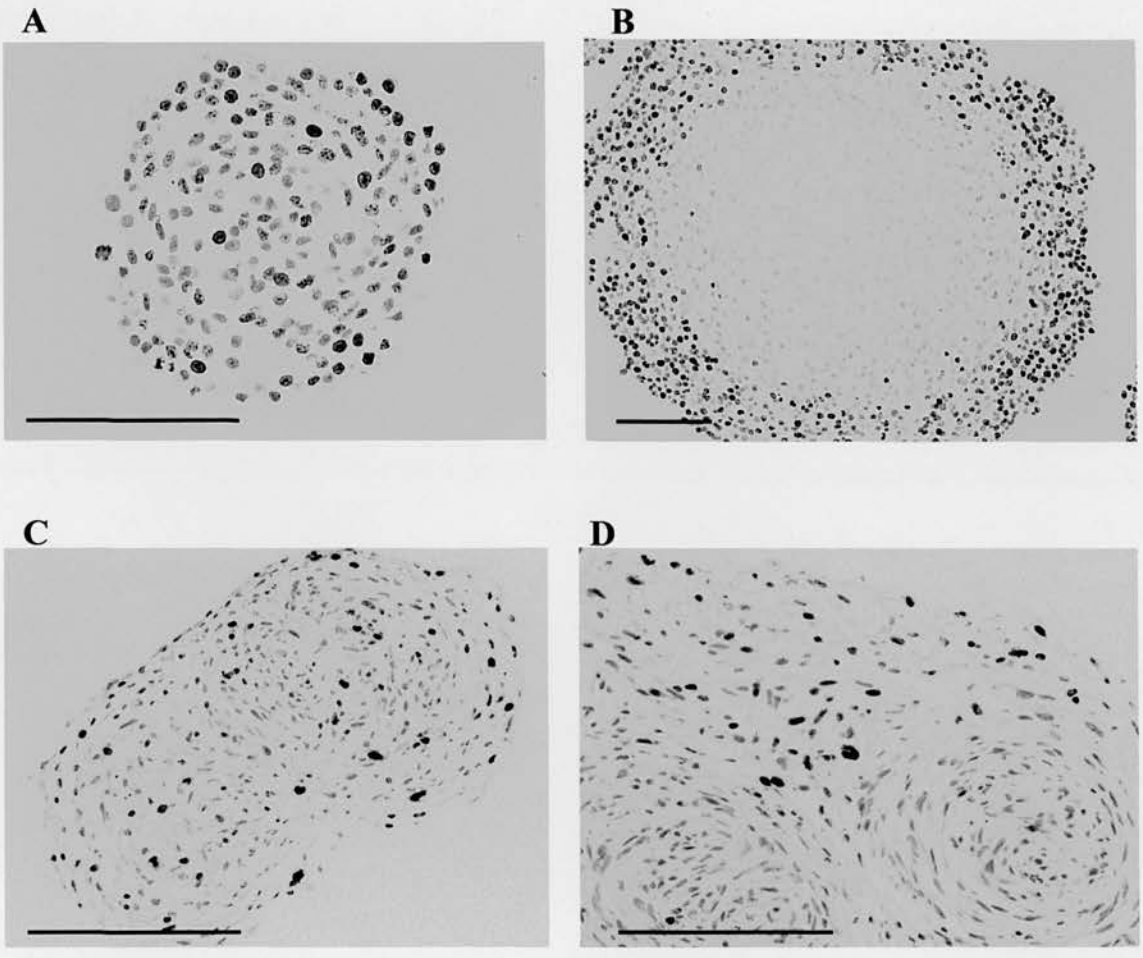

Figure 14. Ki67 labelling in spheroid cultures. A, week 1 U87 spheroids exhibing a random distribution of Ki67 positive cells. B, peripheral localization of Ki67 positive U87 cells (week 3). C, an irregularly shaped week 1 U373 spheroid exhibiting a random distribution of Ki67 labelling. D, peripheral localization of Ki67 positive U373 cells (week 3). All bars=100μm.

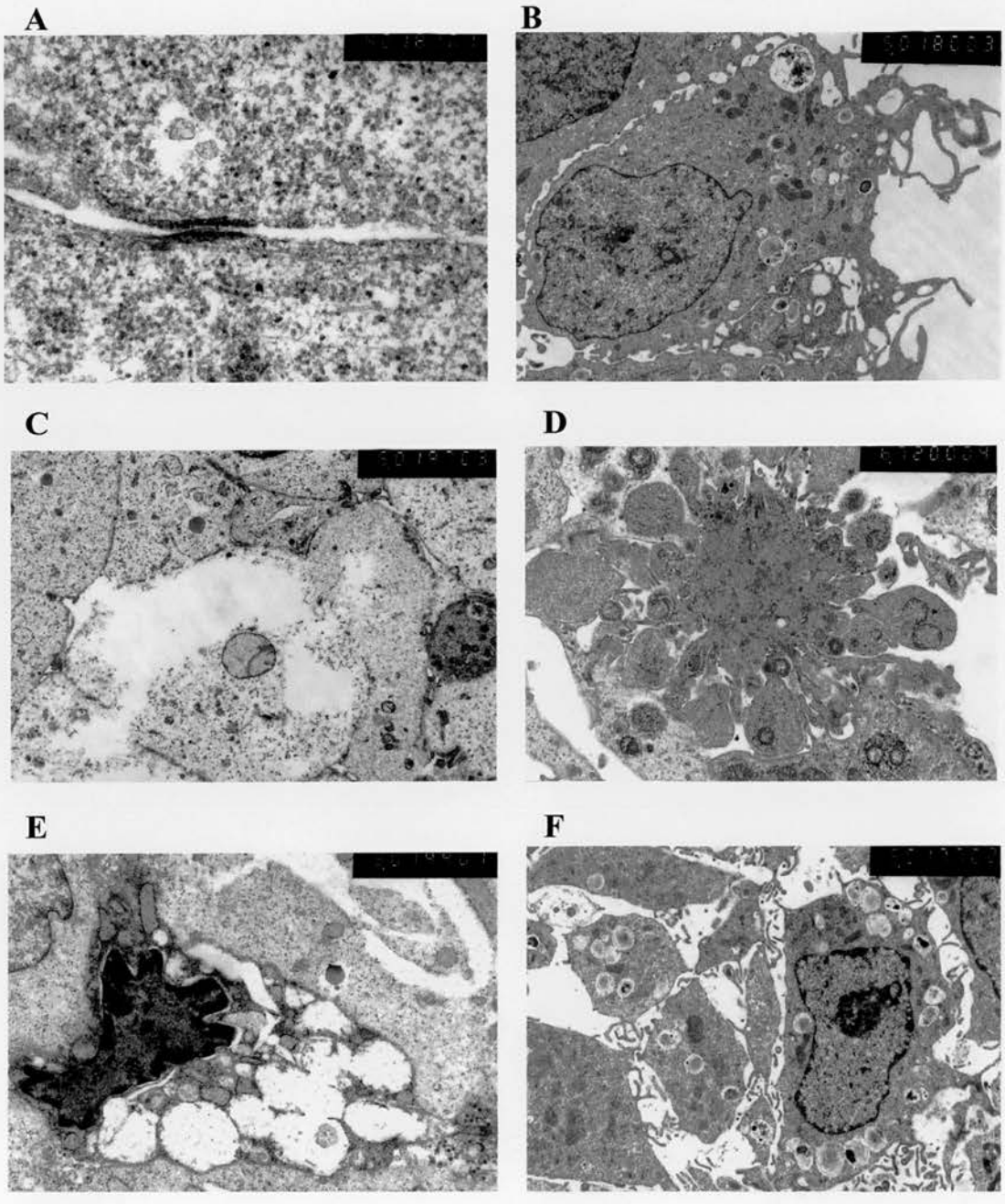

Figure 15. Electron micrographs showing A, an intermediate junction formed between adjacent cells in A172 cell line (x 51000). B, a MOG-G-CCM cell showing evidence of nuclear polarization and autophagic activity (x 16000). C, an A172 necrotic cell (x 16000). D, a U373 apoptotic cell (x 16000). E, a U87 cell exhibiting a vacuolar phenotype (x 16000). F, a MOG-G-CCM cell showing an autophagic morphology (x 16000).

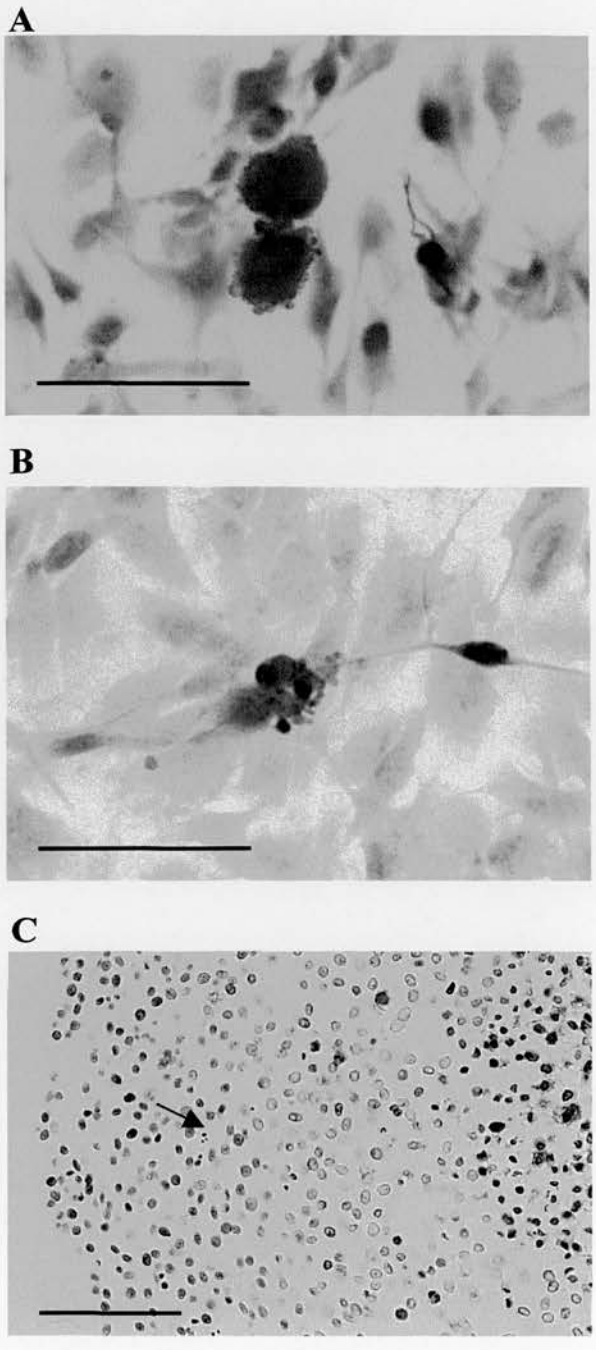

Figure 16. Photomicrographs of A, an H&E stained apoptotic cell in monolayer culture (U87) (Bar=20μm). B, an H&E stained apoptotic cell in monolayer culture (U373) (Bar=20μm). C, a TUNEL labelled U87 (week 3) spheroid (Bar=100μm). Arrow points to a TUNEL negative apoptotic cell.

(resulting from cell shrinkage), condensation of chromatin, nuclear fragmentation and a convoluted cell membrane (Figure 15D). A distinct pattern of cell death emerged where the central area of cell death was necrotic and apoptotic cells were seen scattered in the surrounding viable rim. This pattern was present in all of the cell lines examined.

A third type of cell death observed was termed vacuolar cell death. Here, the cells contained huge vacuoles, which often appeared to arise from the dilation and fusion of organelles. The cytoplasm was very electron dense and the cell membrane appeared to be intact, although in some instances a slight blebbing effect was observed (Figure 15E).

In addition, an autophagic morphology was identified in some cells (Figure 15F). This phenotype was present in all of the cell lines to some extent, but was particularly prevalent in MOG-G-CCM cell line. It was not clear whether these cells were involved in a cell injury/death response. These cells contained lysosomal vacuoles, often containing myelin whorls or fragments of organelles. In addition, these cells were often slightly more electron dense then normal cells although it was unclear whether this was due to cell shrinkage. In the MOG-G-CCM cell line, some cells in the proliferative zone exhibited this phenotype.

TUNEL labelling was present in the centre of week 3 to week 5 spheroids in all of the cell lines (Figure 16C). These were cells which had ultrastructurally been shown to have a necrotic pattern of cell death. Scattered cells within the viable rim and zone of differentiation were also observed, although there was a sharp decline in TUNEL labelling from the centre of the spheroid to the periphery. Close examination using high power light microscopy revealed that many apoptotic cells around the spheroid centre were not TUNEL positive. For this reason, the TUNEL results were not quantitatively assessed.

3.2.6. Quantitative assessment of cell death in monolayer and spheroid cultures

The mean apoptotic indices of the four cell lines differed in monolayer culture. U373 cell line and MOG-G-CCM cell lines had the highest apoptotic indices at 1.0% and 0.9% respectively. U87 and A172 cell lines had lower apoptotic indices at 0.5% and 0.2% respectively (Table 11). Approximately 1000 cells were counted for each cell line.

In the spheroid cultures, morphological counts of apoptotic cells using H&E stained sections showed that at weeks 1-2 the apoptotic index was between 0.04% and 0.05% for all of the cell lines studied (Table 11). This increased by week 3 once the central core of cells had begun to necrose. By week 5, the apoptotic index had increased, ranging from 0.61% in A172 cell line to 2.75% in U87 cell line (Figure 12F and Table 11). Statistical analysis revealed that at week 5, U87 had a significantly higher apoptotic index over time than the other 3 cell lines ($p<0.001$). A172 had a significantly lower apoptotic index than U373 and U87 cell lines ($p<0.001$).

Cell line	Monolayer	Week 1 Spheroid	Week 5 Spheroid
U87	0.50±0.16%	0.04±0.02%	2.75±0.23%
U373	1.00±0.21%	0.05±0.02%	1.60±0.19%
MOG-G-CCM	0.90±0.18%	0.04±0.02%	0.84±0.11%
A172	0.20±0.13%	0.04±0.02%	0.61±0.08%

Table 11. Table showing the apoptotic indices (using morphological counts) of monolayer, week 1 spheroids and week 5 spheroids in the cell lines U87, U373, MOG-G-CCM and A172 (±SEM).

For spheroid cultures at week 3, the numbers of cells demonstrating each type of cell death/injury on ultrastructural examination were recorded for each cell line (Table 12). This was done using the above described criteria (i.e., apoptosis, necrosis, autophagic and lysosomal cell death). The distribution of apoptotic versus necrotic cells was compared across the cell lines at week 3 and the results statistically analysed. Relative levels of apoptosis and necrosis were found to differ between cell lines ($p<0.001$). The largest contribution to this variation was accounted for by A172 which demonstrated the largest number of necrotic cells. The remaining cell lines still showed a significant variation in the proportions of apoptosis vs. necrosis ($p<0.05$), accounted for by higher levels of apoptotic cells in U87. Therefore the apoptotic indices graphed at week 3 in Figure 12F are lower than those in Table 12. Due to better resolution, larger numbers of apoptotic cells were identified using EM than found with the apoptotic counts using the H&E stained cells. Overall, the electron microscopy results compared favourably with levels of cell death found using light microscopical techniques. The latter was found to be the best way of assessing apoptosis and necrosis, because large numbers of spheroids could be

examined. The distribution of autophagic and vacuolar phenotypes were not analysed statistically, but the vacuolar morphology was observed most frequently in U87, and autophagic cells were observed most frequently in MOG-G-CCM cell line.

Cell line	Apoptosis	Necrosis	Autophagic	Vacuolar
U87	52	35	5	18
U373	37	46	2	4
MOG-G-CCM	11	21	21	8
A172	6	67	2	0

Table 12. Levels of apoptotic, necrotic, autophagic and vacuolar cell death phenotypes observed per spheroid using electron microscopy.

To further quantify apoptosis and necrosis in glioma spheroids, Annexin V flow cytometry was employed. Although this method confirmed that the proportions of non-viable cells present in spheroids increased over time, it did not distinguish between apoptosis and necrosis in a substantial proportion of the cells analysed (Figure 17). All cells derived from spheroid cultures were either labelled with both Annexin V and propidium iodide or neither (the healthy cell population). It is possible that the trypsinisation process required for disaggregation was too aggressive causing permeablization of the cell membranes of non-necrotic cells allowing the entry of propidium iodide. Monolayer experiments using the same techniques showed valid apoptotic cell populations, suggesting that the high trypsin concentrations required for spheroid disaggregation may be the reason for the lack of detection of an apoptotic cell population in these experiments. Morphologically, viable and nonviable cells in spheroid cell populations were distinguished by their laser scatter characteristics. Using the U87 cell line as an example, two distinct populations with different forward and side scatter were observed in disaggregated spheroid cell populations (Figure 17B1 and 5). The Annexin V labelling in the total cell populations are shown in Fig 17B2&6 and was 1.68%+/- 0.53% at 2 weeks in U87 spheroids and 7.68%+/-4.16% at four weeks of culture of the same U87 spheroid preparation. This therefore shows a decrease in cell viability in U87 spheroid cultures over 2 weeks of approximately 6%. During spheroid culture, U373 and MOG-G-CCM had similar decreases in viability (5-6%) and A172 spheroids had an overall decrease in viability of 3.5%+/-1.2%. The use of flow cytometry in this study

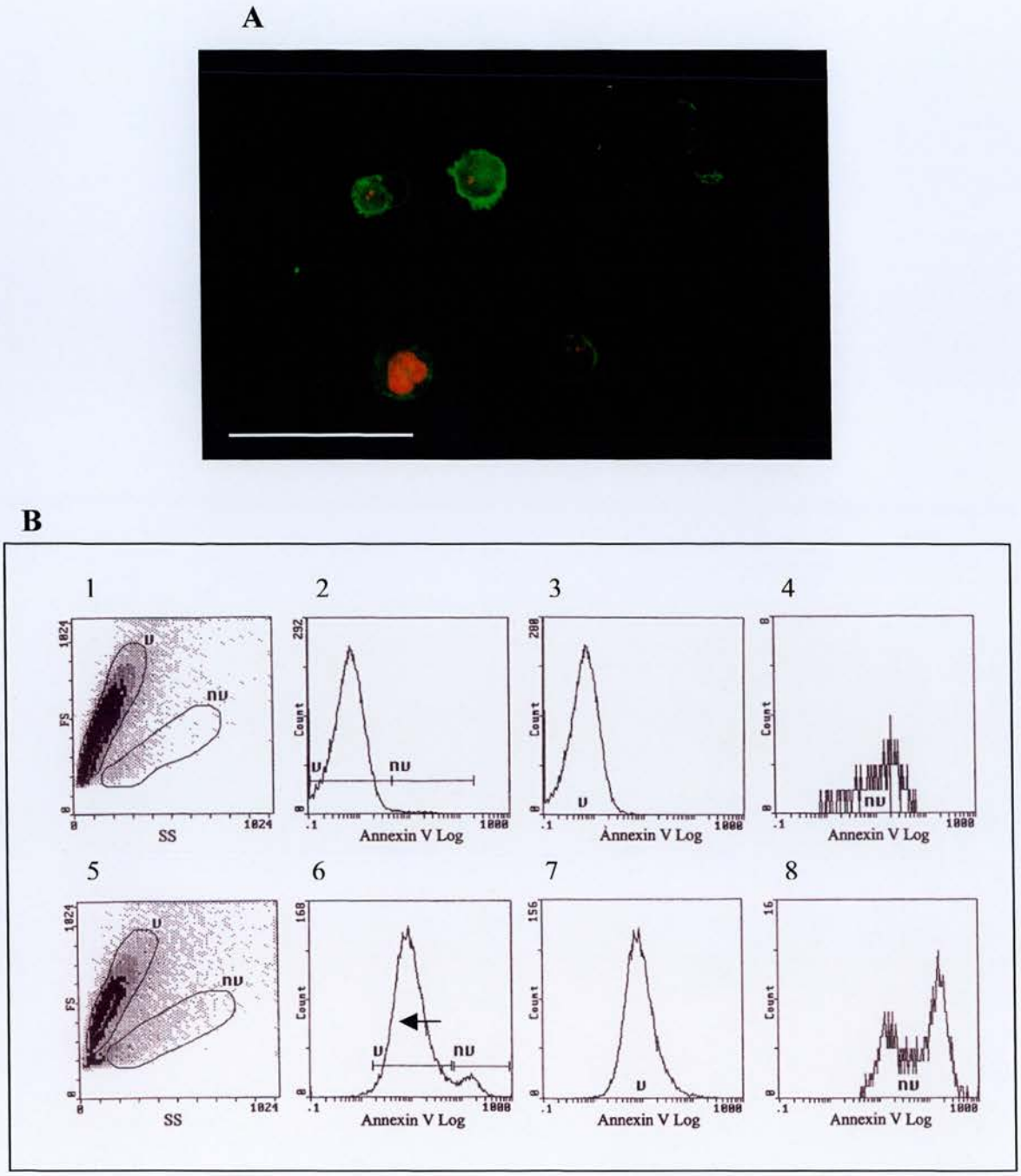

Figure 17. A, Annexin V/propidium iodide labelled U87 cells (Bar=20μm). B, flow cytometric analysis of the U87 cell line grown as spheroids at week 2 (1-4) and week 4 (5-8). 1 & 5 are the flow laser scatter characteristics where SS= side scatter and FS= forward scatter. 2 & 6 show the Annexin V labeling index of the whole cell population in each group where **v**= viable cells and **nv**=non-viable cells. 3 & 7 show Annexin V labelling in the viable cell population (population **n** from scatter plot A). 4 & 8 show the number of cells Annexin V positive in the non-viable cell population (population **nv** from scatter plot 5).

allowed the proportion of dead cell cells to be identified. However, the type of cell death occurring was not distinguishable.

3.2.7. HIF-α expression in monolayer cultures, hypoxic monolayer cultures and spheroids

Very little endogenous HIF-1α expression was present in untreated U373 and U87 monolayer cultures. Darker labelling was however visible within the 3-dimensional aggregates present in U87 monolayer cultures (Figure 18C).

HIF-1α expression was upregulated in response to hypoxia in monolayer U87 and U373 cell cultures (Figures 18A and B). Western blotting experiments showed that HIF-1α was present after one hour exposure to 0.5% oxygen and this increased over a 24hour period. HIF-1α was therefore upregulated irrespective of the p53 status of the cell lines.

HIF-1α expression was upregulated in the centre of spheroids derived from the two cell lines U87 and U373 (Figures 18D and E). Similar experiments were not performed on MOG-G-CCM and A172 cell lines. Positive nuclei were identified in a small number of cells in the centre of the spheroids at week 3. Where necrotic cell loss had occurred, a few positive cells were scattered amongst the perinecrotic tissue. Levels of HIF-1α expression increased over time as the spheroids became larger. By week 5, when the necrotic central regions of spheroid derived from the cell lines were very large, HIF-1α expression was present in 100% of cells situated inside the proliferative rim (Figure 18F).

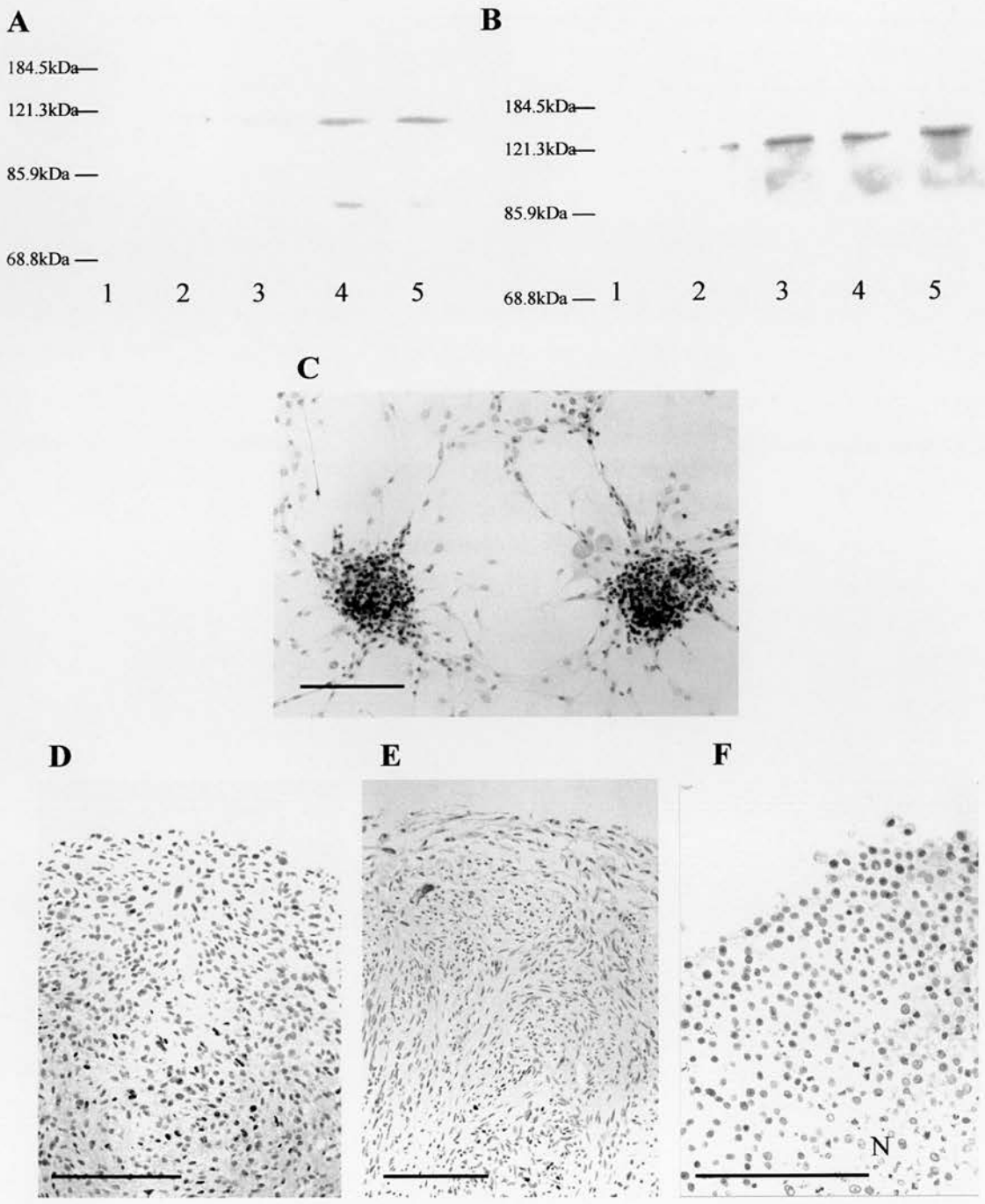

Figure 18. HIF-1α expression in U87 and U373 cell lines. A, western blots shows an upregulation in HIF-1α (120kDa) expression in U87 (A) and U373 (B) cell lines in response to hypoxia (1-5=0, 1, 2, 6, 24hrs exposure to 0.5% O_2). C, HIF-1α immunopositivity in the centre of U87 monolayer aggregates. D and E, week 3 U87 and U373 spheroids with central HIF-1 α labelling. F, week 5 U87 spheroid showing HIF-1 α positive cells adjacent to the proliferative rim (N=necrosis). All bars=100μm.

3.3. Discussion

3.3.1. Summary of results

The phenotypic organisation of growing glioma spheroid cultures have been established in this section. The morphology of glioma spheroid cultures was shown to compare favourably with the organisation of glioblastoma tissue *in vivo*, from the initial avascular growth stage of maligancies to the arrangement of heterogeneous cell populations as determined by the distance from the vasculature These heterogeneous cell populations were observed as regions of peripheral proliferation, GFAP positive non-cycling cells and a central core of cell death. Central cell death occurred at the same time point (week 3) in all four cell lines examined and was initially observed as necrotic foci which became enlarged as the spheroids increased in size. Subsequent increases in apoptotic index were observed around this area of necrosis. HIF-1α, which is expressed in response to hypoxia/hypoglycaemia in many cell types (Moley and Mueckler, 2000; An et al., 1998), was present in central regions from week 3 onwards.

3.3.2. Morphology and differentiation of glioma spheroid cultures

As multicellular tumour spheroids grow larger in culture, they become spherical creating a diffusion-limited tissue model where spatially distinct regions proliferation, differentiation, non-cycling cells and dying cells can be monitored in a concentric pattern outwards from the spheroid centre. It is thought that these three dimensional aggregates retain characteristics similar to *in vivo* tumour cell populations which co-exist at varying distances from the vasculature. The brain tumour spheroids grown in this study showed similar characteristics. Monolayer cultures derived from the four cell lines U87, U373, MOG-G-CCM and A172, exhibited markedly different cellular morphologies. However, as multicellular spheroids, all exhibited similar phenotypes, both at early and late stages of development. Therefore, spheroids derived from different cell lines, like individual tumours with different genetic backgrounds, formed tumour cell populations with a phenotypically similar end point. In addition, the concentric arrangement of heterogeneous cell populations within each spheroid could be compared with similar areas of heterogeneity *in vivo*. Other morphological observations such as the presence of intermediate junctions within the central spheroid regions confirmed this system as a good phenotypic representation of glioblastoma.

GFAP expression was observed in three of the cell lines (U87, MOG-G-CCM and A172) in an intermediate zone between the spheroid centre and periphery. In these cultures, the outer proliferative zone did not express GFAP. This is consistent with reports that GFAP is rarely expressed in cycling cells in human glioma *in vivo* (Schiffer et al., 1986; Kleihues et al., 2000). The cell line U373 did not exhibit this pattern of GFAP labelling. GFAP positive cells were observed throughout the spheroid mass irrespective of their position. It is unclear why this is the case. Because U373 spheroids are irregularly shaped compared to spheroids derived from the other lines, the distinct concentric arrangement is not as pronounced. Therefore, it is possible that the distribution of metabolites within the spheroid mass may not occur as a uniform decrease from the spheroid periphery to the centre. However, other evidence such as the distribution of the proliferating cell population and position of regions of cell death suggests this is unlikely. In addition, U373 cell line exhibited the greatest number of GFAP positive cells in monolayer culture (>80%), and a Ki67 labelling index of approximately 60%. This suggests that some U373 cells are cycling and expressing GFAP simultaneously.

3.3.3. Growth characteristics of glioma spheroid cultures

Past research has shown that if spheroids are cultured from genetically stable cell lines at low passage numbers, spheroid growth kinetics and histological structure are relatively reproducible. This means that volume growth kinetics, viable rim thickness and onset/diameters of necrosis averaged over a certain number of spheroids are relatively invariant between different sets of experiments (Mueller-Klieser, 2000). However, in some cases a considerable amount of inherent variance, is present between individual spheroids within the same culture, particularly in terms of spheroid size (Acker et al., 1984). In terms of growth measurements in this study, these findings were not relevant as the 10 largest spheroids from each weekly sample were used for further analysis. Variation between cell lines and different cell types is to be expected.

All four cell lines showed identical patterns of proliferation. Ki67 positivity was restricted to an outer zone of 100μm in width, thus implying that the cell lines required similar metabolic requirements in which to stimulate proliferation around the nutrient rich periphery of the spheroids. Within the proliferative zone, virtually all cells were Ki67 positive. Because the diameter of the proliferative zone was limited to 100μm, the ratio of the proliferative zone to total volume decreased as the volume of the spheroid increased.

The consequent decline in growth fraction would itself therefore contribute to the slowing of overall growth at high volumes in spheroids, as in solid tumours. The diameter of the proliferative zone itself may well be a reflection and measure of the ability of tumour cells to proliferate under conditions of variable metabolite accessibility. Thus together with the cell death response, ability to proliferate under less than optimal conditions may be another way by which the tumour cells response to stress determines the growth characteristics of the tumour. These findings are consistent with the proliferative characteristics of cell lines derived from other glioma cell lines (Tamaki et al., 1997). All the cells situated inside the proliferative zone were essentially quiescent.

Although complex growth dynamics were not analysed using this system, there were some basic differences between the cell lines in terms of overall growth. A172 cell lines showed significantly increased growth rates compared to the other lines in monolayer culture and similar findings were observed in spheroid culture. Although the thickness of the proliferative band remained consistent in all four cell lines, the A172 cell line grew larger as spheroids than the other three cell lines (up to a diameter of nearly 1.4mm compared to an average of 1mm for the other lines). This was not due to any increases in cell size as the cell packing density remained consistent between the four cell lines. Cell number was consistently higher in A172 spheroids from weeks 4-5 of spheroid culture. It was thought that less overall cell loss occurred within spheroids derived from A172 cells.

3.3.4. Phenotypic onset of central cell death

The predictable onset of cell death in this model has allowed for the examination of the earliest structural changes present in the central regions of brain tumour spheroids as they become larger. Ultrastructural examination of the spheroids at 3 weeks, when onset of necrosis occurred in all four cell lines, revealed the presence of both apoptotic and necrotic cells in a particular pattern. In all four cell lines cell death in the centre of the spheroids was necrotic in type (Figure 19). Apoptotic cells surrounded this area and decreased in number towards the spheroid periphery. The cells within the central area of cell death were labeled with the TUNEL reaction, despite the fact that death in this area was proven ultrastructurally to be necrotic. The TUNEL method has previously been shown to lack specificity, in that it may label necrotic as well as apoptotic cells (Grasl-Kraupp et al., 1995; Gold et al., 1994). In our system too, TUNEL lacked the ability to

discriminate between different cell death patterns. It may also label very actively transcribing nuclei (Kockx and Knaapen, 2000).

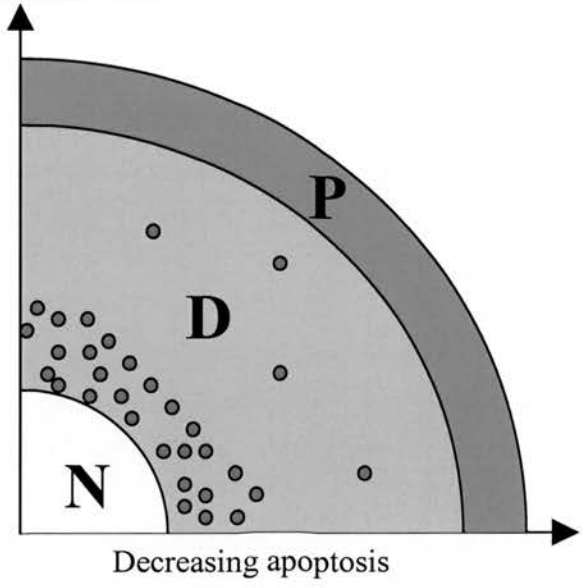

Figure 19. Distribution of necrosis (N), apoptosis (red spheres), region of differentiation (D) and region of proliferation (P) through a quarter cross-section of a glioma spheroid

It was hypothesised that the area of central cell death might arise by apoptosis rather than necrosis. Sublethal injury may induce apoptosis in a variety of settings including hypoxic states *in vivo* (Ruan et al., 1999; Banasiaka et al., 2000) and in cell lines grown in monolayer culture (Lennon et al., 1991). In the case of the spheroid model, an increase in cell stress associated with increasing diameter might initially be expected to produce a sublethal insult. Certainly, in some spheroid systems the onset of an apoptotic response preceeding a necrotic response, appears to occur. For example, in rhabomyosarcoma spheroids the occurance of central apoptosis preceeds the onset of central necrosis (Mueller-Klieser et al, 1997). V79 hamster lung spheroids also show pre-necrotic, centrally located increases in TUNEL positive cells (Mueller-Klieser et al, 1997). However, in the glioma spheroid cultures in this study, the central area of cell death appeared necrotic at the earliest time point, although a few admixed cells with apoptotic morphology were seen. This was apparent in all four lines examined. There is emerging evidence that apoptosis and necrosis are not entirely distinct processes, but may coexist, with the energy status of the cell determining whether apoptosis or necrosis occurs (Leist et al., 1997; Nicotera et al., 1997). Thus, an initially apoptotic process might become

necrotic. Such a pattern has been documented in human and experimental myocardial infarction (Veinot et al., 1997; Olivetti et al., 1996; Akiyama et al., 1997). A very early apoptotic phase preceeding necrosis cannot be entirely excluded in this glioma spheroid model, but certainly completion of cell death for most of the central cells is necrotic in type, indicating that central energy depletion rapidly becomes too severe to allow an apoptotic mode of death. EMT6 spheroids show a similar cell death phenotype to glioma spheroids, where sudden onset of necrosis occurs without any pre-apoptotic phase. EMT6 spheroids exhibit a rapid reduction in ATP levels immediately before the onset of necrosis. The morphological similarities between the two systems again suggests a sudden decrease in energy levels leading to a primary centrally located necrotic response in glioma spheroids.

Although variations existed between cell lines, nearly all the apoptotic cells observed within the spheroids were surrounding the central area of necrosis. This could be a result of sublethal injury to these cells as the radius of the spheroid became larger. However, this seemed unlikely as apoptosis was not stimulated to any great extent when the central regions of pre-necrotic spheroids were subjected to a similar stress. It is likely that necrotic tissue in the centre of the spheroids may have stimulated an apoptotic response in surrounding cells, suggesting the presence of a relationship between the two processes. Products of phospholipase degradation of membranes and reactive oxygen intermediates released during necrosis are possible candidate pro-apoptotic agents (Leaver et al., 1998). This is supported by the increase in the number of apoptotic figures observed elsewhere within the spheroid cell mass from weeks 3-5, after areas of necrosis have formed. Whereas the apoptotic index was nearly zero from weeks 1-2, the index rose rapidly following the onset of necrosis.

Although necrosis was the predominant form of centrally located cell death in spheroids derived from all 4 lines, ultrastructural examination revealed two other cell injury morphologies. In one process, termed vacuolar cell death, contained huge vacuoles, which often appeared to arise from the dilation and fusion of organelles. The cytoplasm was very electron dense and the cell membrane appeared to be intact, although in some instances a slight blebbing effect was observed. Some of the features appeared intermediate between classical apoptotic and necrotic morphologies and it was thus difficult to classify this form of cell death. Vacuolar cell death patterns were mostly associated with the U87 cell line

and were observed mainly in the centre of the spheroid admixed with necrotic cells. Examples of non-apoptotic/necrotic cell death featuring cytoplasmic vacuolation have been observed in other biological systems and pathologies, such as neural development and degeneration (Clarke,1998), *in vivo* rat hepatocarcinoma when exposed to SBA (sodium 5,6-benzylidene-L-ascorbate) (Asano et al., 1999) and in neurons in patients with ALS (amyotrophic lateral schlerosis) (Mourelatos et al., 1996). It is interesting that the latter two circumstances involve the abnormal production of free radicals (ascorbate radicals and H_2O_2 in hepatocarcinoma experiments and hydroxyl radicals in the ALS patients). Perhaps, like the onset of apoptotic cell death as described above, the close association of perinecrotic cells to the toxic waste products of the necrotic tissue resulted in this phenotype in spheroid cultures. A vacuolar morphology is also associated with a type of cell death termed 'parapoptosis' (Sperandio et al., 2000). Again, this phenotype was identified in neurons during development and in some cases of neurodegeneration. 'Parapoptosis' is associated with a caspase-9 activity which is Apaf-1 independent (Sperandio et al., 2000; Wyllie and Golstein, 2001). It is possible therefore, that the vacuolar phenotype observed in spheroid cultures may have arisen via a cell death programme distinct from those normally associated with apoptosis or necrosis.

Another phenotype that was particularly prevalent in the MOG-G-CCM cell line was characterised by the presence of abundant myelin-like membrane whorls within the cytoplasm. It was unclear whether this autophagic pattern was an injury response which would eventually lead to the death of the cells concerned, as many of the cells around the periphery of the spheroids derived from MOG-G-CCM cell line also express this autophagic pattern as well as cells towards the centre. Similar autophagic patterns of cell injury have been observed in developing neurons (Clarke, 1998).

The significance of the varying morphological patterns which we have observed in the spheroid model suggests that there may be other mechanisms and/or intermediate phenotypes involved in cell death in glioma besides those of necrosis and apoptosis.

3.3.5. Quantitative analysis of cell death

Even though the four cell lines used in this study were derived from different tumours, onset of central cell death occurred over week 3 in all 4 lines. Around 60% (38% in A172 cell line to 80% in U87 cell line) of spheroids derived from the 4 cell lines possessed

some element of cell loss from central regions. The remaining 40% of spheroids contained central regions phenotypically consistent with dead or dying cells. An element of variability within spheroid cultures derived from each cell line is to be expected as the spheroid diameters vary by a coefficient of approximately 8% at this time point, despite being selected for their size.

Although central cell death appeared in all of the cell lines at week 3, the spheroids exhibited marginal differences in size. A172 cell line for example, had a diameter of nearly 800μm whereas MOG-G-CCM cell line had a diameter nearer 600μm. These measurements are crucial as the spheroid radius is the limiting factor for the passage of metabolites from the spheroid periphery to the centre. These results are at the upper end of the scale compared to spheroids derived from other tumour types. Spheroids derived from WiDr human colon carcinoma cells and EMT6 mammalian sarcoma spheroids begin to necrose at diameters of 400-500μm (Mueller-Klieser, 2000). MR1 oncogene-transformed rat embryonic fibroblast spheroids are a similar size to glioma spheroids at onset of necrosis at around 700-800μm (Mueller-Klieser, 2000). As the glioma spheroids increased in size, the extent of central necrosis varied between cell lines over time. In A172 cell line, the central necrotic area remained small over time (<10%) but in the other cell lines this area increased to over 60% by week 5. This is surprising as in other spheroid systems including U87, U373 and MOG-G-CCM spheroids the area of necrosis increases in size at almost exactly the same rate as the whole spheroid (Mueller-Klieser, 2000). As a consequence, the thickness of the viable rim remains constant at various spheroid sizes. Centrally located cells in the A172 spheroid therefore appeared to be more resistant to death than the other 3 glioma cell lines.

Apoptotic index over time was measured using 3 techniques, morphological counts using H&E stained sections, TUNEL labeling and Annexin V flow cytometry. Using H&E staining stained sections, significant differences in apoptotic index between cell lines were observed. Between weeks 1and 2 the apoptotic index in all of the cell lines was nearly zero but by week 3, U87 spheroids had significantly more apoptotic figures than the other three cell lines. U373 and MOG-G-CCM cell lines had intermediate levels of apoptosis. A172 had the least number of apoptotic figures over time and this was confirmed by the ultrastructural data at week 3. Annexin V flow cytometery reflected these results in terms of cell viability i.e. U87, MOG-G-CCM and U373 lines had significantly larger non-

viable cell populations over time compared to the A172 cell line. However, it could not distinguish accurately between apoptotic and necrotic cell populations due to membrane damage during trypsin disaggregation. As TUNEL was not accurate in labelling all of the observed apoptotic figures present and often labelled necrotic cells as well as apoptotic cells, H&E stained sections of paraffin embedded spheroids proved to be the best method of quantifying apoptosis in glioma spheroids.

Overall, A172 showed decreased susceptibility to cell death compared to the cell lines U373, MOG-G-CCM and U87, and this was reflected in terms of apoptotic index and the extent of necrosis. This reinforced the earlier evidence suggesting that necrosis may play a role in the stimulation of apoptosis in this model. It certainly implies that inducible apoptosis in the glioma spheroid system does not occur independently of necrosis.

3.3.6. Spheroid metabolism and HIF-1α distribution within glioma spheroids

It is not surprising that for many years the development of central necrosis was attributed to an insufficient oxygen supply. Recent evidence has shown that this may not necessarily be the case. Most spheroids that are commonly used in such studies have not shown a particularly hostile intra-spheroidal environment that would induce either cell-cycle arrest in the areas within the proliferative rim, or central cell death. It has been demonstrated in many spheroid types, that cells inside the proliferative zone adapt their metabolism to specific environmental conditions in a 3-dimensional arrangement by reducing their metabolic turnover rates (Mueller-Klieser, 1997). Other factors, such as cell-cell and cell-matrix interactions, availability of growth factors, expression and accessibility of growth factor receptors and adhesion molecules may be involved in emergence of cell cycle arrest in these spheroids thus preparing them for an environment that would otherwise be highly toxic if they were rapidly proliferating (Mueller Klieser, 1997). Because the metabolic requirements of such cells are so low, these cells become resistant to both various intratumoural stresses but also to various therapeutic drugs (Acker et al., 1984). Onset of necrosis is likely to be the result of a variety of factors leading to a sudden drop in ATP content as mentioned previously. This variety of factors are likely to include a sudden reduction in oxygen and glucose content plus an increase in highly toxic acidic waste products (Mueller Klieser, 2000). A variety of studies have shown that glucose, oxygen and ATP content can remain at normal levels up until just before a necrotic response occurs (Mueller Klieser, 2000; Durand et al., 1998; Walenta et al., 2000). This supports

the earlier findings in this study, where increases in apoptotic index are not observed until a core of central necrosis appears. Then, toxic waste products and subsequent acidosis and free radical production from the necrotic core may be to blame.

The only way of absolutely determining the metabolite and waste product distribution is to measure intraspheroidal O_2, glucose and lactate levels. However, because HIF-1α (hypoxia inducible factor 1 alpha) expression is seen to increase in response to glucose deprivation and hypoxia (<0.05%pO_2) in glioma cells *in vivo* and *in vitro* (An et al., 1998; Zagzag et al., 2000; Zundel et al., 2000; Moley and Mueckler, 2000), in this study it was used as a marker of the distribution of metabolic stress within the spheroid mass. HIF-1α expression was initially observed in spheroid central regions at week 3 in the cell lines (U87 and U373) examined. Labelling was rather faint and only a small number of cells were labelled. This distribution suggested that hypoxia and/or hypoglycaemia occurred just before and during the onset of central necrosis. Subsequent high levels of HIF-1α expression within perinecrotic tissue suggested that central spheroid regions were continually being exposed to high levels of metabolic stress. The western blotting experiments examining HIF-1α expression using monolayer cultures in response to hypoxia over time showed that HIF-1α could be upregulated in less than 2 hours post-hypoxia, and this expression increased over the 24 hour exposure period. Therefore, it was unlikely that other regions of spheroid were severely hypoxic before week 3. These findings using HIF-1α therefore supported the morphological assessment of cell death in the glioma spheroid cultures, which suggested that the distribution of metabolites remained relatively high until a crucial central event occurred centrally at a specific spheroid size.

It is important to mention that three of the four cell lines, U87, U373 and A172 cell lines have previously been shown to possess mutations/polymorphisms in the *PTEN* gene (Ishii et al., 1999). The *PTEN* tumour suppressor gene has been shown to negatively regulate HIF-1α expression by downregulating Akt and PI(3)K kinases (Zundel et al., 2000). Therefore mutations in the gene may result in abnormal expression in these kinases and/or HIF-1α. However, monolayer studies examining HIF-1α expression in the two glioma cell lines studied showed no abnormal expression of the protein.

3.3.7. Characterisation summary

Although using cell lines it is impossible to completely replicate the highly heterogeneous *in vivo* scenario, the spheroid system provides a good reproduction of regions of differentiation, cell death and proliferation present *in vivo*. Necrosis appeared to be the preliminary central cell death event, most probably due to a combination of oxygen depletion, hypoglaecemia and waste product build up. Corresponding increases in HIF-1α expression were observed around this time period. Apoptosis and variety of other intermediate morphologies were observed interspersed with the necrotic cells, and surrounding the necrotic cells, following the initial onset of necrosis. Overall onset of central cell death was predictable within all four cell lines examined which was vital for further experiments measuring onset and extent of death in response to genetic manipulation. The extent of central cell death and apoptotic index varied between cell lines with A172 showing the least necrosis and apoptosis and U87 showing the greatest.

CHAPTER 4

P53 AND THE EXPRESSION OF P53 RELATED PROTEINS

4.1. Introduction

Knowledge of the strategies that tumour cells employ when faced with hypoxia, nutrient withdrawal and waste product build-up may be of relevance when targeting specific cell death pathways therapeutically. Preliminary research completed using this spheroid system showed that the primary central cell death event was consistent with necrosis. This initially implied that regulatory pathways present around such areas of cell death may be limited. However, evidence demonstrating the presence of regulatory molecules in pre or peri necrotic cells (Bootman et al., 2001; Wharton et al., 2000; Fukunaga-Johnson et al, 1995; Kane et al, 1995) together with the observed increase in perinecrotic apoptotic indices, suggests that a variety of regulatory pathways may operate in relation to cell death in the spheroids. In addition, the diversity of cell death morphologies observed both within individual spheroids and between cell lines suggests that the distribution of cell death associated proteins may vary across the radius of spheroids as well as between cell lines harbouring a variety of genetic aberrations. The concentric arrangement of cell morphologies within glioma spheroid cultures means that apoptosis and necrosis can be individually assessed in terms of protein content.

The p53 protein is central to the cell death response in many tissue types. Although most glioblastomas harbour genetic alterations in the p53 system (Rasheed et al., 1999), implying defective operation, a role for p53 and associated proteins in regulating aspects of cell death seems likely. Previous studies have shown the presence of poly (ADP-ribosyl)ation (Wharton et al., 2000), Fas/Fas ligand (Tachibana et al., 1996; Tohma et al., 1998) and HIF-1α (Zagzag et al., 2000) around areas of necrosis in GBM. Poly ADP-ribose polymerase activity (PARP), Fas and HIF-1α have all been associated with a p53-mediated apoptotic response either upstream (HIF-1α) (An et al., 1998), down stream (Fas) (Fulda et al., 1998; Sheard et al., 2001) or both (PARP) (Simbulan-Rosenthal et al., 1999). However, it is not known whether p53 itself is directly involved. Upregulation of wild-type p53 and other directly associated target molecules within perinecrotic tissue may suggest a role for the p53 system in endogenous cell death in glioblastoma. It was therefore hypothesised that p53 and p53 related proteins may play a role in the pathogenesis and regulation of cell death in glioblastoma In addition, it was hypothesised that the distribution of p53 related proteins may vary according to the p53 status of the tumour cell populations examined. In this part of the study, the aims

were (i) to compare the *P53* genetic status of the cell lines with basal levels of p53, Bax, p21 and MDM2 protein expression in the cell lines U87, U373, MOG-G-CCM and A172, (ii) to establish whether p53, Bax, p21 and MDM2 proteins are upregulated in response to oxidative and free radical stress in the four cell lines, (iii) to determine whether there is an increase in these proteins within and around areas of central cell death in spheroid cultures and in biopsy tissue and (iv) to compare *P53* status and levels of protein expression with the levels of cell death within the glioma spheroid cultures.

.

4.2. Results

4.2.1. *P53* sequencing

Of the four cell lines sequenced, the two cell lines U373 and MOG-G-CCM contained *P53* mutations (Figure 20). U373 had a mutation at codon 273 (CGT→CAT). This mutation leads to an Arginine being replaced by a Histidine at codon 273 on exon 5. The mutation in the MOG cell line results in an Alanine being replaced by a Valine at codon 159(GCC→GTC). Cell lines U87 and A172 had no mutations between exons 2 and 11 of the *P53* gene.

4.2.2. p53, p21, Bax, MDM2 and $p14^{ARF}$ expression in monolayer and spheroid cultures

The p53 antibodies used in this study were; p53 (Bp53-12) and p53 (Pab1801). Bp53-12 labels the p53 molecule between residues 32-79. Pab1801 antibody labels the carboxyl terminal of the p53 molecule. In monolayer, spheroid cultures and biopsy specimens the two p53 antibodies generally showed similar patterns of nuclear expression, although Bp53-12 showed slightly stronger staining compared to Pab1801 (Figure 21A-D, Table 13). In addition, Pab1801 often labelled the cytoplasm of positive cells as well as the nucleus. In monolayer, strong staining was present in 70-80% of cells in the mutant U373 cell line (3++++). Moderately strong p53 labelling was observed in MOG-G-CCM cell lines in approximately 60% of cells (3+++). U87 and A172 cell lines showed considerably weaker p53 labelling which was in approximately 40-50% of cells (2++). This labelling pattern was confirmed by western blotting (Figures 21E and F). U373 cell line had the strongest band at 53kDa and U87 and A172 the weakest. Like the immunohistochemistry, p53Bp53-12 antibody showed stronger bands than the Pab1801 antibody.

Nearly 100% of cells were strongly p53 positive (3++++) within spheroids derived from the U373 cell line at week 1 (Figure 22, Table 13). Slightly weaker labelling was seen in MOG-G-CCM cell lines at this time point. Weaker labelling was seen in U87 and A172 cell lines at week 1 in approximately 30-50% of cells. There was no perinecrotic enhancement of p53 labelling as the spheroids became larger in any of the cell lines. In U373 cell line there was an actual decrease in p53 labelling in cells directly adjacent to the central core of necrosis (Figure 22F). By weeks 4 and 5, p53 labelling was only found around the spheroid periphery in the cell lines U87, A172 (Figure 22B and C).

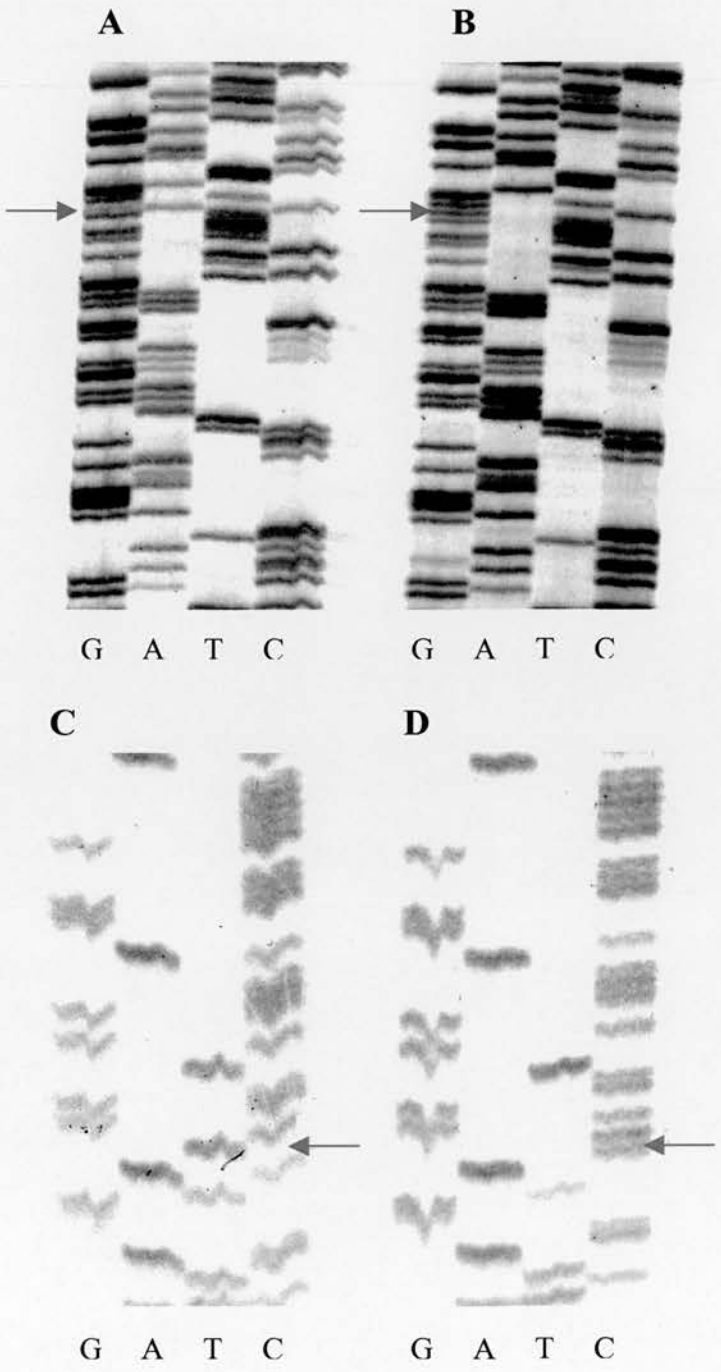

Figure 20. P53 mutation analysis. A, shows the mutation at codon 273 (CGT→CAT) in U373 cell line. B, shows the wild-type sequence of the same region. C, mutation at codon 159 (GCC→GTC) in the MOG-G-CCM cell line. D, shows the wild-type sequence of the same region. The red arrow points to the mutation sites. G=guanine, A=adenosine, T=thymidine, C=cytosine.

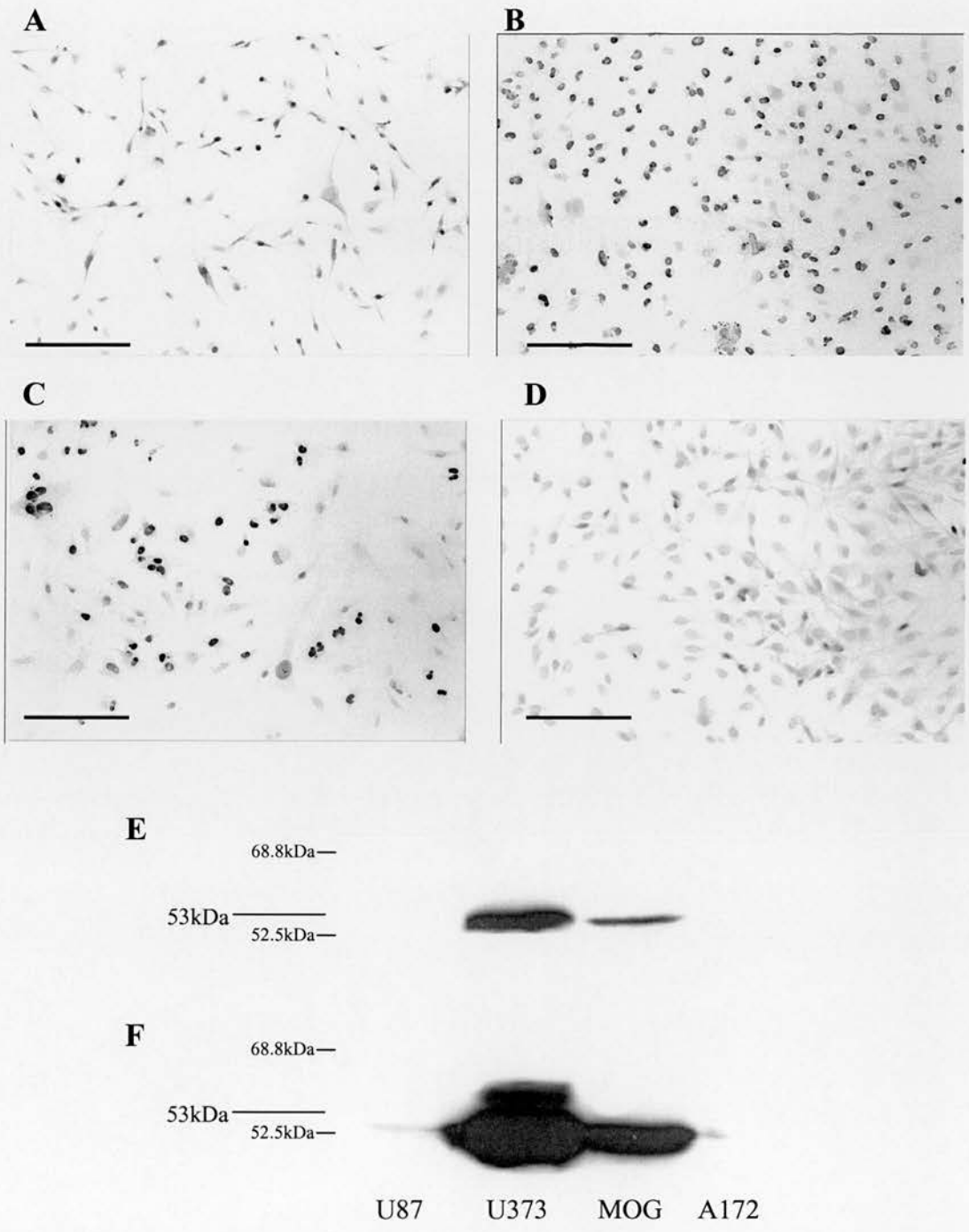

Figure 21. P53 (Bp53-12) immunohistochemistry in U87 (A), U373 (B), MOG-G-CCM (C) and A172 (D) cell lines in monolayer culture. Note the significantly darker and more prolific labelling in U373 (B) and MOG-G-CCM (C) cell lines (all bars=100μm). E&F show p53 western blots using whole cell lysates from the four cell lines. Antibody P53(Pab1801)=E. Antibody P53 (Bp53-12)=F.

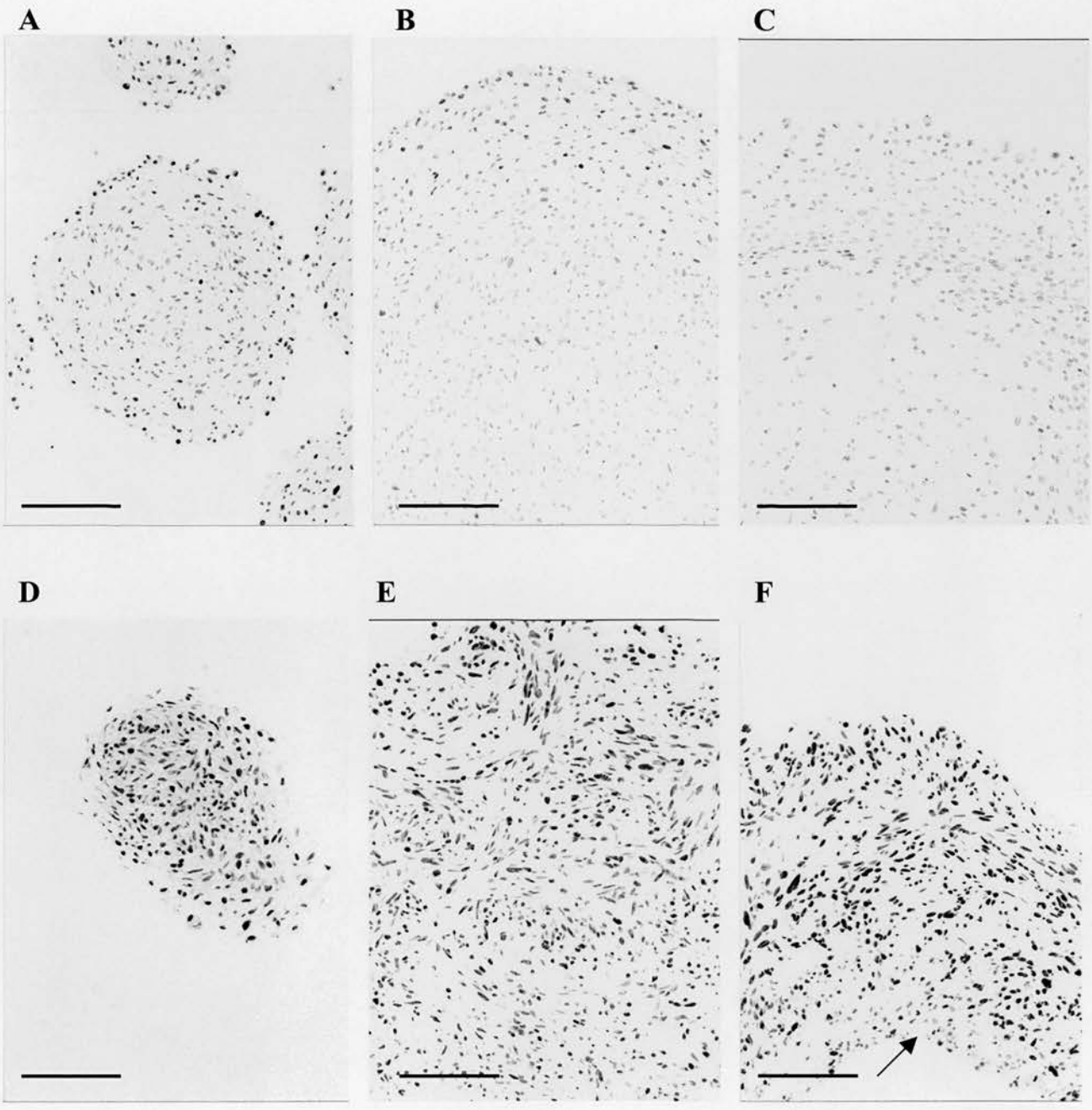

Figure 22. P53 labelling in spheroid cultures. A, week 2 U87 spheroid showing moderate strength diffuse p53 labelling. B, week 3 U87 spheroid showing peripheral localization of p53. C, weak peripheral p53 labelling in a U87 week5 spheroid. D, strong diffuse p53 labelling in a week2 U373 spheroid. E, week 3 U373 spheroid showing strong p53 labelling across the spheroid radius. F, p53 negative cell adjacent to the necrotic centre at week4 (see arrow). All bars=100μm.

	Cell line	Weeks					
		Monolayer	1	2	3	4	5
P53 Bp53-12	U87	2++	2+++	3++	2+++	2++	3++
	U373	3+++	3++++	2+++	3++++	3++++	3++++
	MOG	3+++	3++++	3+++	3++++	3+++	3+++
	A172	2++	2++	3++	3+	2++	3+
P53 Pab1801	U87	2++	3++	3+	2+	2+	2+
	U373	3+++	3+++	3+++	3++++	3++++	3++++
	MOG	3++	3+++	3+++	3+++	3++	3++
	A172	2++	2+	2++	2+	2+	2+
P21	U87	3+	2+	0	2+	2+	3+
	U373	1+	0	0	0	0	0
	MOG	1+	1+	0	0	0	0
	A172	2++	2+	2+	0	1+	2+
Bax	U87	2++++	1+	2++++	1+	1+	2++
	U373	1++++	1++	1++	3++++	3++++	2+++
	MOG	1++++	2++++	2+++	2++++	2++++	2+++
	A172	1++++	2++++	2++++	2++++	2++	3+++
MDM2 (SMP-14)	U87	3++++	2+++	3+++	2+	3+	3+++
	U373	3++++	3+++	2+	3++	3+++	3++
	MOG	3++++	2+++	2++	3+	3+	3+++
	A172	3+++	2++++	3+++	2++	2++	3++
MDM2 (C-18)	U87	2++	1++	1++	1++	1+	1+
	U373	2++	1++	1+	1+	1+	1+
	MOG	2++	1++	1+	1++	1+	1+
	A172	2++	1++	1++	1+	1+	1+
$P14^{ARF}$	U87	0	0	0	0	0	0
	U373	0	0	0	0	0	0
	MOG	2+++	1+	0	0	0	0
	A172	0	0	0	0	0	0

Table 13. Semi-quantitative assessment of the staining intensity (0 absent, 1 weak, 2 moderate, 3 strong) and proportion of cells staining (+ <25%, ++ 25-50%, +++ 50-75%, ++++ 75-100%) for p53 (BP53-12 and Pab1801), Bax, p21, MDM2 (SMP-14 and C-18) and $p14^{ARF}$ in monolayer cultures and brain tumour spheroids derived from U87, U373, A172 and MOG-G-CCM cell lines.

Weak to moderate cytoplasmic Bax expression was noted in monolayer cultures in 80-90% of cells from each cell line (1++++ to 2++++) (Figures 23A-D, Table 13). U87 cells exhibited the strongest Bax labelling followed by U373, MOG and A172 cell lines although there was little difference between them. These differences were not apparent on the photomicrographs as U87 cells were smaller and more rounded. The Bax labelling therefore tended to be more condensed into the smaller cell volume. The Bax western blots using the wild-type cell lysates confirmed that Bax expression was slightly higher in monolayer U87 cells compared to the other cell lines (Figure 23E).

A similar percentage of cells were Bax positive in small spheroids as were found in monolayer culture (Figures 24A and D, Table 13). There was a very slight perinecrotic enhancement in U87 cell line at week 3 (Figure 24B). However this disappeared by week 4 (Figure 24C). The outermost layer of cells at week 4 in U87, MOG-G-CCM and A172 cell lines showed very high levels of Bax expression (Figure 24C). At this time point few Bax positive cells were observed in central regions of the spheroid mass in these three lines. U373 cell line showed consistently high levels of Bax across the spheroid radius and this did not change over the 5 week period (Figures 24D-F). There appeared to be no relationship in the quantity or distribution of Bax labelling between p53 mutant and non-mutant cell lines.

In monolayer, A172 exhibited moderate intensity nuclear p21 labelling in approximately 30-40% of cells (Figure 25D, Table 13). U87 cell line possessed stronger intensity labelling in approximately 20-30% of cells (Figure 25A). Labelling was particularly strong around the periphery of the 3-dimensional aggregates present in this cell line. Uniform nuclear labelling was present in the U87 cell line whereas A172 cell line exhibited a more granular, nuclear labelling pattern. In MOG-G-CCM cell line, a very small percentage of cells exhibited weak nuclear labelling pattern (<2%) (Figure 25C). In U373 cell line, a fine, granular staining pattern was observed in approximately 5% of cells, similar to that found in A172 cell line (Figure 25B). The western blotting experiments confirmed these findings where U87 and A172 cell lines had stronger bands at 21kDa than MOG-G-CCM and U373. No band was seen for U373 cell line (Figure 25E).

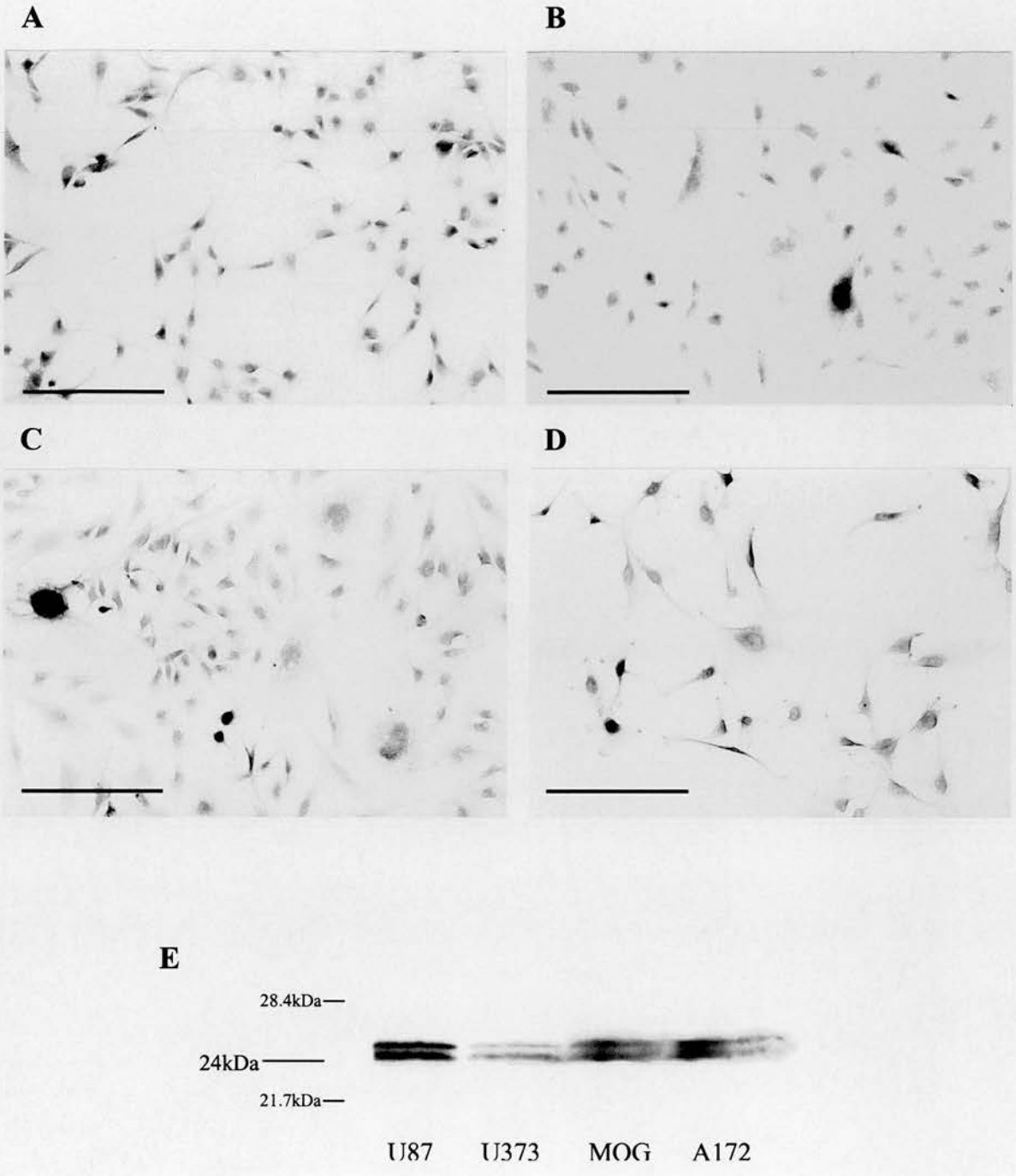

Figure 23. Bax immunohistochemistry in U87 (A), U373 (B), MOG-G-CCM (C) and A172 (D) cell lines in monolayer culture (all bars=100μm). E, shows the western blot analysis using Bax antibody on the four whole cell lysates. Note that U87 cell line has a slightly darker band than the other 3 lines.

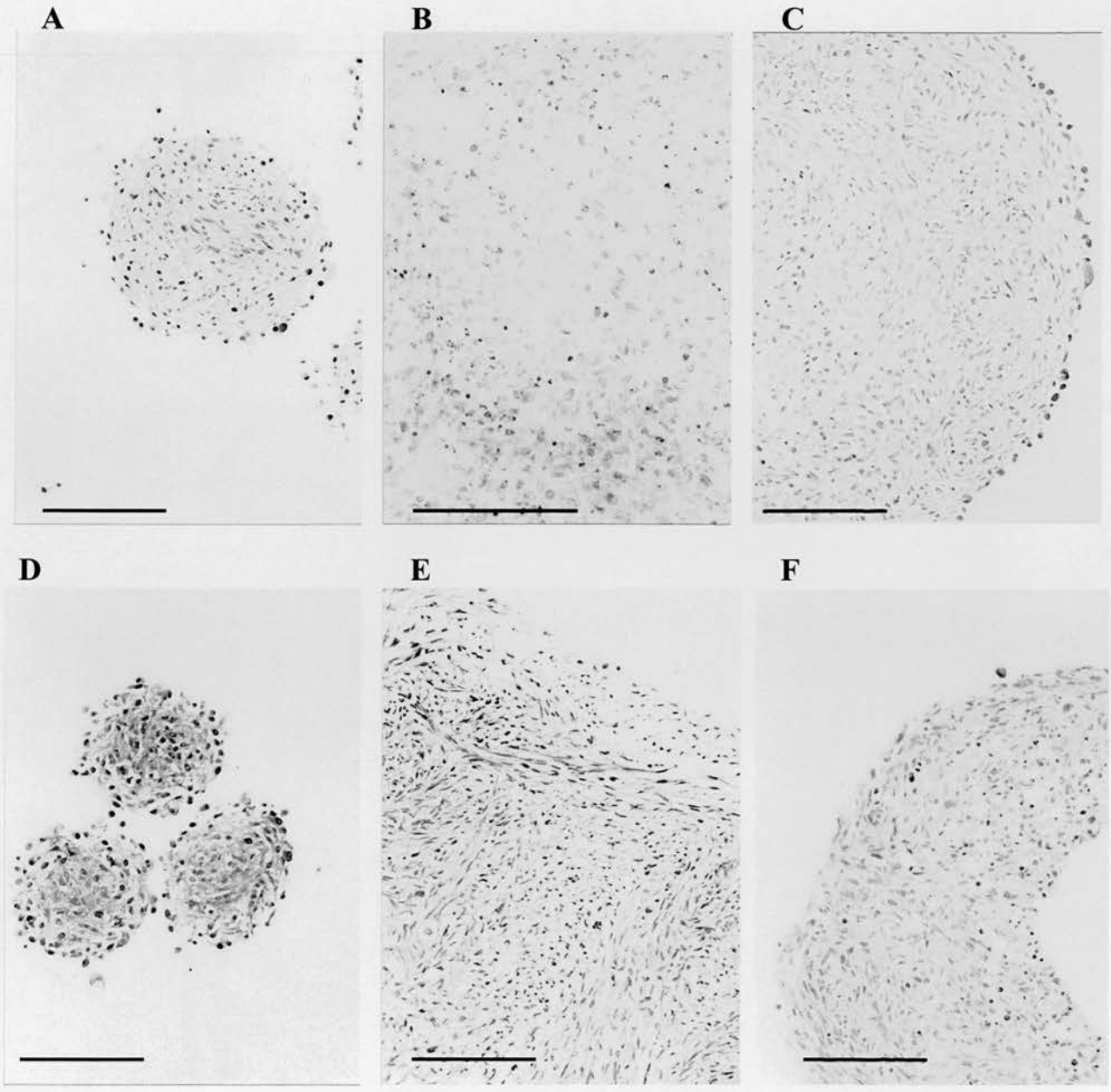

Figure 24. Bax immunohistochemistry in spheroid cultures. A, week 1 U87 spheroid. B, central region of a week 3 U87 spheroid showing a slight increase in perinecrotic expression of Bax. C, week 4 U87 spheroid showing peripheral Bax labelling. D, strong Bax labelling in a week 1 U373 spheroid. E and F, strong Bax labelling across the spheroid radius in week 3 and 4 U373 spheroids respectively. All bars=100μm.

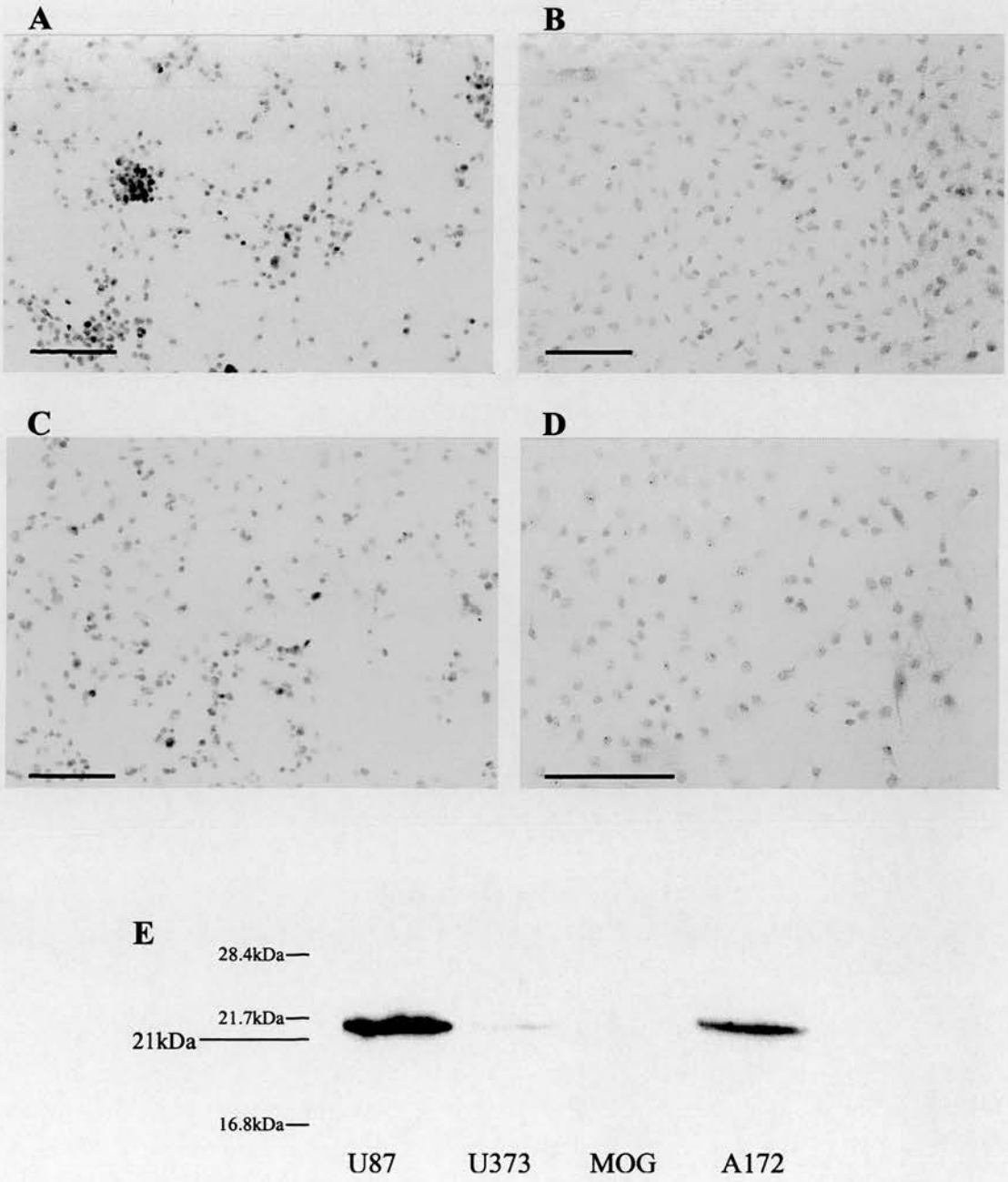

Figure 25. p21 immunohistochemistry in U87 (A), U373 (B), MOG-G-CCM (C) and A172 (D) cell lines in monolayer culture (all bars=100μm). E, shows the western blot analysis using p21 antibody on the four whole cell lysates. Note that U87 and A172 cell lines exhibit considerably darker p21 labelling than the two p53 mutant lines, U373 and MOG-G-CCM.

In spheroid cultures, no visible p21 labelling was observed in U373 cell line at any stage of spheroid development (Figure 26C and D, Table 13). MOG-G-CCM exhibited weak focal labelling in around 1-2% cells at week 1 and this disappeared from week 2 onwards. In U87 and A172 cell lines, moderate focal labelling (2+) was present in approximately 5% of cells from weeks 1-5 (Figure 26A and B, Table 13). p21 labelling was most apparent around the spheroid periphery in these lines over weeks 3-5 (Figure 26B). No perinecrotic enhancement was observed in any of the cell lines.

Two MDM2 antibodies were used in this study; MDM2 (SMP-14) and MDM2 (C-18). SMP-14 binds to an epitope corresponding to amino acids 154-167 of the human MDM2 molecule. C-18 labels the carboxy terminal of the human MDM2 molecule. High levels of MDM2 expression were recorded in all four cell lines in monolayer culture, using the monoclonal antibody SMP-14 (Figure 27, Table 13). U87, U373 and MOG-G-CCM cell lines showed strongly labelled cytoplasm and/or nucleus in nearly 100% of cells (Figure 27A-C). A172 cell line exhibited strong labelling in approximately 60% of cells (Figure 27D). Western blotting confirmed these findings in terms of strength of labelling. However, the most prominent bands on the gel were at 60kDa. Fainter bands were observed at 94kDa (Figure 27E).

In spheroid cultures, SMP-14 levels remained high in all four cell lines at weeks 1 and 2, in terms of both staining intensity and number (Figures 28D and G, Table 13). This labelling was both in the cytoplasm and in the nuclei of all cell lines examined at this time point. By week 3, MDM2 (SMP-14) labelling had become localized towards the centre of the spheroids preceding the onset of central cell death in U373 and MOG-G-CCM cell lines (Figures 28A, B and E). Again, equal amounts of labelling were present in both the nuclei and in the cytoplasm. Staining around the spheroid periphery became weak and almost disappeared in these lines by week 4 (Figure 28C). The cells directly adjacent to the region of central necrosis were MDM2 (SMP-14) negative in U373 cell line (Figure 28F). In A172 and U87 cell lines, perinecrotic MDM2 (SMP-14) was present in slightly larger amounts than elsewhere within the tumour cell mass (Figures 28H and I). The perinecrotic labelling and absence of MDM2 (SMP-14) in surrounding tissue was not as marked in U87 and A172 cell lines as in the MOG and U373 cell lines. Like the p53 mutant lines, perinecrotic MDM2

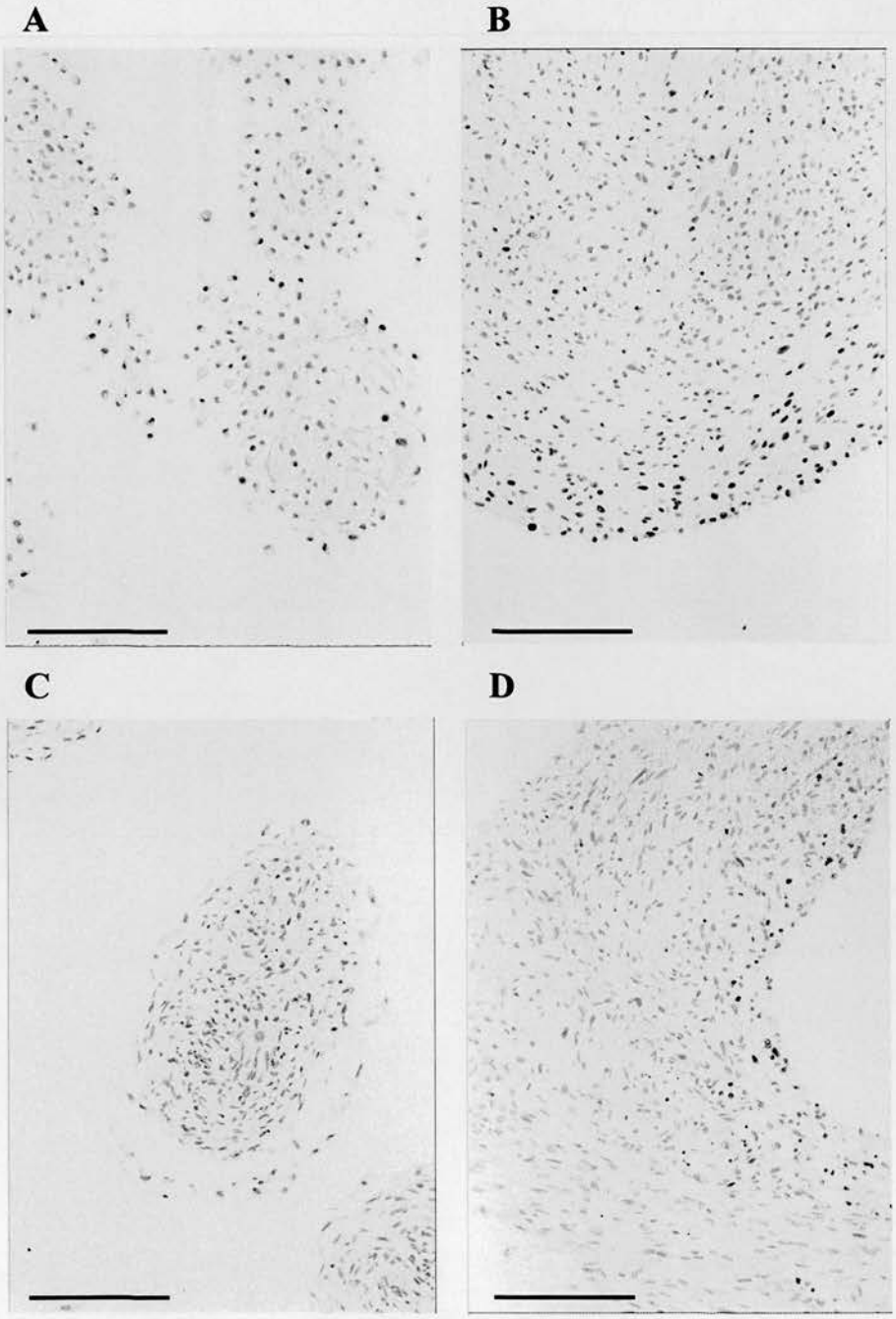

Figure 26. P21 immunohistochemistry in spheroid culture. A, week 1 U87 spheroid showing positive p21 labelling in approximately 5% of cells. B, week 3 U87 spheroid showing peripheral p21 labelling. C and D, week 1 and 3 U373 spheroids showing complete absence of p21 labelling. All bars=100μm.

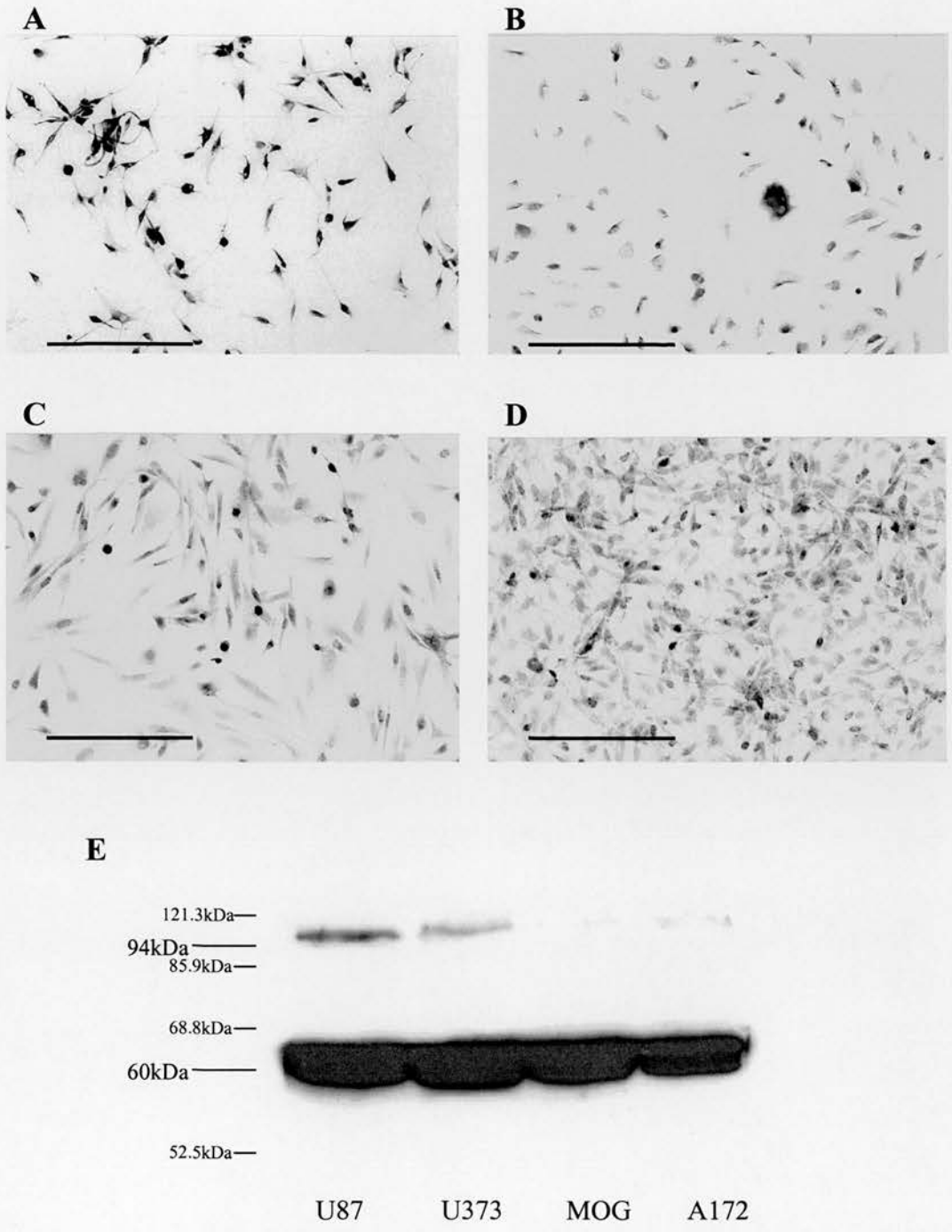

Figure 27. MDM2 (SMP-14) immunohistochemistry in U87 (A), U373 (B), MOG-G-CCM (C) and A172 (D) cell lines in monolayer culture (all bars=100μm). E, western blot showing the MDM2 (smp-14) antibody binding mainly to a 60kDa product as well as to the full-length 94kDa form in monolayer whole cell lysates from the 4 cell lines.

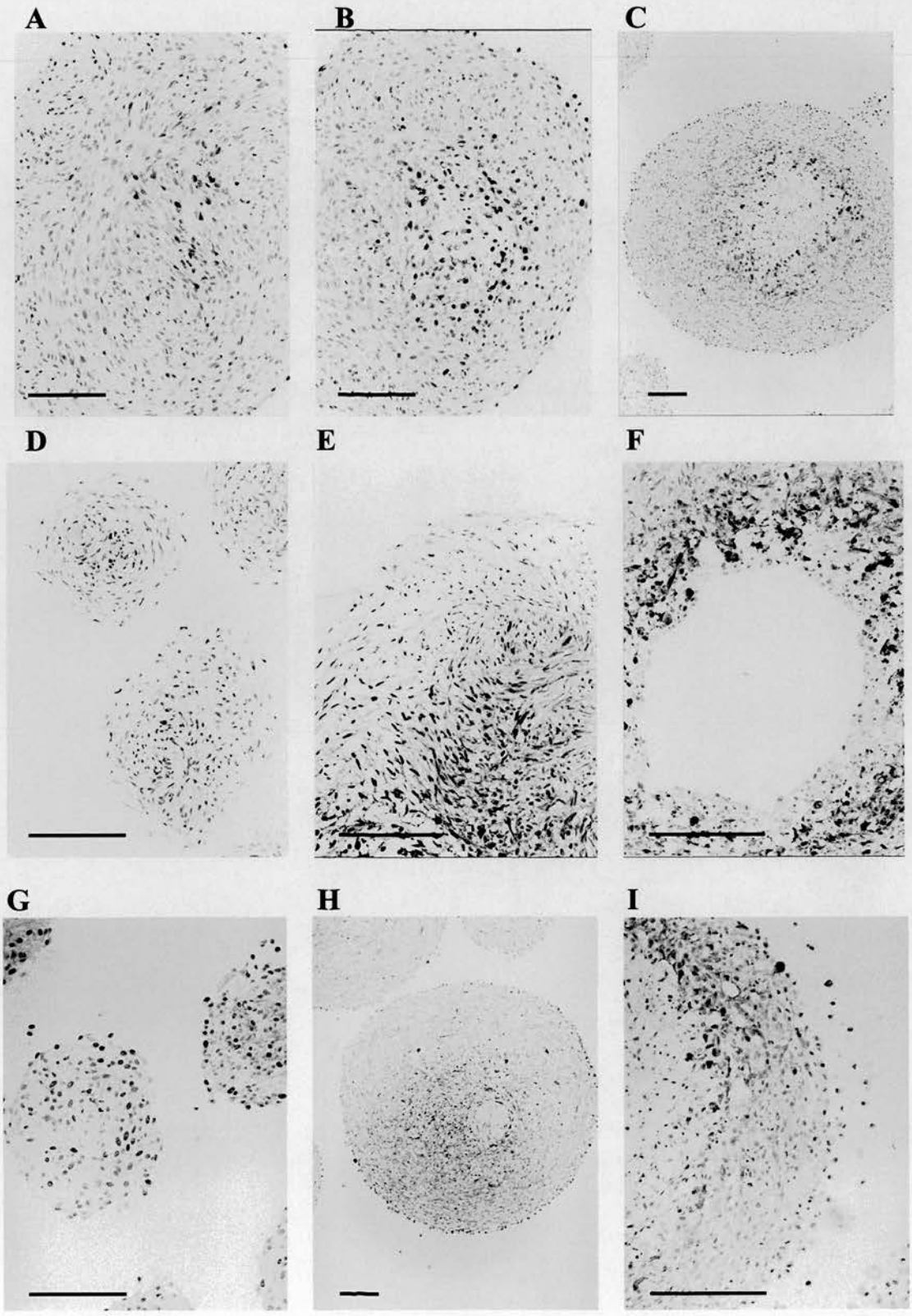
A
B
C
D
E
F
G
H
I

labelling was both nuclear and cytoplasmic in all spheroid regions examined. Therefore the two mutant *P53* cell lines (U373 and MOG-G-CCM) exhibited greater amounts of perinecrotic MDM2 (SMP-14) labelling than the wild-type cell lines (U87 and A172).

The antibody that recognises the carboxyl-terminal of MDM2, C-18, labelled monolayer cultures only weakly and in isolated cells. Western blots of these monolayer cultures revealed that the C-18 antibody labelled only the 94kDa MDM2 protein (Figure 29). No obvious band was seen at 60kDa for this antibody in contrast to the SMP-14 antibody. It was therefore clear that the 60kDa MDM2 isoform (recognised by the SMP-14 antibody) was lacking a carboxyl-terminal domain (as recognised by the C-18 antibody). In spheroid cultures, the distribution of C-18 expression was markedly different from the SMP-14 antibody (Figure 30). No peri-necrotic labelling was observed with this antibody. Morphologically healthy cells situated across the spheroid radius were labelled weakly positive for C-18 in U373, MOG-G-CCM and U87 spheroid cultures. Labelling was predominantly cytoplasmic in spheroids derived from all four cell lines.

In monolayer culture $p14^{ARF}$ expression was highest in MOG-G-CCM cell line (Figure 31). Labelling in this cell line consisted of small dark disks situated within the nucleus (Figure 31A). This occurred in approximately 90% of cells. U373 contained a few isolated cells with this pattern of labelling (2-3%) and A172 and U87 cell lines contained no visible $P14^{ARF}$ labelling. Western blotting confirmed these findings (Figure 31B).

In spheroid culture $p14^{ARF}$ labelling was found only in MOG-G-CCM cell line. Random positively labelled cells were distributed across the spheroid radius. $p14^{ARF}$ labelling was not present in spheroids derived from U87, U373 and A172 cell lines. Some weak peripheral labelling was observed in MOG-G-CCM spheroids from weeks 1-5.

4.2.3. p53, p21, Bax and MDM2 expression in biopsy tissue

As in the spheroid study, both p53 antibodies, Pab1801 and BP53-12, yielded similar results when applied to the biopsy material, apart from the presence of some focal cytoplasmic staining of tumour cells with Pab1801 in most cases (Table 14). Some expression of p53 was detected in 80% (20) of the cases. 52% (13) of cases were classed as being high expressors

Figure 28. MDM2 (SMP-14) immunohistochemistry in spheroid cultures. A, a pre-necrotic MOG-G-CCM spheroid exhibiting central MDM2 localisation . B, a post-necrotic MOG-G-CCM spheroid showing peri-necrotic MDM2 labelling. C, a large week 4 MOG-G-CCM spheroid exhibiting strong peri-necrotic MDM2 labelling. D, week 1 U373 spheroids exhibiting nuclear MDM2 labelling. E, centrally located MDM2 positive cells in a week 3 U373 spheroid. F, peri-necrotic MDM2 labelling in week4 U373 spheroid. Note the absence of MDM2 labelling in cells directly adjacent to the necrotic centre. G, nuclear and cytplasmic MDM2 labelling in a week1 U87 spheroid. H, slight increase in central MDM2 labelling in a week 3 pre-necrotic U87 spheroid. I, week5 U87 spheroid exhibiting lack of staining within the necrotic cell population and positive cells surrounding the necrotic centre. All bars=100μm.

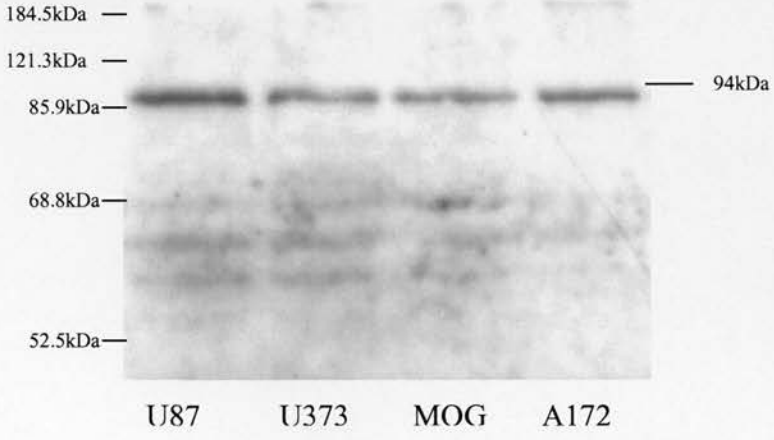

Figure 29. MDM2 (C-18) western blots using cell lysates from the 4 cell lines U87, U373, MOG-G-CCM and A172. Note the absence of a clear band at 60kDa.

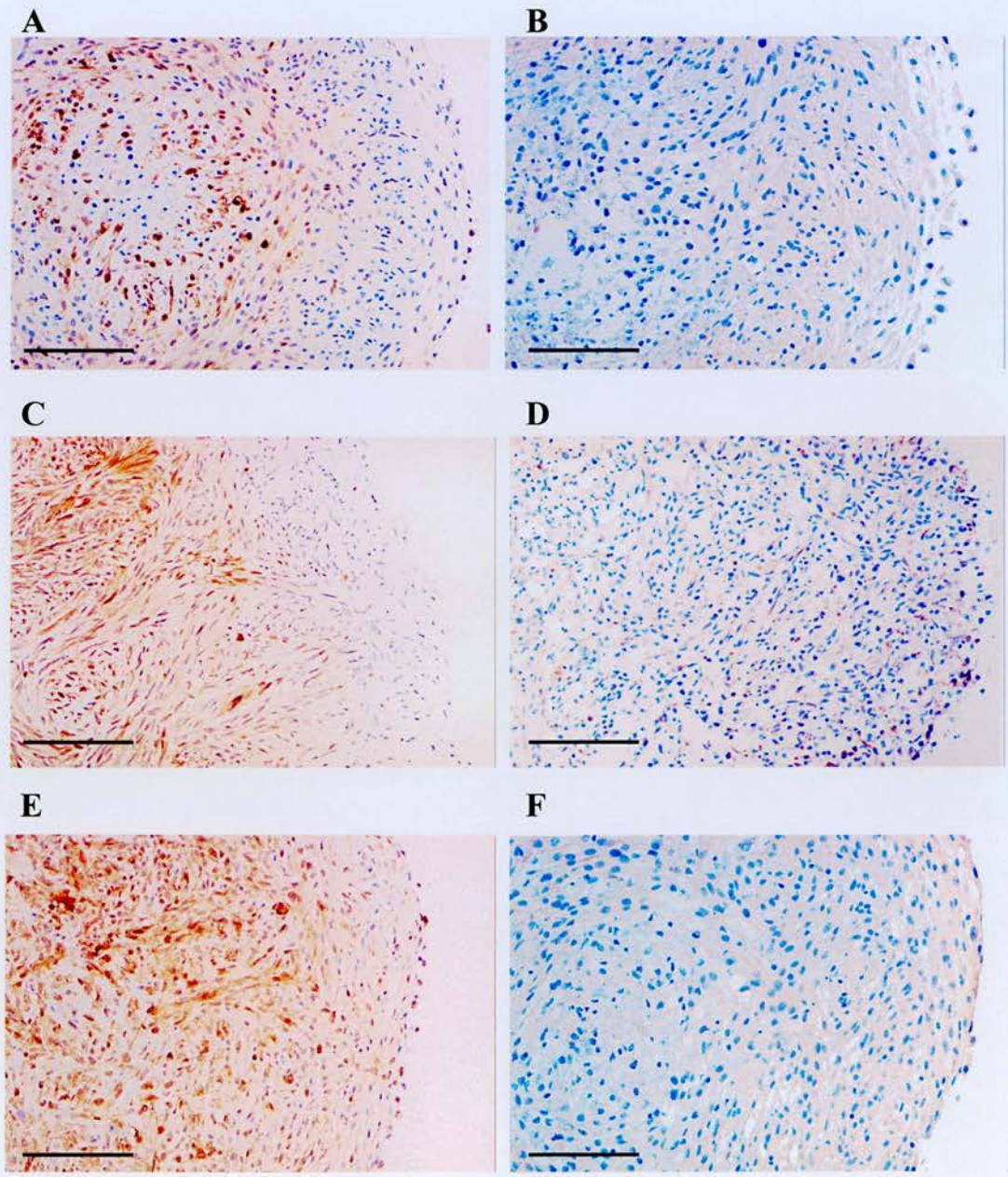

Figure 30. Comparisons between MDM2 (SMP-14) and MDM2 (C-18) immunohistochemistry in spheroid cultures. MOG-G-CCM week 3 spheroid labelled with MDM2 (SMP-14) in A and MDM2 (C-18) in B. U373 week 3 spheroid labelled with MDM2 (SMP-14) in C and MDM2 (C-18) in D. U87 week 3 spheroid labelled with MDM2 (SMP-14) in E and MDM2 (C-18) in F. Note the absence of perinecrotic MDM2 using the C-18 antibody in any of the cell lines. All bars=100μm.

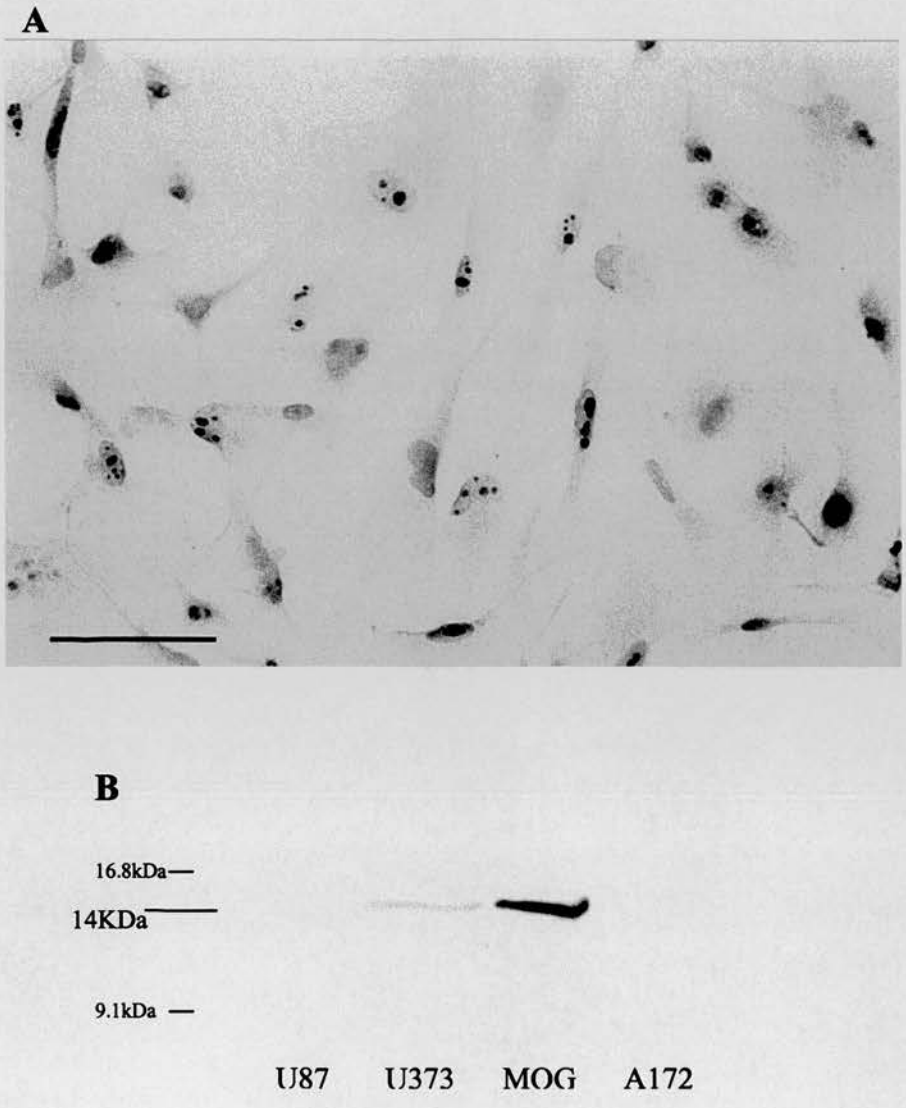

Figure 31. P14^{ARF} labelling in MOG-G-CCM monolayer culture (A) (bar=20μm). Western blot using P14^{ARF} antibody on whole cell lysates of the four monolayer cell lines U87, U373, MOG-G-CCM and A172 (B).

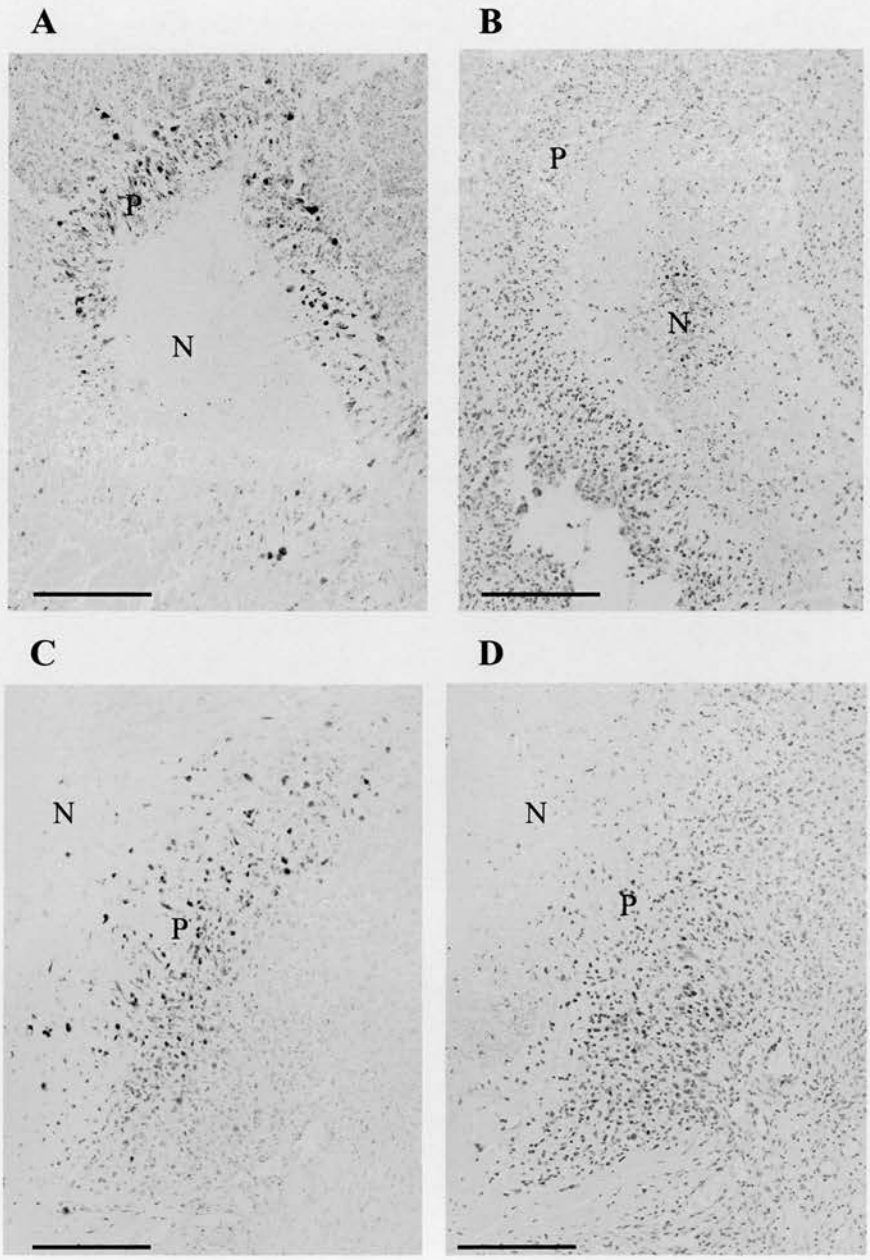

Figure 32. Comparisons between MDM2 (SMP-14) and MDM2 (C-18) immunohistochemistry in glioblastoma biopsy material. Note the peri-necrotic labelling using the MDM2 (SMP-14) antibody in figures A and C and the lack of peri-necrotic labelling using the MDM2 (C-18) antibody. N=necrosis, P=peri-necrotic region. All bars=100μm.

Case	P53 Bp53-12	P53 Pab1801	P21	Bax	MDM2 (SMP-14)	MDM2 (C-18)
1	3++	3++	2+	1++	3+	1+
2	3+	3+	0	0	0	0
3	2+	2+	0	0	0	0
4	2+	2+	0	1+	2+	1+
5	0	2+	0	1+	2+++	1+
6	0	1+	0	3++++	0	1+
7	1+	1+	0	1++	0	0
8	0	2+	0	3++	1+	0
9	3+++	3+++	0	0	1+	0
10	0	0	0	1+	0	0
11	3+++	3+++	0	2+++	1+	1+
12	3++++	3++++	0	2++	2+++	2+
13	3+++	3++	0	1++	0	1+
14	3+++	3+++	3+	2+	1+	0
15	1+	2++	0	1+++	0	ND
16	3++	3+++	0	1+	1+	ND
17	2+	3++	2+	1+++	0	ND
18	1+	1+	0	0	2+	ND
19	1+	1+	0	2+++	1+	0
20	0	1+	0	1++	1+	0
21	2+	2+	0	1++	0	0
22	2+	2++	0	1+	1+	1+
23	3+	2+	0	3+++	2+	ND
24	1+	1+	0	3+++	0	1+
25	3++	3++	0	2+	0	0

Table 14. Semi-quantitative assessment of the staining intensity (0 absent, 1 weak, 2 moderate, 3 strong) and proportion of cells staining (+ <25%, ++ 25-50%, +++ 50-75%, ++++ 75-100%) for p53 (BP53-12 and Pab1801), Bax, p21 and MDM2 (SMP-14 and C-18) in 25 brain tumour biopsies. ND=not done.

(>2+ with either of the two antibodies). Nuclear expression of p21 was observed in 12% (3) of cases (Table 14). Expression of MDM2 (SMP-14) was detected in 80% (20) of cases with 24% of cases showing greater than focal weak expression (>1+) (Table 14). SMP-14 expression in tumour cells was mainly nuclear, although some cytoplasmic staining was also observed. MDM2 (C-18) showed considerably less overall staining than MDM2 (SMP-14). C-18 labelling was observed in around 50% of cases with no cases showing more than weak cytoplasmic expression (<1++) (Table 14). Antibodies to Bax demonstrated granular cytoplasmic expression in 84% of cases with 64% (16) being high expressors (Table 14). In a few cases, staining was both strong and diffuse. No association was demonstrated between p53 over expression and MDM2 (SMP-14 and C-18), Bax and p21.

All of the proteins examined showed some expression on perinecrotic tumour cells, but for p53, p21 and Bax this was similar to the expression on surrounding viable tumour. In the case of MDM2 (SMP-14) however, an upregulation of expression was noted in 80% of cases, which in some cases was striking (Figures 32A and C). In contrast to the predominantly cytoplasmic staining of intervening viable tumour, peri-necrotic staining was both cytoplasmic and nuclear. The MDM2 (C-18) antibody, which labels the central acidic domain of the MDM2 molecule, exhibited markedly decreased MDM2 labelling compared to MDM2 (Smp-14). No perinecrotic labelling was observed (Figures 32B and D). Only cells within morphologically healthy tumour cell populations labelled positively for this antibody. All MDM2 (C-18) labelling was cytoplasmic. There was no correlation between the presence of perinecrotic MDM2 (SMP-14 or C-18) expression and p53 expression in the tissue samples (Table 14).

4.2.4. p53, p21, Bax and MDM2 expression in monolayer cultures and spheroids exposed to oxidative stress

Western blotting using the p53 antibodies Pab1801 and Bp53-12 revealed that levels of p53 were upregulated in U87 and A172 cell lines after exposure to 1mM H_2O_2 for 6 hours (Figure 33). Visible bands were almost non-existent in the untreated groups of cells. Levels of p53 expression were unchanged in the U373 and MOG cell lines when the cells were exposed to H_2O_2. p21, Bax and MDM2 levels were unchanged in all four cell lines in response to H_2O_2. The western blot for MDM2 failed to pick up 90kDa MDM2 in any of the samples tested.

This is probably due to the lack of sensitivity of the assay. Although levels of apoptosis were not assessed, the wild-type monolayer cultures (U87 and A172) could be seen to be considerably less viable subsequent to H_2O_2 treatment than the p53 mutant cultures. All incubation medium was spun down to capture all non-adherant cells following treatment (see Figure 33 for all blots).

Levels of p53 expression increased in U87 cell line when exposed to 0.5% oxygen for varying lengths of time (Figure 34). An upregulation of p53 was noted after 2 hours exposure and became more pronounced after 6, 12 and 24 hours. No change in p53 expression was seen in the U373 cell line in response to hypoxia (Figure 34). Levels of p21 increased in the U87 cell lines in a similar pattern to p53 in response to hypoxia. No such changes were seen in p21 expression in U373 cell line. There appeared to be a slight increase in 90kDa MDM2 in the U87 cell line in response to hypoxia. No similar increase was seen in the U373 cell line. No changes were observed in the expression of Bax in either cell line in response to hypoxia over the 24hour period (See Figure 34 for all blots).

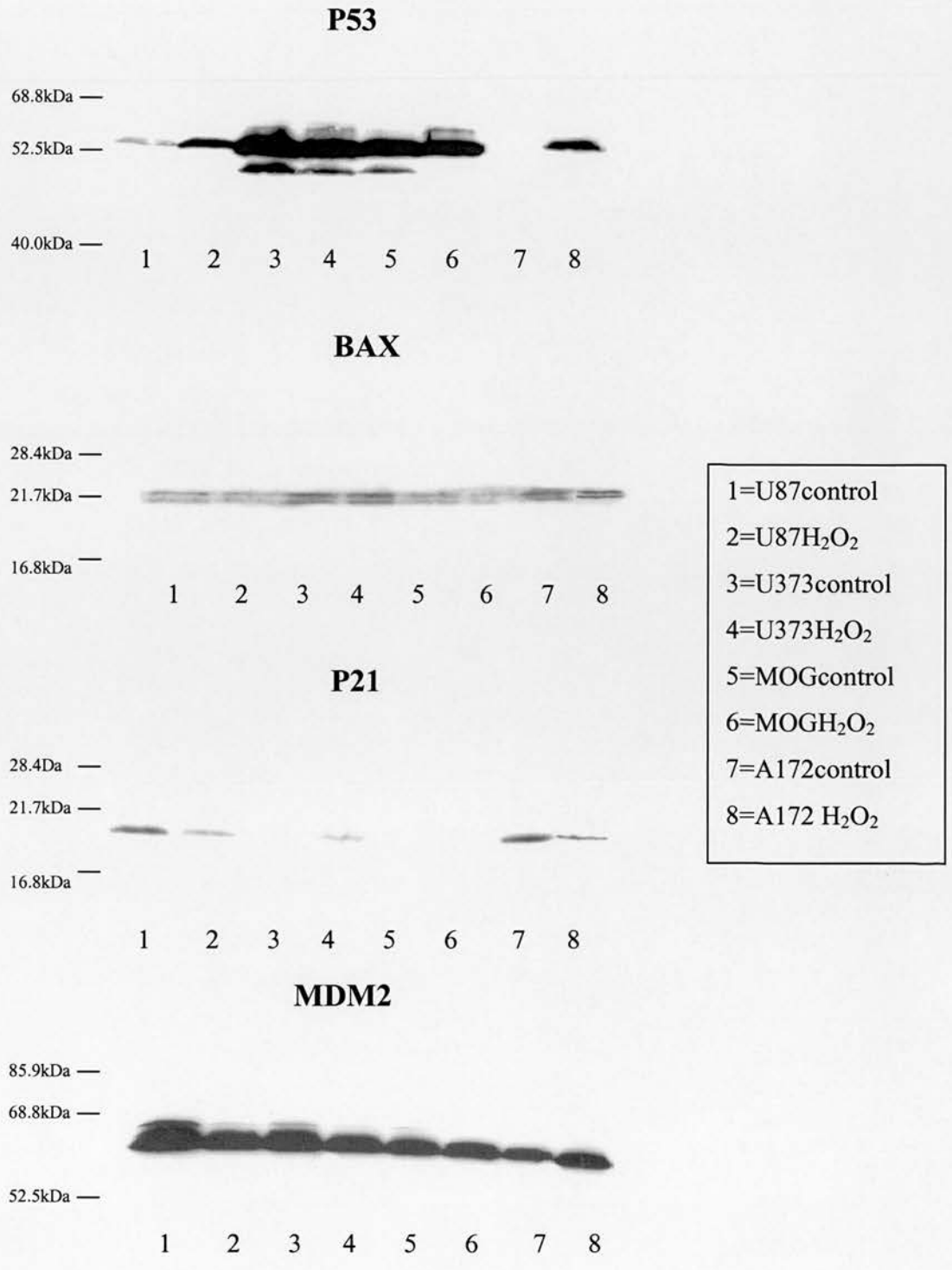

Figure 33. P53 related protein levels in U87, U373, MOG-G-CCM and A172 cell lines in response to H_2O_2. Blots show that U87 and A172 cell lines show upregulation of the p53 after exposure to H_2O_2. control=untreated. H_2O_2=treated with 1mM H_2O_2 for 6hours.

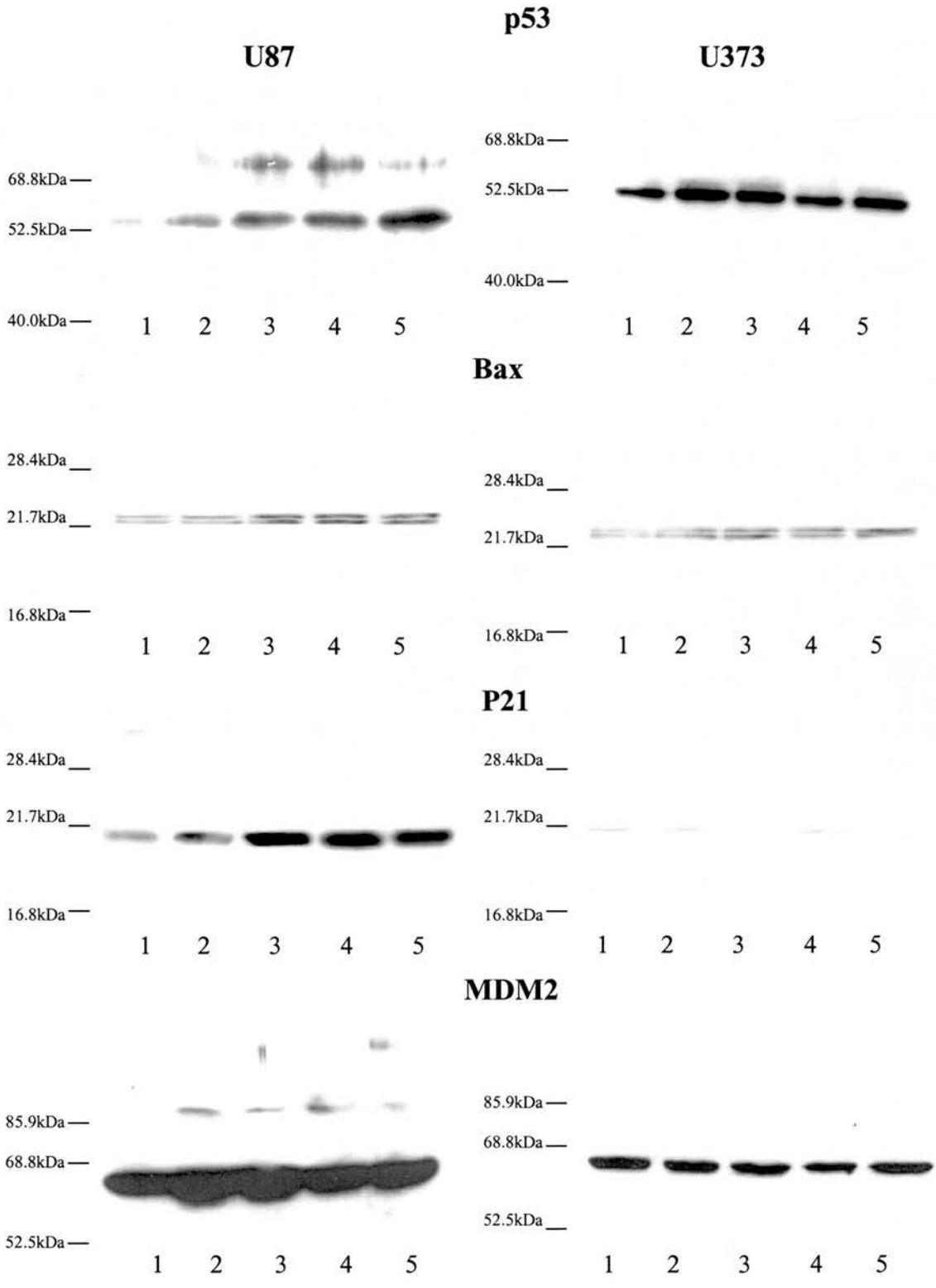

Figure 34. P53 related protein levels in U87 and U373 in response to prolonged exposure to hypoxia (0.5% O_2). 1=non-hypoxic control, 2=1hr, 3=2hrs, 4=6hrs, 5=24hrs. p21, p53 and 94kDa MDM2 show an increase in expression in U87 cell line in response to hypoxia.

4.3. Discussion

4.3.1. Summary of results

Levels of apoptosis and necrosis were not found to differ between p53 mutant lines (U373 and MOG-G-CCM) and p53 wild-type lines (U87 and A172). p53, p21 and 90kDa MDM2 were found to be reactive in the p53 wild-type line U87 in response to hypoxia exposure. Similar findings were observed following exposure to H_2O_2 in both U87 and A172 cell lines. However, there was a decrease in p53 and p21 expression, and no change in 90kDa MDM2 expression, within central regions of pre and post necrotic glioma spheroids derived from these p53 wild-type lines. No upregulation of p53/p21/90kDaMDM2 was identified in the p53 mutant lines U373 and MOG-G-CCM either in response to hypoxia/H_2O_2 or within perinecrotic tissue. High levels of endogenous Bax remained consistent both in monolayer culture and all stages of spheroid growth in all 4 of the cell lines examined. Of the experiments performed in this study, 60kDa MDM2 was the only protein to be localised within perinecrotic tissue *in vitro* and *in vivo*. This expression was found in both p53 wild-type and mutant lines. This 60kDa MDM2 isoform was thought to be lacking a C-terminal domain.

4.3.2. *P53* mutation analysis

Of the four cell lines examined, previous research has shown that U87 and U373 were *P53* wild-type and mutant respectively thus allowing the hypothesis to be addressed (Ishii et al., 1999). In order to confirm these findings and to determine the status of the two other glioma cell lines used in this study, A172 and MOG-G-CCM, the *P53* gene was sequenced in all four cell lines from exons 2-11. U373 possessed a previously identified mutation at codon 273 (CGT→CAT, Arg→His), a mutation 'hotspot' on the *P53* gene*. Approximately 15% of *P53* mutant glioblastomas have mutations at codon 273. This results in the removal of critical residues normally in contact with DNA, causing loss of sequence specific DNA binding (Sigal et al., 2000). However, this mutation retains 98% folding of the wild-type p53 configuration and many experiments have demonstrated the ability of this mutant to bind to and transactivate a p53 responsive reporter (Park et al., 1994; Gollahon et al., 1996; Hachiya et al., 1994). In addition, protection from apoptosis in cells possessing this mutation has been shown to be low when exposed to cisplatin (Sigal et al., 2000). However, marked

decreases in the production of various downstream targets (such p21 and MDM2) have also been reported in various cell lines exhibiting p53His273 mutations suggesting that p53 binding ability may differ between target genes and cell lines (Saintigny et al., 1999). This is further supported by studies examining the dominant/negative characteristics of various *P53* mutants (Kawamura et al., 1996). When a human squamous cell carcinoma cell line exhibiting wild-type *P53* was transfected with a vector containing a *P53*His273 sequence, the resulting protein failed to enhance cell growth (Kawamura et al., 1996). In contrast, normal breast epithelial cells when transfected with a similar vector resulted in an increase in lifespan in all derived clones with one clone actually becoming immortalized (due to subsequent alterations) after a period of growth arrest (Gollahon et al., 1996).

MOG-G-CCM cell line has not previously been sequenced for *P53*. A *P53* mutation was found at codon 159 (GCC→GTC, Ala→Val). Few recorded cases have been found in the literature of this particular mutant and none have been found in astrocytic tumours (van Meyel et al., 1994; Giglia et al., 1998). The DNA binding region of the p53 protein is between residues 102 and 292 thus the *P53*159Val mutation is situated within this section (Prives et al., 1999). However, like the *P53*His273 mutant, the *P53*Val159 mutant is unlikely to result in a protein with a significant configurational change due to the similarity of the replacement amino acid to the original (both have non-polar side chains). Experiments analysing the transcriptional activity of the mutant protein using the yeast functional assay found that 98% of yeast colonies turned red as a result of successful activation of a wild-type *P53* promoter sequence (de Cremoux et al., 1999). This means that the *P53*159Val mutants may retain significant wild-type p53 transactivational ability. The functional status of *P53*159Val mutants have not been functionally assessed in normal or transformed human cells. Analysis of activation of artificial promoter sequences sometimes do not reflect the actual transcription of target mRNA in cell cultures (Tada et al., 1996)

A172 has previously been described as having a mutation at codon 242 (CGT→TTC, Cys→Phe) (Kataoka et al., 2000), but this was not identified in the cells used in this study. In addition, U87 cell line was confirmed as wild-type in these experiments. To summarise

---

* http://perso.curie.fr/Thierry.Soussi/p53_mutation.html

therefore, U87 and A172 cell lines were wild-type for the *P53* gene and U373 and MOG-G-CCM were P53 mutant.

4.3.3. p53 related expression in monolayer cultures and biopsies

In order to fully assess *P53* related protein distribution in spheroid cultures and biopsy tissue, it was first important to review the endogenous expression of these proteins in monolayer culture and on biopsy sections. It is important that expression of these proteins is compared with known genetic aberrations in the cell lines, particularly *P53* status and other known common alterations, such as MDM2 over expression. The biopsy tissue was assessed in terms of general levels of expression, as a mode of comparison with the *in vitro* experiments.

The inability of MDM2 to bind to and inactivate the mutant p53 protein means that many *P53* mutations can be identified immunohistochemically due to an increase in the half life of the mutant p53 protein (Haupt et al., 1997 ; Anker et al., 1993). Using monolayer cultures, this was confirmed in both U373 and MOG-G-CCM cell lines. This suggests that the full length MDM2 protein, which is present in small amounts in these cells, does not recognise the two mutant p53 proteins p53His273 and p53Val159. Although the biopsy material was not sequenced for *P53* status, of the 25 GBM biopsy cases examined, 52% labelled strongly for p53, suggesting the presence of *P53* mutations. This latter result should be taken with caution due to recent studies using 316 breast cancer biopsies which showed that immunohistochemical determination of *P53* mutations can pick up a considerable number of false negatives due to large scale deletions and transversions. These can result in severely truncated forms of the p53 protein which cannot be recognised by commonly used p53 antibodies such as BP53-12 and Pab1801 (Sjogren et al., 1996). In addition, some tumours and tumour cell lines show upregulation of the wild-type p53 protein in the absence of *P53* mutations. This has been observed in smaller studies in glioma where more low and high grade tumours exhibited strong p53 labelling then those possessing detectable *P53* mutations (Marchenko and Moll, 1997; Pykett et al., 1998). All the samples with *P53* mutations in the latter study did have p53 protein upregulation.

To determine whether p53 is likely to be upregulated in relation to necrosis, the expression of several proteins known to be activated by p53, and which may play a role in the pathogenesis

and regulation of cell death were studied. These were p21, Bax, MDM2 and $p14^{ARF}$. In monolayer culture, reductions in p21 labelling were observed in the p53 mutant cell lines U373 and MOG-G-CCM, compared to the other cell lines. No p21 labelling was observed immunohistochemically in either of the p53 mutant cell lines and only a very faint band was observed using western blotting. Mutations at codon 273(CGT →CAT) have previously been shown to reduce transactivation of the WAF1 promotor (Saintigny et al., 1999). Therefore, findings in this study show that the *P53*159Val mutant may also have a reduced WAF1 transactivation ability. In contrast, levels of p21 expression showed no correlation with increased p53 protein expression in the biopsy cases. Only 3 cases were strongly p21 positive and all exhibited high levels of the p53 protein (suggesting the presence of a p53 mutation). These findings are consistent with larger scale studies where no inverse correlation was found between p21 expression and p53 overexpression (Khalid et al., 1998). In addition, other experiments have shown that *P53* genetic status is unrelated to p21 expression (Weller et al., 1998). This may be due to the presence of different *P53* mutations in these tumours, resulting in proteins with varying DNA binding abilities. In addition, recent evidence has suggested a mechanism for p53 independent regulation of p21 via a E2F1/Ras pathway and TNF-α (Kobayashi et al., 2000; Gartel et al., 2000). Other studies have shown that expression of p21 and absence of p53 could confer a selective advantage to healthy tumour cells (Gomez-Mazano et al., 1997).

Constitutive expression of Bax was very high in the four cell lines examined regardless of *P53* status. In the biopsy cases Bax expression was observed in 90% of cases. These findings support the findings of Krajewski et al, where both gliomas and glioma cell lines where shown to exhibit consistently higher levels of constitutive Bax than normal astrocytes, regardless of *P53* status (Krajewski et al., 1997). In addition, phyllodes tumours of the breast harbouring specifically *P53*His273 mutations have been shown to accumulate large quantities of Bax protein (Kuenen-Boumeester et al., 1999). It was not clear in these experiments whether such increases in expression are a result of the mutant p53 protein having some residual transactivation activity or whether Bax is upregulated via a p53 independent pathway. It is clear however that this high endogenous expression of Bax is unlikely to be in the activation of apoptotic pathways in these monolayer cultures and in the biopsy material. In monolayer culture for example, nearly 100% of the cells were Bax

positive in the 4 cell lines examined and basal levels of apoptosis ranged from 0.2% in A172 cell line to 1% in U373 cell line. These data are supported by experiments showing that retroviral transfer of *Bax* into many glioma cell lines fails to have an effect on cell death indices when grown under normal conditions and when exposed to various chemotherapeutic reagents (Naumann et al., 1998).

Like Bax, endogenous MDM2 expression was extremely high in both the *P53* wild-type and mutant cell lines and in monolayer cultures, contrary to evidence suggesting U87, U373 and A172 all exhibit low levels of endogenous protein (He et al., 1994). Using two different MDM2 antibodies (Smp-14 and C-18) which label different parts of the MDM2 molecule, it was clear that the largest proportion of MDM2 in each of the four glioma cell lines was a 60kDa MDM2 protein lacking in a carboxyl terminus. It is thought that this truncated form of MDM2 may provide a new entry point for cellular signals to regulate p53 turnover, both in living and dying cells (Pochempally et al., 1998). The implications, structure and regulation of this truncated 60kDa MDM2 isoform are discussed in 4.3.6-4.3.7.

When the glioblastoma biopsy tissue was examined for both MDM2 isoforms, like the cell lines, a far greater level of the 60kDa MDM2 isoform was found. When examining tissue for the presence of full length MDM2 overexpression, which is common in primary glioblastoma, it is clear that an antibody or a combination of antibodies, that recognise full length MDM2, should be used. There was no correlation between p53 expression and MDM2 (either 90kDa or 60kDa isoform) expression in the biopsy tissue. This was similar to the cell lines where the two mutant lines showed similar levels of 60kDa MDM2 to the *P53* wild-type lines. Initially, it was thought that only cell lines possessing wild-type *P53* contained high levels of various truncated MDM2 isoforms (Landers et al., 1997; Pochempally et al., 1998). However, shortened MDM2 splice variants found in a study by Matsumoto et al together with the data in this study suggests that various MDM2 isoforms exist in tumour cell populations with both *P53* mutant and wild-type backgrounds (Matsumoto et al., 1998).

It is unlikely that the 60kDa MDM2 molecule would be affected by the *CDKN2A* genetic status of the cell lines because the N-terminus of the wild-type $p14^{ARF}$ protein interacts with the C-terminus of the MDM2 molecule. Therefore, if the C-terminus of the MDM2 molecule

is absent, no such interaction can take place. This association would normally lead to repression of the MDM2-dependent suppression of p53 (Pomerantz et al., 1998; Zhang et al., 1998).

Lower levels of the full length 90kDa protein were found in each of the cell lines compared to the 60kDa isoform. Experiments using the MDM2 (C-18) antibody showed that similar levels of 90kDa expression were found in all four lines, thus the expression of both isoforms appeared to be independent of the *P53* status. There appeared to be no relationship between the expression of full length 90kDa MDM2 and $p14^{ARF}$ status/expression. Low levels of $p14^{ARF}$ in three of the lines U87, U373 and A172 were observed. Homozygous deletions have been shown to exist in the *CDKN2A* locus in both U87 and A172 cell lines whereas U373 was wild-type for this locus (Ishii et al., 1999). High levels of $p14^{ARF}$ protein were observed in MOG-G-CCM. MOG-G-CCM was the only cell line not previously characterised for *CDKN2A* mutation status thus it was not known whether the immunoreactive product found in this study was viable. Different proliferative signals, such as c-myc (Zindy et al., 1998), E1A (de Stanchina et al., 1998) and E2F (Bates et al., 1998) lead to $P14^{ARF}$ activation and p53-dependent apoptosis in normal cells. Differences in proliferative signals between lines, in combination with CDKN2A alterations in the U87 and A172 cell lines, are likely to result in the observed variations in $p14^{ARF}$ protein accumulation.

4.3.4. p53 related expression in response to oxidative and free radical stress

In order to test the hypothesis that the accumulation of p53 and its downstream target proteins are associated with areas of endogenous cell death in glioblastoma cell populations, it was first important to establish that at least one cell line was capable of mediating a p53 response to stress. If levels of p53 were not raised in response to different types of oxidative stress in these experiments then it is unlikely they would be raised within glioma spheroid cultures. In addition, any observed upregulation of p53-regulated proteins such as Bax, may be due to a p53 independent mechanism in the absence of a concurrent increase in p53 expression. Many studies have shown that the p53 protein is stabilized after exposure to an oxidative insult (Graeber et al., 1996; An et al., 1998). Tumour cells that develop *P53* mutations demonstrate a diminished apoptotic potential in response to oxidative stress (Graeber et al., 1996). Of 7,202 transcripts known to be induced by p53 before the onset of

apoptosis only 14 have been found to be markedly increased in p53-expressing cells compared to control cells. Nearly all of these encode proteins that could generate reactive oxygen intermediates or respond to oxidative stress (Polyak et al., 1997). The two forms of oxidative stress used in this study, hypoxia and H_20_2 both involve the activity of reactive oxygen species (ROS).

Hypoxia has been shown to generate reactive oxygen species from the mitochondria which regulate the cytosolic redox state and are required for the stablization of the p53 protein (Chandel et al., 2000). In this study, U87 cell line exhibited marked increases in p53 protein over a 24 hour period when exposed to 0.5% oxygen. Not surprisingly, the mutant protein in U373 cells did not show any increase in p53 expression, which remained extremely high. Following p53 protein stabilization, the p53 dependent proteins p21 (Green et al., 2001; Chandel et al., 2000), p27 (Gardner et al., 2000), Bax (Ruan et al., 1999; Kimura et al., 2001) and Fas/FasL (Vogt et al., 1998) have been shown to be expressed which can then activate cell cycle arrest (p21and p27) and/or apoptosis (Bax and Fas/FasL). Levels of p21 were found to gradually increase over time in response to hypoxia in U87 cell line in this study. No changes in p21 expression were observed in the *P53* mutant U373 cell line. Bax remained unchanged in both U87 and U373 cell lines. Levels of 90kDa MDM2 appeared to increase after exposure to hypoxia in U87 cells but not in U373 cells. Levels increased after 1hour and then remained stable over the 24hour period. The 60kDa truncated MDM2 isoform remained unchanged in response to 0.5% oxygen in both lines. Levels of 90kDa MDM2 have previously been shown to be reduced in response to hypoxia in order to allow for the accumulation of the p53 protein (Alarcon et al, 1999). It is possible that the increase in p53 protein stimulated an initial increase in full length MDM2 protein but post-translational modifications and the involvement other proteins, such as $p14^{ARF}$, do not allow any subsequent MDM2 transcription and/or negative association with the active p53 molecule. This is supported by the continual increase in p53 over the 24 hour period. HIF-1α expression was also found to increase after 2 hours exposure to hypoxia. Hypoxia has been shown to activate very high levels HIF-1α which are required help stabilize the p53 protein (Carmeliet et al., 1998) (as discussed in 3.5.6). HIF-1α expression was upregulated in both wild-type and mutant *P53* cell lines thus agreeing with earlier evidence suggesting this to be an event upstream of the p53 protein (An et al., 1998).

In various brain diseases, reactive oxygen intermediates (ROIs) which include H_2O_2, superoxide anions and hydroxyl radicals are important mediators of physical and chemical stresses. For example, ischaemic-reperfusion injured tissue has been shown to excrete large amounts of H_2O_2 (Marx, 1987). NO, another reactive oxygen intermediate has also been shown to increase levels of H_2O_2 and has been implicated around areas of tumour associated hypoxia (Asahi et al., 1995). The addition of large amounts of H_2O_2 (1mM) to cells *in vitro* has a similar effect to hypoxia in that it can increase levels of p53 protein and subsequent levels of p21, GADD45 (Kitamura et al., 1999), Bax (Wang et al., 2001) and Bak (another pro-apoptotic member of the Bcl-2 family)(Kitamura et al., 1999). Low levels of H_2O_2 have been implicated in signal transduction in endothelial cells (Rao and Berk, 1992). The addition of 1M H_2O_2 to the medium of the cell lines in this study resulted in an upregulation of the p53 protein in the two *P53* wild-type lines U87 and A172. No such increase was seen in the *P53* mutant lines, U373 and MOG-G-CCM. p21, MDM2 (60kDa or 90kDa forms) and Bax were not seen to be upregulated in response to H_2O_2 in any of the lines.

The findings in this part of the study suggested that wild-type *P53* was able to be upregulated in two of the cell lines, U87 and A172, in response to stress, irrespective of any other genetic alterations present. This response in monolayer culture to these types of stress raised the possibility that p53 could be important for the regulation of cell death within and around areas of endogenous cell death in glioblastoma. The central areas of glioma spheroids are likely to be subjected to increases in free radical stress due to increases in acidosis, toxic waste build up and lipid peroxidation of necrotic cell membranes (Mueller-Klieser et al., 2000). In addition, levels of intraspheroidal oxygen become very low at large spheroid sizes in central regions, thus p53 could potentially mediate a cell death response within these areas.

4.3.5. *P53* status and levels of apoptosis in spheroid cultures

Quantitative analysis revealed that glioma spheroids derived from U87 cell line, which has a *P53* wild-type status, had significantly more apoptotic figures than the other 3 cell lines. However, U373 which has mutant *P53* contained more apoptotic figures than either MOG-G-CCM (p53 mutant) or A172 cell line which was wild type for *P53*. Therefore, in comparing levels of apoptosis between cell lines, no simple correlation existed with *P53* status. In addition, there was no correlation between *P53* status and susceptibility to necrosis which

occurred at a similar diameter in all four cell lines. These findings support many reports in glioblastoma biopsy material where *P53* wild-type tumours do not show higher apoptotic indices than *P53* mutant tumours. Some investigators have suggested that the reason for this may be due to the fact that over expression of wild-type *P53* often correlates with the expression of pro-survival Bcl-2 thus allowing an escape from p53 mediated apoptosis in wild-type tumour cell populations (Alderson et al., 1995). However, other studies report that no such correlation exists (Tews, 1999). What is most likely is that a combination of genetic alterations and expression patterns are likely to lead to the same functional effect (Rasheed et al., 1999). For example, homozygous deletions in the *CDKN2A* locus in U87 and A172 cell lines may result in a similar apoptotic deficit as *P53* mutations in U373 and MOG-G-CCM lines. Although this is the case, it is possible that the endogenous cell death observed within perinecrotic tissue may arise via different pathways (p53 related or otherwise) in spheroids derived from either *P53* mutant or wild-type lines.

4.3.6. Perinecrotic expression of p53 related proteins

It was hypothesised that increases in p53 expression and other p53 related proteins may be associated with areas of cell death in either pre- or post-necrotic spheroids. Although no increases in p53 expression have been detected previously *in vivo*, it was possible that spatio-temporal monitoring of glioma spheroid cultures may pin-point changes in protein expression within glioma cell populations as areas of cell death form. However, as the spheroids became larger, no increase in p53 protein was apparent in or around the developing area of central necrosis for any of the cell lines examined. In the *P53* mutant lines, p53 protein levels were consistently high across the spheroid radius. This pattern was to be expected due to the inability of the mutant protein to be identified and subsequently degraded. However, in the wild-type cell lines, labelling was faint and peripherally located. There was no increase in centrally located p53 expression at any time point in spheroid development. Peripheral expression was similar to levels in small spheroids and in monolayer culture. Although wild type p53 has a very short half life, it is surprising that expression of the wild type protein should be decreased around areas of cell stress. A comparable pattern of expression was seen in the biopsy sections where p53 labelling in both high and low p53 expression groups appeared to be present within healthy cell populations with no increase in labelling around areas of cell death. It would therefore appear that the regions of cell death present within

glioma cell populations are dying as a result of mechanism not requiring accumulation of the p53 protein. Many different cell types exhibit p53-independent apoptosis. It is possible that endogenous cell death in glioblastoma in both *P53* wild-type and mutant cells are activated via similar p53-independent pathways rather than different pathways resulting from the varying *P53* status of the cells.

In the *P53* wild-type lines, a similar reduction in perinecrotic p21 labelling was observed within inner spheroid regions. Like p53, p21 labelling was present in cells around the spheroid periphery, within the proliferating cell population, at a similar level that was observed in the monolayer cultures. This was surprising as p21 is known to activate cell cycle arrest in similar regions in other spheroid types as a result of cell-cell contact and variations in growth factor availability. In M1(Ha-ras oncogene transformed fibroblasts) spheroids, the inner region of quiescence was characterised by the induction of p21 (LaRue et al., 1998). Cellular quiescence is thought to work as a defence mechanism against likely reductions in metabolites that eventually occur within these areas (Mueller-Klieser, 2000). However, other members of the Cip/Kip family of CDK inhibitors may be responsible for cell cycle arrest within the glioma spheroid cultures. p27 is not thought to be regulated by the p53 pathway and can be induced by IFNs (interferons) and activated post translationally, particularly in response to cell-cell contact and serum deprivation (Pagano et al., 1995; Kuniyasu et al., 1997; Moro et al., 1998; Levenberg et al., 1999). In experiments performed by St Croix et al. (1998), EMT6 cells were transfected with an exogenous E-cahedrin expression vector which resulted in tighter cell adhesion in inner spheroid regions, similar to those found in this study. This resulted in an increase in the CDK inhibitor p27 and subsequent growth arrest. In addition, recent evidence has shown that p21 may be more important in regulating cell cycle re-entry after hypoxic injury rather than activating hypoxia-induced arrest (Green et al., 2001).

Perinecrotic upregulation of Bax was not seen in either the brain tumour spheroids or in biopsy tissue. This, in addition to the lack of Bax upregulation in response to oxidative stress, suggests that Bax is not important for the regulation of cell death in this system. Most cells exhibiting high levels of Bax expression appeared within healthy proliferating cell populations in spheroid culture and in human glioblastoma biopsy material. In some tumour

cell lines high levels of endogenous Bax have been associated with good response to chemotherapeutic agents (McPake et al., 1998). However, because Bax is thought to work as a dimer with other Bcl-2 family members releasing pro-apoptotic factors into the cytoplasm, it is likely that other associated proteins may be be more important for regulating cell death in these cells. Some studies have shown that there is no relationship between Bax and the pro-survival factors Bcl-2, Mcl-1 and Bcl-XL (Krajewski et al., 1997). However, others have suggested that the anti-apoptotic protein Bcl-2 increases during the development of an initial to recurrent glioblastoma (Strik et al., 1999). The heat shock binding protein Bag-1 has also been implicated in providing a survival advantage to glioma cells in deprived microenvironments (Roth et al., 2000). In addition, a novel member of the Bcl-2 family has been discovered called Diva which can interfere with apoptotic signalling downstream from cytochrome C release and upstream form Apaf-1 activation (Naumann et al., 2001). Monitoring levels of Bid, which is transactivated by the p53 protein and is a known mediator of the death receptor superfamily may also be of value, particularly as Fas receptors have found to be expressed around areas of cell death in GBM (Yin, 2000; Tachibana et al., 1996).

4.3.7. Perinecrotic MDM2 expression

One of the most important findings in this study was the localisation of a 60kDa MDM2 isoform around areas of cell death both in the spheroid cultures and the glioblastoma biopsy material. This occurred in spheroid cultures and in glioblastoma biopsies irrespective of *P53* status or p53 protein distribution. This suggested that the accumulation of this protein was distinct from the overexpression/upregulation of full length MDM2 commonly found in primary glioblastoma cells exhibiting wild-type p53. Levels of centrally located, truncated MDM2 appeared at a similar level as that found in monolayer cultures and small spheroids. Therefore, a reduction in levels of this isoform was associated with outer proliferative regions rather than a specific upregulation within perinecrotic tissue. This suggested that 60kDa MDM2 did not actively accumulate as a result of interspheroidal cell stress, such as hypoxia, but may be associated with non-cycling cells. This was confirmed by the lack of a 60kDa MDM2 increase following exposure to oxidative stress. Nevertheless, the existence of this isoform within perinecrotic cells, as compared to healthy proliferating cell populations, could potentially have major implications in the susceptibility of these glioma cell populations to stress. A variety of other MDM2 splice variants have previously been found in

other cell types, including astrocytoma neoplasms (Lukas et al., 2001; Matsumoto et al., 1998). Importantly, the existence of these splice variants have been shown to correlate with malignancy. For example, glioblastomas have shown greater incidence of shortened MDM2 transcripts (69%) than astrocytomas (0%) (Matsumoto et al., 1998).

It has been suggested that truncated MDM2 isoforms can compete with full length MDM2 binding to various target molecules (Pochempally et al., 1999; Damian et al., 2000). Certainly, the cellular distribution of the 60kDa MDM2 isoform showed that it appeared to reside in the nucleus as well as the cytoplasm across the spheroid radius, where it would have preferential access to active transcription factors such as p53, unlike the full length molecule which was predominantly present in the cytoplasm within healthy cell populations. However, nuclear and cytoplasmic extracts would have to be individually assessed to confirm this.

The high expression of the truncated MDM2 protein was initially thought to account for the lack of p53 protein found around perinecrotic areas. However, the 60kDa isoform found in this study is thought to be lacking in a C-terminal domain which contains the ubiquitin ligase E3 which is responsible for mediating ubiquitination of the p53 molecule and/or self ubiquitination of the MDM2 molecule (Figure 35). A RING finger domain also situated on carboxyl terminal is responsible for coordinating this intrinsic E3 activity (Honda et al., 2000). Removal of either the E3 domain or the RING finger domain can result in the loss of ubiquitination capabilities. Therefore, the lack of the whole C-terminal domain would result in an increase in the half life of the truncated MDM2 molecule because MDM2 mediated degradation of p53/MDM2 complexes or MDM2 itself would not occur (Honda et al., 2000; Fang et al., 2000). A similar 60kDa MDM2 has previously been identified in a variety of breast cancer cell lines (Pochempally et al., 1998) (Figure 35). This isoform was found to have a significantly longer half life than 90kDa MDM2 and was found in non-apoptotic tumour cells. The MDM2 splice variants found in astrocytic tumours were found to be lacking regions encoding for the N-terminal p53 binding domain and are different than the 60kDa isoform identified in this study.

Artificially induced, truncated MDM2 isoforms with a similar configuration to the 60kDa isoform found in this study have been shown to bind to and inhibit transactivation of down

stream targets of p53. In all of these experiments, the truncated transcripts encoded proteins with intact N-terminal p53 binding domains and defective C-terminal regions. In experiments performed by Yap et al (2000) and Chen et al (1996), MDM2 mutants (MDM2-Δ(222-437), MDM2-Δ(340-491), MDM2-Δ(440-491)) were created by removing residues over the C-terminus of the MDM2 protein removing either the critical ubiquitin ligase function of the MDM2 and/or the RING finger E3 controlling domain (Figure 35). The antibody combinations used, together with the size of the MDM2 protein found in this study suggests that the endogenous form found in the glioma cell lines is likely to result in the loss of both these domains. These three mutants were found to bind to and inhibit p53 induction of endogenous p21 expression. There was little or no difference between the ability of these 3 mutants and wild-type, full length MDM2 in preventing G_1 arrest by p53. It is possible therefore, that in the glioma spheroid system, the lack of p21 expression situated within spheroid central regions may be explained by the increase in truncated MDM2. Although the interaction of Bax and other down stream target molecules with truncated MDM2 have not been previously investigated, it is likely that a similar p53-independent inhibition may occur. However, it is interesting to note that the transuppression of the pro-survival genes *Bcl-2* and *MAP4* (microtubule associated protein 4) remain unaffected by the artificial addition of truncated MDM2 (Miyashita et al., 1994). It is likely that the E3/degradation function of MDM2 is required to prevent transuppression of these genes.

Using the same MDM2 mutants (MDM2-Δ(222-437), MDM2-Δ(340-491), MDM2-Δ(440-491)), p53-dependent apoptosis was found to be significantly reduced in cell lines expressing high levels of the truncated MDM2 isoforms, although they were not as effective as the full length molecule. It is therefore likely that in spheroids derived from *p53* wild-type cell lines U87 and A172, p53 mediated cell death may be severely compromised by the presence of high levels of 60kda MDM2. Similarly, *in vivo*, stressed glioblastoma cell populations that do not harbour *p53* mutations, but possess large quantities of the 60kDa MDM2 isoform may have a decreased susceptibility to cell death compared to those without high level of this protein. 80% of the biopsies examined in this study also exhibited high levels of endogenous perinecrotic 60kDa MDM2.

Because MDM2 associates with pathways other than the p53 pathway, accumulation of 60kDa MDM2 may be advantageous to both *p53* wild-type and *p53* mutant tumours. This is reflected in the large quantities of 60kDa MDM2 found within perinecrotic tissue in both *P53* wild-type and mutant tumours. Large quantities of intracellular truncated MDM2 may influence levels of cell cycle regulatory molecules including the Rb (retinoblastoma gene product) protein and E2F1. The MDM2 protein can interact physically and functionally with the Rb protein and, as with p53, can inhibit pRB growth regulatory function and allow cell cycle progression (Xiao et al., 1995). Because the MDM2 protein binds the Rb protein with its N-terminus, the truncated molecule may be able to modulate cell cycle progression in a similar way to the wild-type molecule. It is thought that E2F1 has a dual function in regulating cell cycle progression and apoptosis which are partly under the control of p53 and MDM2. Firstly, MDM2 has been found to associate with E2F1 and another transcription factor, DP1 at the activation domain of p53 (Martin et al., 1995). In doing this MDM2 can positively augment proliferation through S-phase. Secondly, high levels of MDM2 can block E2F1 mediated induction of apoptosis and also block the E2F1-mediated accumulation of p53 (Kowalik et al., 1998). Because the N-terminal binding domain on the 60kDa MDM2 isoform found in this study is thought to be intact, it is possible that a similar effect may occur within glioma cell populations. The absence of a C-terminal domain suggests that E2F-1/p14^{ARF} mediated degradation of 60kDa MDM2 will not occur. The resulting abnormal activity of the Rb and E2F-1 pathways could therefore result in variations in the proliferative and survival status of the cell. It is theoretically possible that under periods of stress, high levels of truncated MDM2 could allow aid cell survival, inhibit apoptosis and decrease levels of active p53.

4.3.8. Possible regulation of 60kDa MDM2

The mechanisms responsible for the activation and regulation of the 60kDa MDM2 isoform remain unknown. If the isoform observed in these studies is identical to the similarly sized molecule found by Pochempally et al. (1998), a post translational truncation event is likely to have occurred. A caspase 3 analogue was found to be cleaving full length MDM2 in non-apoptotic tumour cells in these studies. Further experiments would have to be performed using specific caspase 3 inhibitors to examine whether this reduces levels of the 60kDa MDM2 found in these spheroid cultures. Because of the fragment sizes found and the

antibody specificities observed in this study, it is likely that the 60kDa MDM2 isoform found here will have similar physiological functions to that found by Pochempally et al. The one point that contradicts the likelihood of these being identical proteins, is the finding that the *P53* mutant lines in this study exhibit equally high levels of 60kDa MDM2 isoform as the wild-type lines. If the 60kDa MDM2 had accumulated due to a post-translational truncation event, full length MDM2 would have to be translated first. The *P53*His273 mutation in U373 cell line has been shown to result in a reduction in the DNA binding ability of the mutant protein to the *MDM2* promoter and it is likely that the *P53*Val159 mutation in the MOG-G-CCM cell lines has a similar transcriptional deficit (Saintigny et al., 1999). Therefore, if a post-translational truncation event is proven, it is unclear how such high levels of original 90kDa MDM2 isoform can arise in the *P53* mutant cell lines. Perhaps a separate mechanism for the transcription of full length MDM2 exists in the cell lines harbouring *P53* mutations and those without. No p53 independent transcription factors have yet been identified that can actively transactivate the full length *MDM2* promoter sequence in glioma cell lines. However, Ras-driven Raf/MEK/MAP kinase pathway has been shown to regulate MDM2 activation in a p53-independent manner in colon cancer cells (Ries et al., 2000). In addition, thyroid receptors (T3Rs) have been found to transactivate the *MDM2* promoter sequence in GH4C1 pituitary adenoma cells (Qi et al., 1999).

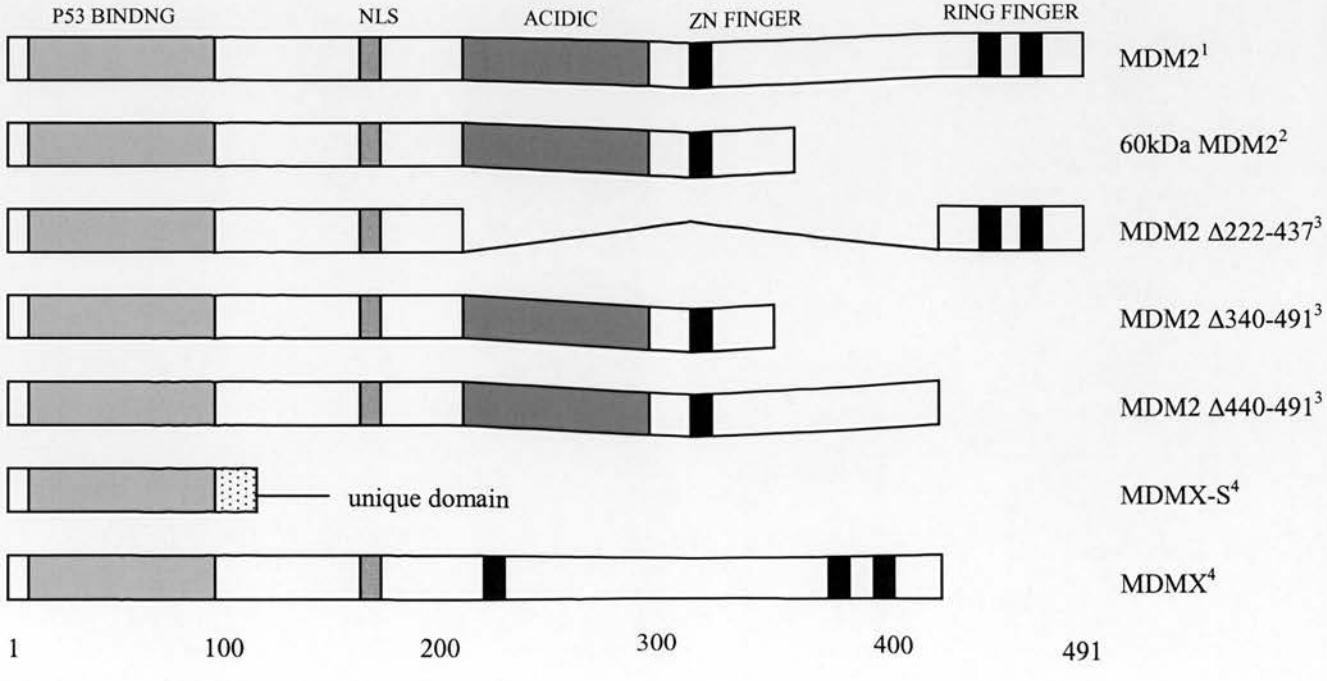

Figure 35. Diagram of previously designed/identified full length and truncated MDM2 molecules. References: [1]Honda et al., 1997; [2]Pochempally et al., 2000; [3]Chen et al., 1997; [4]Strachan et al., 1996.

A separate mechanism for the production of high levels of 60kDa MDM2 could be the direct transcription of truncated alternative mRNA transcripts. Rallapalli et al in 1999 found that alternative splicing of MDM2 transcripts could result in proteins with a similar conformation to those found in this study. An MDM2 isoform MDMX (80kDa), was found to be present in a variety of mouse and human transformed cell lines (Figure 35). This protein has a considerably weaker affinity for p53 than full length MDM2. Although MDMX can bind p53 and block its ability to activate to activate transcription and induce apoptosis, it can also bind to full length MDM2 and increase p53 stability. MDMX is thought to be activated via a p53 independent mechanism as it is not induced by DNA damaging agents that are known to induce full length MDM2. Another protein identified by this group called MDMX-S was also identified in these experiments that, unlike MDMX was missing all three zinc-finger domains and ubiquitin ligase E3 function. Although this protein is considerably smaller than the 60kDa protein found in this study, the interaction with p53 is likely be similar. However, post-translational modifications of this protein are likely to be very different due to differences outwith the p53 binding domain (Figure 35). Post translational modifications by DNA-PKs, for example, can significantly influence the activity of the MDM2 molecule (Khosravi et al., 1999). MDMX-S is actively transcribed by the p53 protein. It is therefore clear that different MDM2 isoforms can arise by post translation truncation events or direct transcription of truncated MDM2, perhaps via a p53-independent mechanism. Interestingly, U87 glioblastoma cells were tested in the Rallapalli study and were found to contain high levels of MDMX and MDMX-S mRNA. Neither of these truncated proteins would be recognised by the two MDM2 antibodies, SMP-14 and C-18 , used in this study.

Further research needs to be completed into the activation of the 60kDa MDM2 molecule found in this study. Defining the amino acid composition of the protein using mass spectrometry should confirm the status of this protein as a definite isoform of the full length MDM2 molecule. In addition, an accurate structural analysis need to be performed in order

to establish the importance of this protein in relation to cell death susceptibility within glioblastoma cell populations. What is clear from previous studies is that a large amount of an MDM2 isoform lacking a C-terminus is likely to significantly influence the interactions of many pro-apoptotic and pro-survival proteins. It is also unknown why this truncated MDM2 becomes localised around and within areas of necrosis in glioblastoma biopsies and spheroids. Perhaps the activation of pro-death pathways actively encourages the accumulation of these abnormal isoforms, which do not occur in normal cells. Or perhaps this 60kDa isoform is lost in the proliferating cell population due to some unknown mechanism. It is however likely that the expression of abnormal MDM2 isoforms in transformed cells may represent an important step in neoplastic transformation in cancer cells. The results in this study suggest that the accumulation of some abnormal MDM2 isoforms may occur in tumours exhibiting both mutant and wild-type *P53*. This implies that that 60kDa MDM2 isoform may increase tumourigenicity in pathways other than those involving p53. Previously studies have shown that abnormal build up of full length MDM2 is normally associated with primary glioblastomas exhibiting wild-type *P53* (Kraus et al., 1999., Rasheed et al., 1999).

4.3.9. MDM2 upregulation and activation of apoptosis

Because p53 accumulation and its downstream targets Bax and p21 appear not to be important for the onset of cell cycle arrest/apoptosis in these experiments, the mechanisms that activate the observed levels of endogenous cell death within these glioblastoma cell populations remain unclear. Interestingly, recent research has highlighted the ability of MDM2 to arrest cell cycle in normal human fibroblasts and promote apoptosis in p53 deficient human medullary thyroid carcinoma cells (Dilla et al., 2000). In addition, various MDM2 overexpression experiments have shown that MDM2 can contribute to an apoptotic response following DNA damage. Genotoxic aryl-hydrocarbons (BPDE) for example, have been shown to augment an MDM2 mediated apoptotic response (Hsing et al., 2000; Wu et al., 1999). The mechanism by which MDM2 contributes to apoptosis in these experiments has not yet been elucidated. However, it has been suggested that the E2F family of transcription factors may be involved. E2F-1, as previously mentioned, is involved in both cell cycle progression and apoptosis (Xiao et al., 1995). MDM2 is known to bind to Rb and derepress E2F-1 activation. Theoretically, high levels of MDM2 (or perhaps truncated

MDM2) could bind to Rb thus allowing E2F-1 overexpression and subsequent acceleration of both cell cycle progression and apoptosis. These suppositions are supported by experiments showing concurrent increases in E2F-1 and MDM2 expression in response to BPDE (Hsing et al., 2000).

Although the above findings are generally associated with direct DNA damage, the involvement of ARNT (HIF-1β)with AhRs (aryl-hydrocarbon receptors) implies similar pathways could be activated in response to various types of free radical and oxidative stress (Dipple, 1995; Hemminki, 1993). As a result, it is possible that the extremely high levels of MDM2 observed in this system around central regions regardless of *P53* status may encourage suppression of p53 mediated apoptosis and induce an apoptotic response through E2F-1. However, the involvement of p53 related proteins, other than those studied here, cannot be ruled out. It is likely that a combination of factors, including intact p53 independent pathways may play a part in activating both apoptosis, necrosis and even some of the other observed cell death morphologies found within glioma spheroid cultures.

4.3.10. Summary of p53 related findings

Given the absence of wild-type p53, Bax and p21 proteins around areas of cell death within glioma spheroids and in biopsy material there is no evidence to suggest that the accumulation of these proteins is important for the onset of cell cycle arrest in intermediate spheroid regions, or the onset of necrosis and subsequent apoptosis within stressed glioblastoma cell populations. This lack of p53 accumulation occurred even when the wild-type *P53* cell lines were known to activate p53 dependent pathways in response to both oxidative and free radical stress, both of which were thought to occur in central spheroid regions. The only p53 related protein investigated in this study that was seen to be increased within perinecrotic tissue was a 60kDa isoform of MDM2. A protein with a similar configuration has previously been identified in a variety of breast cancer cell lines and is expressed in non-apoptotic cells (Pochempally et al., 1998). This protein lacks a C-terminal domain and fails to mark the p53 protein for degradation Previous research has shown that the long half-lives of similar proteins lacking C-terminal regions are likely to result in a decreased susceptibility to cell death due to their capacity to inhibit both p53 transcriptional activity and post-translational modification other cell cycle control checkpoints, such as Rb (Honda et al., 1997; Rallapalli

et al., 1999). Therefore the presence of this isoform could significantly alter cell death susceptibility when the cells in question are exposed to a variety of cell stresses.

It is clear that using the spheroid system to investigate the expression of the various cell death related proteins examined in this study has been invaluable. The use of monolayer cultures has elucidated certain protein-protein interactions and patterns of gene expression when cells are under stress. However, monolayer cultures exposed to both hypoxia and free radical stress cannot accurately reflect the changes in protein expression found endogenously *in vivo*. It is thought that by understanding endogenous cell death *in vivo* we will be in a stronger position to identify intact cell death pathways. These findings prove that growing cells as three dimensional structures can significantly influence the expression of cell death associated proteins under conditions of endogenous stress. The expression of p53, p21, Bax and MDM2 (both 90kDa and 60kDa isoforms) was virtually identical in spheroid cultures and within phenotypically similar areas in glioblastoma biopsy material. The benefits of experimenting with the glioma spheroid system over archival glioblastoma tissue is that it can be used a model for genetic manipulation studies to investigate the properties of various genes and proteins in a more *in vivo*-like environment. Individual zones across the spheroid radius can then be monitored for any changes in size, cellular morphology and protein distribution.

CHAPTER 5

P53 MODULATION AND GLIOMA SPHEROID DYNAMICS

5.1. Introduction

The evidence thus far has suggested that p53 and its downstream target proteins, Bax and p21 are not involved in the stimulation of apoptosis around the center of glioma spheroids. Certainly, the *P53* mutant status of the lines U373 and MOG-G-CCM suggests that p53-mediated perinecrotic apoptosis is unlikely. In addition, the lack of perinecrotic p53 accumulation also implies p53-mediated cell death is unlikely in spheroids derived from the *P53* wild-type U87 and A172 cell lines. However, the examination of protein expression immunohistochemically is insufficient to fully assess the functional capabilities of the p53 molecule in this system. Downregulation of p53 together in the presence of high levels 60kDa MDM2 do not necessarily imply that p53 is redundant in central regions. In fact, because p53 is the known main regulator of MDM2, increases in 60kDa MDM2 suggest p53 may have some function within these cells. Perhaps the presence of 60kDa MDM2 masks the true activity of perinecrotic p53 and the subsequent short half-life of the active p53 molecule means that it may escape detection.

In order to investigate whether p53 has a regulatory role in determining susceptibility to apoptosis and necrosis, *P53* gene transfer technology is utilised. By modulating levels of intracellular p53, variations in the central cell death response and levels of downstream protein expression can be monitored. For example, if in *P53* wild-type spheroids, decreases in endogenous wild-type p53 result in a drop in perinecrotic apoptotic index, wild-type p53 may indeed be involved in the cell death response. This would in turn suggest a role for p53 in endogenous cell death in some glioblastomas harbouring wild-type *P53*. Modulation of intracellular p53 levels would also confirm the importance of a wild-type *P53* gene in the normal regulation cell death in tumours harbouring mutant p53.

To fulfill the hypothesis that p53 has a regulatory role in determining cell death susceptibility in glioblastoma, three *P53* vectors were used, one wild-type *P53* vector (p53wtEGFP), one dominant negative vector (p53mt135EGFP) and a control vector (p53mt144EGFP) (Vogelstein and Kinszer, 1992; Cormack et al., 1996). The wild-type vector encodes a wild-type p53 protein that is capable of activating downstream target sequences such as Bax, p21 and MDM2. The dominant negative vector translates a p53 protein that can bind to and inactivate any endogenous p53 wild-type activity. The control vector was used to assess the

effects of artificially increasing intracellular levels of a similarly sized, totally inactive p53 protein (possesses no wild-type or dominant negative activity). Therefore the aims of these experiments were to establish whether increases in wild-type/dominant negative p53 (i) influence levels of intraspheroidal cell death/growth (ii) alter the expression distribution of Bax and p21 within glioma spheroids (iii) affect the expression and distribution of 60kDa and 90kDa MDM2.

To fulfill these aims, two cell lines, one *P53* wild-type (U87) and one *P53* mutant (U373) were utilised. The cell line U87 has previously been transfected with vectors containing p53 inserts with no subsequent effect on cell viability (Komata et al., 2000; Badie et al., 1999). In contrast, other researchers have observed that all U87 transfected cells die by apoptosis 3 days post-transfection (Cerrato et al., 2001; Li et al., 1997). *P53* mutant cell lines including U373 nearly always show 100% loss of cell viability by apoptosis following wild-type *P53* transfection (Komata et al., 2000; Badie et al., 1999). However, it is thought that His273 mutants, such as U373, may harbour some wild-type p53 transactivation ability Signal et al., 2000 ; Saintigny et al., 1999).

5.2. Results

5.2.1. Verification of p53WT and mutant vectors

To confirm the success of the transformation of the WTp53EGFP vector into chemically competent E.Coli and subsequent plasmid preparation, a PCR was set up to amplify a region(ex2.1-ex6.1) of the *P53* gene. This region was successfully amplified (652bp) in both the samples tested (Figure 36A).

A plasmid-only control vector was produced by removing the *P53* gene from the p53wtEGFP vector. The correct configuraton of the plasmid-only vector (poEGFP) was proven by the presence of specific sized bands after the whole plasmid was digested with AvaI and NcoI restriction enzymes (see Table 6 for correct sized fragments, Figure 36B). Sequencing confirmed the correct plasmid-only sequence over the ligation point after removal of the WT *P53* gene(Figure 36C).

Successful ligation and transformation of the mt135insert into the EGFP vector (p53mt135EGFP) was confirmed by the amplification of a region of DNA from the CMV promoter region (CMV1) into the *P53* gene (630bp) using ten random transformed colony lysates (Figure 36D). All ten colonies were positive, proving that the insert was correctly orientated into the EGFP vector. Once the plasmid preparation had been performed, sequencing over the mutation site (TGC→TAC at codon 135) confirmed the presence of the mutation (Figure 37A).

The amplification of the 518bp fragment between primer sequences 4.1-6.1 confirmed the presence of a *P53* sequence after the ligation of the mt144insert (from the pCp53-scx3 Vogelstein vector) into the EGFP vector (p53mt144EGFP) (Figure 37B). The presence of a 320bp fragment in two of the three cell lysates (instead of a 370bp fragment in the WT sequence) following the HhaI digest confirmed the presence of the mutation at codon 144 (CAG→TAG) (Figure 37C). *P53* gene sequencing of the 2 vectors absolutely confirmed the presence of the mt144 insert (Figure 37D).

Once the cell lines U87 and U373 had been transfected with the appropriate *P53* EGFP vectors and stable transfected colonies had been established, over 90% of the cells exhibited

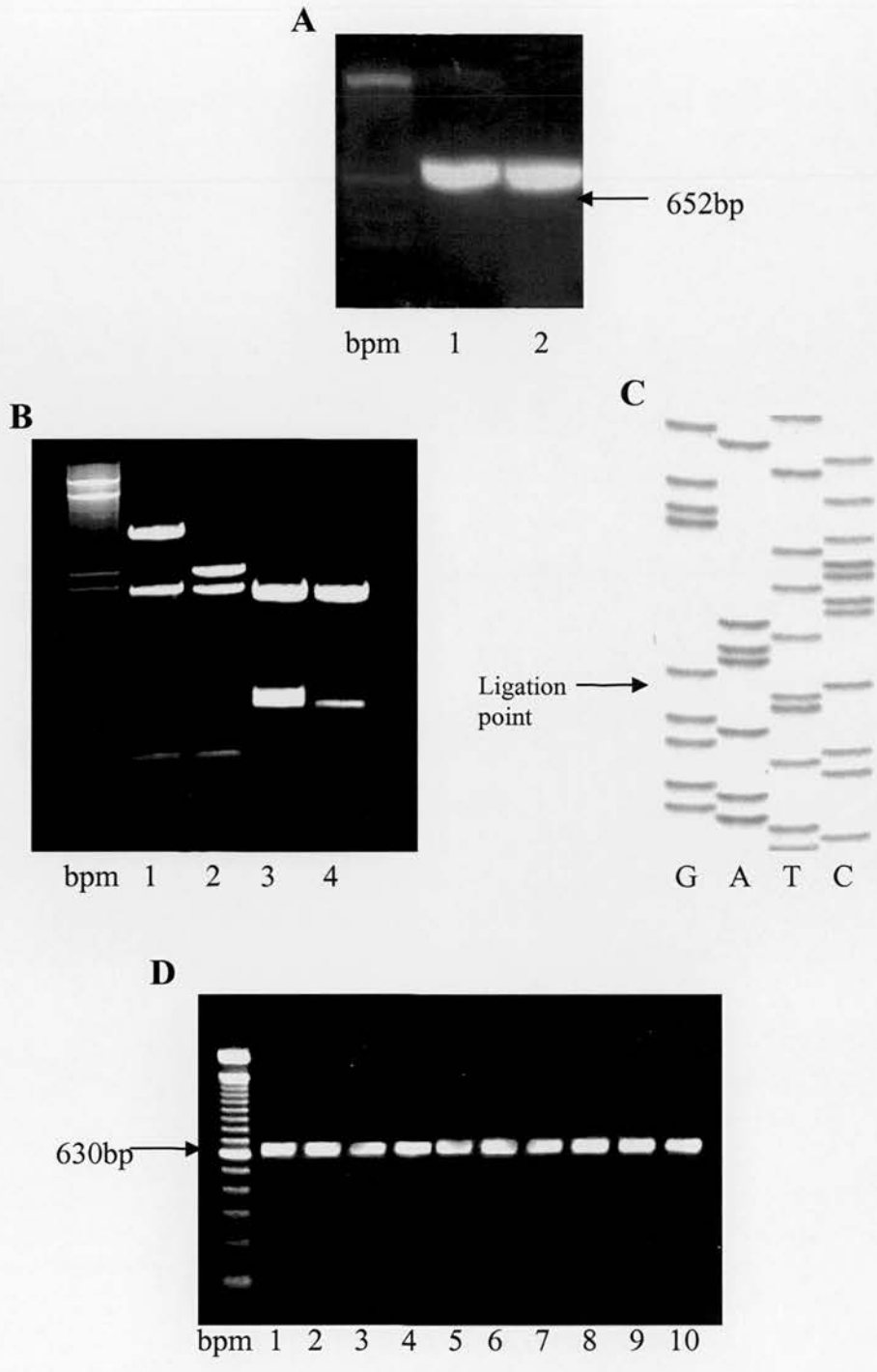

Figure 36. Vector conformation verification. A, gel showing PCR product between ex2.1-ex6.1 in p53wtEGFP (652bp). B, restriction digest of poEGFP and p53wtEGFP. 1=p53wtEGFP digest with AvaII, 2=poEGFP digest with AvaII, 3=p53wtEGFP digest with NcoI, 4=poEGFP digest with NcoI. C, sequencing gel showing the ligation point of the poEGFP vector after the removal of wtp53. D, amplification between CMV1 and ex4.2 of p53mt135EGFP (630bp) using 10 random colony lysates. All were positive.

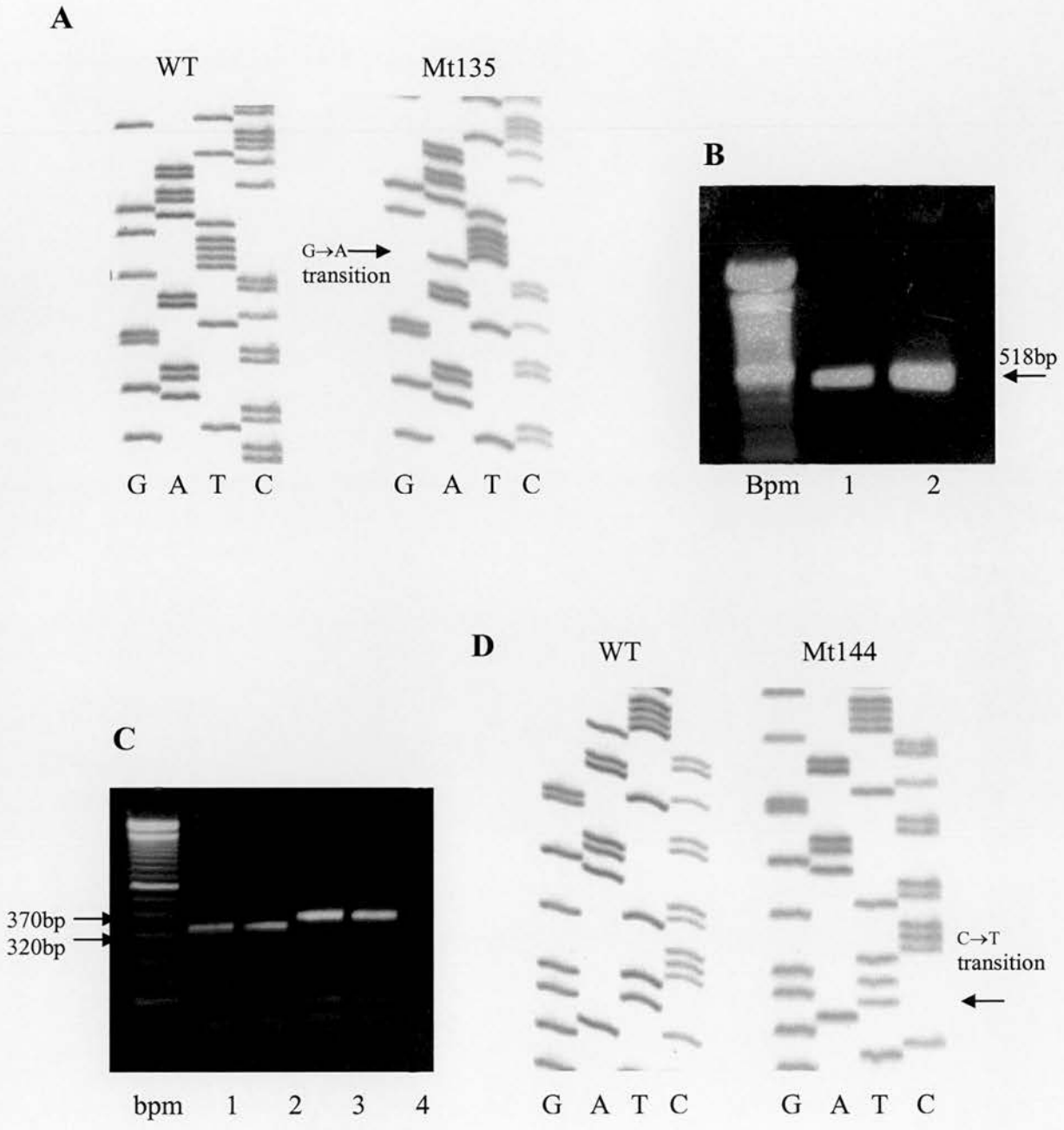

Figure 37. Vector conformation verification continued. A, sequencing gel showing the mutation at codon 135 in p53mt135EGFP compared to the wild-type sequence. B, gel showing the 518bp PCR product from the p53mt144EGFP vector (2 identical samples). C, HhaI restriction digest of p53mt144EGFP vector of PCR product from B. Samples 1 and 2 show the presence of the mt144 vector. Samples 3 and 4 show the wild-type sequence. D, sequencing gel showing the mutation at codon 144 in p53mt144EGFP compared to the wild-type sequence.

strong green fluorescence (Figure 38A). Stable transfectants were not established for the p53wtEGFP vector in U373 cell line because the cells died 3 days post-transfection (Figure 38B). Cells not successfully transfected with the EGFP vector died as a result of the toxic effects of G418. Because the U373p53wtEGFP cells died after 3 days, these cells did not form spheroids and were therefore eliminated from any further experimentation.

5.2.2. p53 protein expression in transfected monolayer and spheroid cultures

As expected, p53 expression was very high in the p53-transfected cell lines. U87 p53wtEGFP, p53mt135EGFP and p53mt144EGFP transfected cell lines showed strong p53 labelling (using both antibodies Bp53-12 and Pab1801) in over 80% of cells (Figure 39A). Many of these cells had positively labelled cytoplasm as well as the expected nuclear staining pattern. When the cells reached approximately 80% confluence the number of cells exhibiting p53 positive nuclei dropped to around 60-70%. As expected, U87 poEGFP (plasmid-only) cultures showed a similar level of p53 labelling as untransfected monolayer U87 cultures (Figure 39A). Western blotting confirmed these findings where strong bands were observed for U87 cells transfected with the three *P53* vectors compared to a faint band for the poEGFP U87 transfectant (Figure 39B).

Although levels of high confluency appeared to decrease the numbers of p53 positive cells in monolayer, in spheroid cultures, 75-80% of cells expressed abnormally high levels of p53 in the U87 spheroid culture for all of the constructs (Figures 40B-D). Levels of p53 labelling were consistent across the radius of U87 spheroids transfected with the 3 vectors, p53wtEGFP, p53mt135EGFP and p53mt144EGFP.

Although U373 cells contained a *P53* mutation and therefore expressed abnormally high levels of the mutant p53 protein, monolayer cultures transfected with the p53mt135EGFP and p53mt144EGFP vectors nevertheless showed considerably darker staining than non-transfected U373 cells (Figure 39A). A large amount of cytoplasmic labelling was observed as well as nuclear staining. All U373 cells transfected with the p53wtEGFP vector died by day five post-transfection and p53 immunohistochemistry was not performed. Western blotting confirmed these findings (Figure 39B). P53mt135EGFP and p53mt144EGFP U373 transfectants showed darker bands than the U373 plasmid-only cells.

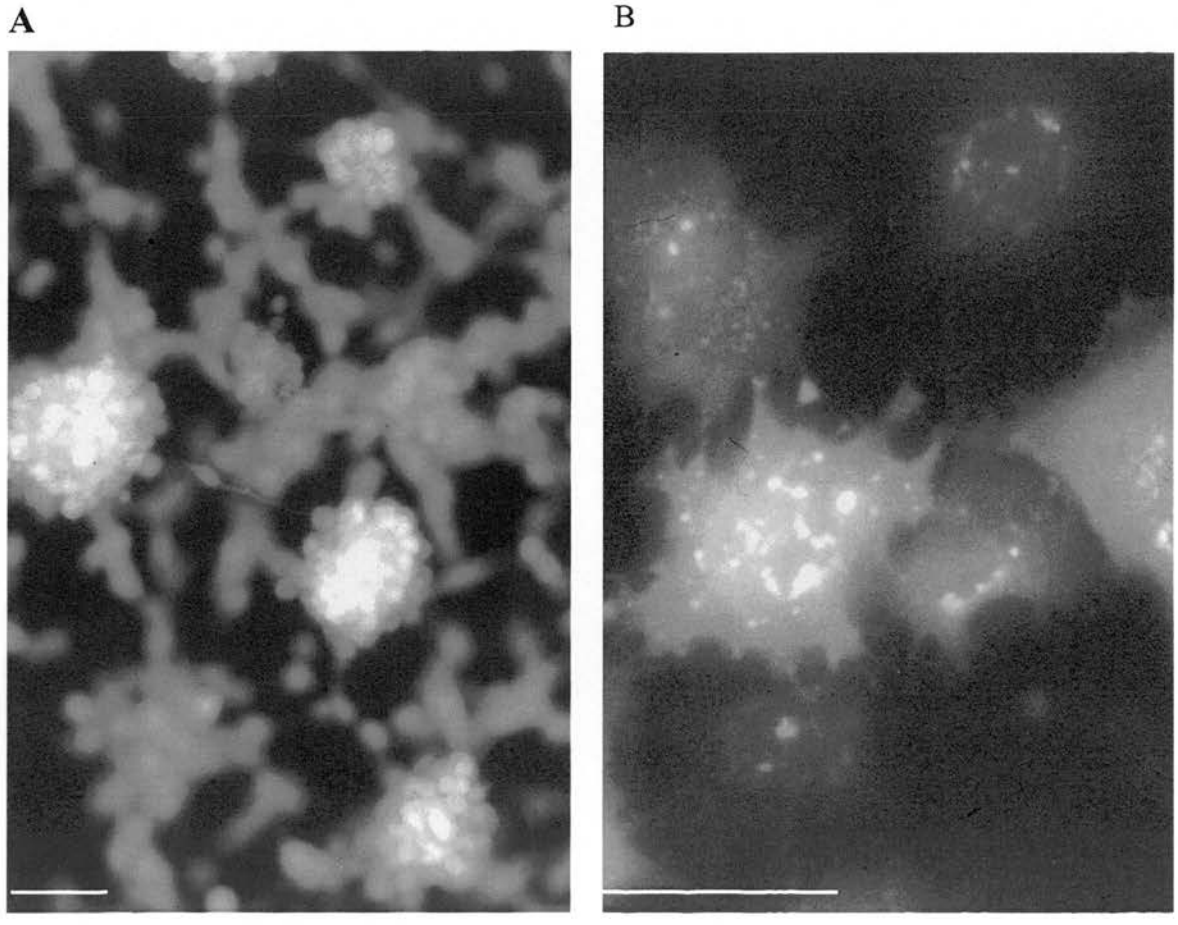

Figure 38. Live U87 and U373 monolayer cultures following transfection with WTp53EGFP. U87 cells remained healthy and formed small spheroids (A) and U373 cells dies 3 days post transfection by apoptosis (B). Bars= 50μm

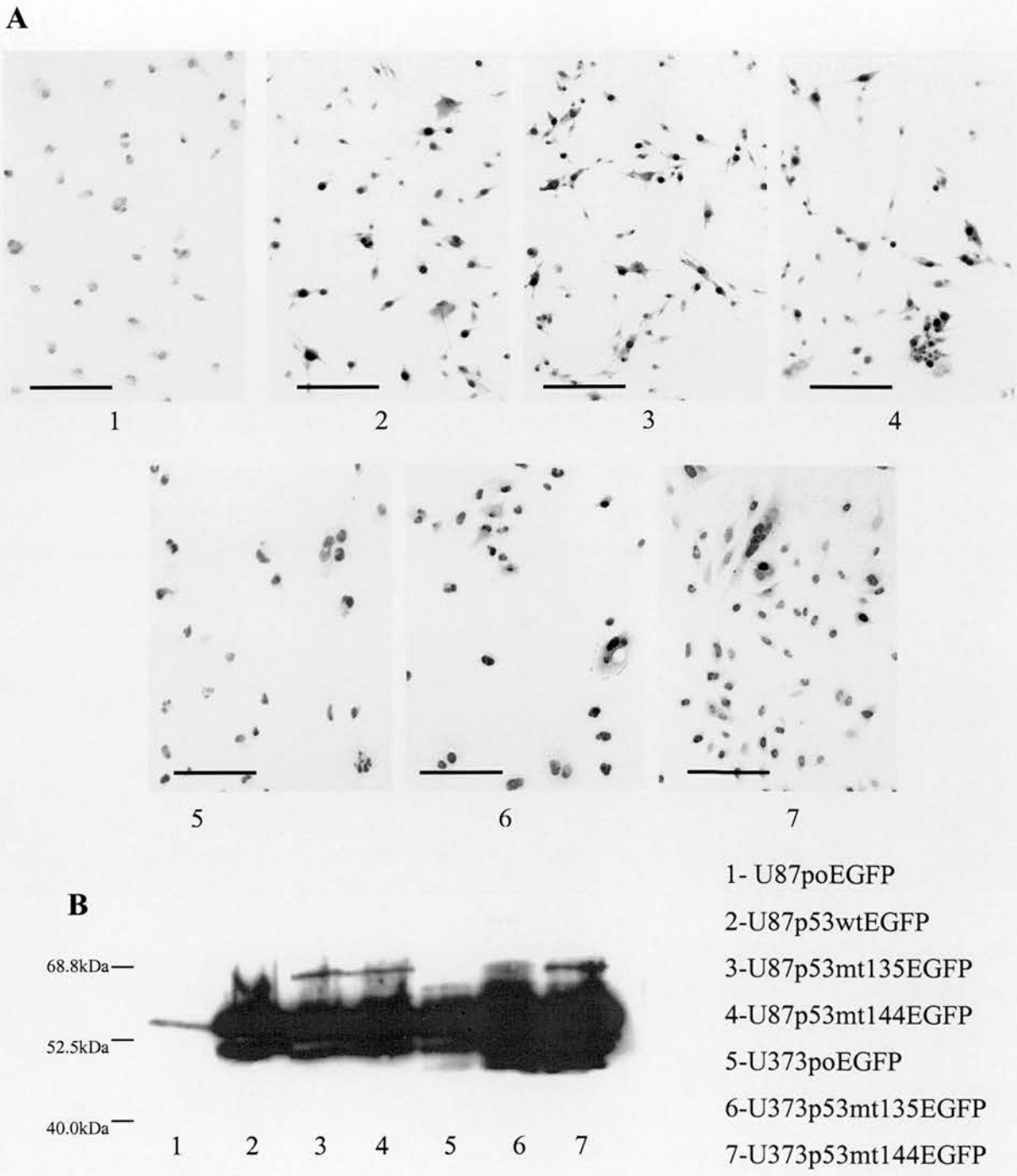

Figure 39. p53 labelling in transfected U87 and U373 monolayer cultures. A, 1, transfected U87 plasmid-only monolayer culture showing basal levels of p53 expression. 2-4, p53 mutant and WT U87 transfectants showing a strong 80% p53 labelling index. 5, U373 plasmid-only monolayer culture showing basal levels of p53 expression. 6-7, p53 mutant U373 tranfectants showing a slightly stronger p53 labelling index including evidence of cytoplasmic labelling. All bars=100μm. B, p53 (53kDa) western blot confirming large increases in p53 expression in p53mutant and WT transfectants.

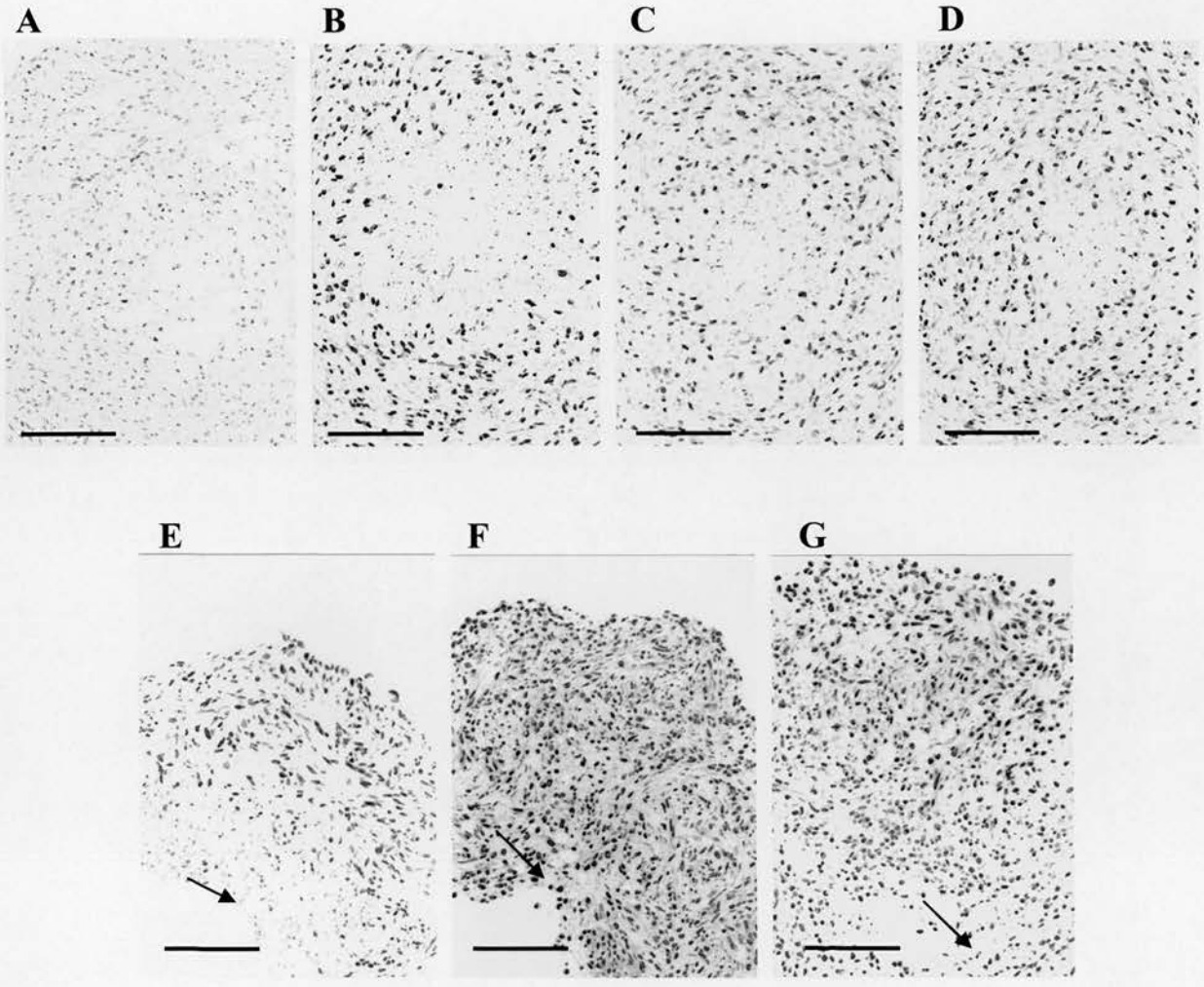

Figure 40. p53 expression in spheroid cultures using transfected U87 and U373 cell lines. A, U87poEGFP showing basal levels p53 expression. Strong p53 labelling across the radius in spheroids derived from U87p53WTEGFP cells(B), U87p53mt135EGFP cells (C), U87p53mt144EGFP cells (D). E, basal levels of p53 expression in U373poEGFP spheroids. p53 mutant U373 transfectants, U373p53mt135EGFP (F) and U373mt144EGFP (G), showing similar labelling patterns when grown as spheroids. Note the absence of a decrease in perinecrotic p53 labelling in the p53 transfectants (F & G) as compared with the plasmid-only U373 spheroids (E) (arrows). All bars=100μm.

In U373 spheroids, darker nuclei and more cytoplasmic p53 labelling was observed across the spheroid radius compared to untransfected and plasmid-only groups (Figures 40F and G). There was no significant difference in the distribution of the p53 protein between the U373 spheroids transfected with the two mutant *P53* vectors. However, no decrease in p53 labelling was observed in the cells directly adjacent to the necrotic centre as in the plasmid-only and untransfected spheroids (Figure 39E). No spheroid cultures were established for the U373p53wtEGFP group as the cells did not survive long enough.

5.2.3. Bax, p21 and MDM2 expression in transfected monolayer and spheroid cultures

The transfection of U87 cell line with the three p53EGFP vectors did not have any significant effect on the expression of Bax or p21 in monolayer culture. There was no variation in intracellular Bax expression in response to the artificial induction of the wild-type and mutant p53 proteins in the U87 cell line (Figure 41A). Notably, there was no increase in Bax expression with the addition of the wild-type *P53* vector and no reduction in Bax expression with the addition of the dominant negative vector (p53mt135EGFP). In the U373 cell line, levels of Bax also remained the same in monolayer culture when the cells were transfected with poEGFP, p53mt135EGFP and p53mt144EGFP vectors (Figure 41A).

In spheroid culture, levels of Bax were similar in U87 spheroids transfected with the three p53EGFP vectors as compared to the plasmid-only cells and wild-type cells. In addition, there was no difference in the distribution of these proteins across the radius of transfected U87 spheroids as compared to untransfected cells (Figure 41B). Similarly, in U373 spheroids, the level and distribution of the Bax protein were not altered with the addition of the p53mt135EGFP and p53mt144EGFP vectors (Figure 41B).

Levels of p21 in monolayer culture appeared unchanged with the addition of the wild-type *P53* and mutant *P53* vectors. Western blotting experiments showed that in U87 cell line, the band size and intensity was the same using the control vector poEGFP, and the p53wtEGFP, p53mt135EGFP and p53mt144EGFP vectors (Figure 42A). Therefore, like Bax, the dominant negative vector mt135EGFP did not reduce intracellular levels of p21 and the wild-type *P53* vector did not result in an increase intracellular levels of p21 in U87 cells. U373

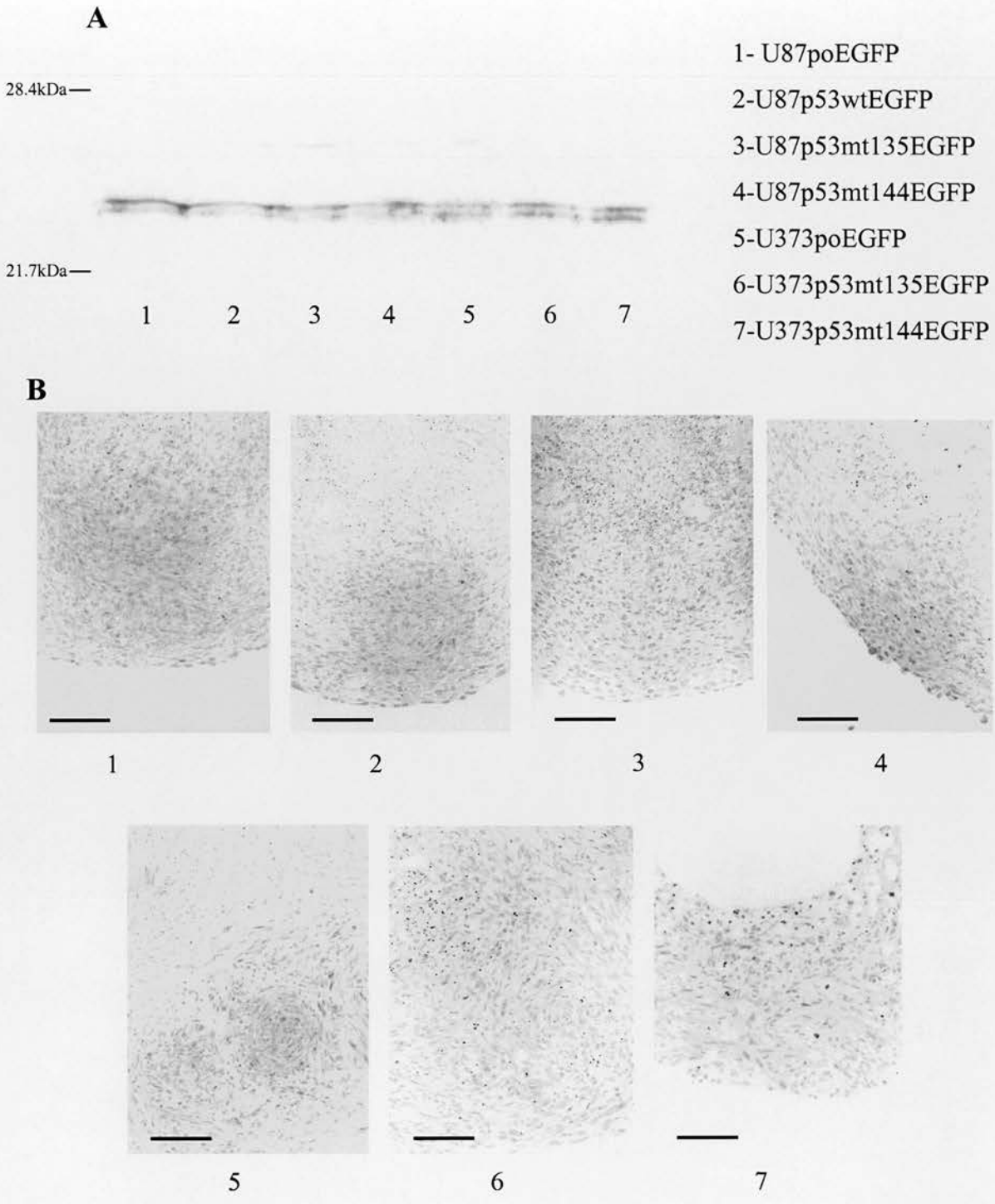

Figure 41. Bax expression in transfected U87 and U373 monolayer and spheroid cultures. A, western blot showing a similar level of Bax expression in both plasmid-only and transfected U87 and U373 monolayer cultures. B, 1-4, U87 transfected spheroid cultures showing no difference in the distribution of Bax protein between plasmid-only (1), mt135 (2), mt144 (3) and wt p53 (4) transfectants. B, 5-7, U373 transfected spheroid cultures showing no difference in the distribution of Bax between plasmid-only (5), mt135 (6), mt144 (7) transfectants. All bars=100μm.

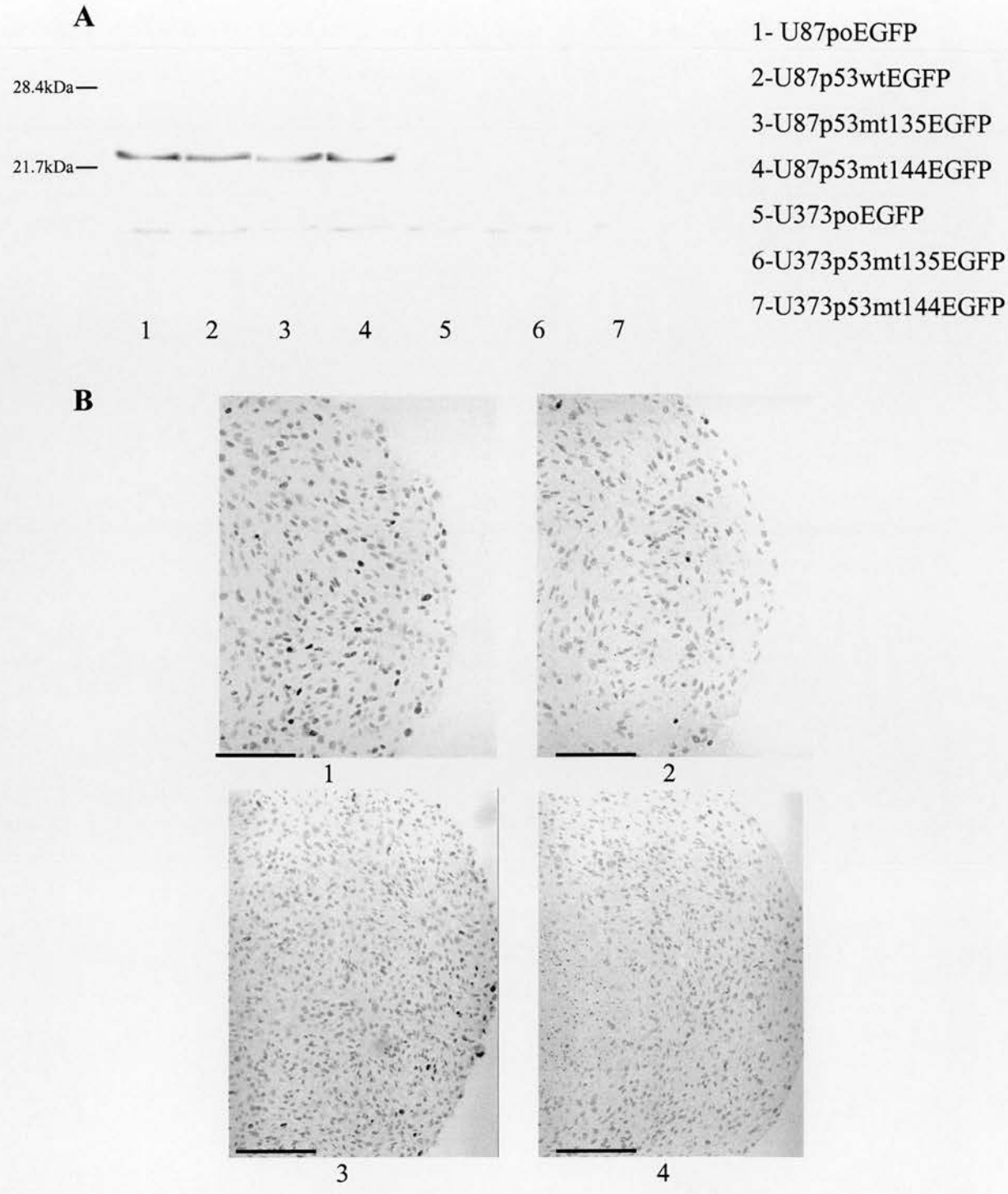

Figure 42. p21 expression in transfected U87 and U373 monolayer and spheroid cultures. A, western blot showing no variation in p21(21kDa) expression between monolayer U87 cells transfected with the p53 EGFP vectors (2-4) and the plasmid-only vector (1). The absence of p21 labelling in U373 cell lines was not altered with the addition of the two mutant p53 vectors, p53mt135 (6) and p53mt144 (7). B, U87 spheroid cultures showing a decrease in p21 expression in spheroids transfected with wtp53 (p53wtEGFP) at weeks 2 and 4 (2 & 4), compared to the plasmid only spheroids at the same time point (1 & 3). All bars=100μm.

poEGFP, p53mt135EGFP and p53mt144EGFP cells all showed a complete absence of p21 protein (Figure 42A).

In spheroid culture, U87 cells transfected with the poEGFP, p53mt135EGFP and p53mt144EGFP vectors all showed similar labelling patterns. However, the p53wtEGFP vector resulted in an unexpected decrease in p21 expression across the radius of the spheroids compared to the plasmid-only and mutant spheroids (Figure 42B). This was mainly apparent at weeks 1-2. At week 3 peripherally labelled cells were much less frequently observed than in plasmid-only and mutant cultures. U373 spheroid did not show any variation in p21 expression with the addition of the two mutant *P53* vectors.

Levels of 60kDa MDM2 appeared to be slightly decreased in monolayer cultures derived from U87 cells transfected with the p53mt135EGFP vector compared to the control poEGFP and p53mt144EGFP cells (Figure 43A). However, this was only apparent in the western blotting experiments. No difference was observed in the in situ labelling of these cells. There was no difference in 60kDa MDM2 expression between cells transfected with p53wtEGFP, p53mt144EGFP and poEGFP (Figure 43A). No variations were observed in 60kDa MDM2 labelling between p53mt135EGFP, p53mt144EGFP and poEGFP transfected U373 cells. In U87 spheroid cultures, there was no difference in 60kDaMDM2 labelling between poEGFP, p53wtEGFP, p53mt135EGFP and p53mt144EGFP vectors in terms of both intensity and distribution (Figure 43B). Similarly, no variation in 60kDa MDM2 labelling was observed in U373 spheroids transfected with poEGFP, p53mt135EGFP and p53mt144EGFP vectors (Figure 43B).

Like the 60kDa MDM2 protein, the 90kDa MDM2 protein appeared to be slightly decreased in monolayer cultures derived from U87 cells transfected with the p53mt135EGFP vector compared to poEGFP and p53mt144EGFP cells (Figure 43A). Again, however, this appeared only in the western blotting experiments. No difference in 90kDa MDM2 expression using monolayer p53mt135EGFP cells was detected immunohistochemically. Levels of 90kDa MDM2 were increased in U87 monolayer cells transfected with the p53wtEGFP vector (Figure 43A). Similarly, in U87p53wtEGFP spheroid cultures, there was an increase in 90kDa MDM2 expression (using the MDM2 C-18 antibody) across the spheroid radius

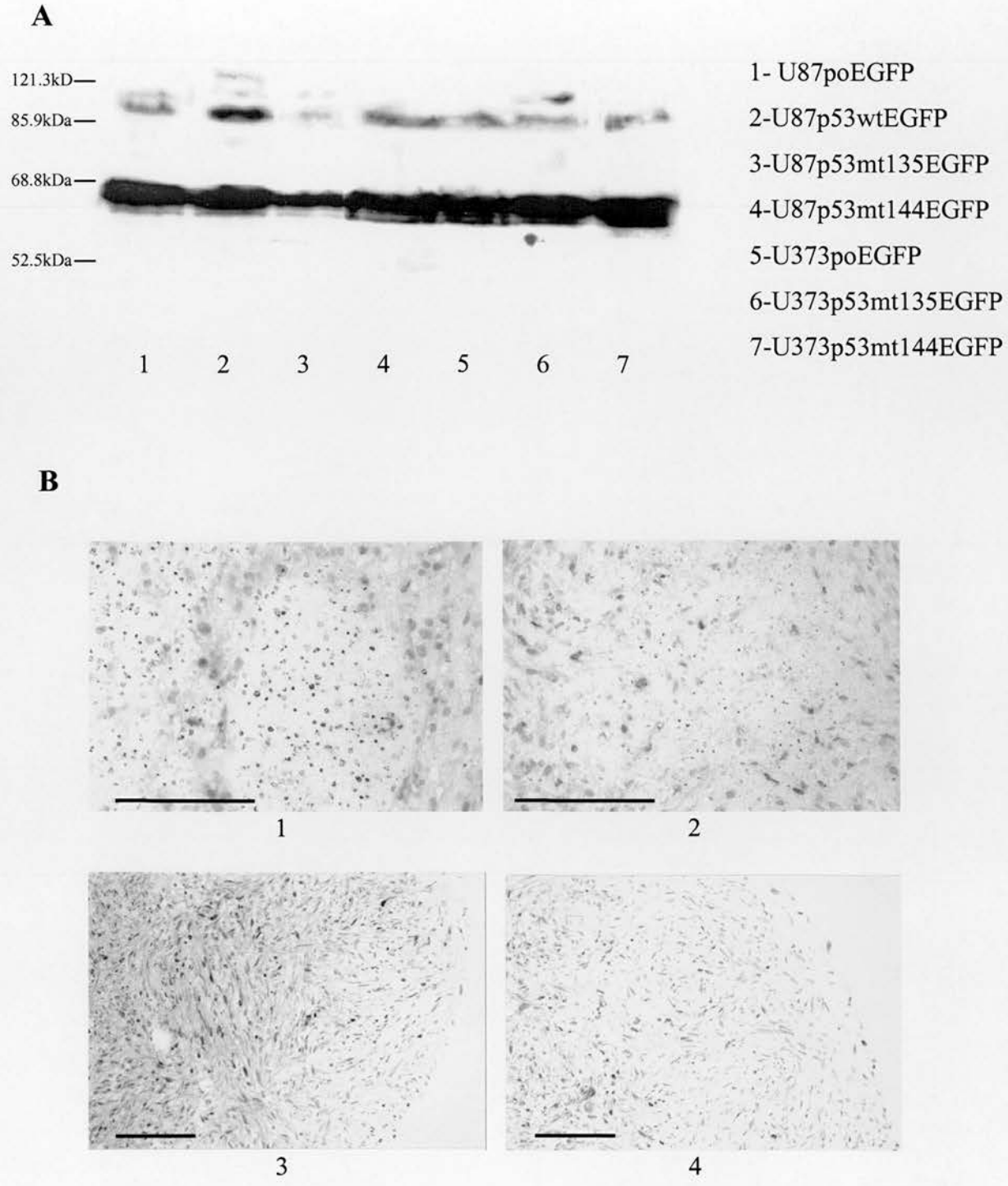

Figure 43. MDM2 expression in transfected U87 and U373 monolayer and spheroid cultures. A, western blot showing 60kDa and 90kDa MDM2 expression in p53 transfected cells in monolayer culture. B, 1 and 2, 60kDa MDM2 immunohistochemical labelling of central regions of U87poEGFP(1) and U87p53wtEGFP(2) spheroid cultures. B, 3 and 4, MDM2 immunohistochemical labeling of peripheral regions of U373poEGFP(3) and U373p53mt135EGFP(4) spheroid cultures. All bars=100μm.

compared to control cultures (Figures 44A and B). The expression of this increased levels of 90kDa MDM2 was primarily cytoplasmically located. In the U373 cell line, no differences were observed between poEGFP, p53mt135EGFP and p53mt144EGFP cells for the 90kDa MDM2 protein in either the monolayer or spheroid cultures (Figures 43A).

5.2.4. The effects of p53 modulation on monolayer growth

Using the MTT proliferation assay, U87poEGFP, U87p53wtEGFP, U87p53mt135EGFP and U87p53mt144EGFP all showed similar growth rates (Figure 45A). Similarly U373poEGFP, U373p53mt135EGFP and U373p53mt144EGFP showed similar growth rates (Figure 45B). Therefore the addition of the above *P53* vectors did not have any effect of monolayer growth in either of the two cell lines. Only transfecting U373 cell line with the p53wtEGFP vector caused significant growth inhibition and subsequent death of the U373 cells.

5.2.5. The effects of p53 modulation on spheroid growth

After following the same protocol as with the wild-type spheroids (2.11.1), the radius measurements taken over the 5 week period from spheroids transfected with the wild-type and mutant p53 vectors showed that there was no statistical difference ($p>0.05$) between transfected, control and non-transfected cells. This was similar for both U87 and U373 spheroids (Figures 45C and D).

5.2.6. P53 gene transfer and cell death in spheroid cultures

Apoptotic counts taken from U87poEGFP, U87p53wtEGFP, U87p53mt135EGFP and U87p53mt144EGFP cell lines showed that the mean apoptotic index for spheroids containing the wild-type insert were slightly higher than the 2 mutant transfectants and the plasmid only spheroids over the 5 week period (Figure 45E). However, statistical analysis (using a split-plot ANOVA) proved this not to be significant ($p>0.05$). Although not graphed, there was also no significant difference in cell number between U87 spheroids transfected with *P53* wild-type and mutant vectors. There was also no difference in the apoptotic indices between transfected and non-transfected U373 spheroids over the 5 week period (Figure 45F). Similar to the U87 transfected cultures, there was also no difference in cell number between transfected and non-transfected U373 spheroids.

There was no difference in the time of onset of central necrosis, in U87 and U373 cells transfected with either the wild-type or mutant *P53* EGFP vectors. Areas of necrosis began to evolve over week 3 in all of the cultures. In addition, subsequent increases in the areas of central necrosis did not vary between cells transfected with control vectors and those transfected with wild-type and mutant *P53* transcripts. In all of the transfectants derived from both U87 and U373 cell lines, areas of central necrosis consisted of, on average, around 5% of the spheroid radius at week 3 and this increased with spheroid diameter over the subsequent 2 weeks.

5.2.7. HIF-1α expression in transfected spheroid cultures

There was no variation in HIF-1α expression in monolayer cultures transfected with poEGFP, p53wtEGFP, p53mt135EGFP and p53mt144EGFP vectors for either U87 or U373 cell lines. In spheroid culture however, there was an increase in HIF-1α expression outside the perinecrotic zone in U87p53wtEGFP transfected cells (Figure 44D). In all other transfected cells lines HIF-1α expression was confined to central regions (Figure 44C). Increased HIF-1α expression in association with wild-type *P53* transfection was confirmed by western blotting experiments using spheroid culture whole cell lysates where HIF-1α expression was higher in U87p53wtEGFP cells than the other U87 transfectants after 3 weeks of spheroid culture.

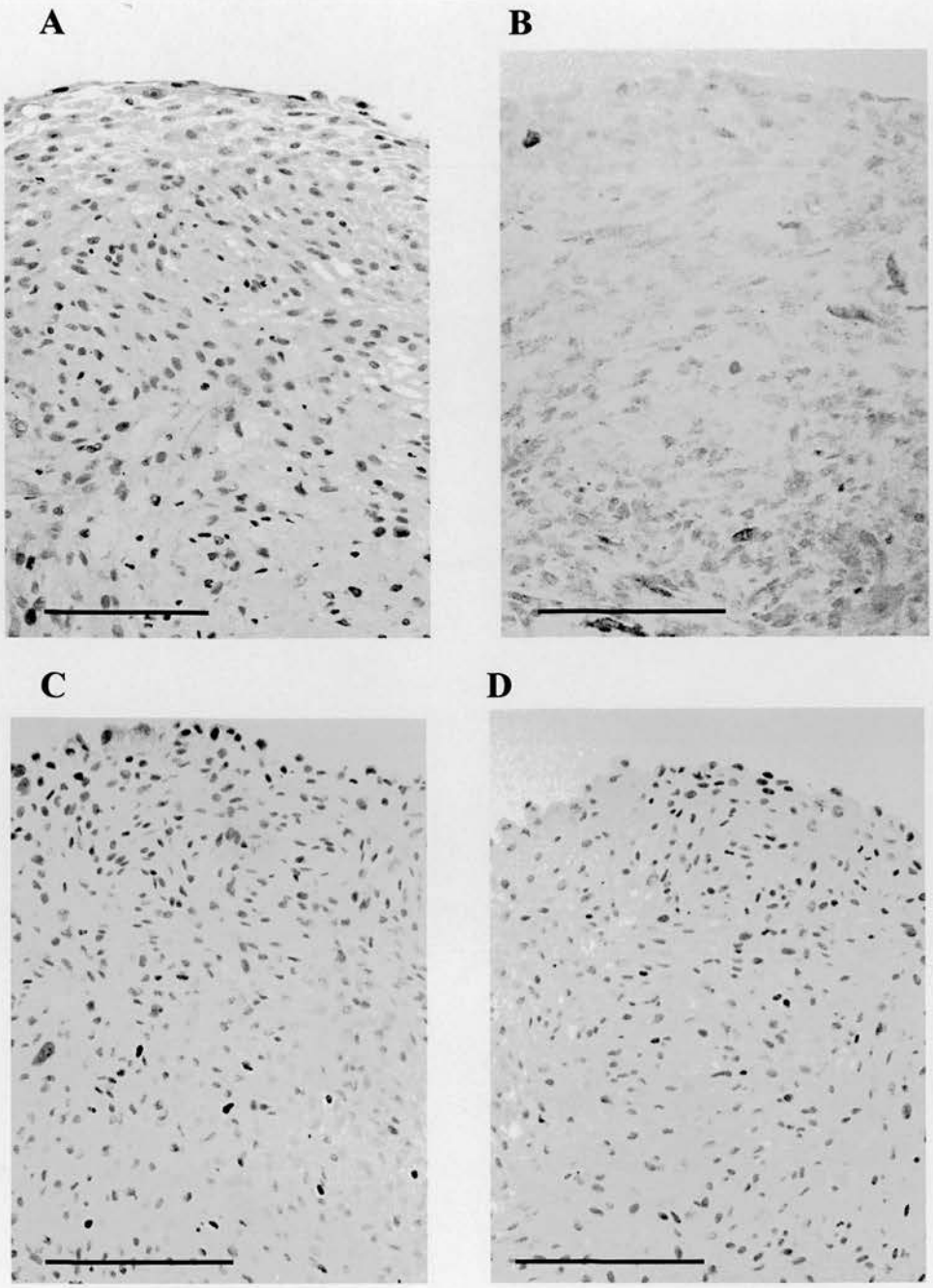

Figure 44. 90kDa MDM2 expression (using MDM2(C-18) antibody) in U87poEGFP spheroids (A) and U87p53wtEGFP spheroids (B). HIF-1□expression was confined to central regions in U87poEGFP spheroids (C) but was present throughout the spheroid mass in U87p53wtEGFP cells (D). All bars=100μm.

Figure 45. Graphs showing the growth characteristics of transfected U87 and U373 monolayer and spheroid cultures. A, MTT assay results using transfected U87 cells. B, MTT assay results using transfected U373 cells. C, spheroid radius over time for transfected U87 cells. D, spheroid radius over time for transfected U373 cells. D, number of observed apoptotic figures per spheroid over time for transfected U87 cells. E, number of observed apoptotic figures per spheroid over time for transfected U373 cells. N=10 for each point on the above graphs. Error bars are shown.

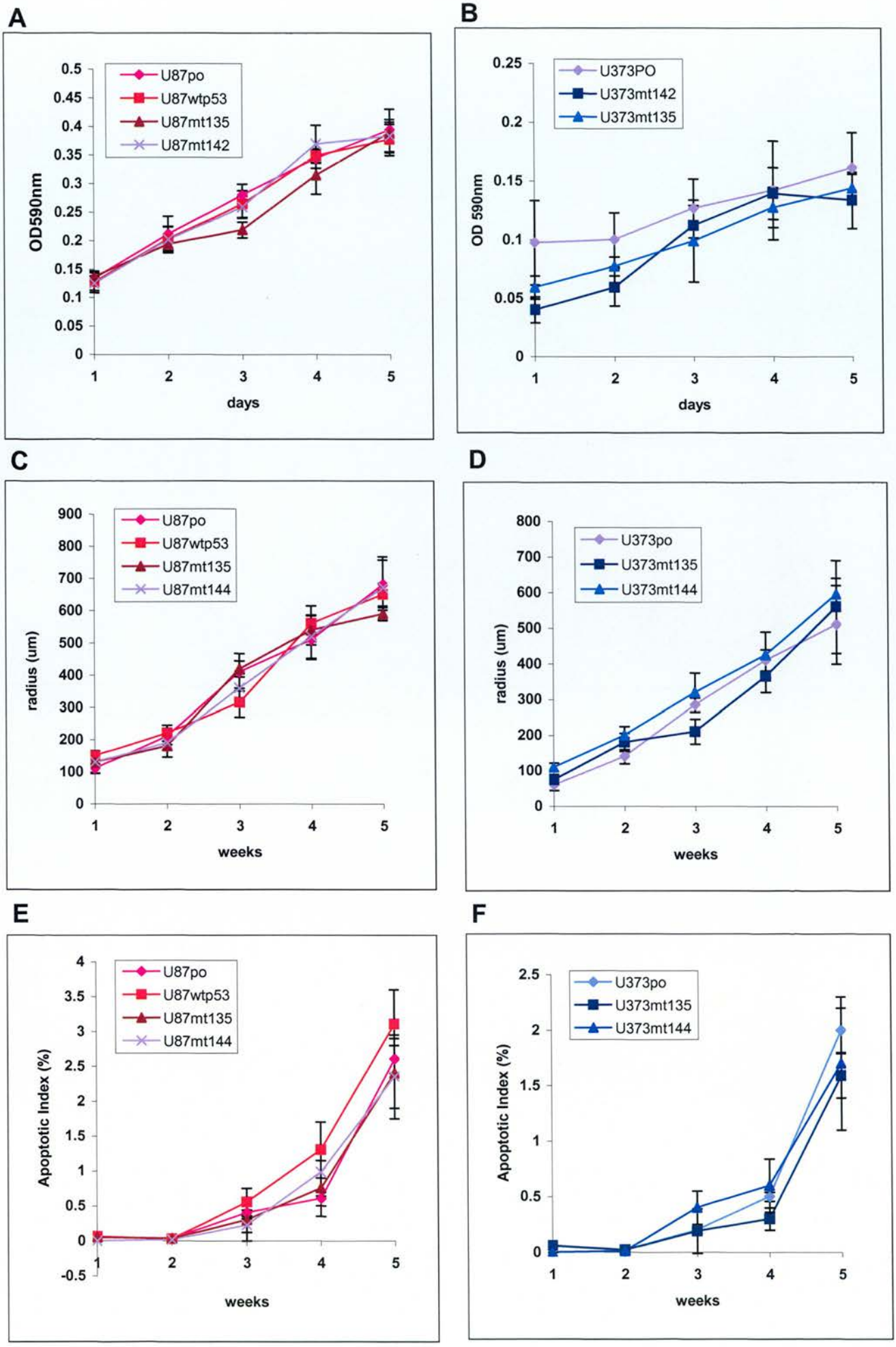
A
U87po
U87wtp53
U87mt135
U87mt142
OD590nm
days
B
U373PO
U373mt142
U373mt135
OD 590nm
days
C
U87po
U87wtp53
U87mt135
U87mt144
radius (um)
weeks
D
U373po
U373mt135
U373mt144
radius (um)
weeks
E
U87po
U87wtp53
U87mt135
U87mt144
Apoptotic Index (%)
weeks
F
U373po
U373mt135
U373mt144
Apoptotic Index (%)
weeks

5.3. Discussion

5.3.1. Summary of results

Levels of spheroid growth and cell death were found not to differ between U87 cells (possesses endogenous wild-type *P53*) transfected with plasmid-only (PO), wild-type *P53* (WTp53), dominant-negative *P53* (Mt135p53) and control *P53* (Mt144p53). Peripheral expression of p21 appeared to be reduced in spheroids derived from cells containing the wild-type *P53* transcript. In the same spheroids, increases in HIF-1α and 90kDa MDM2 were observed whereas levels of 60kDa MDM2 and Bax remained unaffected. In the U373 cell line (possesses endogenous mutant *P53*) transfection with wild-type *P53* resulted in cell death by apoptosis in all of the cultures by 3 days post transfection. The addition of dominant-negative *P53* (Mt135p53) and control *P53* (Mt144p53) did not have any effect on U373 spheroid growth or death. In addition, these two vectors failed to influence levels of endogenous Bax, p21 and MDM2 (60kDa and 90kDa) expression in U373 spheroid culture.

5.3.2. p53 expression in monolayer and spheroid cultures

U87 and U373 monolayer cultures were stably transfected with each of the *P53* vectors preceding spheroid formation. Although over 90% of cells appeared EGFP positive in live culture conditions, only 75-80% of cells in U87 (p53wild-type) appeared to be strongly p53 positive at high confluency levels. It has previously been shown that cell-cell contact can discourage the activity of the transfected vector which governs both the activity of the neo^r cassette and p53 protein production (Sasaki et al., 1992). However, in spheroid cultures, the p53 labelling index was very high, even within spheroid central regions where cell-cell contact was maximal. It was more difficult to monitor exogenous p53 expression in U373 cultures due to the presence of large amounts of mutant protein. EGFP was present in nearly 100% of live monolayer U373 cultures and p53 immunoblots showed considerably stronger bands in the transfected lines compared to the plasmid only controls. P53 immunohistochemical labelling was also noticeably stronger in U373 spheroid cultures, even including spheroid central regions where p53 labelling was low in the plasmid-only controls. These findings confirmed that when the two cell lines were grown as spheroids there were consistently high levels of exogenous p53 across the spheroid radius.

5.3.3. Monolayer and spheroid growth following *P53* gene transfer

U87 monolayer cultures transfected with the 4 vectors (p53mt135EGFP, p53mt144EGFP, p53wtEGFP and poEGFP) showed similar growth curves once stable transfectants were obtained. The addition of wild-type *P53* (p53wtEGFP) to this cell line failed to reduce cell numbers over a five day period. Similar results have been found using this cell line by other investigators (Cerrato et al., 2001; Shinoura et al., 2001; Badie et al., 1999). Other researchers have observed a rapid drop in U87 monolayer viability following transfection with similar *P53* containing vectors, but this was not found in this study (Li et al., 1997; Komata et al., 2000). As has been suggested previously, cell lines with similar names have been found to possess different genotypic alterations, possibly due to the transformation of the lines in culture and/or mix up of cell line samples (Van Meir et al., 1997).

Similar growth results were observed when the U87p53wtEGFP transfectants were grown as spheroid cultures. There was no decrease in size in spheroids derived from cells transfected with p53wtEGFP compared to the control lines. Therefore growing U87p53wtEGFP cells as 3-dimensional structures did not stimulate any reduction in spheroid growth as a result of exogenous wild-type *P53*.

Transcripts encoding *P53* with a p53135Val mutation express a highly stable p53 protein with a conformation-dependent loss of wild-type activity and the ability to eliminate any endogenous p53 wild-type activity (and often p63 and p73 activity) in a dominant negative manner (Shaulian et al., 1992; Unger et al., 1993; Di Como et al., 1999; Strano et al., 2000; Strano et al., 2002). The addition of the p53135Val dominant negative vector failed to alter U87 monolayer growth in this study. In addition, when U87p53mt135 cells were grown as spheroids, no increase in spheroid size was observed compared to control spheroids over the 5 week period. Studies have shown that induction of p53135Val and other dominant negative p53 proteins to wild-type p53 cultures can result in an increase in the transformation ability of various cell lines by increasing proliferative potential (Slingerland and Benchimol, 1991; Signal et al., 2000). Core domain mutants such as p53135Val have been shown to be able to transactivate the c-myc promoter (Frazier et al., 1998), the proliferating cell nuclear antigen promoter (Deb et al., 1992), the human heat shock protein 70 promoter (Tsutsumi-Ishii et al., 1995) and the human epidermal growth factor receptor promoter (Ludes-Meyers et al., 1996).

However, aberrations in proliferative pathways in the U87 cell line may render it unsusceptible to further transformation. Other studies have shown that the introduction of dominant negative p53 proteins to cell lines can block differentiation (Shaulsky et al., 1991). However, the morphology and GFAP positivity of cells situated within the so-called 'region of differentiation' appeared unchanged in the presence of p53135Val compared to control cultures. The size of this region also remained consistent between spheroids derived from the various transfected clones.

The addition of wild-type p53 to the *P53* mutant U373 cell line resulted in loss of the entire cell population 3 days following transfection. This is consistant with a central role for loss of p53 function in the transformation of this cell line. *P53* mutations are often early transformation events vital for the survival of tumour cells and are common in secondary glioblastomas (Rasheed et al., 1999). Subsequent alterations often occur that add transformation potential to the cells, although this is rarely sufficient to prevent death following addition of exogenous wild-type p53. Similar findings have been found using the U373 cell line by other researchers (Badie et al., 1999; Komata et al., 2000; Shinoura et al., 2001). Badie et al observed that U373 cells undergo massive apoptosis and die within 48hours of treatment with adenoviral *P53* (Adp53). There has been some suggestion that p53273His mutants retain wild-type configuration and can activate CAT p53 reporter sequences. As a result, it was thought that this mutant is capable of activating, at least partially, some downstream targets of the p53 protein. However, in terms of monolayer and spheroid overall growth, the addition of the dominant negative *P53* vector had no positive effect on U373 cell numbers compared to the plasmid-only and p53mt144EGFP controls suggesting that the p53273His mutant molecule has little capacity for overall growth inhibition.

5.3.4. Intraspheroidal cell death following *P53* gene transfer

The addition of exogenous wild-type *P53* to the U87 cell line failed to increase the basal level of apoptotic cells present in monolayer culture. In some glioma cell lines, such as the C6 rat glioma cell line, cell cycle arrest/apoptosis does occur directly as a result of *P53* transfection (Timiryasova et al., 1999). However, it has been shown that adding exogenous wild-type p53 to other cell lines that already possess a wild-type *P53* gene increases p53

pathway activation following cellular insults, rather than stimulating an apoptotic response directly as a result of increasing levels of exogenous protein (Badie et al., 1999). This was of particular interest when studying glioblastoma cell populations, where areas of extreme cell stress occur within densely populated regions of tissue distinct from the tumour vasculature. The cell line A172, for example, contains wild-type *P53* and demonstrates minimal apoptosis after infection with Adp53; however, apoptosis increases following treatment with increasing doses of irradiation compared to non-transfected A172 cells (Badie et al., 1999). This suggested that some *P53* wild-type tumours may be sensitive to wild-type *P53* gene transfer only when exposed to stress. However, when central regions of cell stress were observed in U87 spheroids, no increases in apoptotic or necrotic cell death were observed between spheroids derived from U87p53wt vectors and U87mt144 and U87plasmid-only vectors. Onset and subsequent growth of the area of necrosis occurred at the same time point and perinecrotic apoptotic indices remained similar between the different transfected clones. The differing responses of Adp53A172 (Badie et al., 1999) and p53WTU87EGFP cells (in this study) to stress were initially thought to be a result of exposure to different types of stress (A172 was exposed to p53 inducing irradiation in studies by Badie et al, and intraspheroidal U87 cells were likely to be exposed to a combination of hypoxia, metabolite depletion and waste product build up). However, U87 cells have previously shown a intrinsic resistance to increasing doses of irradiation following infection with Adp53 (Badie et al., 1999).

Although there will be variations between gene transfer techniques, particularly in terms of transfection efficiency, it is clear that different *P53* wild-type lines have variable responses to wild-type *P53* gene transfer. For example, C6 cells die directly following Adp53 infection, A172 cells infected with Adp53 die following irradiation and U87 cells transfected with WTp53 vectors are resistant to high levels of wild-type p53 protein and both irradiation and perinecrotic stress in spheroid cultures. Other studies have even shown that using a 9L (a rat *P53* wild-type cell line) brain tumour model *in vivo*, exogenous wild-type p53 expression conferred an additional survival advantage when exposed to radiation compared to non-transfected 9L cells (Bampoe et al., 2000). Conversely, the addition of rVV(recombinant vaccina virus)-WTp53 to monolayer 9L cells results in total growth inhibition and subsequent apoptosis (Timiryasova et al., 1999). The combination of these findings between different cell lines and different brain tumour models accentuates the need for studies

examining a variety of wild-type *P53* lines using 3 dimensional systems to assess the efficacy of *P53* wild-type gene transfer methods and the susceptibility to endogenous cell death within *in vivo* glioblastoma cell populations.

Dominant/negative gene transfer into U87 cells failed to reduce the observed basal levels of apoptosis observed in monolayer culture and/or the increases apoptotic observed around perinecrotic areas in spheroid culture. It has previously been shown that transfection of *P53* wild-type cell lines with dominant negative *P53* can increase resistance to chemotherapeutic agents. For example, the transfection of human ovarian carcinoma cells (A2780 cell line) possessing wild-type *P53* with p53135Val results in a resistance to the chemotherapeutic reagent CCNU (N-(2-chloroethyl)-N'-cyclohexyl-N-nitrosourea) (Aquilina et al., 2000). However, this is unlikely to occur in U87 cell line due to the resistance of the U87 cells to radiation following Adp53 infection and the lack of resistance of U87 cells to perinecrotic cell death following dominant negative transfection.

As previously described, 100% of U373 successfully transfected cells died apoptotically 3 days post transfection therefore U373p53wtEGFP cells did not form spheroid cultures. Nearly all studies examining wild-type *P53* gene transfer on *P53* mutant lines result in a significant reduction in survival of the cells. Commonly used *P53* mutant glioma lines include U373, GB-1, T98G, U251-MG and LG. All of these lines die a week post transfection following Adp53 infection (Shinoura et al., 2000; Komata et al., 2000; Shinoura et al., 2001; Badie et al., 1999; Hong et al., 2000). These findings suggested that there were no other genetic alterations present that were sufficient to allow survival of these lines. U373p53mt135EGFP and U373p53mt144EGFP cells did form spheroids, although there was no difference in the onset of central necrosis and/or the surrounding perinecrotic apoptotic index. This implies that there is no evidence to suggest that inhibiting residual mutant *P53* function has any effect on spheroid growth and/or death.

5.3.5. *P53* gene transfer and Bax expression in glioma spheroid culture

Wild-type *P53* gene transfer into U87 cells did not affect levels of Bax protein in monolayer or spheroid cultures. These findings are consistent with those of Badie et al (1999) and Shinoura (2001), where there was no change in the high levels of endogenous Bax with the

addition of Adp53 and/or Adp53 combined with irradiation in this line. In addition, no increase in Bax expression was observed within perinecrotic tissue in response to exogenous wild-type p53 expression. These results confirmed the findings in the hypoxia experiments where an upregulation of wild-type p53 was not followed by an increase in Bax. Therefore it is clear that in the U87 cell line, there is no p53 dependent stimulation of Bax, even under conditions of extreme metabolic stress.

To further confirm that there was no relationship between Bax and p53 in this cell line, the consistently high levels of endogenous Bax present in U87 cells were not affected by the addition of the dominant negative p53135Val vector. If p53 were responsible for influencing endogenous levels of Bax, the p53mt135 protein would bind to and nullify further transcription of Bax mRNA (Signal and Rotter, 2000). These observations were consistent over a long period of time incorporating many subsequent generations using stable p53135Val transfectants. Therefore, in addition to previous evidence in this study showing that endogenous Bax expression is present within perinecrotic tissue in the absence of wild-type *P53,* these further experiments have shown that endogenous expression of Bax in U87 cell line is almost certainly p53 independent. Although the mechanisms behind p53-independent activation of Bax require elucidation, other investigators have recorded both high levels of endogenous Bax and an upregulation of Bax following exposure to chemotherapeutic agents in tumour cell populations that do not express wild-type p53 (Strobel et al., 1996).

Although wild-type p53 was unable to upregulate levels of Bax in U87 cell line, it is interesting to note that when increasing amounts of exogenous Bax are added to these cells there is no stimulation of apoptosis or necrosis (Naumann and Weller, 1998). These findings appear to be cell line specific (Vogelbaum et al., 1999; Shinoura, 2001). Adenoviral transfection of Bax into the *P53* wild-type cell line A172 results in necrotic cell death (Shinoura et al., 1999). A high level of Bcl-XL (a pro-survival member of the Bcl-2 family) was found to prevent Bax-induced apoptosis in this cell line. When levels of Bax were further increased, the necrotic mode of death was replaced by an apoptotic mode of death.

Levels of Bax were not measured in U373 cells following the induction of p53wtEFGP because the cells died before spheroids could be grown. However, other studies have shown that transfection of U373 cells with Adp53 does result in an upregulation of Bax protein and subsequent cell death by apoptosis, as was seen in this study (Shinoura et al., 2001; Badie et al., 1999). High levels of endogenous Bax in U373 cell line were not effected by the expression of the dominant negative *P53* vector. Therefore, it is possible that endogenous Bax, like that found in U87 cells, may accumulate independently of p53.

The inactivity of endogenous Bax in U373, may occur as a result of equally high endogenous levels of pro-survival proteins such as Bcl-2 and Bcl-XL. When exogenous p53 is added to the cell, levels of Bax increase thus allowing Bax homodimerisation on the mitochondrial membrane and subsequent cytochrome C release (Hengartner, 2000). U373 cells and other *P53* mutant lines such as U251 appear to be more sensitive to adenoviral induction of Bax than *P53* wild-type lines such as U87 and A172 (Naumann and Weller, 1998; Shinoura et al. 1999; Yin et al., 1997).

The presence of active and inactive forms of Bax and other pro-apoptotic Bcl-2 family members in tumour cells has also been hypothesized. High levels of endogenous Bax, Bid and Bad proteins found in tumours with increasing grade with or without corresponding decreases in pro-survival family members. This suggests that basal levels of these so-called pro-apoptotic proteins may have little or no pro-apoptotic function (Kurabayashi et al., 2001; Korsmeyer et al., 1999).

The findings involving the ability of p53 to activate Bax in the 3 lines U87, U373 and A172 appear to reflect levels of cell death both in the spheroid system and in experiments performed by others. *P53* gene transfer did not result in increasing levels of Bax and no apoptosis occurred in U87 cell line. Apoptosis arises in response to p53 and subsequent Bax expression gene transfer in U373 cells. A172 appears to fall into an intermediate group were increasing levels of Adp53 result in apoptosis only when exposed to an element of cell stress (eg irradiation) and/or very high levels of Bax accumulation (Shinoura et al., 1999).

5.3.6. *P53* gene transfer and p21 expression in glioma spheroid culture

p21 expression in large U87 untransfected spheroid cultures was localized around the spheroid periphery. Surprisingly, the addition of wild-type p53 to the U87 cell line resulted in a dramatic decrease in this p21 expression, whereas no decrease in p21 expression was seen in monolayer U87 cultures as a result of exogenous wild-type p53. There can be no simple explanation for these findings. The cells in both monolayer and spheroid cultures are situated within close proximity to the medium. The only difference that is apparent is that more cells are proliferating within the spheroid periphery and the cells are more closely associated. Even the levels of peripheral 60kDa MDM2 in U87 cell line were similar to monolayer levels thus transactivation of the p21 promoter was not inhibited by the presence of abnormal levels of this protein on the spheroid periphery. It is clear that whatever is causing this phenomena is specific to cells growing in 3-dimensional culture. Therefore, the cell-cell interactions that occur in spheroid culture and *in vivo* may significantly influence the expression and interaction of p53 related proteins. Gene transfer studies using monolayer cultures may not accurately reflect the likely response of glioblastoma cell populations *in vivo* to various gene transfer strategies.

Due to the *P53* null status of the U373 cell lines, levels of p21 in U373 were not altered using the dominant/negative p53 vector. p21 levels remained extremely low/non-existent in both monolayer and spheroid cultures.

5.3.7. *P53* gene transfer and MDM2 expression in glioma spheroid culture

Increases in wild-type p53 expression due to hypoxia and transfection with the p53wtEGFP vector resulted in a slight increase in full length 90kDa MDM2 in monolayer U87 cultures. In addition, when the dominant negative p53mt135EGFP vector was transfected into U87 cells a reduction in 90kDa MDM2 was seen compared to the control cells, U87poEGFP and U87p53mt144EGFP. These findings suggested that the levels 90kDa MDM2 found in this cell line are under control of the p53 protein. This was further supported by the finding that higher levels of 90kDa MDM2 and p53 co-exist around the spheroid periphery in untransfected U87 spheroid cultures. Full length 90kDa MDM2 is known to be upregulated by p53, and is often seen to be upregulated concurrently with p53, as a means of controlling p53 levels within the cell (Kubbutat et al., 1997). Most of the 90kDa MDM2 expression was cytoplasmically located, suggesting that it had translocated from the nucleus. Cytoplasmic

localization of MDM2 occurs when p53 is being shuttled by full length MDM2 into the cytoplasm following ubiquitination (Honda et al., 1997). This allows degradation of the MDM2/p53 complex by the proteosome. Because of the high level of exogenous wild-type p53 in U87p53wtEGFP cells, full length MDM2 is likely to be active in this role. P53 labelling was also seen to be present in the cytoplasm of some cells. Because a homozygous deletion has been identified in the CDKN2A locus endcoding the $p14^{ARF}$ protein in the U87 cell line, $P14^{ARF}$ inhibitory activity in regulating this translocation is likely to be compromised.

In contrast, 60kDa MDM2 did not appear to be regulated by wild-type p53. The addition of p53wtEGFP to U87 cells did not increase levels of 60kDa MDM2 either in monolayer or in spheroid culture compared to the control lines. Levels of this protein did appear to be slightly reduced using the dominant negative *P53* vector in the western blotting experiments but this was not confirmed when examining monolayer cultures in situ or in the spheroid cultures. Possibilities for the p53 independent induction of 60kDa MDM2 are discussed in 4.3.7. The absence of a corresponding increase in 60kDa MDM2 with increasing 90kDa MDM2 expression suggests transcriptional activation of a truncated mRNA splice variant, rather then post translational caspase cleavage of the full length molecule. Although the relative stability of a 30kDa MDM2 C-terminal fragment is not known, the absence of such a fragment on the various western blotting experiments performed is again indicative of a direct transcriptional event.

Similar levels of endogenous 90kDa MDM2 were found in untransfected U373 cells as in untransfected U87 cells. Considering that the regulation of full length MDM2 appears to be under control of the p53 in the U87 cell line, these findings are surprising. Siantigny et al (2000) demonstrated that p53273His mutants are capable of activating the MDM2 promoter sequence on average at 30% of the activity of the wild-type protein. Therefore it was initially suggested that this 90kDa isoform may be produced as a result of some residual transactivation activity of the p53 transcription factor. However, the dominant mutant p53135Val when transfected into U373 cells failed to inhibit production of full length MDM2. Similar levels of full length MDM2 were observed in both monolayer and spheroid cultures between control and dominant negative p53 U373 cells. Therefore it appeared that

both 90kDa and 60kDa MDM2 were activated independently of p53 in this cell line. The question was raised as to whether the dominant negative p53135Val mutant could effectively bind to and inhibit the p53273His molecule. It was assumed that heteromerization would occur due to the wild-type configuration of the both molecules. In addition, the oligomerization regions (residues 319-360) of the two molecules are known to be fully functional in these two mutants. However, further investigation may be required to confirm this.

It is possible that intrinsic *MDM2* gene amplification may have occurred in this line. However, this finding would be unusual as *CDKN2A* mutations and *MDM2* amplification are rarely found in glioblastomas or glioma cell lines harbouring *P53* mutations (Fulci et al., 1998; Rasheed et al., 1999; Ishii et al., 1999).

5.3.8. *P53* gene transfer and HIF-1α expression in glioma spheroid culture

The addition of the dominant negative vector p53mt135Val to either U87 or U373 cell lines failed to have an effect on the expression of HIF-1α either in monolayer or spheroid culture. This was not surprising as p53 is thought to play a role downstream of HIF-1α. Dephosphorylated HIF-1α is known to bind to the p53 protein to activate p53 dependent apoptosis (Suzuki et al., 2001). The phoshorylation status of HIF-1α was not monitored in this study. Therefore it was not possible to determine whether the HIF-1α found in this study was of the type that associates with p53 and promotes apoptosis or whether is was the phosphorylated form that associates with HIF-1β (ARNT) to promote VEGF expression and neovascularisation (Suzuki et al., 2001). In this study, HIF-1α expression was largely used as a marker of the oxygenation/metabolic status of the central core of the spheroid cultures for the characterization part of the study (3.4.5).

When wild-type *P53* was added to U87 cells, a definite increase in HIF-1α was observed within spheroid cultures that was not apparent in monolayer culture. HIF-1α was observed across the spheroid radius, not localized within pre or perinecrotic tissue as in the untransfected/control groups. Although HIF-1α is thought to have an upstream effect stabilizing p53, there is no evidence in the literature to suggest that p53 has a regulative role

in modulating levels of HIF-1α. Certainly, p53 is known to repress phosphorylated HIF-1α mediated transcription of genes such as VEGF and PDEGF (platelet derived endothelial growth factor) (Blagosklonny et al., 2001; Dachs and Tozer, 2000). Perhaps high levels of exogenous p53 can, under some circumstances, be involved in a positive feed back loop resulting in an increase in pro-apoptotic dephosphorylated HIF-1α.. However, in some cells possessing wild-type p53, HIF-1α mediated accumulation of p53 may be largely redundant, such as in U87 cell line, where the addition of wild-type p53 does not increase intraspheroidal apoptotic index. These findings may be more relevant to wild-type and mutant *P53* cells lines that have altered cell viability following p53 gene transfer.

5.3.9. Summary of *P53* modulation experiments

The aim of these experiments was to examine whether altering endogenous levels of intracellular p53 has an effect on tumour cell death susceptibility in *P53* wild-type U87 spheroids and in *P53* mutant U373 spheroids. Contrary to some reports, U87 monolayer culture viability was not affected by increasing or decreasing intracellular wild-type p53 levels (Cerrato et al., 2001; Li et al., 1997). Similarly, when U87 cells were metabolically stressed within large glioma spheroid cultures, the modulation of intracellular wild-type p53 did not effect the onset of central death or apoptotic index. This occurred irrespective of alterations in p21, HIF-1α and full length MDM2 expression. These findings show that it is highly unlikely that p53 plays a direct role in the activation of endogenous cell death in U87 spheroids. The implications of these findings for wild-type *P53* glioblastoma populations are limited, due to the fact that only one cell line (U87) was used in this study. *P53* gene transfer experiments done by others show (Timiryasova et al., 199; Badie et al., 1999) that this response is likely to vary between cell lines, thus a wide variety of cell lines need to be tested in order to fully investigate the importance of p53 in endogenous cell death within 3-dimensional cell populations harbouring a wild-type *P53* gene. However what is clear, is that when situated within metabolically deprived environments, some *P53* wild-type tumour cells do not activate p53 mediated pathways resulting in an apoptotic phenotype, even following the addition of large amounts of exogenous wild-type p53. This could have implications for therapeutic targeting of specific p53 related pathways in tumours with a similar genetic background.

The addition of exogenous wild-type p53 to p53 mutant U373 cells resulted in apoptotic cell death in the entire cell population 3 days following transfection. This is often seen to occur *P53* mutant cell populations derived from most cancer types (Komata et al., 2000; Badie et al., 1999). This confirms that the *P53* mutation is likely to be the single most important transformation event in this line. Because the dominant negative vector failed to have an effect on either cell death or the transcription of downstream genes, the mutant p53His 273 protein is likely to possess very little residual pro-apoptotic activity. This is contrary to findings using artificial luciferase promoter sequences suggesting that p53His 273 mutants can activate the WAF1 (p21) and MDM2 promoter sequences at up to 30% of wild-type p53 (Saintigny et al., 1999). However, these latter observations utilising the dominant negative *P53* vector should be taken with care as the binding affinity of the mutant p53135Val protein to the p53273His protein has not been fully elucidated in this study. However, all of above results support the conclusion that endogenous cell death observed in U373 spheroids is unlikely to occur via a p53 related mechanism.

The origins of the 60kDa MDM2 isoform could be further elucidated using the *P53* gene transfer studies. In experiments using the U87 cell line, 60kDa MDM2 was unaffected by increases in p53 expression and subsequent 90kDa MDM2 upregulation. Therefore it is likely that 60kDa MDM2 arises independently of p53 and is not derived from the 90kDa MDM2 molecule. This was further supported by the presence of equally high levels of 60kDa MDM2 in the *P53* mutant U373 line. More importantly, because a lack of p53 mediated apoptosis was demonstrated within the transfected spheroid cultures, the presence of the 60kDa MDM2 isoform may be largely redundant in its inhibition of p53 dependent transcription. Therefore as previously suggested, 60kDa MDM2 may be involved in other pro-apoptotic or even cell survival pathways, perhaps involving E2F-1 and Rb. This would explain the selection for high levels of 60kDa MDM2 expression in glioma cell lines exhibiting both *P53* mutant and wild-type genotypes in the absence of a p53 mediated apoptotic response.

One of the most important conclusions of this part of the study was that successful production of spheroids derived from transfected cell lines was demonstrated. This is means that future studies investigating protein function through genetic modification will be

possible. One particular line of interest may be to create inserts encoding truncated *MDM2* sense and anti-sense transcripts. The effect of modulating levels of 60kDa MDM2 on cell death susceptibility/ tumourgenicity within glioma spheroids could then be assessed.

5.4. General conclusions and further work

The killing of tumour cells *in vivo* is the single most important factor in reducing tumour volume. Many researchers have devised potential therapeutic strategies based on their efficacy using monolayer culture systems using permanent cell lines. However, the homogeneity and morphology of these systems often does not reflect the *in vivo* scenario. Avoiding the expense and time consuming nature of animal experimentation, the spheroid system has been shown in these experiments to possess many of the features present within *in vivo* glioblastoma, particularly those relating to cell death.

One of the first conclusions of this study was that large glioma spheroid cultures appeared highly representative of glioblastoma mutiforme in terms of patterns of cell death, differentiation and proliferation. These compared favourably with cross sections of glioblastoma biopsy material spanning from blood vessels to nutritionally compromised tissue distinct from the vasculature. The formation of central areas of necrosis and subsequent onset of apoptosis in spheroid cultures resulted in morphologies very similar to the small foci of necrosis surrounded by pseudopallisading layers of tumour cells seen *in vivo*. The observed predictable onset of necrosis in spheroids derived from the four cell lines examined allowed the cultures to be examined at a particular time point and any changes could be monitored that were associated with individual cell lines and also following alterations to the genotype of the lines.

Many current studies involve targeting pro-death genes, such as *P53*, depending on the genotype of the representative cell lines in question. However, in this study, regions of endogenous intra-spheroidal cell death were monitored in order to assess the activity of specific proteins/pathways that may be important for glioma cell death susceptibility. In the *P53* wild-type cell lines U87 and A172, the p53 protein and its downstream targets p21 and Bax were found not to be important for the onset of endogenous cell cycle arrest or cell death in 3-dimensional spheroid cultures. This appeared to be the case even when p53 accumulation was found to be associated with monolayer exposure to oxidative and free radical stresses. In addition, when U87 cells were transfected with vectors encoding a variety of *P53* wild-type and mutant transcripts, no effect on cell death susceptibility was observed.

Therefore, even when levels of wild-type p53 were extremely high in this cell line, subsequent increases in cell death were not observed.

High levels of perinecrotic apoptosis in the *P53* mutant lines U373 and MOG-G-CCM lines suggested that p53 was not responsible for endogenous cell death in these lines. The addition of wild-type p53 to U373 cells resulted in the death of the whole monolayer population 3 days post transfection, whereas addition of the dominant negative transcript had no effect on endogenous Bax expression or on cell death. This confirmed that the p53273His mutant possessed little or no pro-apoptotic function. Therefore apoptosis in spheroids derived from this line must arise via a p53 independent mechanism.

These experiments using spheroid cultures suggest that p53 accumulation is not important for the onset of endogenous cell death not only in *P53* mutant tumours, but also in some tumours harbouring a wild-type *P53* gene. It is possible that growing cell lines as 3-dimensional cultures may be the best way of testing the potential of targeting p53 related pathways, even when p53 accumulation and subsequent cell death is seen using monolayer culture systems. Further experimental analysis utilizing a variety of *P53* wild-type cell lines grown as 3-dimensional cultures should hopefully further elucidate these findings.

The presence of high levels of a perinecrotic 60kDa MDM2 isoform could have significant implications in cell death susceptibility in tumours harbouring both wild-type and mutant p53. Although the *P53* gene in both the *P53* wild-type cell line U87 and the *P53* mutant line U373 appeared to be essentially redundant within perinecrotic tissue, high levels of truncated MDM2 could associate with Rb allowing E2F family mediated cell cycle progression and resistance to cell death depending on the *RB* status of the tumours in question. These interactions may theoretically protect centrally located cells against very low pO_2 levels and even allow E2F-1 mediated apoptosis to occur depending on specific, as yet unidentified, pathophysiological stimuli. Other p53 independent pro-apoptotic molecules may also be involved. Further work examining the relationship between 60kDaMDM2 and Rb/E2F family members is therefore required. A series of experiments examining the effect of increasing levels of 60kDa MDM2 in cell lines exhibiting low levels of 60kDa MDM2 in response to various types of stress may implicate a pro-survival/pro-death role for such high

levels of this novel protein. In addition, the 60kDa MDM2 isoform needs to be comprehensively assessed in terms of its amino acid composition and mechanism/s of regulation.

REFERENCES

Acker H, Carlsson J, Durand R, et al. Spheroids in cancer research. Berlin: Springer, 1984.

Acker H, Carlsson J, Mueller-Klieser W, Sutherland RM. Comparative pO2 measurements in cell spheroids cultured with different techniques. Br J Cancer. 1987 Sep;56(3):325-7.

Acker H, Pietruschka F, Deutscher J. Endothelial cell mitogen released from HT29 tumour cells grown in monolayer or multicellular spheroid culture. Br J Cancer. 1990 Sep;62(3):376-7.

Adachi J, Ohbayashi K, Suzuki T, Sasaki T. Cell cycle arrest and astrocytic differentiation resulting from PTEN expression in glioma cells.
J Neurosurg. 1999 Nov;91(5):822-30.

Adams JM, Cory S. The Bcl-2 protein family: arbiters of cell survival. Science. 1998 Aug 28;281(5381):1322-6. Review.

Akiyama K, Gluckman TL, Terhakopian A, Jinadasa PM, Narayan S, Singaswamy S, Massey B, Bing RJ. Apoptosis in experimental myocardial infarction in situ and in the perfused heart in vitro. Tissue Cell 1997;29:733-743.

Alarcon R, Koumenis C, Geyer RK, Maki CG, Giaccia AJ. Hypoxia induces p53 accumulation through MDM2 down-regulation and inhibition of E6-mediated degradation. Cancer Res. 1999 Dec 15;59(24):6046-51.

Alvarez-Tejado M, Alfranca A, Aragones J, Vara A, Landazuri MO, del Peso L. Lack of evidence for the involvement of the phosphoinositide 3-kinase/Akt pathway in the activation of hypoxia inducible factors by low oxygen tension. J Biol Chem. 2002 Jan 28 [epub ahead of print]

Alvord ED. Is necrosis helpful in the grading of gliomas? Editorial opinion. J Neuropathol Exp Neurol 1992; 51: 127-132.

An WG, Kanekal M, Simon MC, Maltepe E, Blagosklonny MV, Neckers LM. Stabilization of wild-type p53 by hypoxia-inducible factor 1alpha. Nature. 1998 Mar 26;392(6674):405-8.

Anker L, Ohgaki H, Ludeke BI, Herrmann HD, Kleihues P, Westphal M. p53 protein accumulation and gene mutations in human glioma cell lines. Int J Cancer. 1993 Dec 2;55(6):982-7.

Aquilina G, Ceccotti S, Martinelli S, Soddu S, Crescenzi M, Branch P, Karran P, Bignami M.Mismatch repair and p53 independently affect sensitivity to N-(2-chloroethyl)-N'-cyclohexyl-N-nitrosourea.Clin Cancer Res. 2000 Feb;6(2):671-80.

Arafat WO, Gomez-Navarro J, Xiang J, Barnes MN, Mahasreshti P, Alvarez RD, Siegal GP, Badib AO, Buchsbaum D, Curiel DT, Stackhouse MA. An adenovirus encoding proapoptotic Bax induces apoptosis and enhances the radiation effect in human ovarian cancer. Mol Ther. 2000 Jun;1(6):545-54.

Arsham AM, Plas DR, Thompson CB, Simon MC. PI3K/Akt signaling is neither required for hypoxic stabilization of HIF-1alpha nor sufficient for HIF-1-dependent target gene transcription. J Biol Chem. 2002 Feb 21 [epub ahead of print]

Asahi M, Fujii J, Suzuki K, Seo HG, Kuzuya T, Hori M, Tada M, Fujii S, Taniguchi N.Inactivation of glutathione peroxidase by nitric oxide. Implication for cytotoxicity. J Biol Chem. 1995 Sep 8;270(36):21035-9.

Asano K, Satoh K, Hosaka M, Arakawa H, Inagaki M, Hisamitsu T, Maeda M, Kochi M, Sakagami H. Production of hydrogen peroxide in cancerous tissue by intravenous administration of sodium 5,6-benzylidene-L-ascorbate. Anticancer Res. 1999 Jan-Feb;19(1A):229-36.

Ashkenazi A, Pai RC, Fong S, Leung S, Lawrence DA, Marsters SA, Blackie C, Chang L, McMurtrey AE, Hebert A, DeForge L, Koumenis IL, Lewis D, Harris L, Bussiere J, Koeppen H, Shahrokh Z, Schwall RH. Safety and antitumor activity of recombinant soluble Apo2 ligand. J Clin Invest. 1999 Jul;104(2):155-62.

Ashkenazi A. The Apo2L/TRAIL system: therapeutic oppertunities. Proc. Am. Assoc. Cancer Res. Conf. Programmed Cell Death Regulation (2000).

Asschert JG, Vellenga E, De Jong S, de Vries EG. Mutual interactions between p53 and growth factors in cancer. Anticancer Res. 1998 May-Jun;18(3A):1713-25. Review.

Attardi LD, Reczek EE, Cosmas C, Demicco EG, McCurrach ME, Lowe SW, Jacks T. PERP, an apoptosis-associated target of p53, is a novel member of the PMP-22/gas3 family. Genes Dev. 2000 Mar 15;14(6):704-18.

Azam N, Vairapandi M, Zhang W, Hoffman B, Liebermann DA. Interaction of CR6 (GADD45gamma) with proliferating cell nuclear antigen impedes negative growth control. J Biol Chem. 2001 Jan 26;276(4):2766-74.

Badie B, Drazan KE, Kramar MH, Shaked A, Black KL. Adenovirus-mediated p53 gene delivery inhibits 9L glioma growth in rats. Neurol Res. 1995 Jun;17(3):209-16.

Badie B, Goh CS, Klaver J, Herweijer H, Boothman DA. Combined radiation and p53 gene therapy of malignant glioma cells. Cancer Gene Ther. 1999 Mar-Apr;6(2):155-62.

Baker SJ, Markowitz S, Fearon ER, Willson JK, Vogelstein B. Suppression of human colorectal carcinoma cell growth by wild-type p53. Science. 1990 Aug 24;249(4971):912-5.

Banasiaka KJ, Xiab Y, Haddadbc GG. Mechanisms underlying hypoxia induced neuronal apoptosis. Prog Neurobiol 2000; 62(3): 215-249.

Bartel F, Meye A, Wurl P, Kappler M, Bache M, Lautenschlager C, Grunbaum U, Schmidt H, Taubert H. Amplification of the MDM2 gene, but not expression of splice

variants of MDM2 MRNA, is associated with prognosis in soft tissue sarcoma.Int J Cancer. 2001 May 20;95(3):168-75.

Basu S, Kolesnick R. Stress signals for apoptosis: ceramide and c-Jun kinase. Oncogene. 1998 Dec 24;17(25):3277-85. Review.

Bates S, Phillips AC, Clark PA, Stott F, Peters G, Ludwig RL, Vousden KH. p14ARF links the tumour suppressors RB and p53. Nature. 1998 Sep 10; 395(6698):124-5.

Bauman GS, MacDonald W, Moore E, Ramsey DA, Fisher BJ, Amberger VR, Del Maestro RM. Effects of radiation on a model of malignant glioma invasion. J Neurooncol. 1999;44(3):223-31.

Bayle JH, Elenbaas B, Levine AJ. The carboxyl-terminal domain of the p53 protein regulates sequence-specific DNA binding through its nonspecific nucleic acid-binding activity. Proc Natl Acad Sci U S A. 1995 Jun 6;92(12):5729-33.

Bell HS, Wharton SB, Leaver HA, Whittle IR. Effects of N-6 essential fatty acids on glioma invasion and growth: experimental studies with glioma spheroids in collagen gels. J Neurosurg. 1999 Dec;91(6):989-96.

Bellamy CO, Malcomson RD, Harrison DJ, Wyllie AH. Cell death in health and disease: the biology and regulation of apoptosis. Semin Cancer Biol. 1995 Feb;6(1):3-16. Review.

Bernardi P, Petronilli V. The permeability transition pore as a mitochondrial calcium release channel: a critical appraisal. J Bioenerg Biomembr. 1996 Apr;28(2):131-8.

Bernstein JJ, Goldberg WJ, Laws ER Jr. Human malignant astrocytoma xenografts migrate in rat brain: a model for nervous system cancer research. J Neurosci Res 1987; 22: 134-143.

Biernat W, Kleihues P, Yonekawa Y, Ohgaki H. Amplification and overexpression of MDM2 in primary (de novo) glioblastomas. J Neuropathol Exp Neurol. 1997 Feb;56(2):180-5.

Bilzer T, Stavrou D, Dahme E, Keiditsch E, Burrig KF, Anzil AP, Wechsler W. Morphological, immunocytochemical and growth characteristics of three human glioblastomas established in vitro. Virchows Arch A Pathol Anat Histopathol. 1991;418(4):281-93.

Bilzer T, Stavrou D, Wechsler W, Wohler B, Keiditsch E. Antigen variation in a human glioblastoma: from the primary tumor to the second recurrence, permanent cell line and xenotransplantation tumors. Anticancer Res. 1991b Mar-Apr;11(2):547-53.

Bjerkvig R, Laerum OD, Mella O. Glioma cell interactions with fetal rat brain aggregates in vitro and with brain tissue in vivo. Cancer Res 1986; 46: 4071-4079.

Bjerkvig R, Tonnesen A, Laerum OD, Backlund EO. Multicellular tumor spheroids from human gliomas maintained in organ culture. J Neurosurg. 1990 Mar;72(3):463-75.

Blagosklonny MV, Giannakakou P, Romanova LY, Ryan KM, Vousden KH, Fojo T. Inhibition of HIF-1- and wild-type p53-stimulated transcription by codon Arg175 p53 mutants with selective loss of functions.Carcinogenesis. 2001 Jun;22(6):861-7.

Blaydes JP, Gire V, Rowson JM, Wynford-Thomas D. Tolerance of high levels of wild-type p53 in transformed epithelial cells dependent on auto-regulation by mdm-2. Oncogene. 1997 Apr 17;14(15):1859-68.

Bögler O, Huang HJ, Kleihues P, Cavenee WK. The p53 gene and its role in human brain tumors. Glia. 1995 Nov;15(3):308-27. Review.

Bonventre JV. Mechanisms of ischemic acute renal failure. Kidney Int. 1993 May;43(5):1160-78.

Bootman MD, Lipp P, Berridge MJ. The organisation and functions of local Ca(2+) signals. J Cell Sci. 2001 Jun;114(Pt 12):2213-22.

Bostrom J, Cobbers JM, Wolter M, Tabatabai G, Weber RG, Lichter P, Collins VP, Reifenberger G. Mutation of the PTEN (MMAC1) tumor suppressor gene in a subset of glioblastomas but not in meningiomas with loss of chromosome arm 10q. Cancer Res. 1998 Jan 1;58(1):29-33.

Bouterfa H, Picht T, Kess D, Herbold C, Noll E, Black PM, Roosen K, Tonn JC. Retinoids inhibit human glioma cell proliferation and migration in primary cell cultures but not in established cell lines. Neurosurgery. 2000a Feb;46(2):419-30.

Bouterfa HL, Sattelmeyer V, Czub S, Vordermark D, Roosen K, Tonn JC. Inhibition of Ras farnesylation by lovastatin leads to downregulation of proliferation and migration in primary cultured human glioblastoma cells.
Anticancer Res. 2000b Jul-Aug;20(4):2761-71.

Bouvier-Labit C, Chinot O, Ochi C, Gambarelli D, Dufour H, Figarella-Branger D. Prognostic significance of Ki67, p53 and epidermal growth factor receptor immunostaining in human glioblastomas.Neuropathol Appl Neurobiol. 1998 Oct;24(5):381-8.

Bredel-Geissler A, Karbach U, Walenta S, Vollrath L, Mueller-Klieser W. Proliferation-associated oxygen consumption and morphology of tumor cells in monolayer and spheroid culture. J Cell Physiol. 1992 Oct;153(1):44-52.

Buchhop S, Gibson MK, Wang XW, Wagner P, Sturzbecher HW, Harris CC. Interaction of p53 with the human Rad51 protein. Nucleic Acids Res. 1997 Oct 1;25(19):3868-74.

Bueso-Ramos CE, Manshouri T, Haidar MA, Yang Y, McCown P, Ordonez N, Glassman A, Sneige N, Albitar M. Abnormal expression of MDM-2 in breast carcinomas. Breast Cancer Res Treat. 1996;37(2):179-88.

Burger PC, Dubois PJ, Schold SC Jr, Smith KR Jr, Odom GL, Crafts DC, Giangaspero F. Computerized tomographic and pathologic studies of the untreated, quiescent, and recurrent glioblastoma multiforme. J Neurosurg. 1983 Feb;58(2):159-69.

Burger PC, Green SB. Patient age, histologic features, and length of survival in patients with glioblastoma multiforme. Cancer 1987;59(9):1617-25.

Burger PC, Kleihues P. Cytologic composition of the untreated glioblastoma with implications for evaluation of needle biopsies. Cancer. 1989 May 15;63(10):2014-23.

Byeon IJ, Li J, Ericson K, Selby TL, Tevelev A, Kim HJ, O'Maille P, Tsai MD. Tumor suppressor p16INK4A: determination of solution structure and analyses of its interaction with cyclin-dependent kinase 4. Mol Cell. 1998 Feb;1(3):421-31.

Byers SW, Sommers CL, Hoxter B, Mercurio AM, Tozeren A. Role of E-cadherin in the response of tumor cell aggregates to lymphatic, venous and arterial flow: measurement of cell-cell adhesion strength. J Cell Sci. 1995 May;108 (Pt 5):2053-64.

Carmeliet P, Dor Y, Herbert JM, Fukumura D, Brusselmans K, Dewerchin M, Neeman M, Bono F, Abramovitch R, Maxwell P, Koch CJ, Ratcliffe P, Moons L, Jain RK, Collen D, Keshert E, Keshet E. Role of HIF-1alpha in hypoxia-mediated apoptosis, cell proliferation and tumour angiogenesis. Nature. 1998 Jul 30;394(6692):485-90.

Carroll RS, Zhang J, Chauncey BW, Chantziara K, Frosch MP, Black PM. Apoptosis in astrocytic neoplasms. Acta Neurochir (Wien). 1997;139(9):845-50.

Catsicas M, Clarke PGH. Cyclohexamide prevents neuronal death during embryogenesis. Experientia 1990, 46: A78.

Celli J, Duijf P, Hamel BC, Bamshad M, Kramer B, Smits AP, Newbury-Ecob R, Hennekam RC, Van Buggenhout G, van Haeringen A, Woods CG, van Essen AJ, de Waal R, Vriend G, Haber DA, Yang A, McKeon F, Brunner HG, van Bokhoven H. Heterozygous germline mutations in the p53 homolog p63 are the cause of EEC syndrome. Cell. 1999 Oct 15;99(2):143-53.

Cerrato JA, Yung WK, Liu TJ. Introduction of mutant p53 into a wild-type p53-expressing glioma cell line confers sensitivity to Ad-p53-induced apoptosis. Neuro-oncol. 2001 Apr;3(2):113-22.

Chandel NS, Vander Heiden MG, Thompson CB, Schumacker PT. Redox regulation of p53 during hypoxia. Oncogene. 2000 Aug 10;19(34):3840-8.

Chao DT, Korsmeyer SJ. BCL-2 family: regulators of cell death. Annu Rev Immunol. 1998;16:395-419. Review.

Chen J, Wu X, Lin J, Levine AJ. mdm-2 inhibits the G1 arrest and apoptosis functions of the p53 tumor suppressor protein. Mol Cell Biol. 1996 May;16(5):2445-52.

Chen L, Marechal V, Moreau J, Levine AJ, Chen J. Proteolytic cleavage of the mdm2 oncoprotein during apoptosis. J Biol Chem. 1997 Sep 5;272(36):22966-73.

Cheng SY, Huang HJ, Nagane M, Ji XD, Wang D, Shih CC, Arap W, Huang CM, Cavenee WK. Suppression of glioblastoma angiogenicity and tumorigenicity by inhibition of endogenous expression of vascular endothelial growth factor. Proc Natl Acad Sci U S A. 1996 Aug 6;93(16):8502-7.

Chintala SK, Gokaslan ZL, Go Y, Sawaya R, Nicolson GL, Rao JS. Role of extracellular matrix proteins in regulation of human glioma cell invasion in vitro. Clin Exp Metastasis. 1996 Sep;14(4):358-66.

Chou D, Miyashita T, Mohrenweiser HW, Ueki K, Kastury K, Druck T, von Deimling A, Huebner K, Reed JC, Louis DN. The BAX gene maps to the glioma candidate region at 19q13.3, but is not altered in human gliomas. Cancer Genet Cytogenet. 1996 Jun;88(2):136-40.

Clarke PGH. Apoptosis Versus Necrosis: How Valid a Dichotomy for Neurons? In Cell Death and Diseases of the Nervous System. VE Koliatos and RR Ratan eds. Humana Press Inc., Totowa, NJ (1998).

Collins VP. Progression as exemplified by human astrocytic tumors. Semin Cancer Biol. 1999 Aug;9(4):267-76.

Cormack BP, Valdivia RH, Falkow S. FACS-optimized mutants of the green fluorescent protein (GFP). Gene. 1996;173(1 Spec No):33-8.

Craperi D, Vicat JM, Nissou MF, Mathieu J, Baudier J, Benabid AL, Verna JM. Increased bax expression is associated with cell death induced by ganciclovir in a herpes thymidine kinase gene-expressing glioma cell line. Hum Gene Ther. 1999 Mar 1;10(4):679-88.

Creutz CE. The annexins and exocytosis. Science 1992; 258(5084): 924-31.

Crook T, Vousden KH. Properties of p53 mutations detected in primary and secondary cervical cancers suggest mechanisms of metastasis and involvement of environmental carcinogens. EMBO J. 1992 Nov;11(11):3935-40.

Cummings MC, Winterford CM, Walker NI. Apoptosis. In: Sternberg SS, eds. Histology for Pathologists, 2nd edition. Philadelphia; Lippencott-Raven Publishers; 3-21.

Dachs GU, Tozer GM. Hypoxia modulated gene expression: angiogenesis, metastasis and therapeutic exploitation.Eur J Cancer. 2000 Aug;36(13 Spec No):1649-60. Review.

D'Amours D, Desnoyers S, D'Silva I, Poirier GG. Poly(ADP-ribosyl)ation reactions in the regulation of nuclear functions. Biochem J. 1999 Sep 1;342 (Pt 2):249-68. Review.

Davis PK, Dowdy SF. p73. Int J Biochem Cell Biol. 2001 Oct;33(10):935-9.

de Cremoux P, Salomon AV, Liva S, Dendale R, Bouchind'homme B, Martin E, Sastre-Garau X, Magdelenat H, Fourquet A, Soussi T. p53 mutation as a genetic trait of typical medullary breast carcinoma. J Natl Cancer Inst. 1999 Apr 7;91(7):641-3.

de Stanchina E, McCurrach ME, Zindy F, Shieh SY, Ferbeyre G, Samuelson AV, Prives C, Roussel MF, Sherr CJ, Lowe SW. E1A signaling to p53 involves the p19(ARF) tumor suppressor.Genes Dev. 1998 Aug 1;12(15): 2434-42.

Deb S, Jackson CT, Subler MA, Martin DW. Modulation of cellular and viral promoters by mutant human p53 proteins found in tumor cells. J Virol. 1992 Oct;66(10):6164-70.

Deckert M, Reifenberger G, Wechsler W. Determination of the proliferative potential of human brain tumors using the monoclonal antibody Ki-67.
J Cancer Res Clin Oncol. 1989;115(2):179-88.

Deisboeck TS, Berens ME, Kansal AR, Torquato S, Stemmer-Rachamimov AO, Chiocca EA. Pattern of self-organization in tumour systems: complex growth dynamics in a novel brain tumour spheroid model. Cell Prolif. 2001 Apr;34(2):115-34.

Di Como CJ, Gaiddon C, Prives C.p73 function is inhibited by tumor-derived p53 mutants in mammalian cells.Mol Cell Biol. 1999 Feb;19(2):1438-49.

Dilla T, Velasco JA, Medina DL, Gonzalez-Palacios JF, Santisteban P. The MDM2 oncoprotein promotes apoptosis in p53-deficient human medullary thyroid carcinoma cells. Endocrinology 2000; 141(1): 420-429.

Dipple A. DNA adducts of chemical carcinogens. Carcinogenesis. 1995 Mar;16(3):437-41. Review.

Donaldson EA, McKenna DJ, McMullen CB, Scott WN, Stitt AW, Nelson J.
The expression of membrane-associated 67-kDa laminin receptor (67LR) is modulated in vitro by cell-contact inhibition. Mol Cell Biol Res Commun. 2000 Jan;3(1):53-9.

Du C, Fang M, Li Y, Li L, Wang X. Smac, a mitochondrial protein that promotes cytochrome c-dependent caspase activation by eliminating IAP inhibition. Cell. 2000 Jul 7;102(1):33-42.

Daumas-Duport C, Scheithauer B, O'Fallon J, Kelly P.Grading of astrocytomas. A simple and reproducible method. Cancer. 1988 Nov 15;62(10):2152-65.

Durand RE, Sham E.The lifetime of hypoxic human tumor cells. Int J Radiat Oncol Biol Phys. 1998 Nov 1;42(4):711-5.

Dyson N.The regulation of E2F by pRB-family proteins. Genes Dev. 1998 Aug 1;12(15):2245-62. Review.

Earnshaw WC, Martins LM, Kaufmann SH. Mammalian caspases: structure, activation, substrates, and functions during apoptosis. Annu Rev Biochem. 1999;68:383-424. Review.

Eguchi Y, Shimizu S, Tsujimoto Y. Intracellular ATP levels determine cell death fate by apoptosis or necrosis. Cancer Res. 1997 May 15;57(10):1835-40.

El-Deiry WS, Kern SE, Pietenpol JA, Kinzler KW, Vogelstein B. Definition of a consensus binding site for p53. Nat Genet. 1992 Apr;1(1):45-9.

Ellison DW, Steart PV, Gatter KC, Weller RO. Apoptosis in cerebral astrocytic tumours and its relationship to expression of the bcl-2 and p53 proteins. Neuropathol Appl Neurobiol. 1995 Aug;21(4):352-61.

Engebraaten O, Bjerkvig R, Pedersen PH, Laerum OD. Effects of EGF, bFGF, NGF and PDGF(bb) on cell proliferative, migratory and invasive capacities of human brain-tumour biopsies in vitro. Int J Cancer. 1993 Jan 21;53(2):209-14.

Evtodienko YV, Teplova VV, Sidash SS, Ichas F, Mazat JP. Microtubule-active drugs suppress the closure of the permeability transition pore in tumour mitochondria. FEBS Lett. 1996 Sep 9;393(1):86-8.

Fang S, Jensen JP, Ludwig RL, Vousden KH, Weissman AM.Mdm2 is a RING finger-dependent ubiquitin protein ligase for itself and p53. J Biol Chem. 2000 Mar 24;275(12):8945-51.

Felderhoff-Mueser U, Taylor DL, Greenwood K, Kozma M, Stilbenz D, Joashi UC, Edwards AD, Mehmet H. Fas/CD95/APO-1 can function as a death receptor for neuronal cells in vitro and in vivo and is upregulated following cerebral hypoxic-ischemic injury to the developing rat brain. Brain Pathology 2000; 10(1): 17-29.

Franks AJ, Burrow HM. In vitro heterogeneity in human gliomas. Are all transformed cells of glial origin? Anticancer Res. 1986 Jul-Aug;6(4):625-9.

Frazier MW, He X, Wang J, Gu Z, Cleveland JL, Zambetti GP.Activation of c-myc gene expression by tumor-derived p53 mutants requires a discrete C-terminal domain.Mol Cell Biol. 1998 Jul;18(7):3735-43.

Fu H, Subramanian RR, Masters SC. 14-3-3 proteins: structure, function, and regulation. Annu Rev Pharmacol Toxicol. 2000;40:617-47.

Fuchs E, Dowling J, Segre J, Lo SH, Yu QC. Integrators of epidermal growth and differentiation: distinct functions for beta 1 and beta 4 integrins. Curr Opin Genet Dev. 1997 Oct;7(5):672-82. Review.

Fukunaga-Johnson N, Ryan JJ, Wicha M, Nunez G, Clarke MF. Bcl-2 protects murine erythroleukemia cells from p53-dependent and -independent radiation-induced cell death. Carcinogenesis. 1995 Aug;16(8):1761-7.

Fulci G, Ishii N, Van Meir EG. p53 and brain tumors: from gene mutations to gene therapy. Brain Pathol. 1998 Oct;8(4):599-613. Review.

Fulci G, Labuhn M, Maier D, Lachat Y, Hausmann O, Hegi ME, Janzer RC, Merlo A, Van Meir EG. p53 gene mutation and ink4a-arf deletion appear to be two mutually exclusive events in human glioblastoma. Oncogene. 2000 Aug 3;19(33):3816-22.

Fulda S, Scaffidi C, Pietsch T, Krammer PH, Peter ME, Debatin KM. Activation of the CD95 (APO-1/Fas) pathway in drug- and gamma-irradiation-induced apoptosis of brain tumor cells. Cell Death Differ. 1998 Oct;5(10):884-93.

Gansbacher B, Rosenthal FM, Zier K. Retroviral vector-mediated cytokine-gene transfer into tumor cells.Cancer Invest. 1993;11(3):345-54. Review.

Gardner LB, Li Q, Park MS, Flanagan WM, Semenza GL, Dang CV.Hypoxia inhibits G1/S transition through regulation of p27 expression.
J Biol Chem. 2001 Mar 16;276(11):7919-26.

Gartel AL, Najmabadi F, Goufman E, Tyner AL.A role for E2F1 in Ras activation of p21(WAF1/CIP1) transcription. Oncogene. 2000 Feb 17;19(7):961-4.

Gerdes J, Schwab U, Lemke H, Stein H. Production of a mouse monoclonal antibody reactive with a human nuclear antigen associated with cell proliferation. Int J Cancer. 1983 Jan 15;31(1):13-20.

Giese A, Loo MA, Reif MD, Tran N, Berens ME. Substrates for astrocytoma invasion. Neurosurgery 1995; 37: 294-302.

Giglia G, Dumaz N, Drougard C, Avril MF, Daya-Grosjean L, Sarasin A. p53 mutations in skin and internal tumors of xeroderma pigmentosum patients belonging to the complementation group C. CancerRes 1998; Oct1; 58(19): 4402-9.

Giordana MT, Bradac GB, Pagni CA, Marino S, Attanasio A. Primary diffuse leptomeningeal gliomatosis with anaplastic features. Acta Neurochir (Wien). 1995;132(1-3):154-9. Review.

Gold R, Schmied M, Giegerich G, Breitschopf H, Hartung HP, Toyka KV, Lassmann H. Differentiation between cellular apoptosis and necrosis by the combined use of in situ tailing and nick translation techniques. Lab Invest. 1994 Aug;71(2):219-25.

Gollahon LS, Shay JW. Immortalization of human mammary epithelial cells transfected with mutant p53 (273his). Oncogene. 1996 Feb 15;12(4):715-25.

Gomez-Manzano C, Fueyo J, Alameda F, Kyritsis AP, Yung WK. Gene therapy for gliomas: p53 and E2F-1 proteins and the target of apoptosis. Int J Mol Med. 1999 Jan;3(1):81-5. Review.

Gomez-Manzano C, Fueyo J, Kyritsis AP, McDonnell TJ, Steck PA, Levin VA, Yung WK. Characterization of p53 and p21 functional interactions in glioma cells en route to apoptosis. J Natl Cancer Inst. 1997 Jul 16;89(14):1036-44.

Gomez-Manzano C, Fueyo J, Kyritsis AP, Steck PA, Roth JA, McDonnell TJ, Steck KD, Levin VA, Yung WK. Adenovirus-mediated transfer of the p53 gene produces rapid and generalized death of human glioma cells via apoptosis. Cancer Res. 1996 Feb 15;56(4):694-9.

Gorgoulis VG, Rassidakis GZ, Karameris AM, Papastamatiou H, Trigidou R, Veslemes M, Rassidakis AN, Kittas C. Immunohistochemical and molecular evaluation of the mdm-2 gene product in bronchogenic carcinoma. Mod Pathol. 1996 May;9(5):544-54.

Graeber TG, Osmanian C, Jacks T, Housman DE, Koch CJ, Lowe SW, Giaccia AJ. Hypoxia-mediated selection of cells with diminished apoptotic potential in solid tumours. Nature. 1996 Jan 4;379(6560):88-91.

Grasl-Kraupp B, Ruttkay-Nedecky B, Koudelka H, Bukowska K, Bursch W, Schulte-Hermann R. In situ detection of fragmented DNA (TUNEL assay) fails to discriminate among apoptosis, necrosis and autolytic cell death: a cautionary note. Hepatology 1995; 21: 1465-1468.

Green SL, Freiberg RA, Giaccia AJ. p21(Cip1) and p27(Kip1) regulate cell cycle reentry after hypoxic stress but are not necessary for hypoxia-induced arrest. Mol Cell Biol. 2001 Feb;21(4):1196-206.

Greenberg AH. Granzyme B-induced apoptosis. Adv Exp Med Biol. 1996;406:219-28. Review.

Greenblatt MS, Bennett WP, Hollstein M, Harris CC. Mutations in the p53 tumor suppressor gene: clues to cancer etiology and molecular pathogenesis. Cancer Res. 1994 Sep 15;54(18):4855-78. Review.

Groebe K, Mueller-Klieser W. On the relation between size of necrosis and diameter of tumor spheroids. Int J Radiat Oncol Biol Phys. 1996 Jan 15;34(2):395-401.

Hachiya M, Chumakov A, Miller CW, Akashi M, Said J, Koeffler HP. Mutant p53 proteins behave in a dominant, negative fashion in vivo. Anticancer Res. 1994 Sep-Oct;14(5A):1853-9.

Hao C, Beguinot F, Condorelli G, Trencia A, Van Meir EG, Yong VW, Parney IF, Roa WH, Petruk KC. Induction and intracellular regulation of tumor necrosis factor-related apoptosis-inducing ligand (TRAIL) mediated apotosis in human malignant glioma cells. Cancer Res. 2001 Feb 1;61(3):1162-70.

Hara E, Smith R, Parry D, Tahara H, Stone S, Peters G. Regulation of p16CDKN2 expression and its implications for cell immortalization and senescence. Mol Cell Biol. 1996 Mar;16(3):859-67.

Haupt Y, Maya R, Kazaz A, Oren M. Mdm2 promotes the rapid degradation of p53.Nature. 1997 May 15;387(6630):296-9.

Hauptmann S, Zardi L, Siri A, Carnemolla B, Borsi L, Castellucci M, Klosterhalfen B, Hartung P, Weis J, Stocker G, et al. Extracellular matrix proteins in colorectal carcinomas. Expression of tenascin and fibronectin isoforms. Lab Invest. 1995 Aug;73(2):172-82.

He J, Reifenberger G, Liu L, Collins VP, James CD Analysis of glioma cell lines for amplification and overexpression of MDM2. Genes Chromosomes Cancer. 1994 Oct;11(2):91-6.

Hemminki K. DNA adducts, mutations and cancer. Carcinogenesis. 1993 Oct;14(10):2007-12. Review.

Hengartner MO. The biochemistry of apoptosis. Nature. 2000 Oct 12;407(6805):770-6. Review.

Hirato J, Nakazato Y, Ogawa A. Expression of non-glial intermediate filament proteins in gliomas.Clin Neuropathol. 1994 Jan-Feb;13(1):1-11.

Hirose Y, Berger MS, Pieper RO. p53 effects both the duration of G2/M arrest and the fate of temozolomide-treated human glioblastoma cells. Cancer Res. 2001 Mar 1;61(5):1957-63.

Hoekstra MF. Responses to DNA damage and regulation of cell cycle checkpoints by the ATM protein kinase family. Curr Opin Genet Dev. 1997 Apr;7(2):170-5. Review.

Hoffman HJ, Duffner PK. Extraneural metastases of central nervous system tumors. Cancer. 1985 Oct 1;56(7 Suppl):1778-82.

Honda R, Tanaka H, Yasuda H. Oncoprotein MDM2 is a ubiquitin ligase E3 for tumor suppressor p53. FEBS Lett. 1997 Dec 22;420(1):25-7.

Honda R, Yasuda H. Activity of MDM2, a ubiquitin ligase, toward p53 or itself is dependent on the RING finger domain of the ligase. Oncogene. 2000 Mar 9;19(11):1473-6.

Hong YK, Joe YA, Yang YJ, Lee KS, Son BC, Jeun SS, Chung DS, Cho KK, Park CK, Kim MC, Kim HK, Yung WK, Kang JK.Potentials and limitations of adenovirus-p53 gene therapy for brain tumors.J Korean Med Sci. 2000 Jun;15(3):315-22.

Hsing A, Faller DV, Vaziri C. DNA-damaging aryl hydrocarbons induce Mdm2 expression via p53-independent post-transcriptional mechanisms. J Biol Chem. 2000 Aug 25;275(34):26024-31.

Humphrey PA, Gangarosa LM, Wong AJ, Archer GE, Lund-Johansen M, Bjerkvig R, Laerum OD, Friedman HS, Bigner DD. Deletion-mutant epidermal growth factor receptor in human gliomas: effects of type II mutation on receptor function. Biochem Biophys Res Commun. 1991 Aug 15;178(3):1413-20.

Hupp TR, Lane DP. Allosteric activation of latent p53 tetramers.Curr Biol. 1994 Oct 1;4(10):865-75.

Ichimura K, Bolin MB, Goike HM, Schmidt EE, Moshref A, Collins VP. Deregulation of the p14ARF/MDM2/p53 pathway is a prerequisite for human astrocytic gliomas with G1-S transition control gene abnormalities. Cancer Res. 2000 Jan 15;60(2):417-24.

Ishii N, Maier D, Merlo A, Tada M, Sawamura Y, Diserens AC, Van Meir EG. Frequent co-alterations of TP53, p16/CDKN2A, p14ARF, PTEN tumor suppressor genes in human glioma cell lines. Brain Pathol. 1999 Jul;9(3):469-79.

Ivanchuk SM, Mondal S, Dirks PB, Rutka JT. The INK4A/ARF locus: role in cell cycle control and apoptosis and implications for glioma growth. J Neurooncol. 2001 Feb;51(3):219-29.

Janka M, Fischer U, Tonn JC, Kerkau S, Roosen K, Meese E. Comparative amplification analysis of human glioma tissue and glioma derived fragment spheroids using reverse chromosome painting (RCP). Anticancer Res. 1996 Sep-Oct;16(5A):2601-6.

Jeffrey PD, Gorina S, Pavletich NP. Crystal structure of the tetramerization domain of the p53 tumor suppressor at 1.7 angstroms. Science. 1995 Mar 10;267(5203):1498-502.

Jen J, Harper JW, Bigner SH, Bigner DD, Papadopoulos N, Markowitz S, Willson JK, Kinzler KW, Vogelstein B. Deletion of p16 and p15 genes in brain tumors. Cancer Res. 1994 Dec 15;54(24):6353-8.

Jeremic B, Jovanovic D, Djuric LJ, Jevremovic S, Mijatovic LJ. Advantage of post-radiotherapy chemotherapy with CCNU, procarbazine, and vincristine (mPCV) over chemotherapy with VM-26 and CCNU for malignant gliomas. J Chemother. 1992 Apr;4(2):123-6.

Jiang BH, Agani F, Passaniti A, Semenza GL. V-SRC induces expression of hypoxia-inducible factor 1 (HIF-1) and transcription of genes encoding vascular endothelial growth factor and enolase 1: involvement of HIF-1 in tumor progression.Cancer Res. 1997 Dec 1;57(23):5328-35.

Joki T, Heese O, Nikas DC, Bello L, Zhang J, Kraeft SK, Seyfried NT, Abe T, Chen LB, Carroll RS, Black PM. Expression of cyclooxygenase 2 (COX-2) in human glioma and in vitro inhibition by a specific COX-2 inhibitor, NS-398. Cancer Res. 2000 Sep 1;60(17):4926-31.

Jung JM, Bruner JM, Ruan S, Langford LA, Kyritsis AP, Kobayashi T, Levin VA, Zhang W. Increased levels of p21WAF1/Cip1 in human brain tumors. Oncogene. 1995 Nov 16;11(10):2021-8.

Kaghad M, Bonnet H, Yang A, Creancier L, Biscan JC, Valent A, Minty A, Chalon P, Lelias JM, Dumont X, Ferrara P, McKeon F, Caput D. Monoallelically expressed gene related to p53 at 1p36, a region frequently deleted in neuroblastoma and other human cancers. Cell. 1997 Aug 22;90(4):809-19.

Kajstura J, Cheng W, Reiss K, Clark WA, Sonnenblick EH, Krajewski S, Reed JC, Olivetti G, Anversa P. Apoptotic and necrotic myocyte cell deaths are independent contributing variables of infarct size in rats. Lab Invest 1996;74:86-107.

Kamijo T, Weber JD, Zambetti G, Zindy F, Roussel MF, Sherr CJ. Functional and physical interactions of the ARF tumor suppressor with p53 and Mdm2. Proc Natl Acad Sci U S A. 1998 Jul 7;95(14):8292-7.

Kamijo T, Zindy F, Roussel MF, Quelle DE, Downing JR, Ashmun RA, Grosveld G, Sherr CJ. Tumor suppression at the mouse INK4a locus mediated by the alternative reading frame product p19ARF. Cell. 1997 Nov 28;91(5):649-59.

Kane DJ, Ord T, Anton R, Bredesen DE. Expression of bcl-2 inhibits necrotic neural cell death. J Neurosci Res. 1995 Feb 1;40(2):269-75.

Karbach U, Gerharz CD, Groebe K, Gabbert HE, Mueller-Klieser W. Rhabdomyosarcoma spheroids with central proliferation and differentiation. Cancer Res. 1992 Jan 15;52(2):474-7.

Kataoka Y, Murley JS, Patel R, Grdina DJ. Cytoprotection by WR-1065, the active form of amifostine, is independent of p53 status in human malignant glioma cell lines. Int J radiat Biol 2000; 76(5): 633-639.

Kawamura M, Yamashita T, Segawa K, Kaneuchi M, Shindoh M, Fujinaga K. The 273rd codon mutants of p53 show growth modulation activities not correlated with p53-specific transactivation activity. Oncogene. 1996 Jun 6;12(11):2361-7.

Kawata M, Sekiya S, Kera K, Kimura H, Takamizawa H. Neural rosette formation within in vitro spheroids of a clonal human teratocarcinoma cell line, PA-1/NR: role of extracellular matrix components in the morphogenesis. Cancer Res. 1991 May 15;51(10):2655-69.

Kerr JF, Winterford CM, Harmon BV. Apoptosis. Its significance in cancer and cancer therapy. Cancer. 1994 Apr 15;73(8):2013-26. Review.

Kerr JF, Wyllie AH, Currie AR. Apoptosis: a basic biological phenomenon with wide-ranging implications in tissue kinetics.Br J Cancer. 1972 Aug;26(4):239-57. Review.

Khalid H, Yagi N, Hiura T, Shibata S. Immunohistochemical analysis of p53 and p21 in human primary glioblastomas in relation to proliferative potential and apoptosis. Brain Tumour Pathol. 1998; 15: 89-94.

Khosravi R, Maya R, Gottlieb T, Oren M, Shiloh Y, Shkedy D.Rapid ATM-dependent phosphorylation of MDM2 precedes p53 accumulation in response to DNA damage. Proc Natl Acad Sci U S A. 1999 Dec 21;96(26):14973-7.

Kieser A, Weich HA, Brandner G, Marme D, Kolch W. Mutant p53 potentiates protein kinase C induction of vascular endothelial growth factor expression. Oncogene. 1994 Mar;9(3):963-9.

Kimura M, Mizukami Y, Miura T, Fujimoto K, Kobayashi S, Matsuzaki M.Orphan G protein-coupled receptor, GPR41, induces apoptosis via a p53/Bax pathway during ischemic hypoxia and reoxygenation. J Biol Chem. 2001 Jul 13;276(28):26453-60.

Kischkel FC, Hellbardt S, Behrmann I, Germer M, Pawlita M, Krammer PH, Peter ME. Cytotoxicity-dependent APO-1 (Fas/CD95)-associated proteins form a death-inducing signaling complex (DISC) with the receptor. EMBO J. 1995 Nov 15;14(22):5579-88.

Kitamura Y, Ota T, Matsuoka Y, Tooyama I, Kimura H, Shimohama S, Nomura Y, Gebicke-Haerter PJ, Taniguchi T. Hydrogen peroxide-induced apoptosis mediated by p53 protein in glial cells. Glia. 1999 Jan 15;25(2):154-64.

Kleihues P, Burger PC, Collins VP, Newcomb EW, Ohgaki H, Cavenee WK. Glioblastoma. In: Kleihues P and Cavanee WK, eds. Tumours of the nervous system. Lyon: IARC Press, 2000: 10-21.

Kleihues P, Burger PC, Scheithauer BW. Histological typing of tumour of the central nervous system. 2nd edition (1993).

Knudson CM, Tung KS, Tourtellotte WG, Brown GA, Korsmeyer SJ. Bax-deficient mice with lymphoid hyperplasia and male germ cell death. Science. 1995 Oct 6;270(5233):96-9.

Knuechel R, Keng P, Hofstaedter F, Langmuir V, Sutherland RM, Penney DP. Differentiation patterns in two- and three-dimensional culture systems of human squamous carcinoma cell lines. Am J Pathol. 1990 Sep;137(3):725-36.

Kobayashi N, Takada Y, Hachiya M, Ando K, Nakajima N, Akashi M. TNF-apha induced p21(WAF1) but not Bax in colon cancer cells WiDr with mutated p53: important role of protein stabilization. Cytokine 2000; 12(12): 1745-1754.

Kock H, Harris MP, Anderson SC, Machemer T, Hancock W, Sutjipto S, Wills KN, Gregory RJ, Shepard HM, Westphal M, Maneval DC. Adenovirus-mediated p53 gene transfer suppresses growth of human glioblastoma cells in vitro and in vivo. Int J Cancer. 1996 Sep 17;67(6):808-15.

Kockx MM, Knaapen WM. The role of apoptosis in vascular disease. J Pathol 2000;190(3):267-280.

Koh J, Enders GH, Dynlacht BD, Harlow E. Tumour-derived p16 alleles encoding proteins defective in cell-cycle inhibition. Nature. 1995 Jun 8;375(6531):506-10.

Komata T, Kondo Y, Koga S, Ko SC, Chung LW, Kondo S. Combination therapy of malignant glioma cells with 2-5A-antisense telomerase RNA and recombinant adenovirus p53. Gene Ther. 2000 Dec;7(24):2071-9.

Kordek R, Hironishi M, Liberski PP, Yanagihara R, Gajdusek DC.Apoptosis in glial tumors as determined by in situ nonradioactive labeling of DNA breaks. Acta Neuropathol (Berl). 1996;91(1):112-6.

Korsmeyer SJ, Gross A, Harada H, Zha J, Wang K, Yin XM, Wei M, Zinkel S. Death and survival signals determine active/inactive conformations of pro-apoptotic BAX, BAD, and BID molecules.Cold Spring Harb Symp Quant Biol. 1999;64:343-50. Review.

Kowalik TF, DeGregori J, Leone G, Jakoi L, Nevins JR. E2F1-specific induction of apoptosis and p53 accumulation, which is blocked by Mdm2. Cell Growth Differ. 1998 Feb;9(2):113-8.

Krajewski S, Krajewska M, Ehrmann J, Sikorska M, Lach B, Chatten J, Reed JC. Immunohistochemical analysis of Bcl-2, Bcl-X, Mcl-1, and Bax in tumors of central and peripheral nervous system origin. Am J Pathol. 1997 Mar;150(3):805-14.

Krammer PH. CD95's deadly mission in the immune system. Nature. 2000 Oct 12;407(6805):789-95. Review.

Kraus A, Neff F, Behn M, Schuermann M, Muenkel K, Schlegel J.Expression of alternatively spliced mdm2 transcripts correlates with stabilized wild-type p53 protein in human glioblastoma cells. Int J Cancer. 1999 Mar 15;80(6):930-4.

Kroemer G. The proto-oncogene Bcl-2 and its role in regulating apoptosis. Nat Med. 1997 Jun;3(6):614-20. Review.

Kubbutat MH, Jones SN, Vousden KH. Regulation of p53 stability by Mdm2. Nature. 1997 May 15;387(6630):299-303.

Kuenen-Boumeester V, Henzen-Logmans SC, Timmermans MM, van Staveren IL, van Geel A, Peeterse HJ, Bonnema J, Berns EM. Altered expression of p53 and its regulated proteins in phyllodes tumours of the breast. J Pathol 1999; 189(2):169-175.

Kuniyasu H, Yasui W, Kitahara K, Naka K, Yokozaki H, Akama Y, Hamamoto T, Tahara H, Tahara E. Growth inhibitory effect of interferon-beta is associated with the induction of cyclin-dependent kinase inhibitor p27Kip1 in a human gastric carcinoma cell line. Cell Growth Differ. 1997 Jan;8(1):47-52.

Kunz-Schughart LA, Groebe K, Mueller-Klieser W. Three-dimensional cell culture induces novel proliferative and metabolic alterations associated with oncogenic transformation. Int J Cancer. 1996 May 16;66(4):578-86.

Kunz-Schughart LA, Kreutz M, Knuechel R. Multicellular spheroids: a three-dimentional in vitro culture system to study tumour biology. Int J Exp Path 1998; 79: 1-23.

Kurabayashi A, Furihata M, Matsumoto M, Ohtsuki Y, Sasaguri S, Ogoshi S. Kurabayashi A, Furihata M, Matsumoto M, Ohtsuki Y, Sasaguri S, Ogoshi S. Expression of Bax and apoptosis-related proteins in human esophageal squamous cell carcinoma including dysplasia. Mod Pathol. 2001 Aug;14(8):741-7.

Kwon D, Choi C, Lee J, Kim KO, Kim JD, Kim SJ, Choi IH. Hydrogen peroxide triggers the expression of Fas/FasL in astrocytoma cell lines and augments apoptosis. J Neuroimmunol. 2001 Feb 1;113(1):1-9.

Laderoute KR, Grant TD, Murphy BJ, Sutherland RM. Enhanced epidermal growth factor receptor synthesis in human squamous carcinoma cells exposed to low levels of oxygen. Int J Cancer. 1992 Sep 30;52(3):428-32.

Laderoute KR, Murphy BJ, Short SM, Grant TD, Knapp AM, Sutherland RM. Enhancement of transforming growth factor-alpha synthesis in multicellular tumour spheroids of A431 squamous carcinoma cells. Br J Cancer. 1992 Feb;65(2):157-62.

Lam EW, La Thangue NB. DP and E2F proteins: coordinating transcription with cell cycle progression. Curr Opin Cell Biol. 1994 Dec;6(6):859-66. Review.

Landers JE, Cassel SL, George DL.Translational enhancement of mdm2 oncogene expression in human tumor cells containing a stabilized wild-type p53 protein.Cancer Res. 1997 Aug 15;57(16):3562-8.

Lang FF, Miller DC, Koslow M, Newcomb EW. Pathways leading to glioblastoma multiforme: a molecular analysis of genetic alterations in 65 astrocytic tumors. J Neurosurg. 1994 Sep;81(3):427-36.

Lang FF, Yung WK, Raju U, Libunao F, Terry NH, Tofilon PJ. Enhancement of radiosensitivity of wild-type p53 human glioma cells by adenovirus-mediated delivery of the p53 gene. J Neurosurg. 1998 Jul;89(1):125-32.

Lantos PL, VandenBurg SR, Kliehues P (1996). Tumours of the central nervous system, Graham DI, Lantos PL (eds), Greenfields Neuropathology. 9, 6th edition, pp583-879, Arnold: London.

LaRue KE, Bradbury EM, Freyer JP. Differential regulation of cyclin-dependent kinase inhibitors in monolayer and spheroid cultures of tumorigenic and nontumorigenic fibroblasts. Cancer Res. 1998 Mar 15;58(6):1305-14.

Laske DW, Ilercil O, Akbasak A, Youle RJ, Oldfield EH. Efficacy of direct intratumoral therapy with targeted protein toxins for solid human gliomas in nude mice. J Neurosurg. 1994 Mar;80(3):520-6.

La Thangue NB. DP and E2F proteins: components of a heterodimeric transcription factor implicated in cell cycle control. Curr Opin Cell Biol. 1994 Jun;6(3):443-50. Review.

Leaver HA, Whittle IR, Wharton SB, Ironside JW. Apoptosis in human primary brain tumours. Br J Neurosurg 1998;12:539-546.

Lee GH, Osanai M, Tokusashi Y. Morphology, proliferation and apoptosis of mouse liver epithelial cells cultured as spheroids. Jpn J Cancer Res. 1999 Oct;90(10):1109-16.

Lee KH, Kim KC, Jung YJ, Ham YH, Jang JJ, Kwon H, Sung YC, Kim SH, Han SK, Kim CM. Induction of apoptosis in p53-deficient human hepatoma cell line by wild-type p53 gene transduction: inhibition by antioxidant. Mol Cells. 2001 Aug 31;12(1):17-24.

Leist M, Single B, Castoldi AF, Kuhnle S, Nicotera P. Intracellular adenosine triphosphate (ATP) concentration: a switch in the decision between apoptosis and necrosis. J Exp Med 1997;185:1481-1486.

Lemasters JJ, Qian T, Bradham CA, Brenner DA, Cascio WE, Trost LC, Nishimura Y, Nieminen AL, Herman B. Mitochondrial dysfunction in the pathogenesis of necrotic and apoptotic cell death. J Bioenerg Biomembr. 1999 Aug;31(4):305-19.

Lennon SV, Martin SJ, Cotter TG. Dose-dependent induction of apoptosis in human tumour cell lines by widely diverging stimuli. Cell Prolif 1991;24:2-3-214.

Levenberg S, Yarden A, Kam Z, Geiger B. p27 is involved in N-cadherin-mediated contact inhibition of cell growth and S-phase entry. Oncogene. 1999 Jan 28;18(4):869-76.

Levin VA, Silver P, Hannigan J, Wara WM, Gutin PH, Davis RL, Wilson CB. Superiority of post-radiotherapy adjuvant chemotherapy with CCNU, procarbazine, and vincristine (PCV) over BCNU for anaplastic gliomas: NCOG 6G61 final report.

Li H, Lochmuller H, Yong VW, Karpati G, Nalbantoglu J. Adenovirus-mediated wild-type p53 gene transfer and overexpression induces apoptosis of human glioma cells independent of endogenous p53 status. J Neuropathol Exp Neurol. 1997 Aug;56(8):872-8.

Li R, Waga S, Hannon GJ, Beach D, Stillman B. Differential effects by the p21 CDK inhibitor on PCNA-dependent DNA replication and repair. Nature. 1994 Oct 6;371(6497):534-7.

Li YJ, Hoang-Xuan K, Zhou XP, Sanson M, Mokhtari K, Faillot T, Cornu P, Poisson M, Thomas G, Hamelin R. Analysis of the p21 gene in gliomas. J Neurooncol. 1998 Nov;40(2):107-11.

Ludes-Meyers JH, Subler MA, Shivakumar CV, Munoz RM, Jiang P, Bigger JE, Brown DR, Deb SP, Deb S.Transcriptional activation of the human epidermal growth factor receptor promoter by human p53. Mol Cell Biol. 1996 Nov;16(11):6009-19.

Lukas J, Gao DQ, Keshmeshian M, Wen WH, Tsao-Wei D, Rosenberg S, Press MF.Alternative and aberrant messenger RNA splicing of the mdm2 oncogene in invasive breast cancer.Cancer Res. 2001 Apr 1;61(7):3212-9.

Lund-Johansen M., Bjerkvig R and Rucklidge GJ (1992). Tumor spheroids from monolayer culture. In Spheroid culture in cancer research (Ed by Bjerkvig R.), pp. 4 - 18, CRC Press Boca Raton.

Mainprize TG, Taylor MD, Rutka JT, Dirks PB. Cip/Kip cell-cycle inhibitors: a neuro-oncological perspective. J Neurooncol. 2001 Feb;51(3):205-18.

Malkin D. The role of p53 in human cancer. J Neurooncol. 2001 Feb;51(3):231-43.

Mansbridge JN, Ausserer WA, Knapp MA, Sutherland RM. Adaptation of EGF receptor signal transduction to three-dimensional culture conditions: changes in surface receptor expression and protein tyrosine phosphorylation. J Cell Physiol. 1994 Nov;161(2):374-82.

Marchenko ND, Moll UM. Nuclear overexpression of p53 protein does not correlate with gene mutation in primary peritoneal carcinoma. Hum Pathol. 1997 Sep;28(9):1002-6.

Marmorstein LY, Ouchi T, Aaronson SA. The BRCA2 gene product functionally interacts with p53 and RAD51. Proc Natl Acad Sci U S A. 1998 Nov 10;95(23):13869-74.

Martin K, Trouche D, Hagemeier C, Sorensen TS, La Thangue NB, Kouzarides T. Stimulation of E2F1/DP1 transcriptional activity by MDM2 oncoprotein. Nature. 1995 Jun 22;375(6533): 691-4.

Marx JL. Oxygen free radicals linked to many diseases. Science. 1987 Jan 30;235(4788):529-31.

Matsumoto R, Tada M, Nozaki M, Zhang CL, Sawamura Y, Abe H.Short alternative splice transcripts of the mdm2 oncogene correlate to malignancy in human astrocytic neoplasms.Cancer Res. 1998 Feb 15;58(4):609-13.

Matsumura K, Kawamoto K. Long-term passage results of glioma cells and their cell kinetics. Hum Cell. 1994 Sep;7(3):158-66.

Maxwell PH, Dachs GU, Gleadle JM, Nicholls LG, Harris AL, Stratford IJ, Hankinson O, Pugh CW, Ratcliffe PJ.Hypoxia-inducible factor-1 modulates gene

expression in solid tumors and influences both angiogenesis and tumor growth. Proc Natl Acad Sci U S A. 1997 Jul 22;94(15):8104-9.

McPake CR, Tillman DM, Poquette CA, George EO, Houghton JA, Harris LC. Bax is an important determinant of chemosensitivity in pediatric tumor cell lines independent of Bcl-2 expression and p53 status. Oncol Res. 1998;10(5):235-44.

Meier P, Finch A, Evan G. Apoptosis in development.Nature. 2000 Oct 12;407(6805):796-801. Review.

Mercer WE, Shields MT, Amin M, Sauve GJ, Appella E, Romano JW, Ullrich SJ. Negative growth regulation in a glioblastoma tumor cell line that conditionally expresses human wild-type p53. Proc Natl Acad Sci U S A. 1990 Aug;87(16): 6166-70.

Merzak A, Raynal S, Rogers JP, Lawrence D, Pilkington GJ. Human wild type p53 inhibits cell proliferation and elicits dramatic morphological changes in human glioma cell lines in vitro. J Neurol Sci. 1994 Dec 20;127(2):125-33.

Migheli A, Cavalla P, Marino S, Schiffer D.A study of apoptosis in normal and pathologic nervous tissue after in situ end-labeling of DNA strand breaks. J Neuropathol Exp Neurol. 1994 Nov;53(6):606-16.

Miller LK. An exegesis of IAPs: salvation and surprises from BIR motifs. Trends Cell Biol. 1999 Aug;9(8):323-8. Review.

Miyashita T, Krajewski S, Krajewska M, Wang HG, Lin HK, Liebermann DA, Hoffman B, Reed JC. Tumor suppressor p53 is a regulator of bcl-2 and bax gene expression in vitro and in vivo. Oncogene. 1994 Jun;9(6):1799-805.

Moley KH, Mueckler MM. Glucose transport and apoptosis. Apoptosis. 2000 Apr;5(2):99-105. Review.

Momand J, Zambetti GP, Olson DC, George D, Levine AJ.The mdm-2 oncogene product forms a complex with the p53 protein and inhibits p53-mediated transactivation.Cell. 1992 Jun 26;69(7):1237-45.

Montes de Oca Luna R, Wagner DS, Lozano G. Rescue of early embryonic lethality in mdm2-deficient mice by deletion of p53. Nature. 1995 Nov 9;378(6553):203-6.

Moro A, Calixto A, Suarez E, Arana MJ, Perea SE. Differential expression of the p27Kip1 mRNA in IFN-sensitive and resistant cell lines. Biochem Biophys Res Commun. 1998 Apr 28;245(3):752-6.

Mueller-Klieser W, Freyer JP, Sutherland RM. Influence of glucose and oxygen supply conditions on the oxygenation of multicellular spheroids. Br J Cancer. 1986 Mar;53(3):345-53.

Mueller-Klieser W. Multicellular spheroids. A review on cellular aggregates in cancer research. J Cancer Res Clin Oncol. 1987;113(2):101-22. Review.

Mueller-Klieser W. Three-dimensional cell cultures: from molecular mechanisms to clinical applications. Am J Physiol. 1997 Oct;273(4 Pt 1):C1109-23. Review.

Mueller-Klieser W. Tumor biology and experimental therapeutics. Crit Rev Oncol Hematol. 2000 Nov-Dec;36(2-3):123-39. Review.

Murphy BJ, Laderoute KR, Vreman HJ, Grant TD, Gill NS, Stevenson DK, Sutherland RM. Enhancement of heme oxygenase expression and activity in A431 squamous carcinoma multicellular tumor spheroids.Cancer Res. 1993 Jun 15;53(12):2700-3.

Nagane M, Su Huang HJ, Cavenee WK. Advances in the molecular genetics of gliomas. Current Opinion in Oncology 1997; 9: 215-222.

Nagashima T, Hoshino T, Cho KG. Proliferative potential of vascular components in human glioblastoma multiforme. Acta Neuropathol (Berl). 1987;73(3):301-5.

Narla RK, Liu XP, Klis D, Uckun FM. Inhibition of human glioblastoma cell adhesion and invasion by 4-(4'-hydroxylphenyl)-amino-6,7-dimethoxyquinazoline (WHI-P131) and 4-(3'-bromo-4'-hydroxylphenyl)-amino-6,7-dimethoxyquinazoline (WHI-P154). Clin Cancer Res. 1998 Oct;4(10):2463-71.

Naumann U, Weit S, Wischhusen J, Weller M. Diva/Boo is a negative regulator of cell death in human glioma cells. FEBS Lett. 2001 Sep 7;505(1):23-6.

Naumann U, Weller M. Retroviral BAX gene transfer fails to sensitize malignant glioma cells to CD95L-induced apoptosis and cancer chemotherapy. Int J Cancer. 1998 Aug 12;77(4):645-8.

Ness GO, Pedersen PH, Bjerkvig R, Laerum OD, Lillehaug JR. Three-dimensional growth of glial cell lines affects growth factor and growth factor receptor mRNA levels. Exp Cell Res. 1994 Sep;214(1):433-6.

Nicholson DW. From bench to clinic with apoptosis-based therapeutic agents. Nature. 2000 Oct 12;407(6805):810-6. Review.

Nicholson SA, Okby NT, Khan MA, Welsh JA, McMenamin MG, Travis WD, Jett JR, Tazelaar HD, Trastek V, Pairolero PC, Corn PG, Herman JG, Liotta LA, Caporaso NE, Harris CC. Alterations of p14ARF, p53, and p73 genes involved in the E2F-1-mediated apoptotic pathways in non-small cell lung carcinoma. Cancer Res. 2001 Jul 15;61(14):5636-43.

Nicotera P, Leist M, Fava E, Berliocchi L, Volbracht C. Energy requirement for caspase activation and neuronal cell death. Brain Pathol 2000;10:276-282.

Nip J, Strom DK, Eischen CM, Cleveland JL, Zambetti GP, Hiebert SW. E2F-1 induces the stabilization of p53 but blocks p53-mediated transactivation. Oncogene. 2001 Feb 22;20(8):910-20.

Nishikawa R, Ji XD, Harmon RC, Lazar CS, Gill GN, Cavenee WK, Huang HJ. A mutant epidermal growth factor receptor common in human glioma confers enhanced tumorigenicity. Proc Natl Acad Sci U S A. 1994 Aug 2;91(16):7727-31.

Ohgaki H, Schauble B, zur Hausen A, von Ammon K, Kleihues P. Genetic alterations associated with the evolution and progression of astrocytic brain tumours. Virchows Arch. 1995;427(2):113-8. Review.

Olson DC, Marechal V, Momand J, Chen J, Romocki C, Levine AJ. Identification and characterization of multiple mdm-2 proteins and mdm-2-p53 protein complexes. Oncogene. 1993 Sep;8(9):2353-60.

Pagano M, Tam SW, Theodoras AM, Beer-Romero P, Del Sal G, Chau V, Yew PR, Draetta GF, Rolfe M. Role of the ubiquitin-proteasome pathway in regulating abundance of the cyclin-dependent kinase inhibitor p27. Science. 1995 Aug 4;269(5224):682-5.

Park DJ, Nakamura H, Chumakov AM, Said JW, Miller CW, Chen DL, Koeffler HP. Transactivational and DNA binding abilities of endogenous p53 in mutant cell lines. Oncogene 1994; 9(7): 1899-1906.

Patsouris E, Davaki P, Kapranos N, Davaris P, Papageorgiou K.A study of apoptosis in brain tumors by in situ end-labeling method. Clin Neuropathol. 1996 Nov-Dec;15(6):337-41.

Paulus W, Huettner C, Tonn JC. Collagens, integrins and the mesenchymal drift in glioblastomas: a comparison of biopsy specimens, spheroid and early monolayer cultures. Int J Cancer. 1994 Sep 15;58(6):841-6.

Penar PL, Khoshyomn S, Bhushan A, Tritton TR. Inhibition of epidermal growth factor receptor-associated tyrosine kinase blocks glioblastoma invasion of the brain.Neurosurgery. 1997 Jan;40(1):141-51.

Phelps PC, Smith MW, Trump BF. Cytosolic ionized calcium and bleb formation after acute cell injury of cultured rabbit renal tubule cells.
Lab Invest. 1989 May;60(5):630-42.

Plate KH, Breier G, Weich HA, Risau W.Vascular endothelial growth factor is a potential tumour angiogenesis factor in human gliomas in vivo.Nature. 1992 Oct 29;359(6398):845-8.

Pochampally R, Fodera B, Chen L, Lu W, Chen J. Activation of an MDM2-specific caspase by p53 in the absence of apoptosis. J Biol Chem. 1999 May 21;274(21):15271-7.

Pochampally R, Fodera B, Chen L, Shao W, Levine EA, Chen J. A 60 kd MDM2 isoform is produced by caspase cleavage in non-apoptotic tumor cells. Oncogene. 1998 Nov 19;17(20):2629-36.

Polyak K, Xia Y, Zweier JL, Kinzler KW, Vogelstein B. A model for p53-induced apoptosis. Nature. 1997 Sep 18;389(6648):300-5.

Pomerantz J, Schreiber-Agus N, Liegeois NJ, Silverman A, Alland L, Chin L, Potes J, Chen K, Orlow I, Lee HW, Cordon-Cardo C, DePinho RA. The Ink4a tumor suppressor gene product, p19Arf, interacts with MDM2 and neutralizes MDM2's inhibition of p53. Cell. 1998 Mar 20;92(6):713-23.

Popp JA, Shinozuka H, Farber E. The protective effects of diethyldithiocarbamate and cycloheximide on the multiple hepatic lesions induced by carbon tetrachloride in the rat. Toxicol Appl Pharmacol. 1978 Aug;45(2):549-64.

Prados MD, Levin V. Biology and treatment of malignant glioma. Semin Oncol. 2000 Jun;27(3 Suppl 6):1-10. Review.

Prives C, Hall PA. The p53 pathway. J Pathol. 1999 Jan;187(1):112-26. Review.

Pykett MJ, Azzam E, Dahlberg W, Little JB. Differential p53, p21, mdm2 and Rb regulation in glioma cell lines that overexpress wild-type p53. Int J Oncol. 1998 Aug;13(2):213-6.

Qi JS, Yuan Y, Desai-Yajnik V, Samuels HH. Regulation of the mdm2 oncogene by thyroid hormone receptor.Mol Cell Biol. 1999 Jan;19(1):864-72.

Rainaldi G, Calcabrini A, Arancia G, Santini MT. Differential expression of adhesion molecules (CD44, ICAM-1 and LFA-3) in cancer cells grown in monolayer or as multicellular spheroids. Anticancer Res. 1999 May-Jun;19(3A):1769-78.

Rallapalli R, Strachan G, Cho B, Mercer WE, Hall DJ.A novel MDMX transcript expressed in a variety of transformed cell lines encodes a truncated protein with potent p53 repressive activity. J Biol Chem. 1999 Mar 19;274(12):8299-308.

Rao GN, Berk BC.Active oxygen species stimulate vascular smooth muscle cell growth and proto-oncogene expression. Circ Res. 1992 Mar;70(3):593-9.

Rasheed BK, Wiltshire RN, Bigner SH, Bigner DD. Molecular pathogenesis of malignant gliomas.Curr Opin Oncol. 1999 May;11(3):162-7.

Rasper DM, Vaillancourt JP, Hadano S, Houtzager VM, Seiden I, Keen SL, Tawa P, Xanthoudakis S, Nasir J, Martindale D, Koop BF, Peterson EP, Thornberry NA, Huang J, MacPherson DP, Black SC, Hornung F, Lenardo MJ, Hayden MR, Roy S, Nicholson DW. Cell death attenuation by 'Usurpin', a mammalian DED-caspase homologue that precludes caspase-8 recruitment and activation by the CD-95 (Fas, APO-1) receptor complex. Cell Death Differ. 1998 Apr;5(4):271-88.

Reifenberger G, Liu L, Ichimura K, Schmidt EE, Collins VP. Amplification and overexpression of the MDM2 gene in a subset of human malignant gliomas without p53 mutations. Cancer Res. 1993 Jun 15;53(12):2736-9.

Ries S, Biederer C, Woods D, Shifman O, Shirasawa S, Sasazuki T, McMahon M, Oren M, McCormick F. Opposing effects of Ras on p53: transcriptional activation of mdm2 and induction of p19ARF. Cell. 2000 Oct 13;103(2):321-30.

Romero FJ, Zukowski D, Mueller-Klieser W. Glutathione content of V79 cells in two- or three-dimensional culture. Am J Physiol. 1997 May;272(5 Pt 1):C1507-12.

Rosen A, Casciola-Rosen L. Macromolecular substrates for the ICE-like proteases during apoptosis. J Cell Biochem. 1997 Jan;64(1):50-4. Review.

Roth W, Grimmel C, Rieger L, Strik H, Takayama S, Krajewski S, Meyermann R, Dichgans J, Reed JC, Weller M. Bag-1 and Bcl-2 gene transfer in malignant glioma: modulation of cell cycle regulation and apoptosis. Brain Pathol. 2000 Apr;10(2):223-34.

Roussel MF. The INK4 family of cell cycle inhibitors in cancer. Oncogene. 1999 Sep 20;18(38):5311-7. Review.

Ruan H, Wang J, Hu L, Lin CS, Lamborn KR, Deen DF. Killing of brain tumor cells by hypoxia-responsive element mediated expression of BAX. Neoplasia 1999; 1(5): 431-7.

Ruas M, Peters G. The p16INK4a/CDKN2A tumor suppressor and its relatives. Biochim Biophys Acta. 1998 Oct 14;1378(2):F115-77. Review.

Russo AA, Jeffrey PD, Patten AK, Massague J, Pavletich NP. Crystal structure of the p27Kip1 cyclin-dependent-kinase inhibitor bound to the cyclin A-Cdk2 complex. Nature. 1996 Jul 25;382(6589):325-31.

Saintigny Y, Rouillard D, Chaput B, Soussi T, Lopez BS. Mutant p53 proteins stimulate spontaneous and radiation-induced intrachromosomal homologous recombination independently of the alteration of the transactivation activity and of the G1 checkpoint. Oncogene. 1999 Jun 17;18(24):3553-63.

Sasaki A, Ishiuchi S, Kanda T, Hasegawa M, Nakazato Y.Analysis of interleukin-6 gene expression in primary human gliomas, glioblastoma xenografts, and glioblastoma cell lines. Brain Tumor Pathol. 2001;18(1):13-21.

Sasaki K, Mizusawa H, Ishidate M, Tanaka N. Regulation of G418 selection efficiency by cell-cell interaction in transfection. Somat Cell Mol Genet. 1992 Nov;18(6):517-27.

Sawada M, Nakashima S, Kiyono T, Nakagawa M, Yamada J, Yamakawa H, Banno Y, Shinoda J, Nishimura Y, Nozawa Y, Sakai N. p53 regulates ceramide formation by neutral sphingomyelinase through reactive oxygen species in human glioma cells. Oncogene. 2001 Mar 15;20(11):1368-78.

Scherer HJ. Cerebral astrocytomas and their derivatives. Am J Cancer 1940; 159-198.

Schiffer D, Cavalla P, Migheli A, Chio A, Giordana MT, Marino S, Attanasio A. Apoptosis and cell proliferation in human neuroepithelial tumors. Neurosci Lett. 1995 Aug 4;195(2):81-4.

Schiffer D, Giordana MT, Germano I, Mauro A. Anaplasia and heterogeneity of GFAP expression in gliomas. Tumori. 1986 Apr 30;72(2):163-70.

Schmidt EE, Ichimura K, Reifenberger G, Collins VP. CDKN2 (p16/MTS1) gene deletion or CDK4 amplification occurs in the majority of glioblastomas. Cancer Res. 1994 Dec 15;54(24):6321-4.

Schmitt CA, McCurrach ME, de Stanchina E, Wallace-Brodeur RR, Lowe SW. INK4a/ARF mutations accelerate lymphomagenesis and promote chemoresistance by disabling p53.Genes Dev. 1999 Oct 15;13(20):2670-7.

Schor SL, Schor AM, Winn B, Rushton G. The use of three-dimensional collagen gels for the study of tumor cell invasion in vitro: experimental parameters influencing cell migration into the gel matrix. Int J Cancer 1982; 29: 57-62.

Shapiro JR, Shapiro WR. The subpopulations and isolated cell types of freshly resected high grade human gliomas: their influence on the tumor's evolution in vivo and behavior and therapy in vitro. Cancer Metastasis Rev. 1985;4(2):107-24. Review.

Shaul Y. c-Abl: activation and nuclear targets. Cell Death Differ. 2000 Jan;7(1):10-6. Review.

Shaulian E, Zauberman A, Ginsberg D, Oren M.Identification of a minimal transforming domain of p53: negative dominance through abrogation of sequence-specific DNA binding. Mol Cell Biol. 1992 Dec;12(12):5581-92.

Shaulsky G, Goldfinger N, Rotter V. Alterations in tumor development in vivo mediated by expression of wild type or mutant p53 proteins. Cancer Res. 1991 Oct 1;51(19):5232-7.

Sheard MA. Ionizing radiation as a response-enhancing agent for CD95-mediated apoptosis. Int J Cancer. 2001 Aug 20;96(4):213-20. Review.

Shimada A, Kato S, Enjo K, Osada M, Ikawa Y, Kohno K, Obinata M, Kanamaru R, Ikawa S, Ishioka C. The transcriptional activities of p53 and its homologue p51/p63: similarities and differences. Cancer Res. 1999 Jun 15;59(12):2781-6.

Shinoura N, Muramatsu Y, Asai A, Han S, Horii A, Kirino T, Hamada H.Degree of apoptosis induced by adenovirus-mediated transduction of p53 or p73alpha depends on the p53 status of glioma cells.Cancer Lett. 2000 Nov 10;160(1):67-73.

Shinoura N, Sakurai S, Asai A, Kirino T, Hamada H.Caspase-9 transduction overrides the resistance mechanism against p53-mediated apoptosis in U-87MG glioma cells.Neurosurgery. 2001 Jul;49(1):177-86.

Shinoura N, Yoshida Y, Asai A, Kirino T, Hamada H. Relative level of expression of Bax and Bcl-XL determines the cellular fate of apoptosis/ necrosis induced by the overexpression of Bax. Oncogene. 1999 Oct 7;18(41):5703-13.

Shu HK, Julin CM, Furman F, Yount GL, Haas-Kogan D, Israel MA. Overexpression of E2F1 in glioma-derived cell lines induces a p53-independent apoptosis that is further enhanced by ionizing radiation. Neuro-oncol. 2000 Jan;2(1):16-21.

Shweiki D, Neeman M, Itin A, Keshet E. Induction of vascular endothelial growth factor expression by hypoxia and by glucose deficiency in multicell spheroids: implications for tumor angiogenesis. Proc Natl Acad Sci U S A. 1995 Jan 31;92(3):768-72.

Sigal A, Rotter V. Oncogenic mutations of the p53 tumor suppressor: the demons of the guardian of the genome. Cancer Res. 2000 Dec 15;60(24):6788-93. Review.

Simbulan-Rosenthal CM, Rosenthal DS, Luo R, Smulson ME. Poly(ADP-ribosyl)ation of p53 during apoptosis in human osteosarcoma cells. Cancer Res. 1999 May 1;59(9):2190-4.

Sionov RV, Moallem E, Berger M, Kazaz A, Gerlitz O, Ben-Neriah Y, Oren M, Haupt Y.c-Abl neutralizes the inhibitory effect of Mdm2 on p53.
J Biol Chem. 1999 Mar 26;274(13):8371-4.

Sjogren S, Inganas M, Norberg T, Lindgren A, Nordgren H, Holmberg L, Bergh J. The p53 gene in breast cancer: prognostic value of complementary DNA sequencing versus immunohistochemistry. J Natl Cancer Inst. 1996 Feb 21;88(3-4):173-82.

Slingerland JM, Benchimol S.Transforming activity of mutant human p53 alleles. J Cell Physiol. 1991 Sep;148(3):391-5.

Smith GC, Cary RB, Lakin ND, Hann BC, Teo SH, Chen DJ, Jackson SP. Purification and DNA binding properties of the ataxia-telangiectasia gene product ATM. Proc Natl Acad Sci U S A. 1999 Sep 28;96(20):11134-9.

Smith GC, Jackson SP. The DNA-dependent protein kinase. Genes Dev. 1999 Apr 15;13(8):916-34.

Sommers GM, Alfieri AA. Multimodality therapy: radiation and continuous concomitant cis-platinum and PKC inhibition in a cervical carcinoma model. Cancer Invest. 1998;16(7):462-70.

Sperandio S, de Belle I, Bredesen DE. An alternative, nonapoptotic form of programmed cell death. Proc Natl Acad Sci U S A. 2000 Dec 19;97(26):14376-81.

St Croix B, Sheehan C, Rak JW, Florenes VA, Slingerland JM, Kerbel RS.E-Cadherin-dependent growth suppression is mediated by the cyclin-dependent kinase inhibitor p27(KIP1). J Cell Biol. 1998 Jul 27;142(2):557-71.

Steel GG (1977) Basic theory of growing cell populations. In Growth Kinetics of tumours. Clarendon Press, Oxford, ch 2.

Stewart CL, Soria AM, Hamel PA. Integration of the pRB and p53 cell cycle control pathways. J Neurooncol. 2001 Feb;51(3):183-204.

Stewart DJ. The role of chemotherapy in the treatment of gliomas in adults. Cancer Treat Rev. 1989 Sep;16(3):129-60. Review.

Stott FJ, Bates S, James MC, McConnell BB, Starborg M, Brookes S, Palmero I, Ryan K, Hara E, Vousden KH, Peters G. The alternative product from the human CDKN2A locus, p14(ARF), participates in a regulatory feedback loop with p53 and MDM2. EMBO J. 1998 Sep 1;17(17):5001-14.

Strano S, Fontemaggi G, Costanzo A, Rizzo MG, Monti O, Baccarini A, Del Sal G, Levrero M, Sacchi A, Oren M, Blandino G.Physical interaction with human tumor-derived p53 mutants inhibits p63 activities.J Biol Chem. 2002 Mar 13 [epub ahead of print]

Strano S, Munarriz E, Rossi M, Cristofanelli B, Shaul Y, Castagnoli L, Levine AJ, Sacchi A, Cesareni G, Oren M, Blandino G.Physical and functional interaction between p53 mutants and different isoforms of p73.J Biol Chem. 2000 Sep 22;275(38):29503-12.

Strik H, Deininger M, Streffer J, Grote E, Wickboldt J, Dichgans J, Weller M, Meyermann R. BCL-2 family protein expression in initial and recurrent glioblastomas: modulation by radiochemotherapy. J Neurol Neurosurg Psychiatry. 1999 Dec;67(6):763-8.

Strobel T, Swanson L, Korsmeyer S, Cannistra SA. BAX enhances paclitaxel-induced apoptosis through a p53-independent pathway. Proc Natl Acad Sci U S A. 1996 Nov 26;93(24):14094-9.

Susin SA, Zamzami N, Castedo M, Hirsch T, Marchetti P, Macho A, Daugas E, Geuskens M, Kroemer G. Bcl-2 inhibits the mitochondrial release of an apoptogenic protease. J Exp Med. 1996 Oct 1;184(4):1331-41.

Sutherland RM, Carlsson J, Durand RE, Yunas J. Spheroids in cancer research. Cancer Res. 1981 Aug; 41: 2980-94.

Sutherland RM. Cell and Environment interactions in tumour microregions: the multicellular spheroid model. Science 1988; 240: 177-184.

Suzuki H, Tomida A, Tsuruo T. Dephosphorylated hypoxia-inducible factor 1alpha as a mediator of p53-dependent apoptosis during hypoxia. Oncogene. 2001 Sep 13;20(41):5779-88.

Tachibana O, Lampe J, Kleihues P, Ohgaki H. Preferential expression of Fas/APO1 (CD95) and apoptotic cell death in perinecrotic cells of glioblastoma multiforme. Acta Neuropathol (Berl). 1996 Nov;92(5):431-4.

Tachibana O, Nakazama H, Lampe J, Watanabe K, Kleihues P, Ohgaki H. Expression of Fas/APO-1 during the progression of astrocytoma. Cancer Research 1995; 55(23): 5528-30.

Tada M, Iggo RD, Ishii N, Shinohe Y, Sakuma S, Estreicher A, Sawamura Y, Abe H. Clonality and stability of the p53 gene in human astrocytic tumor cells: quantitative analysis of p53 gene mutations by yeast functional assay.Int J Cancer. 1996 Jul 29; 67(3):447-50.

Takimoto R, El-Deiry WS. Wild-type p53 transactivates the KILLER/DR5 gene through an intronic sequence-specific DNA-binding site. Oncogene. 2000 Mar 30;19(14):1735-43.

Tamaki M, McDonald W, Amberger VR, Moore E, Del Maestro RF. Implantation of C6 astrocytoma spheroid into collagen type I gels: invasive, proliferative, and enzymatic characterisations. J Neurosurg 1997; 87: 602-609.

Tanaka H, Arakawa H, Yamaguchi T, Shiraishi K, Fukuda S, Matsui K, Takei Y, Nakamura Y. A ribonucleotide reductase gene involved in a p53-dependent cell-cycle checkpoint for DNA damage. Nature. 2000 Mar 2;404(6773):42-9.

Terzis AJ, Thorsen F, Heese O, Visted T, Bjerkvig R, Dahl O, Arnold H, Gundersen G. Proliferation, migration and invasion of human glioma cells exposed to paclitaxel (Taxol) in vitro. Br J Cancer. 1997;75(12):1744-52.

Teutsch HF, Goellner A, Mueller-Klieser W. Glucose levels and succinate and lactate dehydrogenase activity in EMT6/Ro tumor spheroids. Eur J Cell Biol. 1995 Mar;66(3):302-7.

Thome M, Schneider P, Hofmann K, Fickenscher H, Meinl E, Neipel F, Mattmann C, Burns K, Bodmer JL, Schroter M, Scaffidi C, Krammer PH, Peter ME, Tschopp J. Viral FLICE-inhibitory proteins (FLIPs) prevent apoptosis induced by death receptors. Nature. 1997 Apr 3;386(6624):517-21.

Timiryasova TM, Chen B, Haghighat P, Fodor I.Vaccinia virus-mediated expression of wild-type p53 suppresses glioma cell growth and induces apoptosis. Int J Oncol. 1999 May;14(5):845-54.

Tohma Y, Gratas C, Van Meir EG, Desbaillets I, Tenan M, Tachibana O, Kleihues P, Ohgaki H. Necrogenesis and Fas/APO-1 (CD95) expression in primary (de novo) and secondary glioblastomas. J Neuropathol Exp Neurol. 1998 Mar;57(3):239-45.

Tonn JC, Kerkau S, Hanke A, Bouterfa H, Mueller JG, Wagner S, Vince GH, Roosen K. Effect of synthetic matrix-metalloproteinase inhibitors on invasive capacity and proliferation of human malignant gliomas in vitro. Int J Cancer. 1999 Mar 1;80(5):764-72.

Torvik A, Heding A. Histological studies on the effect of actinomycin D on retrograde nerve cell reaction in the facial nucleus of mice. Acta Neuropathol (Berl). 1967 Oct 20;9(2):146-57.

Trepel M, Groscurth P, Malipiero U, Gulbins E, Dichgans J, Weller M. Chemosensitivity of human malignant glioma: modulation by p53 gene transfer. J Neurooncol. 1998 Aug;39(1):19-32.

Tribius S, Pidel A, Casper D. ATM protein expression correlates with radioresistance in primary glioblastoma cells in culture.Int J Radiat Oncol Biol Phys. 2001 Jun 1;50(2):511-23.

Trump BF, Berezesky IK, Chang SH, Phelps PC. The pathways of cell death: oncosis, apoptosis, and necrosis. Toxicol Pathol. 1997 Jan-Feb;25(1):82-8. Review.

Trump BF, Berezesky IK. The reactions of cells to lethal injury: Oncosis and Necrosis- The role of calcium. In: Lockshin RA, Zakeri Z, Tilly JL, eds. When Cells Die (1998). New York; Wiley-Liss, Inc; 57-97.

Tsujimoto T, Mochizuchi S, Iwadate Y, Namba H, Nagai M, Kawamoto T, Sunahara M, Yamaura A, Nakagawara A, Sakiyama S, Tagawa M. The p73 gene is not mutated in oligodendrogliomas which frequently have a deleted region at chromosome 1p36.3. Anticancer Res. 2000 Jul-Aug;20(4):2495-7.

Tsutsumi-Ishii Y, Tadokoro K, Hanaoka F, Tsuchida N.Response of heat shock element within the human HSP70 promoter to mutated p53 genes.Cell Growth Differ. 1995 Jan;6(1):1-8.

Ueki K, Ono Y, Henson JW, Efird JT, von Deimling A, Louis DN. CDKN2/p16 or RB alterations occur in the majority of glioblastomas and are inversely correlated. Cancer Res. 1996 Jan 1;56(1):150-3.

Unger T, Mietz JA, Scheffner M, Yee CL, Howley PM.Functional domains of wild-type and mutant p53 proteins involved in transcriptional regulation, transdominant inhibition, and transformation suppression. Mol Cell Biol. 1993 Sep;13(9):5186-94.

Van Meir EG, Roemer K, Diserens AC, Kikuchi T, Rempel SA, Haas M, Huang HJ, Friedmann T, de Tribolet N, Cavenee WK. Single cell monitoring of growth arrest and morphological changes induced by transfer of wild-type p53 alleles to glioblastoma cells. Proc Natl Acad Sci U S A. 1995 Feb 14;92(4):1008-12.

Van Meyel DJ, Ramsay DA, Chambers AF, MacDonald DR, Cairncross JG. Absence of hereditary mutations in exons 5 through 9 of the p53 gene and exon 24 of the neurofibrin gene in families with glioma. Ann Neurol 1994; 35: 120-122.

Van Valen F, Fulda S, Truckenbrod B, Eckervogt V, Sonnemann J, Hillmann A, Rodl R, Hoffmann C, Winkelmann W, Schafer L, Dockhorn-Dworniczak B, Wessel T, Boos J, Debatin KM, Jurgens H. Apoptotic responsiveness of the Ewing's sarcoma family of tumours to tumour necrosis factor-related apoptosis-inducing ligand (TRAIL). Int J Cancer. 2000 Oct 15;88(2):252-9.

Veinot JP, Gattinger DA, Fliss H. Early apoptosis in human myocardial infarcts. Hum Pathol 1997;28:485-492.

Verhagen AM, Ekert PG, Pakusch M, Silke J, Connolly LM, Reid GE, Moritz RL, Simpson RJ, Vaux DL. Identification of DIABLO, a mammalian protein that promotes apoptosis by binding to and antagonizing IAP proteins. Cell. 2000 Jul 7;102(1):43-53.

Vogelbaum MA, Tong JX, Perugu R, Gutmann DH, Rich KM. Overexpression of bax in human glioma cell lines. J Neurosurg. 1999 Sep;91(3):483-9.

Vogelstein B, Kinzler KW. p53 function and dysfunction.Cell. 1992 Aug 21;70(4):523-6. Review.

Vogelstein B, Lane D, Levine AJ. Surfing the p53 network. Nature 2000; 408: 307-310.

Vogt M, Bauer MK, Ferrrari D, Schulze-Osthoff K. Oxidative stress and hypoxia/reoxygenation trigger CD95(APO-1/Fas) ligand expression in microglial cells. FEBs Lett 1998; 429(1): 67-72.

Waga S, Hannon GJ, Beach D, Stillman B. The p21 inhibitor of cyclin-dependent kinases controls DNA replication by interaction with PCNA. Nature. 1994 Jun 16;369(6481):574-8.

Walczak H, Miller RE, Ariail K, Gliniak B, Griffith TS, Kubin M, Chin W, Jones J, Woodward A, Le T, Smith C, Smolak P, Goodwin RG, Rauch CT, Schuh JC, Lynch DH. Tumoricidal activity of tumor necrosis factor-related apoptosis-inducing ligand in vivo. Nat Med. 1999 Feb;5(2):157-63.

Waleh NS, Brody MD, Knapp MA, Mendonca HL, Lord EM, Koch CJ, Laderoute KR, Sutherland RM. Mapping of the vascular endothelial growth factor-producing hypoxic cells in multicellular tumor spheroids using a hypoxia-specific marker.Cancer Res. 1995 Dec 15;55(24):6222-6.

Waleh NS, Gallo J, Grant TD, Murphy BJ, Kramer RH, Sutherland RM. Selective down-regulation of integrin receptors in spheroids of squamous cell carcinoma. Cancer Res. 1994 Feb 1;54(3):838-43.

Walenta S, Doetsch J, Mueller-Klieser W, Kunz-Schughart LA.Metabolic imaging in multicellular spheroids of oncogene-transfected fibroblasts. J Histochem Cytochem. 2000 Apr;48(4):509-22.

Walenta S, Dotsch J, Mueller-Klieser W. ATP concentrations in multicellular tumor spheroids assessed by single photon imaging and quantitative bioluminescence. Eur J Cell Biol. 1990 Aug;52(2):389-93.

Wang R, Xiao XQ, Tang XC.Huperzine A attenuates hydrogen peroxide-induced apoptosis by regulating expression of apoptosis-related genes in rat PC12 cells. Neuroreport. 2001 Aug 28;12(12):2629-34.

Wang XW, Vermeulen W, Coursen JD, Gibson M, Lupold SE, Forrester K, Xu G, Elmore L, Yeh H, Hoeijmakers JH, Harris CC. The XPB and XPD DNA helicases are components of the p53-mediated apoptosis pathway. Genes Dev. 1996 May 15;10(10):1219-32.

Waring P, Müllbacher A. Cell death induced by the Fas/Fas ligand pathway and its role in pathology. Immunol Cell Biol. 1999 Aug;77(4):312-7. Review.

Watanabe K, Tachibana O, Sata K, Yonekawa Y, Kleihues P, Ohgaki H. Overexpression of the EGF receptor and p53 mutations are mutually exclusive in the evolution of primary and secondary glioblastomas. Brain Pathol. 1996 Jul;6(3):217-23; discussion 23-4.

Watanabe K, Tachibana O, Yonekawa Y, Kleihues P, Ohgaki H. Role of gemistocytes in astrocytoma progression. Lab Invest. 1997 Feb;76(2):277-84.

Waters JS, Webb A, Cunningham D, Clarke PA, Raynaud F, di Stefano F, Cotter FE. Phase I clinical and pharmacokinetic study of bcl-2 antisense oligonucleotide therapy in patients with non-Hodgkin's lymphoma. J Clin Oncol. 2000 May;18(9):1812-23.

Wedge SR, Porteus JK, May BL, Newlands ES. Potentiation of temozolomide and BCNU cytotoxicity by O(6)-benzylguanine: a comparative study in vitro. Br J Cancer. 1996 Feb;73(4):482-90.

Weller M, Frei K, Groscurth P, Krammer PH, Yonekawa Y, Fontana A. Anti-Fas/APO-1 antibody-mediated apoptosis of cultured human glioma cells. Induction and modulation of sensitivity by cytokines. J Clin Invest. 1994 Sep;94(3):954-64.

Weller M, Rieger J, Grimmel C, Van Meir EG, De Tribolet N, Krajewski S, Reed JC, von Deimling A, Dichgans J. Predicting chemoresistance in human malignant glioma cells: the role of molecular genetic analyses. Int J Cancer. 1998 Dec 18;79(6):640-4.

Wester K, Bjerkvig R, Cressey L, Engebraaten O, Mork S. Organ culture of a glioblastoma from a patient with an unusually long survival. Neurosurgery. 1994 Sep;35(3):428-32; discussion 432-3.

Wharton SB, Hamilton FA, Chan WK, Chan KK, Anderson JR. Proliferation and cell death in oligodendrogliomas. Neuropathol Appl Neurobiol. 1998 Feb;24(1):21-8.

Wharton SB, McNelis U, Bell HS, Whittle IR. Expression of poly(ADP-ribose) polymerase and distribution of poly(ADP-ribosyl)ation in glioblastoma and in a glioma multicellular tumour spheroid model. Neuropathol Appl Neurobiol. 2000 Dec;26(6):528-35.

Whittle IR. Therapeutic approaches to primary and secondary brain tumours. Neuropathol Appl Neurobiol. 1996 Oct;22(5):424-9.

Wikstrand CJ, Reist CJ, Archer GE, Zalutsky MR, Bigner DD. The class III variant of the epidermal growth factor receptor (EGFRvIII): characterization and utilization as an immunotherapeutic target. J Neurovirol. 1998 Apr;4(2):148-58. Review.

Williams AC, Miller JC, Collard TJ, Bracey TS, Cosulich S, Paraskeva C. Mutant p53 is not fully dominant over endogenous wild type p53 in a colorectal adenoma cell line as demonstrated by induction of MDM2 protein and retention of a p53 dependent G1 arrest after gamma irradiation. Oncogene. 1995 Jul 6;11(1):141-9.

Wu GS, Burns TF, McDonald ER 3rd, Jiang W, Meng R, Krantz ID, Kao G, Gan DD, Zhou JY, Muschel R, Hamilton SR, Spinner NB, Markowitz S, Wu G, el-Deiry WS. KILLER/DR5 is a DNA damage-inducible p53-regulated death receptor gene. Nat Genet. 1997 Oct;17(2):141-3.

Wu J, Gu L, Wang H, Geacintov NE, Li GM. Mismatch repair processing of carcinogen-DNA adducts triggers apoptosis. Mol Cell Biol. 1999 Dec;19(12):8292-301.

Wu X, Bayle JH, Olson D, Levine AJ. The p53-mdm-2 autoregulatory feedback loop. Genes Dev. 1993 Jul;7(7A):1126-32.

Wylie AH. Cell death. A new classification separating apoptosis from necrosis. In : Bowen D, Lockshin RA, eds. Cell death in biology and pathology. London; Chapman and Hall, 1981; 209-242.

Wylie AH. The genetic regulation of apoptosis. Current Opinion in Genetics and Development 1995; 5: 97-104.

Wyllie AH, Golstein P. More than one way to go. Proc Natl Acad Sci U S A. 2001 Jan 2;98(1):11-3.

Wyllie AH. Apoptosis and carcinogenesis. Eur J Cell Biol. 1997(a) Jul;73(3):189-97. Review.

Wyllie AH. Apoptosis: an overview.Br Med Bull. 1997;53(3):451-65. Review.

Xiao ZX, Chen J, Levine AJ, Modjtahedi N, Xing J, Sellers WR, Livingston DM. Interaction between the retinoblastoma protein and the oncoprotein MDM2. Nature. 1995 Jun 22;375(6533):694-8.

Yap DB, Hsieh JK, Lu X. Mdm2 inhibits the apoptotic function of p53 mainly by targeting It for degradation. J Biol Chem. 2000 Nov 24;275(47):37296-302.

Yee D, Hao C, Cheung HC, Chen HT, Dabbagh L, Hanson J, Coupland R, Petruk KC, Fulton D, Roa WH. Effect of radiation on cytokine and cytokine receptor messenger-RNA profiles in p53 wild and mutated human glioblastoma cell lines. Clin Invest Med. 2001 Apr;24(2):76-82.

Yin C, Knudson CM, Korsmeyer SJ, Van Dyke T. Bax suppresses tumorigenesis and stimulates apoptosis in vivo.Nature. 1997 Feb 13;385(6617):637-40.

Yin XM. Signal transduction mediated by Bid, a pro-death Bcl-2 family proteins, connects the death receptor and mitochondria apoptosis pathways. Cell Res. 2000 Sep;10(3):161-7. Review.

Yokomizo A, Mai M, Bostwick DG, Tindall DJ, Qian J, Cheng L, Jenkins RB, Smith DI, Liu W. Mutation and expression analysis of the p73 gene in prostate cancer. Prostate. 1999 May;39(2):94-100.

Yonish-Rouach E, Resnitzky D, Lotem J, Sachs L, Kimchi A, Oren M. Wild-type p53 induces apoptosis of myeloid leukaemic cells that is inhibited by interleukin-6. Nature. 1991 Jul 25;352(6333):345-7.

Yu ZK, Geyer RK, Maki CG. MDM2-dependent ubiquitination of nuclear and cytoplasmic p53. Oncogene 2000; 19(51): 5892-5897.

Yuan J. Apoptosis in the nervous system. Nature. 2000 Oct 12;407: 802-809.

Yuan ZM, Huang Y, Whang Y, Sawyers C, Weichselbaum R, Kharbanda S, Kufe D. Role for c-Abl tyrosine kinase in growth arrest response to DNA damage. Nature. 1996 Jul 18;382(6588):272-4.

Yung WK, Prados MD, Yaya-Tur R, Rosenfeld SS, Brada M, Friedman HS, Albright R, Olson J, Chang SM, O'Neill AM, Friedman AH, Bruner J, Yue N, Dugan M, Zaknoen S, Levin VA. Multicenter phase II trial of temozolomide in patients with anaplastic astrocytoma or anaplastic oligoastrocytoma at first relapse. Temodal Brain Tumor Group. J Clin Oncol. 1999 Sep;17(9):2762-71.

Zagzag D, Zhong H, Scalzitti JM, Laughner E, Simons JW, Semenza GL. Expression of hypoxia-inducible factor 1alpha in brain tumors: association with angiogenesis, invasion, and progression. Cancer. 2000 Jun 1;88(11):2606-18.

Zauberman A, Flusberg D, Haupt Y, Barak Y, Oren M. A functional p53-responsive intronic promoter is contained within the human mdm2 gene. Nucleic Acids Res. 1995 Jul 25;23(14):2584-92.

Zhang H, Hannon GJ, Beach D. p21-containing cyclin kinases exist in both active and inactive states. Genes Dev. 1994 Aug 1;8(15):1750-8.

Zhang S, Endo S, Koga H, Ichikawa T, Feng X, Onda K, Washiyama K, Kumanishi T. A comparative study of glioma cell lines for p16, p15, p53 and p21 gene alterations. Jpn J Cancer Res. 1996 Sep;87(9):900-7.

Zhang XD, Franco A, Myers K, Gray C, Nguyen T, Hersey P. Relation of TNF-related apoptosis-inducing ligand (TRAIL) receptor and FLICE-inhibitory protein expression to TRAIL-induced apoptosis of melanoma. Cancer Res. 1999 Jun 1;59(11):2747-53.

Zhong H, De Marzo AM, Laughner E, Lim M, Hilton DA, Zagzag D, Buechler P, Isaacs WB, Semenza GL, Simons JW. Overexpression of hypoxia-inducible factor 1alpha in common human cancers and their metastases. Cancer Res. 1999 Nov 15;59(22):5830-5.

Zindy F, Eischen CM, Randle DH, Kamijo T, Cleveland JL, Sherr CJ, Roussel MF.Myc signaling via the ARF tumor suppressor regulates p53-dependent apoptosis and immortalization. Genes Dev. 1998 Aug 1;12(15):2424-33.

Zundel W, Schindler C, Haas-Kogan D, Koong A, Kaper F, Chen E, Gottschalk AR, Ryan HE, Johnson RS, Jefferson AB, Stokoe D, Giaccia AJ. Loss of PTEN facilitates HIF-1-mediated gene expression. Genes Dev. 2000 Feb 15;14(4):391-6.

Neuropathology and Applied Neurobiology (2001), **27**, 291–304

The development of necrosis and apoptosis in glioma: experimental findings using spheroid culture systems*

H. S. Bell, I. R. Whittle, M. Walker, H. A. Leaver and S. B. Wharton

Departments of Pathology and Clinical Neurosciences, University of Edinburgh, Western General Hospital, Edinburgh, Scotland

H. S. Bell, I. R. Whittle, M. Walker, H. A. Leaver and S. B. Wharton (2001) *Neuropathology and Applied Neurobiology*, **27**, 291–304

The development of necrosis and apoptosis in glioma: experimental findings using spheroid culture systems

Cell death in gliomas may occur either by apoptosis, or, in the case of high grade tumours, by necrosis, but questions remain as to the pathogenesis and relationship between these processes. The development of cell death was investigated in multicellular glioma spheroid cultures. Spheroids model the development of cell death due to diffusion gradients in a three-dimensional system without confounding influences of immune response, pressure gradients, etc. Spheroid cultures were established from four malignant glioma cell lines: U87, U373, MOG-G-CCM and A172; harvested from culture at weekly intervals and stained with Haematoxylin and Eosin (H&E), TdT-mediated dUTP-X nick end labelling (TUNEL) and by immunohistochemistry for vimentin, Glial Fibrillary Acidic Protein (GFAP) and Ki67. Annexin V flow cytometry and counts of apoptotic cells on H & E stained sections were performed to assess levels of apoptosis. Modes of cell death were also characterized by electron microscopy. Spatially separate zones of proliferation, differentiation and central cell death developed with increasing spheroid diameter. Central cell death developed at a predictable radius (300–400 μm) for each cell line. Ultrastructural examination showed this to be necrotic in type. Apoptosis was most reliably assayed by morphological counts using H & E. Basal levels of apoptosis were low (<0.5%), but increased with increasing spheroid diameter (>2% in U87). In particular, levels of apoptosis rose following development of central necrosis and apoptoses were most abundant in the peri-necrotic zone. There were quantitative differences in the levels of apoptosis and necrosis between glioma cell lines. The predictable onset of necrosis in the spheroids will allow us to investigate the pathogenesis of necrosis and events in prenecrotic cells. There is a relationship between the development of necrosis and apoptosis in this model and these processes can be separately assayed. Further *in vitro* and genetic studies will enable us to study these events and interactions in greater detail than is possible using other cell culture and *in vivo* systems.

Keywords: Glioma, spheroid, apoptosis, necrosis, TUNEL labelling, Annexin V

Introduction

The growth rate of tumours is dependent both on the rate of proliferation and on the rate of cell loss [41]. Cell loss due to the death of cells may occur due to either apoptosis or necrosis. Apoptosis is a process that often requires new gene transcription and the triggering of complex regulatory pathways [49]. In contrast, necrosis is sudden and accidental cell death brought on by a large stimulus sufficient to kill the cell and generate an inflammatory response. Necrotic cell death, sometimes referred to as oncotic necrosis, is characterized by membrane damage and energy depletion. Necrosis is generally regarded as an unregulated process which, in

Correspondence: Helen S Bell, Department of Clinical Neurosciences, Western General Hospital, Crewe Road, Edinburgh, EH4 2XU, Tel.: +44 (0131) 537 2551, Fax: +44 (0131) 537 2561, E-mail: hsb@skull.dcn.ed.ac.uk

*Presented in part at the XIVth International Congress of Neuropathology in Birmingham, April 2000. Abstracted in *Brain Pathology* 2000; 10 [4]: 731–732.

contrast to apoptosis, is not under genetic control [46]. However, necrosis is a poorly understood process and it is possible that there are regulatory mechanisms involved, perhaps separate from those involved in apoptosis [10].

Both apoptosis and necrosis are observed in glioma. Apoptotic bodies are observed in both high and low grade gliomas and apoptotic index generally increases with tumour grade. It tends therefore to be associated with more aggressive behaviour, although it has not been found to be of independent prognostic significance [13,31,38]. In the diffuse astrocytoma group of tumours, necrosis is associated with high grade tumours [2] and is a diagnostic feature to allow the categorization of an astrocytoma as glioblastoma multiforme [23]. In glioblastoma, there is emerging evidence that two distinct types of necrosis exist [22]. The first of these has an infarct-like pattern and is thought to be ischemic in origin. The second type observed is that of smaller areas of necrosis surrounded by pseudopallisading layers of tumour cells. It has been suggested that such areas may have evolved from small clusters of apoptotic cells [22]. Differences between these two types of necrosis have also been found in the perinecrotic tumour cells. Expression of Fas (CD95), a member of the TNF receptor superfamily which mediates some apoptotic signalling pathways, has been found particularly in cells around areas of ischaemic necrosis, whilst cells with apoptotic features are found particularly around pseudopallisaded necrosis [43]. These findings suggest that a relationship may exist between apoptosis and necrosis in glioma, although the relationship between the two is uncertain.

In contrast, there is some evidence to suggest that apoptosis and necrosis are independently regulated. Levels of apoptosis appear to vary according to tumour type [40]. Some CNS tumours, such as oligodendrogliomas and medulloblastomas, have higher apoptotic indices but do not necessarily contain areas of necrosis [38]. Levels of apoptosis and variations between tumour types are likely to be determined in part by the expression of various oncogenes [6,19]. In some systems, susceptibility to necrosis is inversely proportional to apoptosis [3]. In astrocytomas, it is unclear whether apoptosis and necrosis develop in parallel, or whether they are independently determined. It may be important to distinguish between these processes and their associated mechanisms when considering pro-apoptotic therapies.

A number of *in vitro* and *in vivo* models have been developed to study the characteristics of glial tumour cell growth [7,8,16,39]. Monolayer and cell suspension systems are of great value when assessing detailed cell function and studying regulation of apoptosis, but they do not reconstruct the cellular microenvironments present within a tumour cell mass and there are no simulated nutrient gradients. In addition, many *in vitro* models are limited in the study of cell death in that they do not model necrosis. The spheroid system for cell culture is a three-dimensional (3-D) model which creates areas of proliferation, differentiation and cell death within a tumour cell mass [26,42,44]. These areas can be studied individually when the spheroid becomes larger and a nutrient gradient forms across the radius of the spheroid. Brain tumour spheroids have been used to test the response of tumour cells to various therapeutic stimuli within the 3-D tumour cell mass and the invading cell population [5,37]. Many studies have reported the presence of a central area of necrosis within the glial cell spheroids and some groups have examined responses of these oxygen deprived cells [34,35]. However, the exact mechanisms resulting in this area of cell death remain unclear.

The aim of this study was to develop the spheroid model to study the pathogenesis of cell death in glioma. Multicellular tumour spheroids were derived from four different human glioma cell lines, U87, U373, MOG-G-CCM and A172, which have different molecular genetic alterations [20]. It was hypothesized that this model would allow spatial separation of zones of proliferation, differentiation and cell death. The study objectives were: (I) to determine how cell death occurs in glioma spheroids; is it necrotic or apoptotic? (II) to determine the time course of development of central cell death and how levels of apoptosis vary with time and size (III) to establish the best means of quantifying both apoptosis and necrosis in this model, with the aim of comparing cell lines with different genetic backgrounds (IV) to determine the relationship between apoptosis and necrosis within the spheroids.

Methods

Cell culture

Four human glioma cell lines derived from anaplastic astrocytoma or glioblastoma multiforme (GBM) were

used in this study: A172, MOG-G-CCM, U373, and U87. All cell lines were supplied by the European Collection of Cell Cultures, CAMR, Salisbury, UK. They were grown in monolayer in Dulbecco's Modified Eagles Medium (DMEM) supplemented with 10% foetal calf serum (FCS), penicillin and streptomycin (all from GibcoBRL, Life Technologies, Paisley, Scotland).

Spheroid formation

Once the monolayer cultures became confluent the cells were trypsinized and seeded into spinner culture flasks at a density 3×10^6 cells/100 ml of medium (DMEM with 10% FCS), and spun at 180 r.p.m. for 5 weeks (previously described in Bell *et al.* 1999 [6]). Approximately 200 spheroids from each cell line were removed from culture at weekly intervals, 50% of these were used for flow cytometry and 50% for paraffin embedding following fixation. 5 μm sections were then cut for H & E (haematoxylin and eosin) staining, immunohistochemistry and TUNEL labelling. 30–40 spheroids were also removed at these time points for EM processing.

Immunohistochemistry

All immunohistochemistry was performed using the standard immunoperoxidase protocol. The three antibodies used were Glial Fibrillary Acidic Protein (GFAP) (DAKO Ltd, Cambridgeshire, UK, dilution 1 : 1000), Ki67 (Novocastra Ltd, Vector Laboratories Ltd, Peterborough, UK, dilution 1 : 200) and Vimentin (DAKO Ltd, dilution 1 : 200). The slides to be stained with Vimentin and Ki67 were first microwaved in a citrate buffer for 15 min. The secondary antibodies used were swine antirabbit (DAKO Ltd) for GFAP and goat antimouse (Vector Laboratories Ltd) for Ki67 and Vimentin. The avidin-biotinylated enzyme complex used was a vector elite kit (Vector Ltd). The stain was visualized using diaminobenzidine tablets (Sigma-Aldrich Company Ltd, Poole, Dorset, UK), then the sections were counterstained with haematoxylin and examined using light microscopy.

TUNEL labelling

TUNEL (TdT-mediated dUTP-X nick end labelling) labels DNA strand breaks which occur during early apoptosis [28]. Spheroid sections were dewaxed, rehydrated as above and incubated with proteinase K for 20 min at a concentration of 20 μg/ml in 10 mM/HCl, pH 7.6. After washing in PBS, the sections were incubated in TUNEL reaction mixture (TdT-mediated dUTP-X nick end labelling). This was followed by the addition of a secondary detection system that contained a biotinylated antibody to enable visualization of the fluorescent markers for light microscopy (instructions as described for *in-situ* Cell detection kit, AP from Boehringer Mannheim Roche Diagnostics Ltd, Leines, East Sussex). Once the substrate was added (5-Bromo-4-Chloro-3-Indolyl Phosphate/Nitro Blue Tetrazolium Tablets (BCIP/NBT) from Sigma) the sections were washed, dehydrated, counterstained and mounted as above.

Light microscopy

The sections were examined using light microscopy and the regional staining patterns of TUNEL, Ki67, GFAP and vimentin staining were recorded photographically. The slides stained with H & E were used to measure the radius of the spheroids for each cell line at each given time point using a graticule. The 10 largest spheroids were measured on each slide and the average taken. These sections were also used to establish the time point for each cell line when a central area of cell death first appears. The number of cells per spheroid were also counted to determine spheroid packing density. This was done using a specially designed graticule (Graticules Division, Pyser-SGI Ltd, Edenbridge, UK), to count individual segments of each spheroid examined. A segment representing 10% of the area of each spheroid was counted and the 10 largest spheroids (as above) from each slide were chosen. Morphological apoptotic counts were also recorded using H & E stained sections in the technique mentioned in the previous sentence. An apoptotic index was determined for each cell line as a percentage of total cell counts per spheroid (AI).

Electron microscopy (EM)

Spheroids derived from the four cell lines at each time point were fixed for 2 h at 4°C in 3% glutaraldehyde in 0.1 M Sodium Cacodylate/HCl buffer pH 7.2–7.4. They were then washed 3 times in double distilled water for 20 min and fixed for 45 min in 1% osmium tetroxide. Following dehydration to 100% ethanol, the spheroids were submerged in propylene oxide for 30 min

then left overnight in Emix resin (Taab Laboratories, Aldermaston, Berks, UK) at room temperature. Once the spheroids had polymerized (20 h at 70°C), 90 nm sections were cut with a glass knife on a Reichert OMU2 microtome and mounted on 300 mesh copper grids. The sections were then stained by the Uranyl Acetate/Lead Citrate method and examined using a Jeol 100 CXII transmission electron microscope with an operating voltage of 60 KV. Photographs were taken using Kodak 4489 film and developed using a Ilford P & Q Universal developer (Ilford Imaging UK Ltd, Mobberley, Cheshire, UK) on Ilford Multigrade glossy photographic paper. Spheroids derived from each cell line at each time point were assessed and photographed. The ultrastructural types of cell death observed in week three spheroids were morphologically and quantatively assessed in a single spheroid for each of the cell lines.

Flow cytometry

At weekly intervals, the spheroids were disaggregated following centrifugation (3000 *g* for 5 min) in universal tubes using trypsin (0.5 g trypsin and 0.2 g EDTA in 250 ml PBS) in a water bath at 37°C for 5 min. To avoid membrane damage, cycles of resuspension were used to break down spheroids from weeks 4–5. 10 mls of DMEM (containing 10% FCS, as above) was then added to each tube to inhibit the action of the trypsin. The cells were then centrifuged again, the supernatent removed and the cells suspended in 100 µl of Annexin V/propidium iodide solution (Boehringer Mannheim – see instructions for methods) for 15 min at room temperature. 400 µl of PBS was then added and the resulting cell suspensions were analysed using a Coulter EPICS XL flow cytometer (Beckman Coulter Ltd, High Wycombe, Buckinghamshire, UK) with EPICS XL-MCL System II software (Beckman Coulter Ltd, High Wycombe, Buckinghamshire, UK). This identified apoptotic and necrotic cells on the basis of side scatter and fluorescence associated with Fluorescein-labelled Annexin V and propidium iodide [12]. In the early stages of apoptosis, phosphatidyl serine residues flip to the external side of the cell membrane. These can be labelled with the Annexin V probe. The cell membranes of necrotic cells become permeabilized early on, allowing the entry of both the Annexin V probe and propidium iodide. The combination of high Annexin V labelling with low propidium iodide labelling indicates an apoptotic cell, whilst high labelling for both Annexin and Propidium iodide indicates a necrotic cell.

Statistics

A split plot analysis of variance (ANOVA) was used to assess *in situ* cell counts and apoptotic index results. To analyse the former, a null hypothesis was set up where 'the total number of cells per spheroid remains the same between cell lines over time'. After finding that Mauchly's test of sphericity was significant, the *F*-ratio was obtained using the new degrees of freedom calculated using the Huynh-Fel Epsilon value. In order to analyse the distribution of apoptotic index over time, a null hypothesis was set up where 'the apoptotic index of each spheroid remains the same between cell lines over time'. After finding that Mauchly's test of sphericity was significant, again the *F*-ratio was obtained using the new degrees of freedom calculated by using the Huynh-Fel Epsilon value.

Results

Phenotypic characterization of the spheroid system

Positive GFAP staining in all 4 cell lines (MOG-G-CCM, U87, U373, A172) in monolayer culture confirmed their glial nature. In spheroid cultures the staining pattern varied from weeks 1–5. At week one, GFAP positive cells were diffusely scattered across the radius of the spheroid (Figure 1**a**). As the spheroids became larger at week 2, GFAP labelling was observed in the centre of the spheroids (Figure 1**c**). By week four GFAP positive cells were found in a ring around the centre of the spheroid

Figure 1. Light micrographs showing various immunohistochemical staining patterns in U87 cell lines over weeks 1–5. (**a**), Week 1 spheroids showing random GFAP labelling across the radius. (**c**), Central GFAP staining pattern at week 2. (**e**), Ring of GFAP positivity around the spheroid centre at week 4. (**b**), Random distribution of Ki67 labelling across the radius at week 1. (**d**), Localization of Ki67 around the spheroid periphery at week 2. (**f**), Week 4 spheroids show no Ki67 labelling centrally, but a very high peripheral index. (**g**), Central TUNEL positivity in week 4 spheroids, note the absence of TUNEL labelling in some apoptotic cells (arrow) and positively labelled central necrotic tissue. (**h**), H & E showing central areas of necrosis (right) surrounded by apoptotic figures (left) at week 4. All bars = 100 µm.

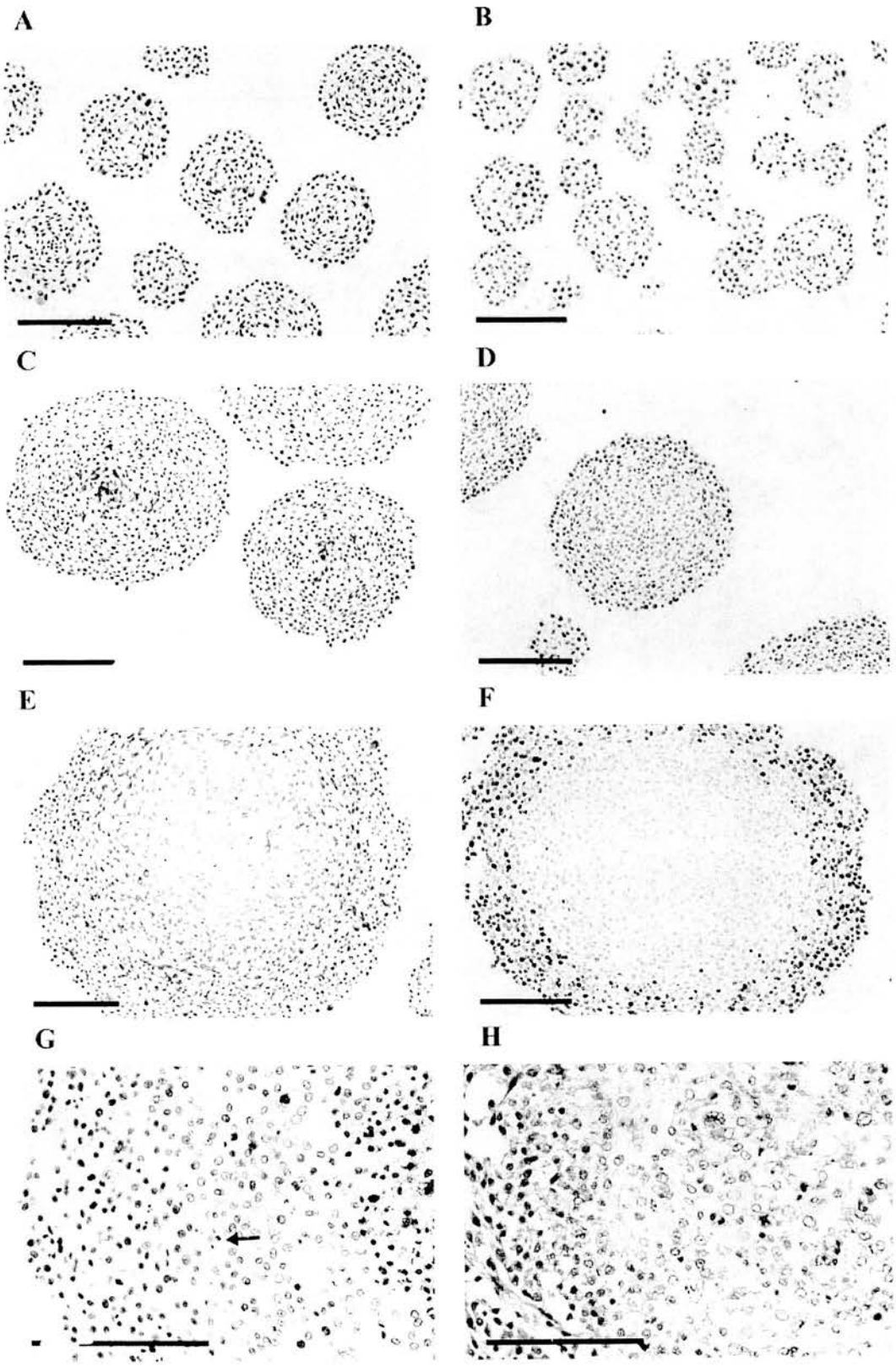
A
B
C
D
E
F
G
H

(Figure 1e), with loss of staining in the spheroid centre and no labelling of the outer proliferating cells. This pattern was the same in all four cell lines examined. The antibody against human vimentin demonstrated a similar pattern to GFAP although the staining was much fainter. At week one the Ki67 antibody labelled cells randomly across the radius of the spheroids in a similar pattern to GFAP with a nuclear pattern of staining (Figure 1b). However, by week 2 Ki67 was confined to the perimeter of the spheroids and no positive cells were observed in the centre (Figure 1d & f). This proliferative rim was approximately 100 μm wide and was consistent in all of the cells lines examined.

Ultrastructural examination of individual spheroids revealed that the cells formed intermediate junctions and became closely packed together as the spheroids became larger (Figure 3a). This was particularly apparent within the viable rim at weeks 3–4. The cells around the periphery of the spheroid became polarized with the nucleus basally situated towards the spheroid centre (Figure 3b).

Glioma spheroid growth kinetics

The four cell lines showed similar growth rates when grown as spheroids (Figure 2a). At the end of the first week, the spheroids had a radius of approximately 50 μm. This increased over 4 weeks until the radius of the spheroids reached approximately 500 μm. On average, A172 spheroids were slightly larger than the other three cell lines but this was not statistically significant. Between weeks 1 and 3 the cell counts remained low (below or around 2000 cells/spheroid). This was followed by a huge increase in cell number from weeks 3–4 (Figure 2b). By week 5 the cell numbers had levelled at approximately 10 000 cells per spheroid (Figure 2b). There were differences in cell number over time between cell lines. A172 spheroids contained the largest number of cells over the 5-week period compared to the other three cell lines ($P<0.001$) with a maximum cell number of 14 000 cells at week 5. This was due to reduced cell loss in the A172 cell line. There was no significant difference ($P>0.05$) in cell numbers between U87, MOG-G-CCM and U373 cell lines. Cell packing density dropped over weeks 1–3 in each cell line as the cells became more loosely packed within the spheroid mass (as observed under EM), but increased from weeks 4–6 as the cells became very tightly packed around the spheroid periphery (Figure 2c). There was a slight increase in packing density in week 5 spheroids derived from the A172 cell line compared to the other cell lines at week 5. This was due to the lack of cell death in the spheroid centre (Figure 2d). As packing density was relatively similar between cell lines, it was not thought to influence the onset of cell death in this model.

The qualitative distribution of cell death in glioma spheroids

Central cell death developed over week 3 in all four cell lines (Figure 2e), although the extent of necrosis varied considerably between lines (Figure 2d). Thus necrosis could be accurately predicted at a certain time point and size for each cell line. By week 5 the areas of necrosis were very large in 3 of the 4 cell lines, U87, MOG-G-CCM and U373 (Figure 2d). A172 exhibited a different pattern of necrosis, where the percentage of the radius that was necrotic over weeks 3–4 did not increase above 10% (Figure 2d).

Using week 3 spheroids it was possible to identify three morphological types of cell death using electron microscopy. The first type was characterised by large swollen cells, dilation of organelles and break up of the cell membrane, features typical of necrosis (Figure 3c). The second type was characteristic of apoptosis: electron dense cells (resulting from cell shrinkage), condensation of chromatin, nuclear fragmentation and a convoluted cell membrane (Figure 3d). A distinct pattern of cell death emerged with necrotic cells in the spheroid centre surrounded by apoptotic cells (Figure 1g & h). This pattern was present in all of the cell lines examined.

Figure 2. Graphs showing the growth characteristics of U373, U87, MOG-G-CCM and A172 cell lines when grown as spheroids. (a), Length of spheroid radius over time for each cell line.(b), Number of cells per spheroid for each cell line over time. (c), Packing density for each spheroid derived from each cell line over time (number of cells per mm^2). (d), Extent of necrosis in each cell line over time, i.e. the percentage of the radius consisting of necrotic cells. (e), Graph showing the percentage of spheroids (derived from all four cell lines) containing areas of necrosis over weeks 1–5. (f), Number of observed apoptotic figures per spheroid over time for each cell line. $n=10$ for each point on the above graphs. Error bars are shown.

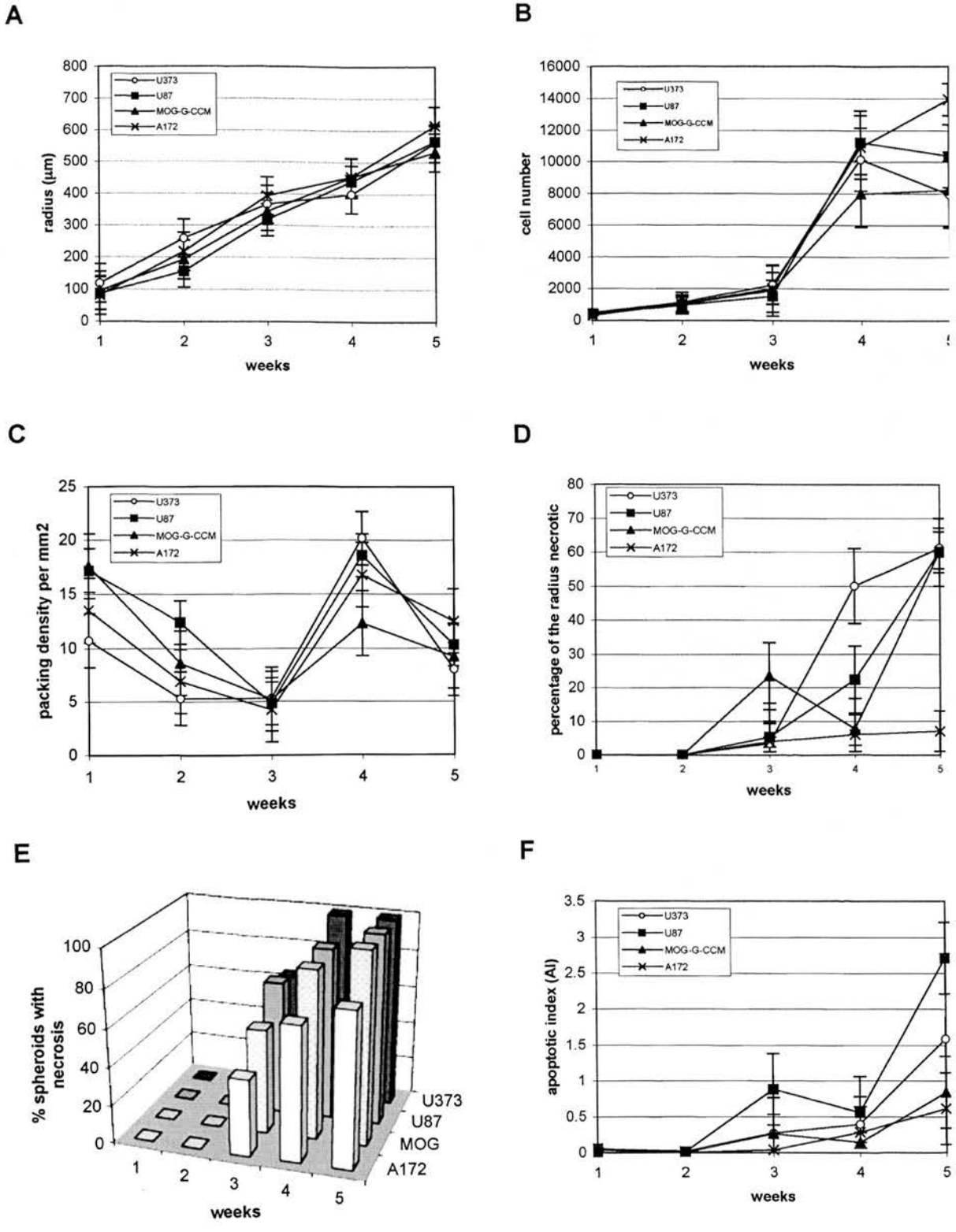
A
radius (µm)
weeks
U373
U87
MOG-G-CCM
A172
B
cell number
weeks
C
packing density per mm2
weeks
D
percentage of the radius necrotic
weeks
E
% spheroids with necrosis
weeks
U373
U87
MOG
A172
F
apoptotic index (AI)
weeks

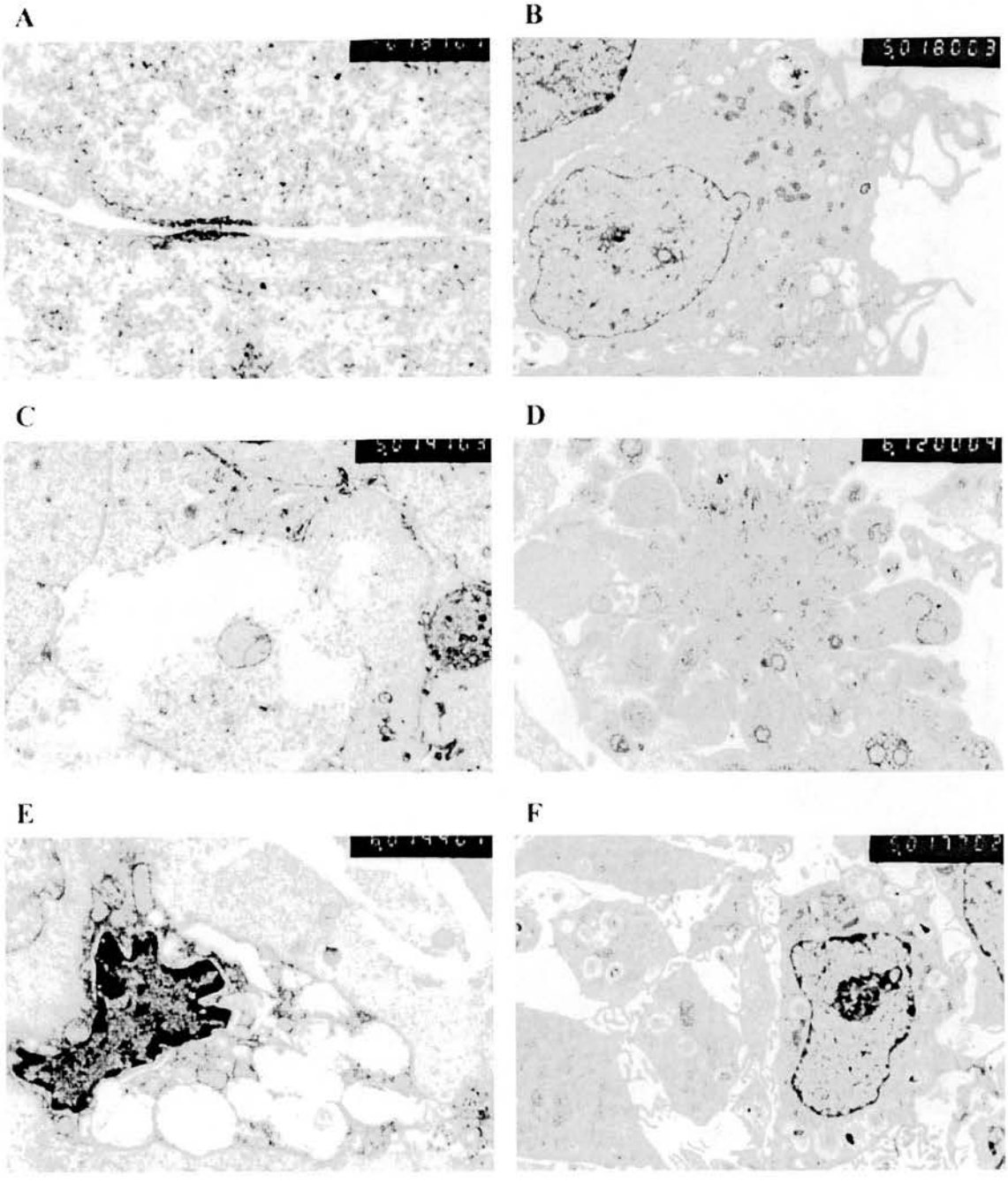

Figure 3. Electron micrographs showing the ultrastructural changes that occur when glioma cell lines are grown as spheroids. (a). An intermediate junction formed between adjacent cells in A172 cell line (× 51 000). (b). Cell showing evidence of nuclear polarization and autophagic activity (MOG-G-CCM). (c). A necrotic cell (A172). (d). An apoptotic cell (U373). (e). Vacuolar cell death (U87). (f). The autophagic phenotype (MOG-G-CCM). (b). (c). (d). (e) & (f): × 16 000.

A third type of cell death observed was termed 'vacuolar cell death'. Here, the cells contained huge vacuoles, which often appeared to arise from the dilation and fusion of organelles. The cytoplasm was very electron dense and the cell membrane appeared to be intact, although in some instances a slight 'blebbing' effect was observed (Figure 3e). In addition, an autophagic pattern of cell injury was identified (Figure 3f). This phenotype was present in all of the cell lines to some extent, but was particularly prevalent in the MOG-G-CCM cell line. These cells contained lysosomal vacuoles, often containing myelin whorls or fragments of organelles. In addition, these cells were often slightly more electron dense than normal cells, although it is unclear whether this is due to cell shrinkage. In the MOG-G-CCM cell line, some cells in the proliferative zone exhibited this phenotype.

TUNEL labelling was present in the centre of week 3–5 spheroids in all of the cell lines (Figure 1g). These were cells which had been ultrastructurally shown to have a necrotic pattern of cell death. Scattered cells within the viable rim and zone of differentiation were also observed, although there was a sharp decline in TUNEL labelling from the centre of the spheroid to the periphery. Close examination using high-power light microscopy revealed that many apoptotic cells around the spheroid centre were not TUNEL positive. For this reason, the TUNEL results were not quantitively assessed.

Quantitative distribution of apoptosis and necrosis in glioma spheroids

Ultra structural examination by means of electron microscopy meant that week 3 spheroids could be quantitatively assessed using the cell death classification criteria described below (Table 1). A172 demonstrated the largest proportion of necrotic cells, and U87 demonstrated the greatest proportion of apoptotic cells. The vacuolar morphology was observed most frequently in U87, and autophagic cells were observed most frequently in MOG-G-CCM cell line.

Morphological counts of apoptotic cells using H & E stained sections showed that at weeks 1–2 the apoptotic index was nearly zero for all of the cell lines studied. This index increased at week 3, when the central core of cells had begun to necrose. By week 5, the apoptotic index ranged from 0.6% in A172 cell line to 2.75% in U87 cell line (Figure 2f). Statistical analysis revealed that U87 had a significantly higher apoptotic index over time than the other 3 cell lines ($P<0.001$) and A172 had a significantly lower apoptotic index than U373 and U87 cell lines ($P<0.001$). These results supported the above quantities observed using electron microscopy (Table 1).

To further quantify apoptosis and necrosis in glioma spheroids, Annexin V flow cytometry was employed. Although this method confirmed an increase in the proportion of non-viable cells present in spheroids over time, it could not distinguish between apoptosis and necrosis in many of the cells derived from larger spheroids. It is possible that the trypsinization process required for disaggregation was too aggressive, causing semi-permeablization of the cell membranes of some non-necrotic cells that allowed the entry of propidium iodide. Monolayer experiments using the same techniques showed valid apoptotic cell populations, suggesting that the high trypsin concentrations required for spheroid disaggregation might be the reason for the lack of an apoptotic cell population in these experiments. Morphologically, viable and non-viable cells in spheroid

Table 1. Quantitative assessment of cell death morphologies observed using EM

	Type of Death			
	Apoptosis	***Necrosis***	***Autophagic***	***Vacuolar***
	Chromatin condensation	*Swollen cell*	*Lysosomes containing*	*Dilation of ER*
	Blebbing	*V. pale cytoplasm*	*myelin/organelles*	*Empty vacuoles*
Cell line	*Nucleus disrupted first*	*Damaged cell membrane*	*Some blebbing*	*Cell membrane breaks rare*
MOG	11	21	4	4
U87	52	35	5	18
U373	37	46	2	8
A172	6	67	2	0

cell populations were distinguished by their laser scatter characteristics. Two distinct populations with different forward- and side-scatter were observed in disaggregated spheroid cell populations. The Annexin V labelling in the total cell populations was approximately 2% for week 2 spheroids derived from each cell line. For week 4 spheroids, 6% Annexin V labelling was observed for week 4 spheroids derived from the cell lines MOG, U87 and U373 and 3% Annexin V labelling for week 4 A172 spheroids.

Discussion

The development of cell death in a multicellular tumour spheroid model of human glioma was studied. The study demonstrated that:

1. the spheroids show spatially distinct regions of proliferation, differentiation and cell death;
2. the central area of cell death is necrotic in nature;
3. central necrosis develops at a predictable radius for each cell line;
4. apoptosis occurs mainly in peri-necrotic cells;
5. apoptosis increases with spheroid radius, particularly after necrosis has developed; and
6. there are differences between the cell lines with respect to susceptibility to apoptosis and necrosis, and in the relative proportions of each.

Glioma spheroid characterization

Certain criteria were initially established to justify the use of this system to study specific interactions usually only found *in vivo*. Spheroid cultures derived from glioma cell lines contained regionally distinct areas of proliferation, differentiation and cell death. GFAP staining confirmed the glial nature of the cell lines. Expression of GFAP was observed in an intermediate zone between the spheroid centre and the spheroid periphery. The outer proliferative zone did not express GFAP. This is consistent with reports that GFAP is rarely expressed in cycling cells in human glioma *in situ* [15]. GFAP expression was lost from the spheroid centre as an area of cell death developed. GFAP is generally expressed when cells leave the cell cycle, become larger and extend their processes [14]. It is not clear whether the expression of GFAP in this model is due to a stress response [27] or a reflection of differentiation. The layer of GFAP positive cells was termed the area of 'differentiation'.

Ultrastructural study of the spheroids over time showed distinct cellular morphologies. The peripheral cells showed evidence of polarization, characterized by a basally located nucleus and the cytoplasm contained many microvilli which extended into the medium. Intermediate junctions were observed between cells as the spheroids became larger, similar to those found *in vivo* [9]. It was probable that together with the entangling of the cell processes, these junctions held the cells within the spheroids tightly together.

The spheroids derived from the four cell lines showed similar growth characteristics. All four cell lines showed identical patterns of proliferation. Ki67 positivity was restricted to an outer zone of 100 μm in width, thus implying that the cell lines required similar metabolic requirements in which to stimulate proliferation around the nutrient-rich periphery of the spheroids. Within the proliferative zone, virtually all cells were Ki67 positive. Because the diameter of the proliferative zone was limited to 100 μm, the ratio of the proliferative zone to total volume decreased as the volume of the spheroid increased. The consequent decline in growth fraction would itself therefore contribute to the slowing of overall growth at high volumes in spheroids, as in solid tumours [45]. The diameter of the proliferative zone itself may well be a reflection and measure of the ability of tumour cells to proliferate under conditions of increasing stress. Thus, together with the cell death response, ability to proliferate under stress may be another way by which the tumour cell response to stress determines the growth characteristics of the tumour.

When examining the behaviour of the spheroids overall, it is clear that when grown in a 3-D environment, the cells become more closely associated and behave differently to monolayer cultures. There is evidence to suggest that cells grown in 3-D culture produce different growth factors than in monolayer cultures [32]. In monolayer culture, the cellular morphologies of the four cell lines are very different (H S Bell, unpublished data), but in 3-D culture, they exhibit very similar behaviour patterns. Although onset and extent of cell death differs between cell lines in 3-D culture, the number of observed apoptotic figures and nonviable cells in spheroid culture is not reflected in monolayer culture (HS Bell, unpublished data), thus confirming the need for such a 3-D system to study these processes. In addition, the spheroid system allows the study of cellular interactions within pure glial tissue. Cell death in this system is not a result of any

immunological or inflammatory response such as those found *in vivo*.

Development of cell death in glioma

The pathogenesis of cell death in glioma remains unclear. The predictable onset of cell death in this model has allowed us to examine the earliest structural changes present in the central regions of brain tumour spheroids as they become larger and the centre becomes nutrient depleted. These can be directly compared to similar situations *in vivo*. Ultrastructural examination of the spheroids at 3 weeks, when the centres are metabolically stressed, revealed the presence of both apoptotic and necrotic cells in a particular pattern. In all four cell lines cell death in the centre of the spheroids was necrotic in type. Apoptotic cells surrounded this area and decreased in number towards the spheroid periphery. The cells within the central area of cell death were labelled with the TUNEL reaction, despite the fact that death in this area was proven ultrastructurally to be necrotic. The TUNEL method has previously been shown to lack specificity, in that it may label necrotic as well as apoptotic cells [17,18]. In our system too, TUNEL lacked the ability to discriminate between different cell death patterns. It may also label very actively transcribing nuclei [25].

It was hypothesized that the area of central cell death might arise by apoptosis rather than necrosis. Sublethal injury may induce apoptosis in a variety of settings including hypoxic states *in vivo* [4,36] and in cell lines grown in monolayer culture [30]. In the case of the spheroid model, the slowly increasing stress associated with increasing diameter might initially be expected to produce a sublethal insult. However, we found no evidence to support this contention, the central area of cell death appears necrotic at the earliest time point, although admixed cells with apoptotic morphology were seen. There is emerging evidence that apoptosis and necrosis are not entirely distinct processes, but may coexist, with the energy status of the cell determining whether apoptosis or necrosis occurs [29,33]. Thus, an initially apoptotic process might become necrotic. Such a pattern has been documented in human and experimental myocardial infarction [1,21,48]. A very early apoptotic phase preceding necrosis cannot be entirely excluded in our model, but certainly completion of cell death for most of the central cells is necrotic in type, indicating that central energy depletion rapidly becomes too severe to allow an apoptotic mode of death.

Although variations existed between cell lines, nearly all the apoptotic cells observed within the spheroids were surrounding the central area of necrosis. This could be a result of sublethal injury to these cells as the radius of the spheroid became larger. However, this seems unlikely as apoptosis was not stimulated to any great extent when the central regions of prenecrotic spheroids were subjected to a similar stress. It is likely that necrotic tissue in the centre of the spheroids may have stimulated an apoptotic response in surrounding cells, suggesting the presence of a relationship between the two processes. Products of phospholipase degradation of membranes and reactive oxygen intermediates released during necrosis [28] are possible candidate pro-apoptotic agents. This is supported by the increase in the number of apoptotic figures observed elsewhere within the tumour cell mass from weeks 3–5, after areas of necrosis have formed. Whereas the apoptotic index was nearly zero from weeks 1–2, the index rose rapidly following the onset of necrosis.

Ultrastructural examination revealed two other cell injury morphologies. In one process, termed 'vacuolar cell death', the cell cytoplasm contained huge vacuoles, which often appeared to arise from the dilation and fusion of organelles. The cytoplasm was very electron dense and the cell membrane appeared to be intact, although in some instances a slight 'blebbing' effect was observed. Some of the features appeared intermediate between classical apoptotic and necrotic morphologies, consequently it was difficult to classify this form of cell death. Vacuolar cell death patterns were mostly associated with the U87 cell line and were observed mainly in the centre of the spheroid admixed with necrotic cells. Another phenotype that was particularly prevalent in the MOG-G-CCM cell line was characterized by the presence of abundant myelin-like membrane whorls within the cytoplasm. It was unclear whether this autophagic pattern was an injury response which would eventually lead to the death of the cells concerned, as many of the cells around the periphery of the spheroids derived from MOG-G-CCM cell line also expressed this autophagic pattern as well as cells towards the centre. Varying cell death morphologies, in addition to classical apoptosis and necrosis, have been observed in other systems. These include vacuolar and autophagic patterns of cell death in developing neurones

[10]. The significance of the varying morphological patterns which we have observed in the spheroid model suggests that there may be other mechanisms and/or intermediate phenotypes involved in cell death in glioma besides those of necrosis and apoptosis.

Quantitative comparison of cell death between cell lines

The group of tumours classed as GBM vary in terms of both histological appearance and genetic background. Differences in the molecular genetics of gliomas range from *p53* mutations resulting in the accumulations of other mutations in secondary GBM, to EGFR amplification having a central role in the development of *de novo* tumours [11]. These differences result in equally aggressive and morphologically similar cancers [24]. Therefore, the development of cell death in spheroids derived from cell lines with differing genetic backgrounds was compared in this study [20,47].

Differences in the susceptibility to cell death between cell lines started to become apparent at week 3. Although central cell death appeared in all of the cell lines at this time point, the spheroids varied in size. For example, the A172 cell line had an average radius of nearly 400 μm whereas U87 cell line had a average radius nearer 300 μm. These measurements are crucial as the spheroid radius is the limiting factor for the passage of metabolites from the spheroid periphery to the centre.

Apoptotic index over time was measured using 3 techniques: morphological counts using H & E stained sections, TUNEL labelling and Annexin V flow cytometry. Using H & E stained sections, significant differences in apoptotic index between cell lines were observed. Between weeks 1 and 2 the apoptotic index in all of the cell lines was nearly zero but by week 3, U87 spheroids had significantly more apoptotic figures than the other three cell lines. U373 and MOG-G-CCM cell lines had intermediate levels of apoptosis. A172 had the least number of apoptotic figures over time and this was confirmed by the ultrastructural data at week 3. Annexin V flow cytometery reflected these results in terms of cell viability i.e. U87, MOG-G-CCM and U373 lines had significantly larger non-viable cell populations over time compared to the A172 cell line. However, it could not distinguish accurately between apoptotic and necrotic cell populations due to membrane damage during trypsin disaggregation. As TUNEL was not accurate in labelling all of the observed apoptotic figures present and often labelled necrotic cells as well as apoptotic cells, H & E stained sections of paraffin embedded spheroids proved to be the best method of quantifying cell death in glioma spheroids.

The extent of central necrosis varied between cell lines over time. At week 3, A172 cell line had a relative excess of necrotic cells compared to apoptotic cells and other cell death morphologies. However, as the spheroids became larger, this small number of necrotic cells ($<10\%$ of the radius) did not increase in size as was observed with the spheroids derived from the other cell lines ($>50\%$), nor was there any observed increase in apoptotic index. Therefore, A172 showed an overall decrease in susceptibility to cell death compared to the cell lines U373, MOG-G-CCM and U87, and this was reflected in terms of apoptotic index and the extent of necrosis. This reinforced the earlier evidence suggesting that necrosis may play a role in the stimulation of apoptosis in this model. It certainly implies that inducible apoptosis in the glioma spheroid system does not occur independently of necrosis. When these results were compared to the genotypic characterizations made by Van Meir *et al.* [27], there was little correlation between the extent of apoptosis and relevant mutations present in these cell lines. However, further analysis is required to include all four cell lines and other genes involved in the regulation of cell death pathways.

In conclusion, we have investigated the development of cell death in a glioma multicellular tumour spheroid model. We have shown that the central area of cell death which develops is necrotic in type and the predictable nature of its onset will enable the study of putative regulatory events in prenecrotic cells. Apoptosis tends to increase with necrosis in this model and comparisons between cell lines suggest that there is a relationship between the susceptibility to necrosis and to apoptosis. The low levels of apoptosis observed at weeks 1 and 2, when the spheroids are small and relatively unstressed, suggests that the effect of the dysregulated cell cycle of these tumour cells alone is a small contributor to levels of apoptosis. In contrast, most of the apoptosis observed appears to be that which is induced, either by stresses caused by increasing diffusion gradients or by breakdown products of necrotic cells. Differences observed in the susceptibility and patterns of cell death in the different cell lines, however, are likely to reflect the interaction between the molecular genetic status of

a cell line with the environment, giving rise to the particular cell death response to increasing stress. The ability to distinctly quantify apoptosis and necrosis using the spheroid model will prove to be a valuable tool to study the interactions in the regulation of both apoptosis and necrosis in gliomas.

Acknowledgments

This work was supported by a grant from the Samantha Dickson Research Trust. Helen Bell is supported by the Brain Tumour Endowment fund at the Department of Clinical Neurosciences, Western General Hospital, Edinburgh. We would like to thank Mr Frank Donelly for technical help in the preparations of spheroids for electron microscopy.

References

1 Akiyama K, Gluckman TL, Terhakopian A, Jinadasa PM, Narayan S, Singaswamy S, Massey B, Bing RJ. Apoptosis in experimental myocardial infarction *in situ* and in the perfused heart *in vitro*. *Tissue Cell* 1997; **29**: 733–43

2 Alvord ED. Is necrosis helpful in the grading of gliomas? Editorial opinion. *J Neuropathol Exp Neurol* 1992; **51**: 127–32

3 Arends MJ, McGregor AH, Wyllie AH. Apoptosis is inversely related to necrosis and determines net growth in tumours bearing constitutively expressed myc, ras and HPV oncogenes. *Am J Pathol* 1994; **144**: 1045–57

5 Banasiaka KJ, Xiab Y, Haddadbc GG. Mechanisms underlying hypoxia induced neuronal apoptosis. *Prog Neurobiol* 2000; **62** (3): 215–49

6 Bell HS, Wharton SB, Leaver HA, Whittle IR. Effects of N-6 essential fatty acids on glioma invasion and growth: experimental studies with glioma spheroids in collagen gels. *J Neurosurg* 1999; **91**: 989–96

7 Bellamy CO, Malcomson RD, Harrison DJ, Wyllie AH. Cell death in health and disease: the biology and regulation of apoptosis. *Semin Cancer Biol* 1995; **6** (1): 3–16

8 Bernstein JJ, Goldberg WJ, Laws ER Jr. Human malignant astrocytoma xenografts migrate in rat brain: a model for nervous system cancer research. *J Neurosci Res* 1987; **22**: 134–43

9 Bjerkvig R, Laerum OD, Mella O. Glioma cell interactions with fetal rat brain aggregates *in vitro* and with brain tissue *in vivo*. *Cancer Res* 1986; **46**: 4071–9

10 Burger PC, Scheithauer BW. Tumours of the central nervous system. In *Atlas of Tumour Pathology*. 3rd series, Fascicle 10. Washington DC: Armed Forces Institute of Pathology, 1994: 49–68.

11 Clarke PGH. Apoptosis Versus Necrosis: How Valid a Dichotomy for Neurons? In *Cell Death and Diseases of the Nervous System*. Eds VE Koliatos, RR Ratan. Totowa, NJ: Humana Press Inc, 1998: 3–28

12 Collins VP. Progression as exemplified by human astrocytic tumours. *Seminars Cancer Biology* 1999; **9**: 267–76

13 Creutz CE. The annexins and exocytosis. *Science* 1992; **258** (5084): 924–31

14 Ellison DW, Steart PV, Gatter KC, Weller RO. Apoptosis in cerebral astrocytic tumours and its relationship to expression of the Bcl-2 and p53 proteins. *Neuropathol Appl Neurobiol* 1995; **21**: 352–61

15 Elobeid A, Bongcam-Rudloff E, Westermark B, Nister M. Effects of inducible glial fibrillary acidic protein on glioma cell motility and proliferation. *J Neuroscience Res* 2000; **60** (2): 245–56

16 Frame MC, Freshney RI, Vaughan PFT, Graham DI, Shaw R. Inter-relationship between differentiation and malignancy-associated properties in glioma. *Br J Cancer* 1984; **49**: 269–80

17 Giese A, Loo MA, Reif MD, Tran N, Berens ME. Substrates for astrocytoma invasion. *Neurosurgery* 1995; **37**: 294–302

18 Gold R, Schmied M, Giegerich G, Breitschopf H, Hartung HP, Toyka KV, Lassmann H. Differentiation between cellular apoptosis and necrosis by the combined use of *in situ* tailing and nick translation techniques. *Lab Invest* 1994; **71** (2): 219–25

19 Grasl-Kraupp B, Ruttkay-Nedecky B, Koudelka H, Bukowska K, Bursch W, Schulte-Hermann R. *In situ* detection of fragmented DNA (TUNEL assay) fails to discriminate among apoptosis, necrosis and autolytic cell death: a cautionary note. *Hepatology* 1995; **21**: 1465–8

20 Guo M, Hay BA. Cell proliferation apoptosis. *Curr Opin Cell Biol* 1999; **11** (6): 745–52

21 Ishii N, Maier D, Merlo A, Tada M, Sawamura Y, Diserens A-C, Van Meir EG. Frequent Co-Alterations of *TP53*, *p16/CDKN2A*, *p14^{ARF}*, *PTEN* tumour suppressor genes in human glioma cell lines. *Brain Pathol* 1999; **9**: 469–79

22 Kajstura J, Cheng W, Reiss K, Clark WA, Sonnenblick EH, Krajewski S, Reed JC, Olivetti G, Anversa P. Apoptotic and necrotic myocyte cell deaths are independent contributing variables of infarct size in rats. *Lab Invest* 1996; **74**: 86–107

23 Kleihues P, Burger PC, Collins VP, Newcomb EW, Ohgaki H, Cavenee WK. Glioblastoma. In: Kleihues P, Cavanee WK, Eds. *Tumours of the Nervous System*. IARC Press: Lyon, 2000: 10–21

24 Kleihues P, Burger PC, Scheithauer BW. *Histological Typing of Tumour of the Central Nervous System*. 2nd edn. Berlin: Springer-Verlag, 1993: 11–16

25 Kleihues P, Ohgaki H. Primary and secondary glioblastomas: from concept to clinical diagnosis. *Neuro-Oncology* 1999; **1**: 44–51

26 Kockx MM, Knaapen WM. The role of apoptosis in vascular disease. *J Pathol* 2000; **190** (3): 267–80
27 Kunz-Schughart LA, Kreutz M, Knuechel R. Multicellular spheroids: a three-dimensional *in vitro* culture system to study tumour biology. *Int J Exp Path* 1998; **79**: 1–23
28 Laping NJ, Teter B, Nichols NR, Rozovsky I, Finch CE. Glial fibrillary acidic protein: regulation by hormones, cytokines and growth factors. *Brain Pathol* 1994; **1**: 259–75
29 Leaver HA, Whittle IR, Wharton SB, Ironside JW. Apoptosis in human primary brain tumours. *Br J Neurosurg* 1998; **12**: 539–46
30 Leist M, Single B, Castoldi AF, Kuhnle S, Nicotera P. Intracellular adenosine triphosphate (ATP) concentration: a switch in the decision between apoptosis and necrosis. *J Exp Med* 1997; **185**: 1481–6
31 Lennon SV, Martin SJ, Cotter TG. Dose-dependent induction of apoptosis in human tumour cell lines by widely diverging stimuli. *Cell Prolif* 1991; **24**: 2–3–214
32 Nakagawa S, Shiraishi T, Kihara S, Tabuchi K. Detection of DNA strand break associated with apoptosis in human brain tumours. *Virchows Arch* 1995; **427**: 175–9
33 Ness GO, Pedersen PH, Bjerkvig K, Laerum OD, Lillehaug JR. Three-dimensional growth of glial cell lines affects growth factor receptor mRNA levels. *Exp Cell Res* 1994; **214** (1): 433–6
34 Nicotera P, Leist M, Fava E, Berliocchi L, Volbracht C. Energy requirement for caspase activation and neuronal cell death. *Brain Pathol* 2000; **10**: 276–82
35 Parliament MB, Allanunis-Turner MJ, Franko AJ, Olive PL, Mandyam R, Santos C, Wolokoff B. Vascular endothelial growth factor expression is independent of hypoxia in human malignant glioma spheroids and tumours. *Br J Cancer* 2000; **82** (3): 635–41
36 Rofstad EK, Eide K, Skoyum R, Hystad ME, Lyng H. Apoptosis, energy metabolism, and fraction of radiobiologically hypoxic cells: a study of human melanoma multicellular spheroids. *Int J Radiat Biol* 1996; **70** (3): 241–9
37 Ruan H, Wang J, Hu L, Lin CS, Lamborn KR, Deen DF. Killing of brain tumor cells by hypoxia-responsive element mediated expression of BAX. *Neoplasia* 1999; **1** (5): 431–7
38 Sano Y, Hoshino T, Bjerkvig R, Denn DF. The relative resistance of non-cycling cells in 9L multicellular spheroids to spirohydantoin mustard. *European J Cancer Clin Oncology* 1983; **19** (10): 1451–6
39 Schiffer D, Cavalla P, Migheli A, Chio A, Giodana MT, Marion S, Attanasio A. Apoptosis and cell proliferation in human neuroepithelial tumours. *Neuroscience Lett* 1995; **195**: 81–4
40 Schor SL, Schor AM, Winn B, Rushton G. The use of three-dimensional collagen gels for the study of tumour cell invasion *in vitro*: experimental parameters influencing cell migration into the gel matrix. *Int J Cancer* 1982; **29**: 57–62
41 Staunton MJ, Gaffney EF. Tumour type is a determinant of susceptibility to apoptosis. *Am J Clin Pathol* 1995; **103**: 300–7
42 Steel GG. Basic theory of growing cell populations. In *Growth Kinetics of Tumours*, chptr. 2. Oxford: Clarendon Press, 1977: 56–85
43 Sutherland RM. Cell and Environment interactions in tumour microregions: the multicellular spheroid model. *Science* 1988; **240**: 177–84
44 Tachibana O, Nakazama H, Lampe J, Watanabe K, Kleihues P, Ohgaki H. Expression of Fas/APO-1 during the progression of astrocytoma. *Cancer Res* 1995; **55** (23): 5528–30
45 Tamaki M, McDonald W, Amberger VR, Moore E, Del Maestro RF. Implantation of C6 astrocytoma spheroid into collagen type I gels: invasive, proliferative, and enzymatic characterisations. *J Neurosurg* 1997; **87**: 602–9
46 Tannock IF. Cell proliferation. In *The Basic Science of Oncology*. 2nd edn. Eds. IF Tannock, RP Hill. New York: McGraw-Hill, Inc, 1992: 154–177
47 Trump BF, Berezesky IK, Chang SH, Phelps PC. The pathways of cell death: oncosis apoptosis, and necrosis. *Toxicol Pathol* 1997; **25** (1): 82–8
48 Van Meir EG, Kikuchi T, Tada M, Li H, Diserens AC, Wojcik BE, Sultuang H-J, Friedmann T, De Tribolet N, Cavenee WK. Analysis of the *p53* gene and its expression in human glioblastoma cells. *Cancer Res* 1994; **54**: 649–52
49 Veinot JP, Gattinger DA, Fliss H. Early apoptosis in human myocardial infarcts. *Hum Pathol* 1997; **28**: 485–92
50 Wylie AH. The genetic regulation of apoptosis. *Current Opinion Genet Dev* 1995; **5** (97–104): 51

Received 20 November 2000
Accepted after revision 5 March 2001